



# **Application of the Cell Painting Assay for Pseudo-Natural Product Projects**

## **Dissertation**

zur Erlangung des akademischen Grades des Doktors der  
Naturwissenschaften (Dr. rer. nat.)

der Fakultät für Chemie und Chemische Biologie der  
Technischen Universität Dortmund

vorgelegt von

**Sarah Zinken, M.Sc.**

geboren am 12.04.1995  
in Mechernich

Dortmund, 2022



Die vorliegende Arbeit entstand im Zeitraum von Oktober 2018 bis Juni 2022 unter der Anleitung von Prof. Dr. Dr. h.c. Herbert Waldmann an der Fakultät für Chemie und Chemische Biologie der Technischen Universität Dortmund und dem Max-Planck-Institut für molekulare Physiologie Dortmund.

1. Gutachter Prof. Dr. Dr. h.c. Herbert Waldmann
2. Gutachter PD Dr. Andreas Brunschweiler



Results presented in this dissertation contributed to the following publications:

D. J. Foley, S. Zinken, D. Corkery, L. Laraia, A. Pahl, Y.-W Wu, H. Waldmann, “Phenotyping Reveals Targets of a Pseudo-Natural-Product Autophagy Inhibitor”, *Angew. Chem.* **2020**, *59*, 12470-12476. DOI:10.1002/anie.202000364.

M. Grigalunas, A. Burhop, S. Zinken, A. Pahl, S. Sievers, D. J. Foley, A. P. Antonchick, H. Waldmann, “Natural Product Fragment Combination to Performance-Diverse Pseudo-Natural Products”, *Nat. Commun.* **2021**, *12*, 1-11. DOI:10.1038/s41467-021-22174-4.

S. Zinken, M. Grigalunas, A. Pahl, H. Waldmann, “Cell-Painting-Assay Guided Design of a novel Pseudo-Natural Product Compound Class“, *in preparation, preliminary title.*



## Acknowledgements

Looking back on the last couple of years, all the ups (and some downs) of a PhD, there are quite a few people who made this a wonderful and most memorable time. My very warmest thanks to all of you!

First, I would like to thank Prof. Dr Dr h. c. Herbert Waldmann who made this doctoral thesis in his group possible in the first place, but also provided me with all the great opportunities to pursue my scientific development. I really appreciate the outstanding scientific environment, the diverse and interdisciplinary research projects and all the freedom and independence I have experienced, while I always could be sure that I could count on your support.

Additionally, I am grateful to PD Dr Andreas Brunschweiler for taking over the responsibilities as my second examiner.

A special thanks goes to Dr Michael Grigalunas, who first became one of my accomplices to solve the cell painting mystery, but then also took on the role of a very inspiring and understanding group leader. I really enjoyed shaping and discussing my projects with you and I am more than thankful for your support and guidance.

A thank you that I can hardly put into words goes to the most fabulous PhDs: Caitlin Davies, Aylin Binici and Lara Dötsch. I will always have fond memories of our teatimes and dinners, our support for each other, our celebration of scientific success (or just ourselves), and most of all our laughter.

Furthermore, I would like to thank the whole chemistry group, and everyone involved in any pseudo-natural product projects. I am grateful for all our scientific discussions, the mutual support and for every shared chemical and idea. I would particularly like to thank Dr Gregor Cremosnik, who was a wonderful mentor straight from the beginning of my PhD time. But also, Dr Daniel Foley, Dr Saad Shaaban and Dr Georg Niggemeyer for every fruitful discussion.

Another group of people I am deeply grateful to is the cell painting team, including Dr Andreas Christoforow, Dr Gregor Cremosnik, Dr Michael Grigalunas, Dr Axel Pahl, Dr Tabea Schneidewind, Dr Julian Wilke and Dr Slava Ziegler. I really enjoyed working on this project with you!

## Acknowledgements

Whenever biological questions arose, Dr Slava Ziegler and her ‘bio-team’ were there to help and to advise. Special thanks go to Dr Nadine Kaiser for her introduction to the autophagy biology and to Dr Julian Wilke for his support with my first CETSA experiences. I would also like to thank Dr Dale Corkery for the collaboration on autophagy-related projects.

I gratefully acknowledge the whole COMAS team for the performance of the phenotypic assays. I am particular grateful to Dr Axel Pahl for all the cell painting assay-related discussions, his incredible work to make this assay and its analysis possible but also for all the cheminformatic analyses he performed on my compounds. Furthermore, I would like to thank everyone involved in the analytical support: Dr Petra Janning and her team for the HRMS measurements as well as Bernhard Griewel and the NMR team of the TU Dortmund for the performance of the NMR experiments. A special thanks goes to Jens Warmers for keeping almost all instruments in the institute always running.

In addition, I would like to thank the whole of Department 4, everyone who came and left during my time here, for a great working atmosphere and a wonderful time.

Last but definitely not least: Zum Schluss möchte ich ein ganz besonderes Dankeschön an meine Eltern und meine Geschwister richten, die in den letzten Jahren, wie auch schon während dem Studium stets mein Rückhalt und meine Sicherheit waren. Ich bin unglaublich froh und stolz darauf ein Teil unserer Familie zu sein. Ebenfalls möchte ich an dieser Stelle Maria Jopen und Jürgen Quadt danken, die in den letzten Jahren eine große Rolle in meinem Leben eingenommen haben und von denen ich stets Unterstützung erfahren habe.

Zu guter Letzt, gilt mein allerherzlichster Dank meinem Freund Max Jopen. Dafür, dass ich immer auf dich zählen kann. Danke für Alles! ♥



## Table of Contents

Acknowledgements.....	V
Abstract.....	1
Zusammenfassung.....	3
1. General Introduction .....	5
1.1 Relevance and Design of Bioactive Small Molecules .....	5
1.1.1 Small Molecules in Chemical Biology.....	5
1.1.2 Small Molecule Libraries inspired by Natural Products .....	5
1.1.2.1 Biology Oriented Synthesis (BIOS).....	6
1.1.2.2 Complexity to Diversity (CtD) .....	7
1.1.2.3 Pseudo-Natural Products (PNPs).....	7
1.2. Evaluation of Diverse Compound Libraries with Unknown Bioactivities .....	12
1.2.1 Phenotypic Screening .....	13
1.2.1.1 A Phenotypic Autophagy Assay .....	14
1.2.2.2 Morphological Profiling: The Cell Painting Assay .....	15
2. Objectives .....	18
3. Part I: Evaluation of a Pseudo-Natural Product Autophagy Inhibitor .....	20
3.1. Introduction .....	20
3.1.1 Autophagy and its Regulation .....	20
3.1.2. PNPs Derived from Cinchona Alkaloids and Indoles .....	23
3.2. Results and Discussion.....	25
3.2.1. Structure Activity Relationship .....	25
3.2.2 Activity in the Cell-Painting Assay .....	36
3.2.3 Cell Painting Guided Target Hypothesis and Target Identification .....	39
3.2.4 Target Validation.....	42
3.2.5 Mode of Inhibition by Enzyme Kinetics .....	47
3.3 Conclusion.....	51

## Table of Contents

4. Part II: Cell-painting assay analysis of NP-fragment combinations.....	52
4.1 Introduction.....	52
4.1.1 CPA comparison of compound classes .....	53
4.2. Results and Discussion.....	55
4.2.1 Influence of the Fusion Pattern on Morphological Activity.....	56
4.2.2 Influence of Fragment Combinations on Morphological Activity .....	57
4.2.3 Prediction of Novel Fragment Combinations .....	59
4.2.3.1 Synthesis of Quinidine Isocoumarins .....	60
4.2.3.2 CPA Analysis of Predicted Compounds .....	65
4.3 Conclusion.....	69
5. Part III: Chromalines – Cell Painting-Aided Design of a Novel PNP Compound Class ....	71
5.1 Introduction.....	71
5.2 Results and Discussion.....	73
5.2.1 Synthesis of Chromalines .....	73
5.2.1.1 Synthesis of a Flavanone Starting Material .....	73
5.2.1.2 Synthesis of Flavan-4-ol from Flavanone.....	76
5.2.1.3 Development of an Intramolecular Flavanol Cyclisation Reaction .....	79
5.2.2 A Preliminary CPA Analysis.....	82
5.2.3 Synthesis of Chromaline Derivatives .....	84
5.2.4 Cheminformatic Analysis of the Chromaline Compound Class .....	86
5.2.5 Cell Painting Assay Analysis of Chromalines.....	90
5.3 Conclusion.....	95
6. Experimental.....	97
6.1 Materials and Methods for Organic Synthesis .....	97
6.2 Chemical Synthesis .....	100
6.2.1 Azaquinidole-1 Derivatives .....	100
6.2.2 Synthesis of Isocoumarin-Quinidines.....	117

6.2.3 Synthesis of Chromalines .....	122
6.3. Materials, Instruments and Methods for Biological Experiments.....	166
6.4 Biological Methods .....	170
6.4.1 Cell Culture.....	170
6.4.2 Phenotypic Assays .....	171
6.4.2.1 High Content Screening for Autophagy Inhibitors.....	171
6.4.2.2 Cell Painting Assay.....	171
6.4.3 Biochemical and Cell-based Assays.....	174
6.4.3.1 Kinase Panel.....	174
6.4.3.2 Immunoblotting (LC3 and ULK1/pULK1) .....	174
6.4.3.3 Selective Viability Assay .....	174
6.4.3.4 Live-Cell Microscopy .....	175
6.4.3.5 Cellular Thermal Shift Assay (CETSA) .....	175
6.4.3.6 Kinase Kinetic Experiments (VPS34) .....	176
6.4. Cheminformatic Analysis.....	177
6.4.1 Reference Data Sets.....	177
6.4.2 Molecular and Physiochemical Investigations .....	177
7. Abbreviations .....	180
8. References.....	186



## Abstract

The exploration of novel areas of chemical space that are covered by bioactive small molecules is of great interest to the chemical biology and medicinal chemistry communities. Small molecules may not only serve as tool compounds for the investigation of cellular processes but may also modulate cellular misregulation in certain diseases. To narrow the search area from all potentially synthesisable compounds and to focus on biologically relevant chemical space, the implementation of molecular design principles is essential. Considering that natural products (NPs) underwent evolutionary selection to bind to their biological targets and therefore represent biologically prevalidated chemical matter, they can serve as a valuable source of inspiration. In the pseudo-NP (PNP) approach, NP fragments are combined by means of chemical methodologies in new arrangements that are not observed in nature. PNPs are designed to share the NP fragments' high probability to bind to macromolecular targets but also may explore novel areas of biological space as they are structurally distinct from NPs. Phenotypic screening methods, particularly the cell-painting assay (CPA), have been investigated as powerful tools for the biological evaluation of PNPs since they may have unexpected bioactivities.

Herein, a PNP class derived from a quinine- and azaindole-fragments was proven to inhibit the autophagy signalling pathway. A structure-activity-relationship was determined, and the most active autophagy inhibitor, azaquindole-1, was chosen for further studies towards its mode of action. Comparison of its morphological profile from the CPA to reference compound profiles with annotated bioactivity hinted towards a kinase target. Further investigation proved this hypothesis and identified VPS34 kinase as a potential autophagy-related target. An *in-vitro* enzyme activity assay, further cellular assays and a cellular thermal shift assay validated the binding and inhibition of VPS34 by azaquindole-1. This study highlighted the impact that the CPA can have on the target identification of bioactive PNPs.

CPA analysis of diverse PNP compound classes derived from a small fragment subset, allowed the investigation of fragment combinations on morphological profiles. It was shown that different fragment connectivities can lead to diverse bioactivities. Furthermore, the observation was made that fragments can either have a dominating or non-dominating effect on the morphological activity of PNPs that could also be proven in behaviour predictions. This led to the suggestion to use non-dominating fragments to design PNPs with unique and potentially novel bioactivities.

## Abstract

Taking inspiration from previous PNP examples, a novel chromane- and 4*H*-quinoline-derived compound class was designed. The development of a suitable synthetic route resulted in a chromaline compound library that was subsequently tested in the CPA. Comparison with the inspiring PNP classes (chromopynone and pyroquinoline) revealed, that both fragments were non-dominating and therefore suitable for the design of unique PNPs. Furthermore, the novel chromaline compound class showed high chemical and morphological diversity.

Overall, design strategies with the guiding principle of PNPs were employed to generate compound libraries that were evaluated and biologically characterised by the cell painting assay (Figure 1).

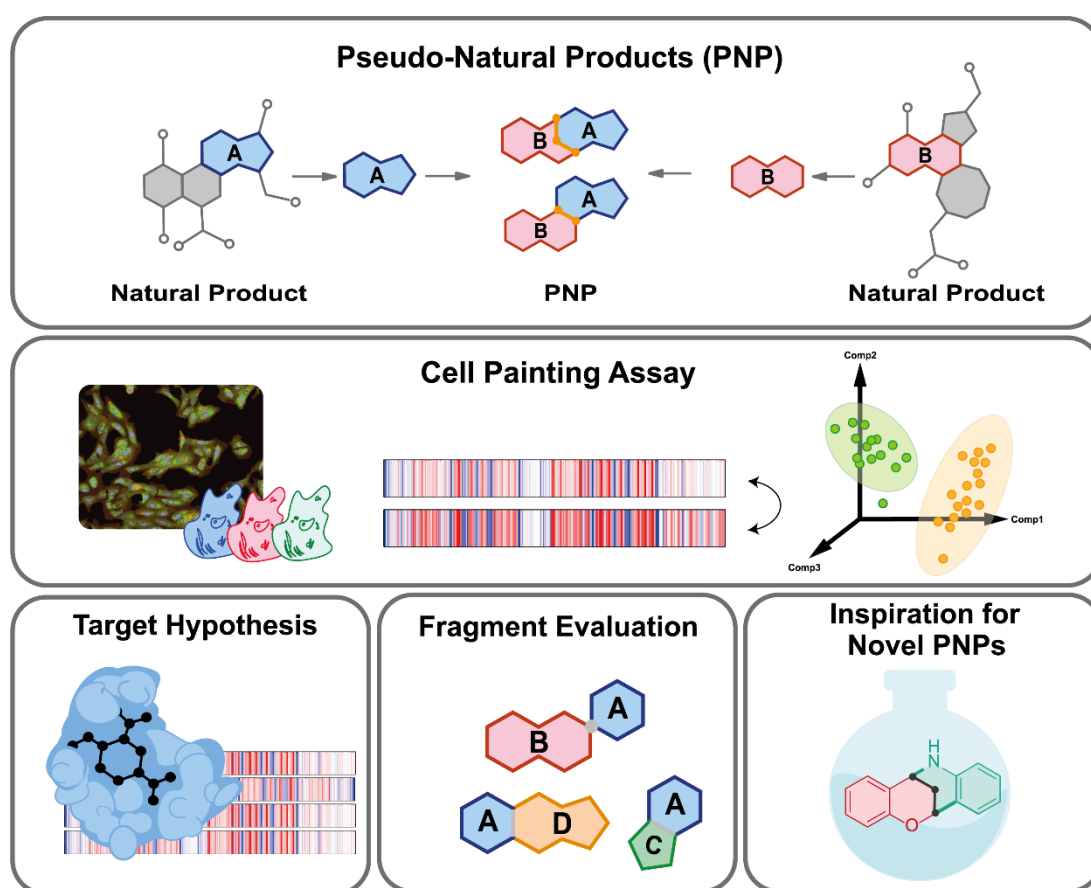


Figure 1: Summary of the PNP concept, the cell painting assay and overview of possible applications of the cell painting assay to study PNPs.

## Zusammenfassung

Die Entwicklung neuartiger, niedermolekularer und bioaktiver Verbindungen ist von großem Interesse für die Chemische Biologie sowie die medizinische Chemie. Niedermolekulare Verbindungen können zum einen als Sonden für die Untersuchung zellulärer Prozesse dienen, aber auch zelluläre Fehlregulationen bestimmter Krankheitsbilder modulieren. Um den Suchbereich aller potenziell synthetisierbaren Verbindungen einzugrenzen, ist die Anwendung molekularer Designprinzipien unerlässlich. Da Naturstoffe (*natural product*, NP) evolutionär selektiert wurden, um effizient an ihre biologischen Zielstrukturen zu binden, können ihre privilegierten Strukturen als wertvolle Inspirationsquelle dienen. Beim Pseudo-NP (PNP)-Ansatz werden NP-Fragmente unter Zuhilfenahme chemischer Synthesemethoden in neuen Anordnungen miteinander kombiniert, welche in der Natur nicht zu finden sind. PNPs teilen daher die hohe Wahrscheinlichkeit von NP-Fragmenten an makromolekulare Zielstrukturen zu binden. Da sie sich strukturell von NPs unterscheiden können PNPs aber auch unerwartete Bioaktivitäten aufweisen. Daher haben sich phänotypische Screening-Methoden, insbesondere das *Cell-Painting-Assay* (CPA), als leistungsfähige Instrumente für ihre biologische Untersuchung erwiesen.

In dieser Arbeit wurde nachgewiesen, dass eine zuvor beschriebene PNP-Klasse, die aus Kombination eines Chinin- und Azaindol-Fragment erhalten wurde, den Autophagie-Signalweg hemmt. Es wurde eine Struktur-Aktivitäts-Beziehung hergeleitet, und der aktivste Autophagie-Inhibitor, Azaquindole-1, wurde für weitere Studien zu seinem Wirkmechanismus ausgewählt. Der Vergleich seines morphologischen Profils aus dem CPA mit Referenzprofilen von Verbindungen mit annotierter Bioaktivität deutete auf ein Kinase-Target hin. Weitere Untersuchungen bestätigten diese Hypothese und identifizierten die VPS34-Kinase als potenzielles biologisches *Target*. Ein *in-vitro*-Enzymaktivitätsassay, weitere zelluläre Assays und ein *Thermal-Shift-Assay* bestätigten die Bindung und Hemmung von VPS34 durch Azaquindole-1. Diese Studie unterstreicht die Bedeutung, die das CPA auf die Identifizierung bioaktiver PNPs haben kann.

Die CPA-Analyse verschiedener PNP-Verbindungsklassen, die aus einer kleinen, definierten Gruppe Fragmente aufgebaut wurden, ermöglichte die Untersuchung des Einflusses von Fragment-Kombinationen auf morphologische Profile. Es wurde gezeigt, dass verschiedene Anordnungen der gleichen Fragmente zu unterschiedlichen Bioaktivitäten führen können. Darüber hinaus wurde die Beobachtung gemacht, dass Fragmente entweder eine dominierende oder eine nicht-dominierende Wirkung auf die morphologische Aktivität von PNPs haben

## Zusammenfassung

können. Dies konnte durch Vorhersagen des entweder dominierenden oder nicht-dominierenden Verhaltens weiterer PNP-Klassen bestätigt werden. Daraus ergibt sich die Empfehlung, für das Design neuer PNPs auf nicht-dominierende Fragmente zurückzugreifen, um Verbindungen mit einzigartigen und potenziell neuartigen Bioaktivitäten zu entwickeln.

In Anlehnung an frühere PNP-Beispiele wurde eine neue, von Chroman und 4*H*-Chinolin abgeleitete Verbindungsklasse entwickelt. Die Entwicklung eines geeigneten Syntheseweges ermöglichte die Synthese einer Chromaline-Substanzbibliothek, die anschließend im CPA getestet wurde. Der Vergleich mit den PNP-Klassen (Chromopynone und Pyrroquinoline) die als Inspirationsquelle dienten bestätigte, dass beide Fragmente nicht dominierend sind und sich daher für die Entwicklung einzigartiger PNPs eignen. Darüber hinaus zeigte die neue Chromaline Verbindungsklasse eine große chemische und morphologische Vielfalt.

Insgesamt wurden Design-Strategien mit dem Leitprinzip der PNPs eingesetzt, um Substanzbibliotheken zu generieren, die dann durch das *Cell-Painting-Assay* bewertet und biologisch charakterisiert wurden (Abbildung 1).

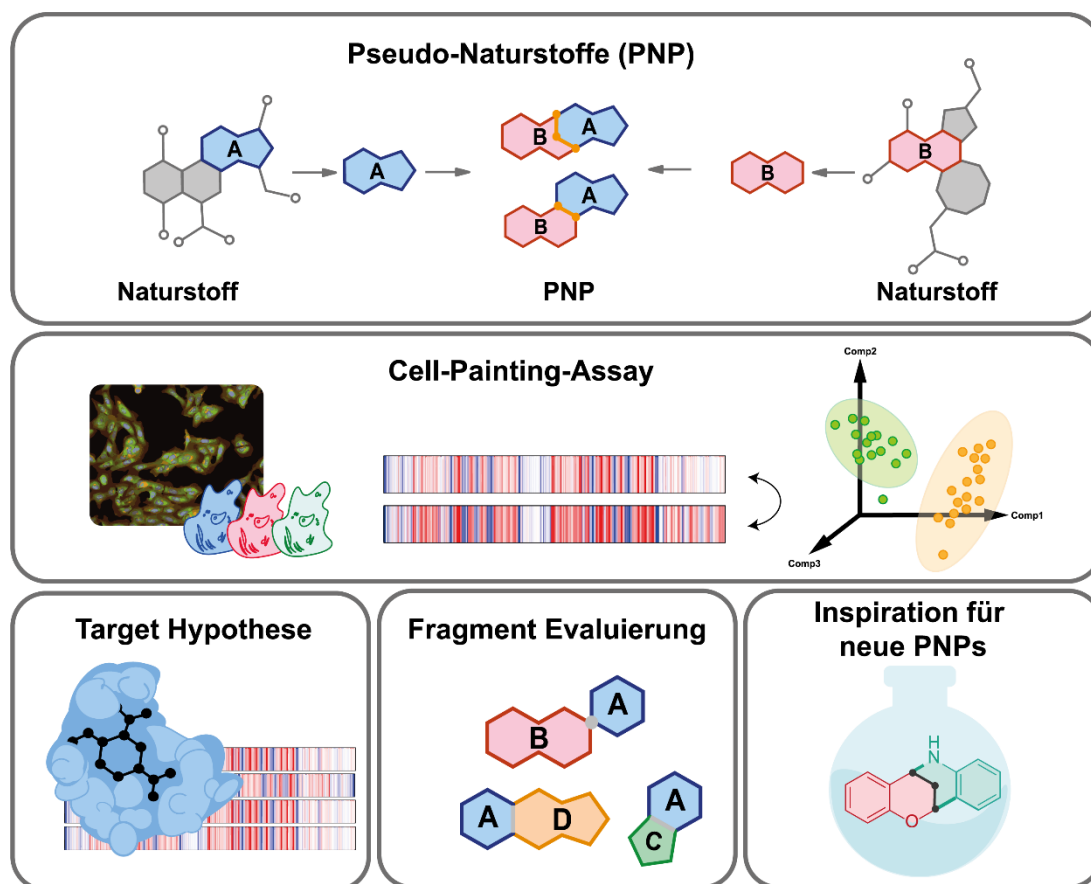


Abbildung 1: Zusammenfassung des PNP-Konzepts, des *Cell-Painting-Assays* und Überblick über mögliche Anwendung des *Cell-Painting-Assays* zur Untersuchung von PNPs.



## 1. General Introduction

### 1.1 Relevance and Design of Bioactive Small Molecules

#### 1.1.1 Small Molecules in Chemical Biology

One of the main objectives of chemical biology is to probe and thereby explore and understand biological systems. Amongst others, bioactive small molecules have proven to be a valuable tool for the exploration of complex signalling networks in living cells. They can modulate biomacromolecules and therefore allow insights into the regulation and organisation of signalling pathways.<sup>[1,2]</sup> The perturbation of protein function by small molecules is reversible, transient, and tuneable by different concentrations, which provides them with a major advantage over gene deletion methods. While gene deletion methods completely remove multifunctional proteins, which may lead to undesired influences on signalling networks, small molecules can deliver more precise information about the role of specific protein functions. Since they can allow insights into complex biological systems and have become a valuable tool for the identification of molecular targets, the discovery of novel bioactive small molecules is of great interest to the chemical biology and medicinal chemistry community.<sup>[1]</sup>

#### 1.1.2 Small Molecule Libraries inspired by Natural Products

Considering the enormous number of small molecules that constitute the drug-like chemical space ( $>10^{60}$  compounds) and the impracticality in to synthesising all of them, it is of great importance to narrow down this number to compounds that are biologically relevant.<sup>[3]</sup> In the past natural products (NPs) have been an invaluable source of inspiration for the development of novel bioactive small molecules. NPs (or secondary metabolites) were designed by nature to fulfil a specific function and to pass an evolutionary advantage to the producing organism. Their structures were evolutionarily selected and adjusted for the binding to protein targets, so they can be considered as biologically prevalidated, privileged scaffolds for molecular interactions.<sup>[4-6]</sup> During the past decades (1981-2019) 32% of all FDA approved small molecule drugs were either NPs or derivatives, highlighting their role as promising models for drug-like molecules.<sup>[6]</sup> Structurally, NPs differ from synthetic small molecules by their high complexity and a high density of stereochemical information. On the one hand this gives them a high selectivity for specific protein targets, but also impacts their availability through chemical synthesis. Chemical modifications to optimise their molecular properties for medicinal use and to evaluate structure activity relationship (SAR) studies can become challenging due to

multistep synthetic routes.<sup>[7]</sup> Therefore, approaches to overcome these chemical restrictions by designing NP-inspired compound collections has gained great interest.

### 1.1.2.1 Biology Oriented Synthesis (BIOS)

The biology-oriented synthesis (BIOS) approach aims to overcome the difficulties in NP synthesis by logical and stepwise simplification of their complex molecular frameworks.<sup>[8-11]</sup> The underlying concept is based on the observation, that the three-dimensional shape of many binding sites is highly conserved among protein subclasses, even though the decorating amino acid combinations are variable.<sup>[12]</sup> Consequently, NP scaffolds require a shape to structurally fit into these sites and exert their biological activity. This leads to the observation, that many NPs share common scaffolds, so called ‘privileged scaffolds’. Nevertheless, NPs can achieve selectivity for their binding site through variable side chains and functionalities interacting with the amino acid backbone.<sup>[9,10]</sup> To reduce NP structures to the relevant scaffolds, a cheminformatic structural analysis was performed and visualised in a tree-like structural classification of natural products (SCONP). Consideration of biological relevance during stepwise and hierarchical simplification of NP structures assures that the core scaffolds maintain their bioactivity, while they might lose affinity and potency.<sup>[13]</sup> Derivatisation by implementing, for example functional groups or stereogenic information, allows the optimisation of potency and of physiochemical properties of the NP-inspired compound collections (Figure 2). In this turn, this led to compounds with improved properties or different bioactivities.<sup>[14,15]</sup>

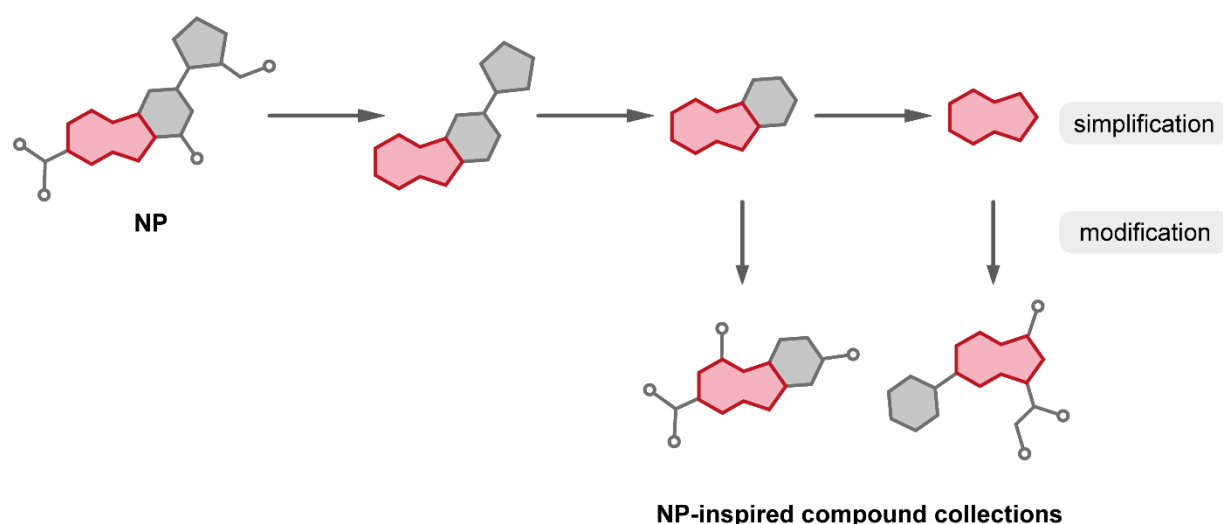


Figure 2: Schematic representation of the BIOS approach. The biologically relevant core scaffold is highlighted in red.

However, since the BIOS approach takes its inspirations from a limited set of privileged NP derived scaffolds, the potential exploration of relevant chemical space is limited. Furthermore,

based on their similar molecular properties, BIOS derived compounds often share the same or similar bioactivity to that of the guiding NPs, restricting the identification of novel biological space.<sup>[16]</sup>

### 1.1.2.2 Complexity to Diversity (CtD)

The Complexity to Diversity (CtD) approach, first introduced by Hergenrother *et al.*, aims to generate novel bioactive compound collections utilising complex NPs as synthetic precursors. Different from other NP modification approaches, the CtD approach not only aims to modify the NP's sidechains and functionalities, but to completely change the NP's core structure. Chemical re-engineering of the rigid and spatially defined ring systems by ring fusion, ring expansion, ring contraction, ring rearrangement or ring cleavage can lead to a drastic change in chemical shape (Figure 3). Consequently, these NP inspired compound collections have a high potential to own new bioactivities compared to their parent NPs and to occupy unknown areas of chemical as well as biological space.<sup>[17-19]</sup>

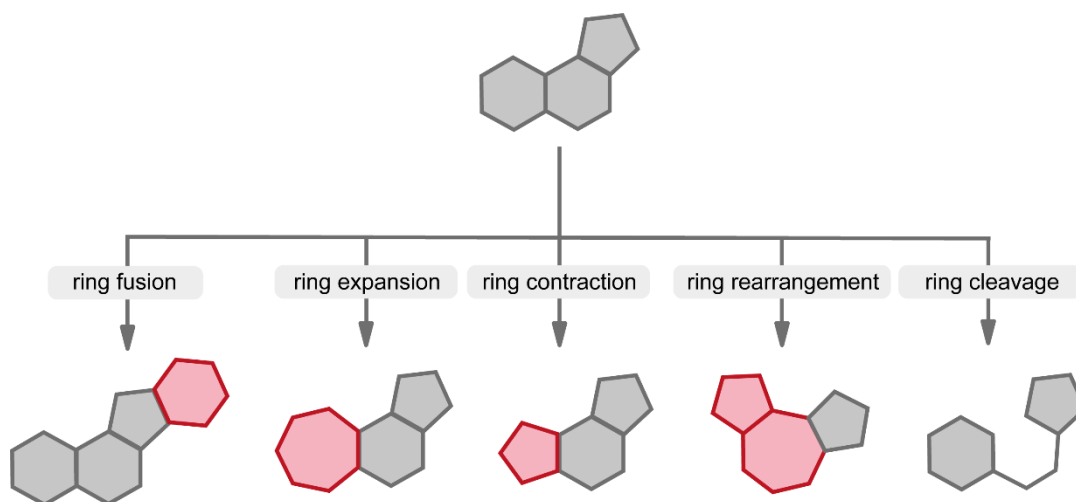


Figure 3: Schematic representation of the CtD approach. Changes of the core scaffold are highlighted in red.

However, several criteria have to be met to qualify a NP for the applicability in this approach. Besides its commercial availability in multigram quantities, the NP should bear orthogonal functional groups that allow the structural transformations. Furthermore, the applicability of the ring-distortion strategies on a limited subset of NP scaffolds confines the area of accessible chemical space.<sup>[17]</sup>

### 1.1.2.3 Pseudo-Natural Products (PNPs)

Previous approaches, like BIOS or CtD, for the design of NP-inspired molecules have led to the successful synthesis of novel bioactivity-enriched compound collections.<sup>[10,17]</sup>

Nevertheless, these concepts have their limitations in the exploration of possible chemical and biological space. Therefore, there is still a great need for the development of novel methods for the design of probe- or drug-like molecules to move forward in the modulation and understanding of biological systems. These concepts should allow extensive and fast navigation through undiscovered chemical space, while the biological relevance of NP structures should be maintained.<sup>[4]</sup>

The design of pseudo-natural products (PNPs) could overcome previous limitations by the combination of NP fragments in arrangements not found in Nature.<sup>[4,15]</sup> Fragments derived from known drugs or drug candidates are valuable starting points for the discovery of novel bioactive compounds. In fragment-based drug design (FBDD) small fragments (“rule of three”:  $\text{AlogP} \leq 3.5$ , a molecular weight of  $< 300$  Da,  $< 3$  hydrogen bond donors,  $\leq 3$  hydrogen bond acceptors) are used in high throughput screening (HTS) campaigns to identify low-affinity ligands via biophysical methods (e.g., NMR or mass spectrometry). Screening of large and diverse fragment collections, followed by combination of fragments occupying the space in the same binding site can result in the identification of drug candidates with high binding affinities.<sup>[20,21]</sup> Even though this approach allows rapid access to novel bioactive molecular scaffolds, the fragments are derived from known drugs that mostly have a flat and  $\text{sp}^2$ -rich structure and therefore only cover a limited area in chemical space.<sup>[22]</sup> However, the validated, combinatorial aspect of the FBDD implies a great advantage to novel methodologies in drug- and probe-development, such as the PNP approach.

In contrast to FBDD, the PNP approach aims to combine fragments derived from NPs instead of classical fragments (Figure 4). In this regard, the identification of relevant fragments can be facilitated by *in silico* fragmentation algorithms, for example the previously mentioned SCONP algorithm that may be modified to allow the retention of structural attachment points and the nature of functional groups.<sup>[23]</sup> Many of the derived NP fragments are enriched in  $\text{sp}^3$  atoms and cover molecular shapes that are prevalidated by nature (see also section 1.12). Their molecular properties are slightly different from the “rule of three” considered for classical fragments (NP-fragments:  $\text{AlogP} \leq 3.5$ , a molecular weight of 120–350 Da,  $\leq 3$  hydrogen bond

donors,  $\leq 6$  hydrogen bond acceptors). Consequently, NPs and derivatives from CtD attempts that meet these criteria can be considered as fragments.<sup>[4,23]</sup>

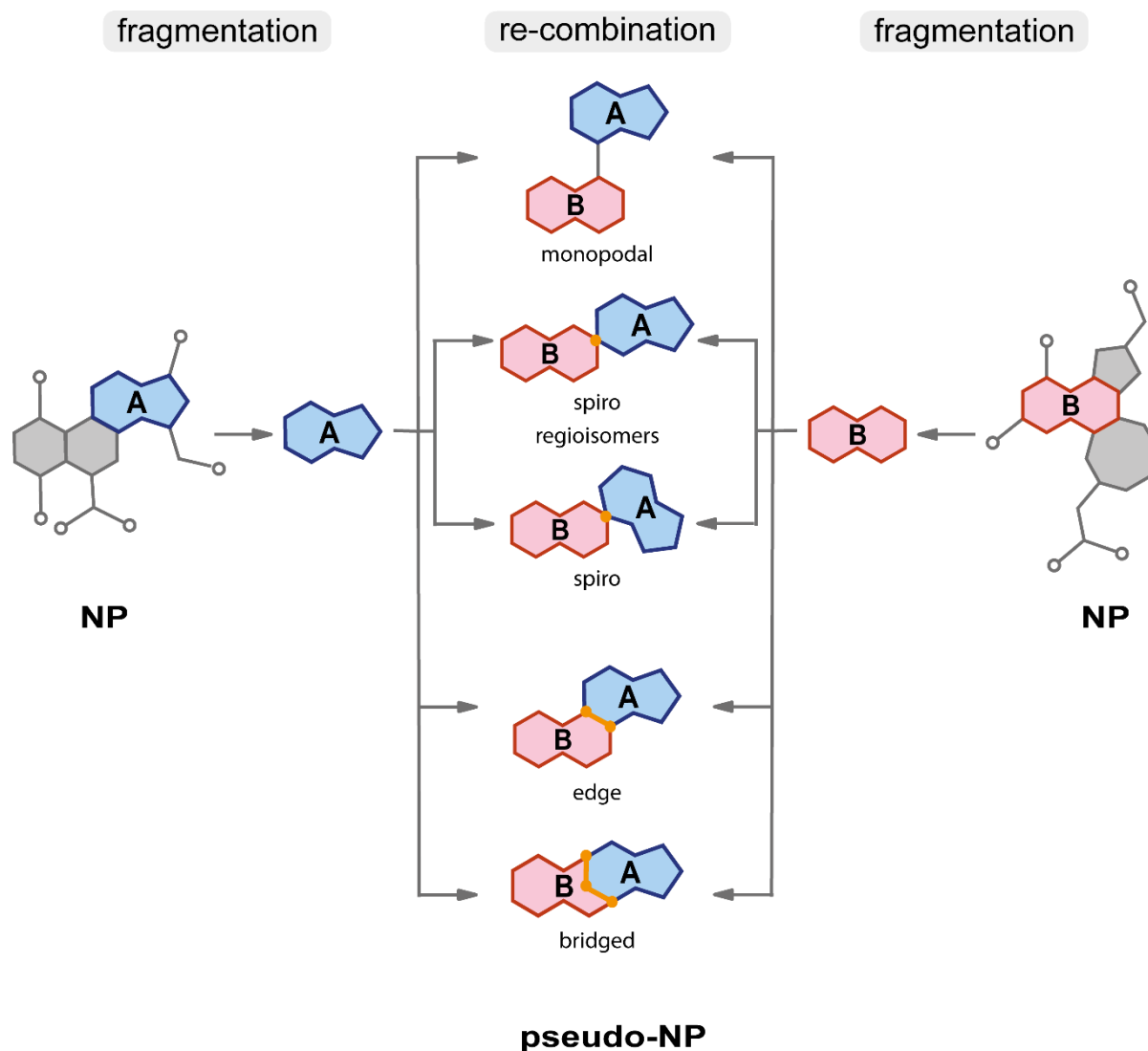


Figure 4: Schematic representation of the PNP approach. NP-fragments are indicated in red and blue and connecting atoms and bonds are indicated in orange.

In PNP design, the recombination of NP fragments should lead to scaffolds, that resemble NPs but have structural deviations that are not known in NPs. Combining fragments that are derived from unrelated biosynthetically pathways or combination in structural arrangements that cannot be reached via biosynthesis may result in structures that are not obtainable by nature. Therefore, PNPs have a high potential to explore novel areas of chemical space while retaining the biological relevance instilled in NPs.

A high degree of diversity within these new designed compound classes may be achieved by utilising different types of connectivity. Connections between two fragments can be classified into four main groups by the number of shared atoms. In monopodal fusions, fragments do not

## General Introduction

share any atoms, in spiro fusions they share 1 atom, in edge fusions they share 2 atoms and in bridged fusions they share  $\geq 3$  atoms (Figure 4). The fusion of fragments in different orientations, i.e. to form different regio-isomers can further expand the diversity of libraries in terms of chemical space and bioactivity.

Since first reporting this novel approach, several PNP examples with diverse bioactivities have been successfully synthesised and evaluated (Figure 5). For example, the combination of chromanes and tetrahydroprimidones led to the first reported PNP compound class (Figure 5 I.). While chromanes are represented in several NPs that cover broad ranges of bioactivity, tetrahydropyrimidones are an antibiotic NP compound class. Recombination of these fragments via a bridged fusion resulted in the novel “chromopynone” class. Biological evaluation of chromopynone-1 revealed their bioactivity in glucose uptake inhibition by selective inhibition of the transporters GLUT-1 and GLUT-3, even though neither of the fragments showed this activity before.<sup>[24]</sup>

Rhonin is a PNP derived from two different 5-membered nitrogen containing heterocycles pyrroline and pyrrolidine, that have a wide occurrence in bioactive NPs (Figure 5 II.). The combination of these fragments via an edge fusion connectivity led to the identification of Rhonin, a novel inhibitor of hedgehog-induced osteogenesis. Further target identification studies revealed that Rhonin is the first small molecule Rho-GDP dissociation inhibitor1 (RHOGDI1) ligand. This finding provided a link between RHOGDI1 and osteogenesis and highlights the potential impact that PNP compounds can have on the investigation of biological systems.<sup>[25]</sup>

Another successful example is the indofulvin class derived from the combination of the fragment-sized NP griseofulvin and indole (Figure 5 III.). Griseofulvin is a modulator of tubulin polymerization and can be isolated from *Penicillium griseofulvin*. Indole on the other hand is a widely occurring fragment in NPs. Combination in a spiro-fusion connection-type resulted in inhibitors of autophagy through perturbation of the mitochondrial function. Moreover, the griseofulvin's original bioactivity was not retained in the PNP, proving that fragment combinations can significantly change an NPs bioactivity and that fragment sized NPs are a suitable starting point in PNP design.<sup>[26]</sup>

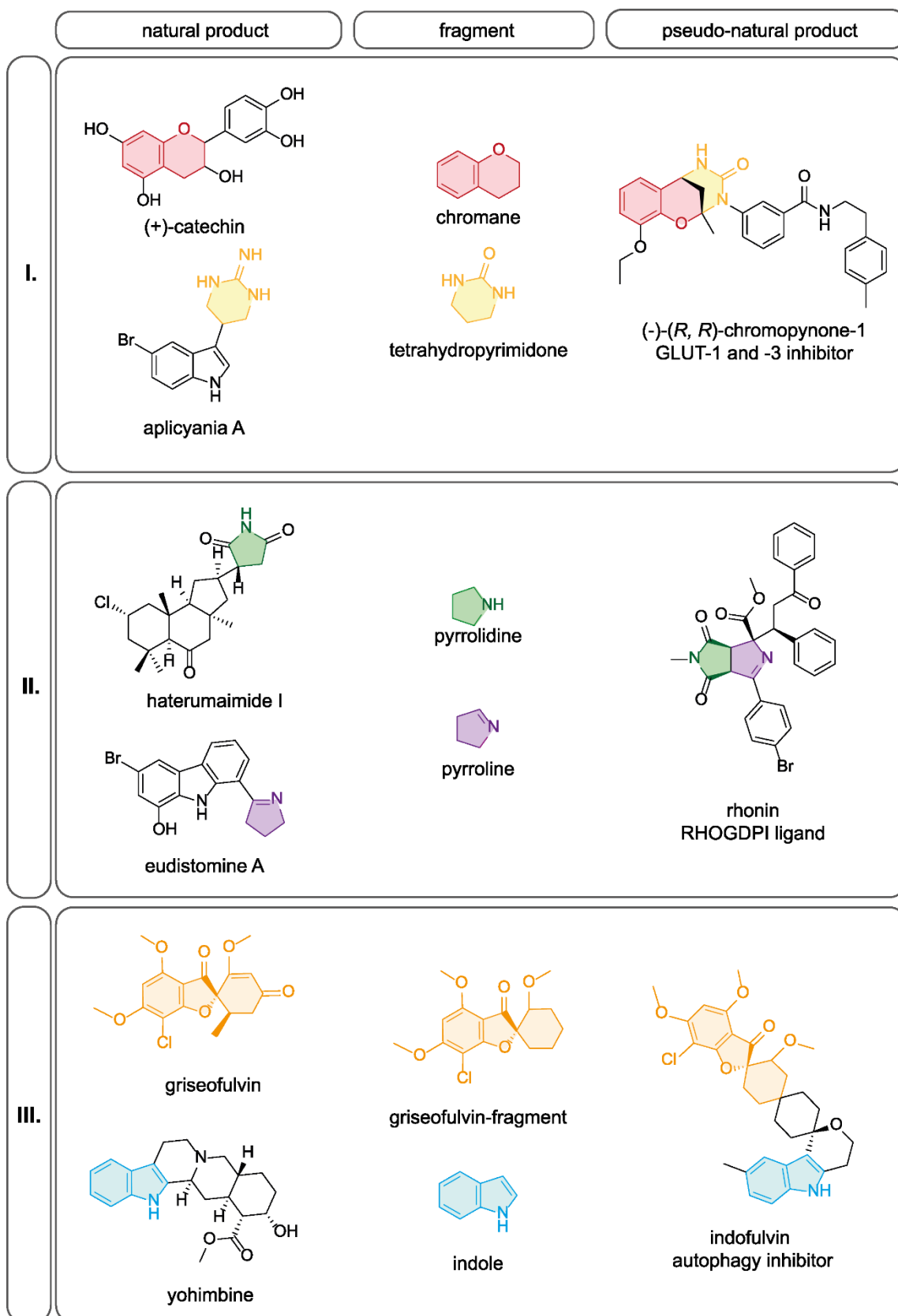


Figure 5: Selected examples for bioactive PNPs; shown are the parent NPs, the used fragments and the structures of most active derivatives: I. chromopynone-1, II. rhonin, III. indofulvin.

Even though the PNP approach was first mentioned by name in the late 2010s, a recent cheminformatic analysis of bioactive compound classes revealed that many compounds meeting the PNP criteria have been synthesised for at least 45 years without being defined as PNPs. The applied methodology considered fragments defined as NP fragments and their arrangement in the final molecule to identify PNPs in the ChEMBL database. The study outlined, that ~23 % of biologically relevant compounds listed in the ChEMBL database met the criteria for the PNP definition. This not only demonstrates the frequent occurrence of PNPs in bioactive small molecules and validates the design principle, but also highlights the relevance of the PNP approach towards the identification of novel bioactive chemical space.<sup>[27]</sup>

## 1.2. Evaluation of Diverse Compound Libraries with Unknown Bioactivities

Besides the design and synthesis of novel compound libraries, a further challenge is their biological evaluation in suitable screening systems. The chemical genetics approach is a valuable general concept for the identification of selective small molecule modulators of specific biological functions. The general idea of this approach was adopted from genetics, which allows the investigation of protein function by genetic manipulations. However, in chemical genetics the protein function is modulated by a small molecule, bearing the advantages of a reversible, temporary and tuneable modification.<sup>[28–30]</sup>

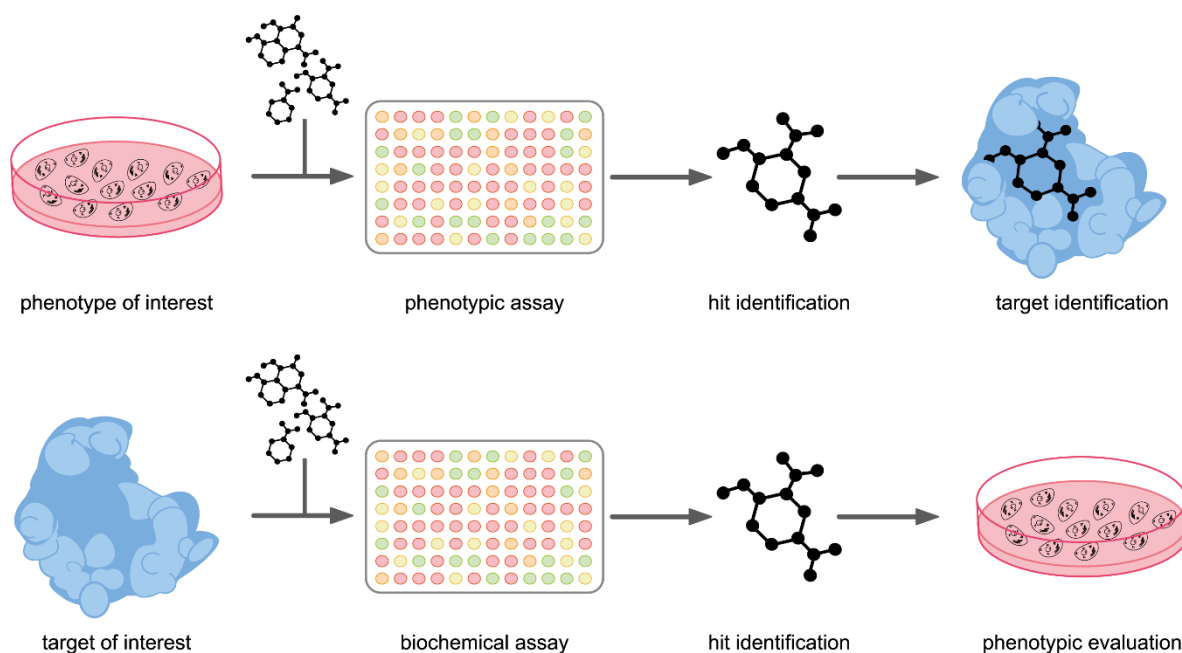


Figure 6: Schematic representation of the forward (a) and reverse (b) chemical genetics approaches.



Chemical genetics encompasses the two fundamental approaches, forward and reverse chemical genetics. In forward chemical genetics compounds are screened in cells or organisms for their induction of a phenotype of interest. Selected compounds, showing the desired phenotypic effect then are further investigated to identify their (protein-) target. Reverse chemical genetic studies on the other hand operate in the opposite direction. Compound libraries are screened on an isolated target protein of interest in biochemical assays. Compounds perturbing the proteins function then are selected and further tested for their phenotypic influences (Figure 6).<sup>[28]</sup>

### 1.2.1 Phenotypic Screening

Along with the increasing number of small molecules and increasing size of libraries, as well as the development of robotic screening platforms, high throughput screening (HTS) methods have gained great importance. In automated systems, large compound libraries can either be tested in phenotypic assays for phenotypic impact, following the forward chemical genetics approach, or in target-based assays for their ability to modulate specific protein functions, following the reverse chemical genetics approach.<sup>[31]</sup> Target-based screening attempts, thereby bear the advantage of a subsequent identification of a specific protein modulation. However, this also limits the method to targets that are already known and furthermore already linked to a specific cellular function. Phenotypic methods, on the other hand, can cover a broad-spectrum of bioactivities, either linked to a pathway of interest or to the entire phenotype of an organism. Therefore, they allow the identification of novel molecular targets or connections in the cellular function network. The identification of a target that is linked to the phenotype can be a challenging process, assuming the number of possible protein- and other macromolecular targets, such as RNA. In addition, a phenotypic effect is not always the result of the direct interaction with a single target. Small molecule ligands can have several targets, either responsible for the phenotype in a superposition of effects or leading to ‘off-target’, meaning side effect activities.<sup>[32,33]</sup>

Nevertheless, phenotypic screening methods are the methods of choice for the biological evaluation of PNP libraries. Not only can these libraries be very diverse, they also are assumed to cover novel biological space and consequently require broad biological screening methods to investigate their activity. Furthermore, in-cell screening methodologies are considered to have a higher physiologically relevance than biochemical assays. The biological target is located in its native, cellular environment. Additionally, the tested compound must be able

enter the cell through the outer membrane to achieve sufficient bioavailability and has to be chemically stable in the cytoplasm.<sup>[33,34]</sup>

### 1.2.1.1 A Phenotypic Autophagy Assay

Phenotypic assays that are linked to a specific pathway are of great interest to the chemical biology and medicinal chemistry fields of research. Often the misregulation of certain pathways is linked to diseases, highlighting the importance for a better understanding and possibilities to regulate these pathways. Among others, fluorescent protein (e.g. green fluorescent protein - GFP) conjugates or reporter genes (e.g. luciferase) that are expressed downstream of a signalling pathway are used as a readout for pathway activity. Fluorescent protein conjugates furthermore can be used to investigate cellular protein localisation and dynamics.<sup>[35]</sup>

One of many cellular pathways, that have come into focus is the autophagy pathway. Autophagy is a conserved process that can be observed at a basal level in most cells, as it is a key regulator in cellular homeostasis. It enables the elimination of misfolded proteins, aggregates and damaged organelles and the subsequent recovery of cellular nutrients. A misregulation of autophagy is therefore often associated with various human disease, such as metabolic conditions, neurodegenerative disease, cancers, and infectious disease.<sup>[36]</sup>

Often, phenotypic assays based on the autophagy marker protein microtubule-associated light-chain 3 (LC3) are applied to monitor autophagy in a cellular context. Under basal cellular conditions, the LC3-I protein is localised and distributed in the cytosol. Upon initiation of autophagy by starvation or autophagy activating modalities, the cytosolic LC3-I protein is conjugated with phosphatidylethanolamine (PE) to LC3-II and delocalised to the outer and inner membrane of phagophores and autophagosomes. Fusion of phagosomes with lysosomes leads to the degradation of LC3-II on the inner membrane by degradative enzymes and a release of LC3-II on the outer membrane by cleavage of PE. Utilising an autophagosome to lysosome fusion inhibitor, such as e.g., chloroquine, therefore leads to an accumulation of phagosomes and consequently of LC3-II on those membranes.<sup>[37-39]</sup>

The distribution and accumulation of LC3 can be monitored by fluorescence microscopy by expressing an enhanced green fluorescent protein (eGFP)-LC3 fusion protein in the cell line of interest. While LC3-I is detectable as an equal distribution of the fluorescence signal throughout the cells, LC3-II on phagosome membranes appears as dense fluorescent puncta, upon accumulation after chloroquine treatment. An autophagy inhibitor acting upstream of the

fusion process can reverse this accumulation of LC3-II in a dose-dependent manner, allowing a quantification of autophagy inhibitors in this assay setup (Figure 7).<sup>[38,40,41]</sup>

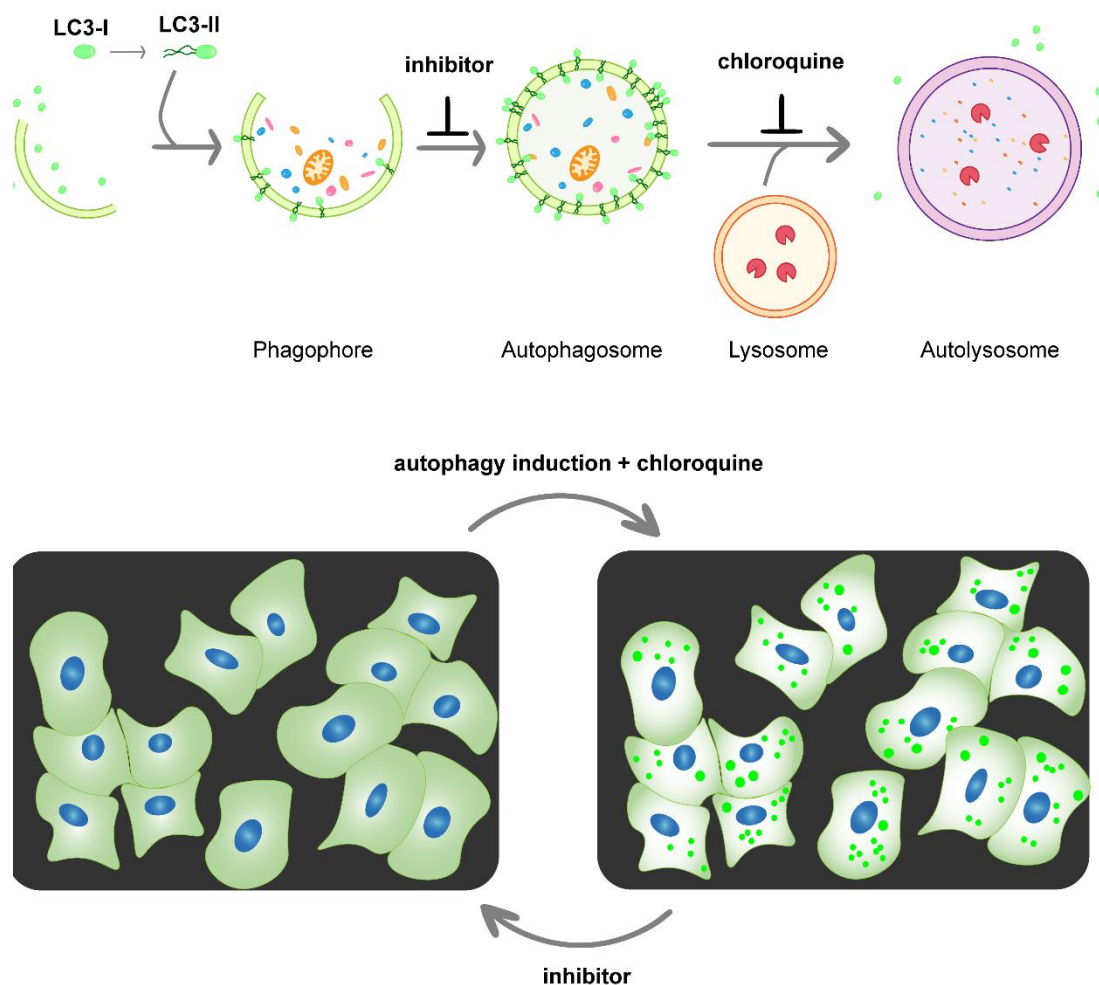


Figure 7: (a) Schematic representation of the phenotypic autophagy assay; (b) schematic representation of microscopic figures obtained in the autophagy assay.

### 1.2.2.2 Morphological Profiling: The Cell Painting Assay

Even though phenotypic screening setups, like the described autophagy assay, bear a lot of advantages, they are still limited to a certain pathway and therefore have a high potential to fail in elucidating a relevant biological target of a small molecule. An approach to overcome this limitation could be a target-agnostic and unbiased morphological assay. The cell painting assay (Figure 8), invented by the Carpenter group, fits these requirements, and furthermore is characterised by an ease of use and relatively low cost, allowing the screening of large compound libraries in automated HTS systems.<sup>[42,43]</sup>

## General Introduction

In the cell painting assay, cells of a suitable cell line (the human osteosarcoma (U-2OS) cell line is commonly used) are treated with compounds for a defined time range (24-48 h). Upon incubation, the cells are fixed and stained with six different fluorescent dyes that selectively stain the different compartments of a cell (nuclei, endoplasmic reticulum, nucleoli, RNA, actin, Golgi apparatus and mitochondria). Subsequent recording of images by fluorescence microscopy at 5 different wavelengths is followed by extraction of several hundred morphological features from obtained figures by the open-source software CellProfiler. These features are normalised to a DMSO control experiment and combined to form a barcode-like morphological profile ('fingerprint') that describes the greater picture of morphological changes induced by compound treatment. Besides that, the percentage of significantly changed parameters, compared to the DMSO control experiment, was defined as 'induction' and can be used as a measure for morphological activity.<sup>[43]</sup>

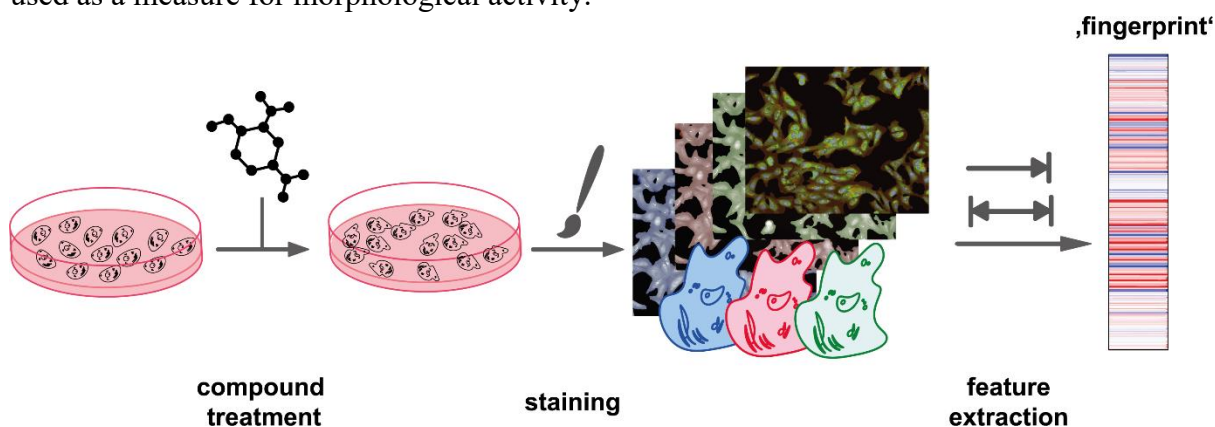


Figure 8: Schematic representation of the CPA workflow.

Even though, the phenotypic fingerprints consisting out of several hundred of cellular features do not allow a direct characterization of a specific mode of action or target, the comparison of obtained morphological profiles with reference and other research compounds can deliver valuable information. Analysis of cell painting assay results have been shown as successful source for mode of action (MoA) hypotheses, structure phenotype relationships as well as off-target identification.<sup>[44]</sup>

Within the investigation of compound collections with unprecedented bioactivities, the cell painting assay has been a valuable tool. Evaluation of the pyrano-furo-pyridones, a PNP compound class derived from pyridine and dihydropyran, in the cell painting assay on a first glance revealed the possibility to elucidate structure phenotype relationships within defined compound classes. Furthermore, comparison with reference compounds with annotated activities revealed a high similarity of the pyranofuro-pyridones profile to the morphological

profile of aumitin. Aumitin is a known inhibitor of mitochondrial respiration, targeting the mitochondrial complex I. Further biological evaluation of the PNPs, confirmed its inhibitory effect of mitochondrial complex I. This finding highlights the impact of the cell painting assay to the investigation of target hypotheses for compounds with unprecedented bioactivities.<sup>[45]</sup>

Another successful example, where the cell painting gave a crucial hint towards a compounds' MoA is the evaluation of the NP-derived autoquin, that was previously shown to inhibit autophagy. Common follow up experiments to identify the target of autoquin based on protein enrichment from cell lysates led to inconclusive results. However, comparing cell painting assay profiles added the essential information for the identification of the non-protein related MoA. Autoquin accumulates in the lysosomes, inhibits the fusion with phagosomes and furthermore sequesters  $\text{Fe}^{2+}$ .<sup>[46]</sup> As demonstrated by these examples, the cell painting assay is a powerful hypothesis-generating tool for the identification of MoAs of small molecules with unprecedented bioactivities.

## 2. Objectives

The identification of bioactive small molecules that are endowed with novel bioactivities is of great interest for the elucidation of cellular processes and to gain an improved understanding of signaling pathways. The general aim of this thesis was to design, synthesize and biologically investigate novel molecular entities. To design compound collections that have a high potential to be enriched in bioactivity and simultaneously have a high potential for the investigation of unknown chemical and biological space, the PNP approach can be implemented. This approach is based on the unprecedented combination of natural product fragments in arrangements that are not observed in nature. The success of this approach has been shown in previous examples. [24-26]

To biologically investigate the resulting PNPs that may have unknown bioactivities, the cell painting assay (CPA) can be facilitated. The CPA is a morphological profiling method that covers a broad range of bioactivities and therefore is a valuable tool to investigate compounds with unexpected bioactivities. The CPA was previously used for mode of action and target identification hypotheses and structure-phenotype-relationship studies. In the context of this work novel, potential applications of this assay for PNP projects should be investigated.

The first part of this thesis focuses on the biological investigation of a previously described azaquinole PNP compound class derived from cinchona alkaloids and indoles. Besides the validation of the autophagy activity of the compounds class and the elucidation of a structure activity relationship, the mode of action should also be further investigated. Since the azaquinole induced morphological changes in the CPA assay, the identification of potential autophagy related targets may be facilitated by the comparison of their morphological profiles with morphological profiles of reference molecules with annotated bioactivities.

To gain further insights into the applicability of the CPA for PNP projects, the second part of this thesis investigates the influence of NP fragments on the morphological activity of PNPs. The aim of this study was to show whether the bioactivity of a PNP is dominated by one of the fragments or a result of their combination. Furthermore, the comparison should give insights into the effects of different connectivities of fragments.

Based on the results of the second part, a novel PNP compound class should be designed. Generally, it was found that fragments either dominate the bioactivity of PNPs or are non-dominating. The combination of non-dominating fragments is preferred, since it can lead to unique bioactivities. The design of a novel compound class by recombination of fragments

used in previous PNPs in the same connectivity pattern was supposed to give further insights into the combination of NP fragments.

### **3. Part I: Evaluation of a Pseudo-Natural Product Autophagy Inhibitor**

#### **3.1. Introduction**

##### **3.1.1 Autophagy and its Regulation**

As mentioned previously, the dysregulation of autophagy as an essential, highly conserved cellular process is involved in several disorders including cancer. Therefore, the identification of suitable probe molecules for understanding and investigating autophagy-related proteins at different stages of this pathway is in high demand.

Autophagy is an adaptive process, that is initiated as response to cellular stress, including starvation, growth factor signalling, infections and hypoxia. Autophagy induction leads to the recruitment of autophagy related genes (ATGs) to the phagophore assembly site (PAS) located at ER membranes and nucleation of an isolation membrane termed phagophore. Upon autophagy signalling, the phagophore membrane matures to a double membraned vesicle, engulfing cytosolic cargos. Fusion with lysosomes then leads to formation of autolysosomes and release to the lysosomal hydrolytic conditions and consequent degradation of the autophagic content.<sup>[47]</sup> More than 15 different, highly conserved ATG proteins, first identified by Yoshinori Ohsumi, are essential for autophagosome formation and delivery to the lysosome.<sup>[48,49]</sup>

The most characterised pathway for autophagy induction occurs via inhibition of the mammalian target of rapamycin (mTOR) through amino acid starvation or through the ATP/AMP ratio sensed by the regulatory kinase 5' AMP-activated kinase (AMPK) (Figure 9). Under nutrient rich conditions, active mTOR is bound to the downstream regulators ATG13 and ULK1. Inhibition of mTOR leads to a release and subsequent autophosphorylation of the unc-51-like-kinase 1 (ULK1) complex. Consequently, ULK1 phosphorylates components of the class III phosphatidylinositol 3-kinase (PI3KC3) complex I, including the class III PI3K vacuolar protein sorting 34 (VPS34), Beclin-1, ATG14 and the activating molecule in Beclin-1 regulated autophagy (AMRA1). Subsequent phosphorylation of membrane-bound phosphatidylinositol to phosphatidylinositol-3-phosphate (PI3P) by VPS34 enables the binding of WD repeat domain phosphoinositide-interacting protein (WIPI), a scaffold protein recruiting the ATG12-ATG5-ATG16L1 complex, to the initiation membrane. A key element in further phagophore expansion is LC3, which was already mentioned previously as important autophagy marker protein and belongs to the ATG8 family. Pro-LC3 is cleaved by the cysteine



protease ATG4 to form cytosolic LC3-I, which allows the lipidation in a ubiquitin like system. The E1-like enzyme ATG7 activates LC3-I and the E2-like ATG3 can conjugate LC3-I to membrane bound PE to form LC3-II. ATG3 requires the stimulation by the E3 -like activity of ATG5-ATG12, recruited to the phagophore membrane by WIPI scaffold proteins. Conjugation of LC3-II to the initiation membrane promotes the phagophore expansion and potentially the sealing to form autophagosomes. Upon autophagosome maturation, LC3-II is released through PE cleavage by ATG4.<sup>[37,47]</sup> This leads to recruitment of microtubule-based kinesin motors, the molecular machinery that is responsible for the migration of the phagosomes to the lysosome-rich regions of the cell using the coordinated microtubule network. Once autophagosome and lysosomes are in close proximity, SNARE-mediated association leads to fusion of the membranes and subsequent release of autophagic cargo to the degradative lysosome.<sup>[50]</sup>

Due to its cellular relevance and involvement in the progression of many metabolic diseases, autophagy has been a target of numerous probes as well as drug identification studies. Thereby both, inhibition and activation of autophagy have moved into focus.

The first ever US Food and Drug administration (FDA) approved autophagy inhibitor was chloroquine, that blocks phagosome lysosome fusion by disrupting lysosomal acidification. chloroquine and its analogue hydroxychloroquine are mainly used in combinatorial cancer therapies, as it was observed that autophagy activation is a side effect of diminish therapy-induced stress in many cancer types. Therefore, inhibition of autophagy is a beneficial strategy to enhance the efficacy of therapies and to overcome resistances.<sup>[51]</sup> Besides the fusion process, earlier stages also have become clinical or preclinical targets of inhibition. The most investigated targets at the early stage of autophagy initiation are ULK1 and VPS34 kinases. The ATP-competitive ULK1 inhibitor SBI-0206965 induces an apoptotic response in lung cancer under starvation conditions<sup>[52]</sup> and VPS34 inhibitors, including VPS34-IN and SAR405, improve the sensitivity of therapy in different cancer types.<sup>[53,54]</sup> However, even if the investigation of these inhibitors in early pre-clinical studies may have looked promising, multiple clinical trials indicated a disappointing efficacy of autophagy inhibitors in patients, that may be due to the not fully understood, complex networks in which autophagy is embedded. While inhibition of autophagy can induce cell death by apoptosis, it may at the same time promote the release of survival factors to the tumour environment, contraindicating a positive therapy outcome.<sup>[37]</sup> This circumstance is reflected in reports, highlighting the increase of efficacy in immunogenic chemotherapies by autophagy activation.<sup>[55]</sup>

Whereas targeting of autophagy in cancer therapies is often referred as double-edged sword, in the treatment of neurodegenerative diseases, autophagy activation associated with the clearance of aggregates of misfolded and unfolded proteins is beneficial to prevent disorders. The most prominent autophagy activation small molecule is rapamycin, an inhibitor of mTOR complex formation.<sup>[37]</sup> However, the selective targeting and optimal dosage to prevent affecting of other cellular processes is still the major challenge in the autophagy-dependent treatment, not only in neurodegenerative diseases.

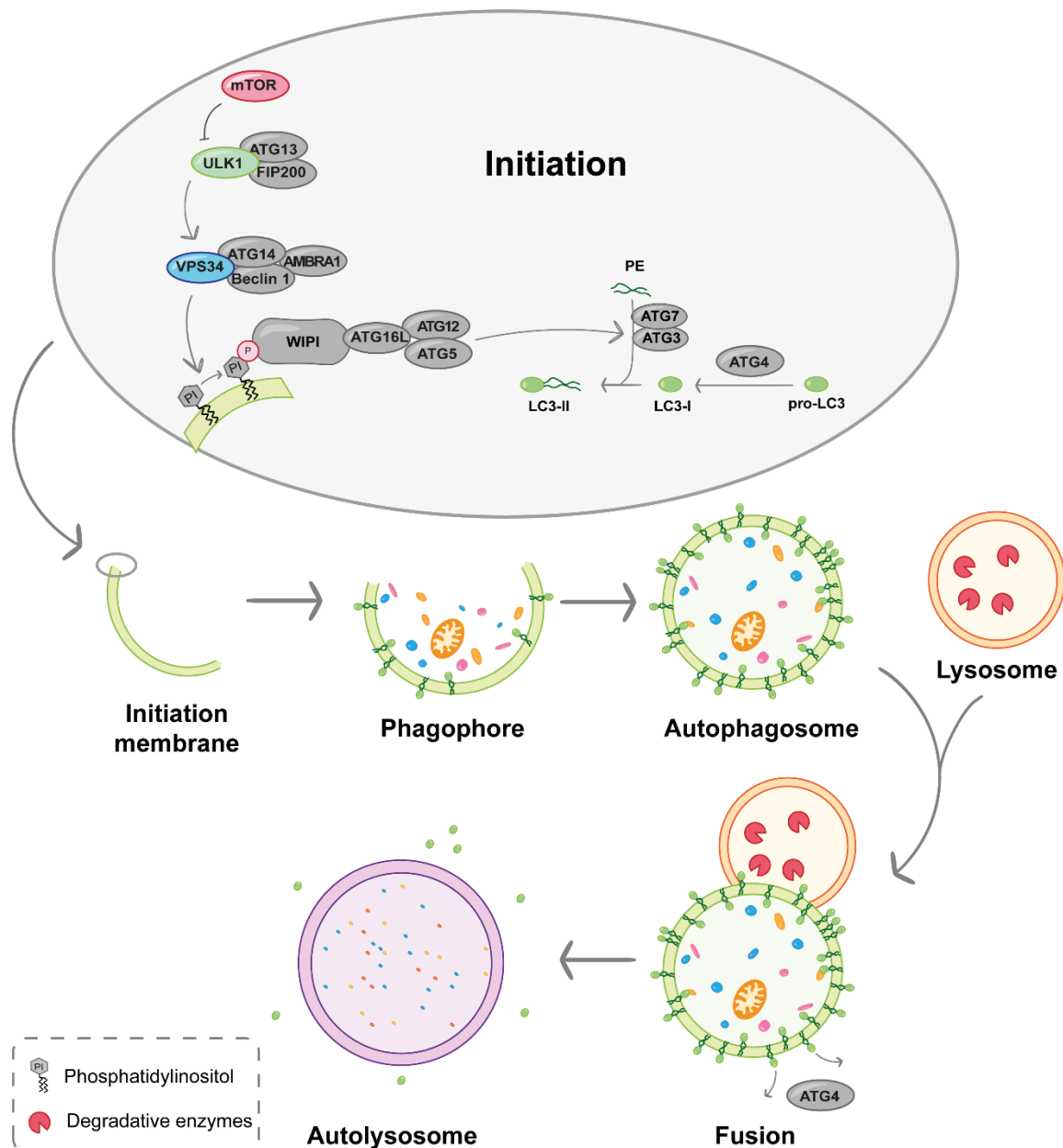


Figure 9: General overview of the autophagy process and the mechanism of autophagy initiation.

### 3.1.2. PNPs Derived from Cinchona Alkaloids and Indoles

In a study preceding this thesis, a novel PNP compound class derived from the cinchona alkaloids quinine and quinidine, and indole was designed and synthesised. Phenotypic screening revealed the 7-azaindole-containing members of the quinine-derived compound class as a novel autophagy inhibitor chemotype. This work aimed to further investigate this class of compounds and their biological activity.

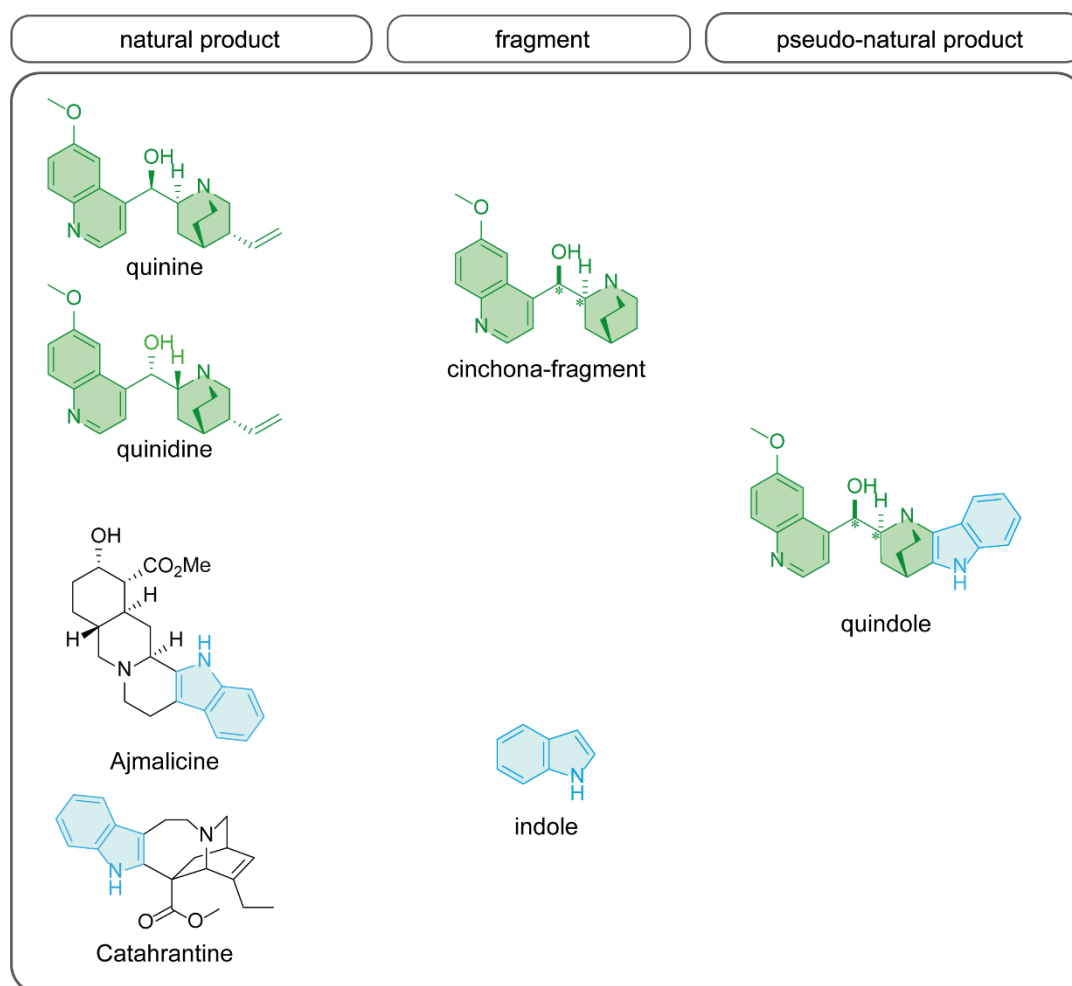
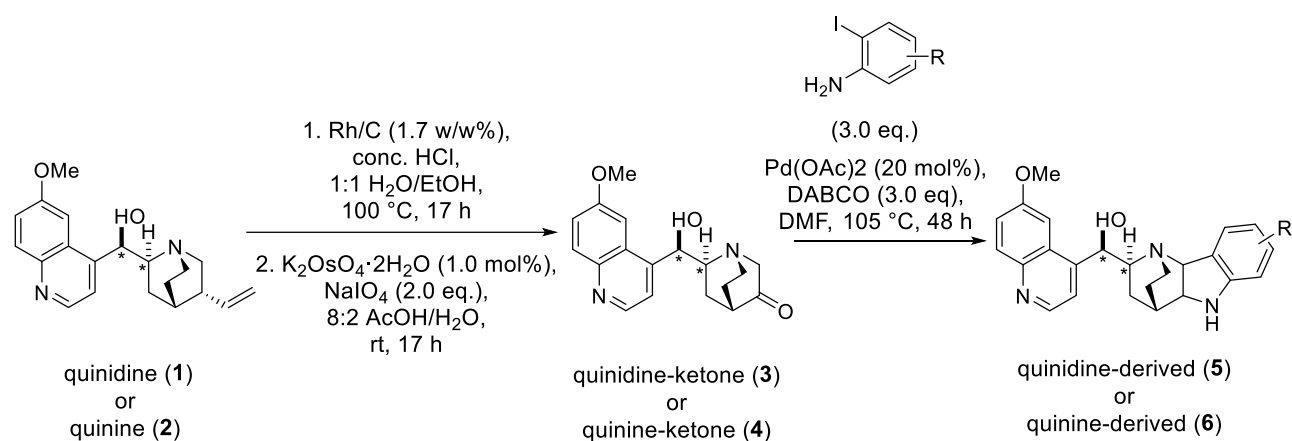


Figure 10: Design principle for of cinchona derived indoles ('quindoles'); shown are the parental NPs, derived fragments, and the structure of the novel PNP class.

The cinchona alkaloids, namely quinine, quinidine, cinchonine and cinchonidine are a class of natural product alkaloids with a long history in medicinal as well as organic chemistry.<sup>[56]</sup> Quinine the first isolated cinchona alkaloid (1820), was identified as the active ingredient in the bark of *Cinchona* trees.<sup>[57]</sup> The bark was originally used in traditional South American medicine to treat fever, shivering and pain but later, after the discovery of its antimalarial activity, it was also introduced to the European market. Today, the isolated quinine is still in medicinal use for antimalaria treatment, whereas its diastereomer quinidine is used in treatment

of cardiac arrhythmias. Besides the medicinal use, the isolated cinchona alkaloids are used in food and beverages industry as bitter flavouring agent.<sup>[56,58]</sup> Furthermore, the molecules or close derivatives have found an important application in organic synthesis as chiral catalysts.<sup>[59]</sup> Following its wide applications, the chemical modification of the alkaloids, especially of quinine and quinidine gained great interest.<sup>[60]</sup> Many of the synthesised NP derivatives have similar or different bioactivities.<sup>[18,61]</sup>

The indole fragment has been suggested to be one of the most privileged scaffolds in the discovery of bioactive molecules.<sup>[62]</sup> The heterocyclic structure is widely distributed among NPs that encompass diverse bioactivities, such as antiviral, antimicrobial, anticancer, anti-inflammatory, antihypertensive, antioxidant, anti-diabetic, and anti-depressive activity. The alkaloid catharanthine<sup>[63]</sup> for example is used in cancer treatments, and ajmalicine<sup>[64]</sup> as an antihypertensive drug.



Scheme 1: Reaction sequence to synthesise quinine- and quinidine derived indoles.

For the fusion of the fragment-sized NPs quinine (1) and quinidine (2) with indoles, a Pd-catalysed annulation reaction of 2-iodoanilins<sup>[65]</sup> with NP-derived ketones was established. The cinchona ketones (3 and 4) were derived from NP material in a two-step procedure (Scheme 1). Isomerization of the terminal alkene was followed by an oxidative cleavage under modified Lemieux-Johnson conditions to give 3 and 4. This reaction sequence turned out to be very robust and yielded a PNP library of 61 cinchona alkaloid-derived indoles.

## 3.2. Results and Discussion

### 3.2.1. Structure Activity Relationship

The PNP library was screened in a range of phenotypic assays at the compound management and screening facility (COMAS) centre in Dortmund since the bioactivities of these chemotypes are unknown. Indeed, some quinine-derived library members, especially 7-azaindole-containing ones, were identified as active hits in a phenotypic autophagy assay. The assay was performed, like previously described in section 1.2.1.1, using starvation conditions or rapamycin to induce autophagy. In a preliminary screen, all compounds were tested at 10  $\mu$ M. For compounds that exhibited an autophagy inhibition of at least 50%, IC<sub>50</sub> values were measured (Table 1). Interestingly, 7-azaindole compounds derived from quinidine showed no autophagy inhibition at all (Table 1, entries 22 and 23). Also, the non-modified cinchona alkaloids (quinine, quinidine, cinchonine and cinchonidine) as well as indoles and azaindoles were not active in the autophagy assay, indicating that by fusion of these fragments a novel bioactivity was created.

Considering the results of the starvation-induced autophagy (SIA) screen, a preliminary SAR was evaluated. Indoles derived from quinine, that were substituted in 5- or 6-position showed a rather weak inhibitory activity (Table 1, entries 1-7), whereas substitution with the polar methoxy group in 7-position led to a significantly better activity (Table 1, entry 8). However, the most potent autophagy inhibitors were the 7-azaindoles (azaquindoles from here on), also containing a polar functionality in 7-position which is important for the PNPs activity. Among the 7-azaindoles (Table 1, entries 9-21) compounds bearing a further polar (NO<sub>2</sub>) or non-polar (Me, CF<sub>3</sub>, Cl, Br, I) substituent in 4- or 5-position were all equivalently active with sub micromolar IC<sub>50</sub> values. Only the smaller fluorine (Table 1, entry 15) and the bigger aryl (Table 1, entry 12) substituent led to a significant decrease or even loss of activity, suggesting a decisive influence of the functional groups' size, whereas the electronic effect may not be important. Substituents in indole 6-position generally were less active and did not further improve the activity compared to the unsubstituted 7-azaindole (Table 1, entries 20 and 21), while a combination of 5-bromo and 6-methyl substitution (azaquindole-1, **6s**) yielded the strongest inhibitory activity (0.04  $\mu$ M; Table 1, entry 19). It is worth mentioning that all azaindoles sharing a sub micromolar inhibition of starvation-induced autophagy were also inhibiting rapamycin-induced autophagy (RIA) in a similar fashion. Based on this finding, it was concluded, that the azaquindoles either inhibit the autophagy pathway downstream or independent of mTOR complex formation (see also Figure 9).

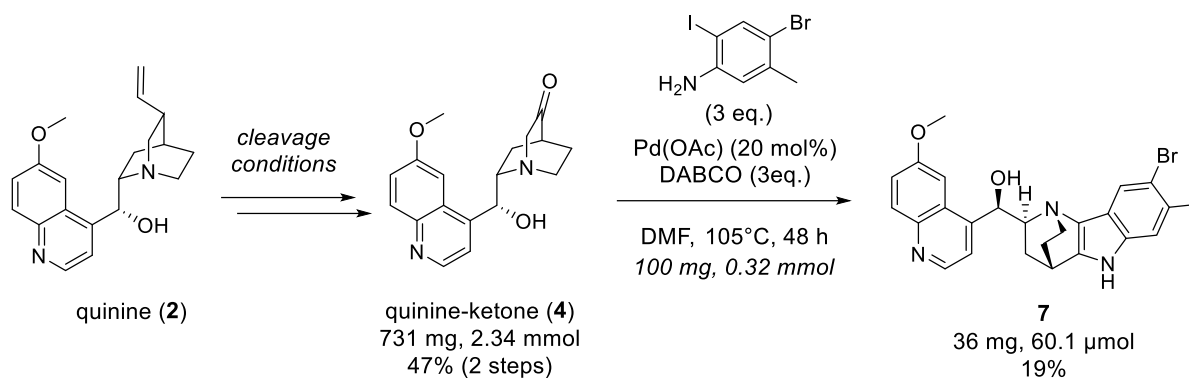
Table 1: Preliminary SAR of quindoles and azaquindoles in starvation- and rapamycin-induced autophagy

Entry	R-group and indole position	Nr	Starvation-induced autophagy IC <sub>50</sub> [ $\mu$ M]*	Rapamycin-induced autophagy IC <sub>50</sub> [ $\mu$ M]*
1	5-CF <sub>3</sub>	6a	7.86 $\pm$ 0.8	n/a
2	5-NO <sub>2</sub>	6b	7.33 $\pm$ 1.5	n/a
3	5-OCF <sub>3</sub>	6c	4.68 $\pm$ 1.4	n/a
4	5-Cl	6d	5.54 $\pm$ 2.5	n/a
5	5-Br	6e	6.78 $\pm$ 1.1	n/a
6	6-CF <sub>3</sub>	6f	5.82 $\pm$ 3.0	n/a
7	6-Cl	6g	8.12 $\pm$ 1.5	n/a
8	7-OMe	6h	2.46 $\pm$ 0.6	2.37 $\pm$ 0.7
9	7-azaindole	6i	4.33 $\pm$ 1.7	4.95 $\pm$ 0.7
10	4-Cl-7-azaindole	6j	0.52 $\pm$ 0.20	0.65 $\pm$ 0.35
11	5-Me-7-azaindole	6k	0.31 $\pm$ 0.09	0.86 $\pm$ 0.26
12	5-Ar-7-azaindole	6l	9.00 $\pm$ 1.1	n/a
13	5-CF <sub>3</sub> -7-azaindole	6m	0.12 $\pm$ 0.03	0.77 $\pm$ 0.29
14	5-NO <sub>2</sub> -7-azaindole	6n	0.67 $\pm$ 0.13	1.26 $\pm$ 0.20
15	5-F-7-azaindole	6o	n/a	n/a
16	5-Cl-7-azaindole	6p	0.11 $\pm$ 0.04	0.85 $\pm$ 0.14
17	5-Br-7-azaindole	6q	0.08 $\pm$ 0.03	0.81 $\pm$ 0.35
18	5-I-7-azaindole	6r	0.08 $\pm$ 0.02	1.24 $\pm$ 0.20
19	<b>5-Br-6-Me-7-azaindole</b>	<b>6s</b>	<b>0.04 <math>\pm</math> 0.02</b>	<b>0.10 <math>\pm</math> 0.02</b>
20	6-Me-7-azaindole	6t	3.15 $\pm$ 0.5	5.11 $\pm$ 1.4
21	6-Cl-7-azaindole	6u	3.09 $\pm$ 0.9	6.21 $\pm$ 2.2
22	7-azaindole <sup>#</sup>	6v	n/a	nd
23	5-Me-7-azaindole <sup>#</sup>	6w	n/a	nd

\*IC<sub>50</sub>-values (as mean  $\pm$  SD) were determined in biological triplicates at the COMAS- Center Dortmund (N = 3, n = 3). <sup>#</sup>quinidine derived azaindoles. Ar = 4-Cl-C<sub>6</sub>H<sub>4</sub>.

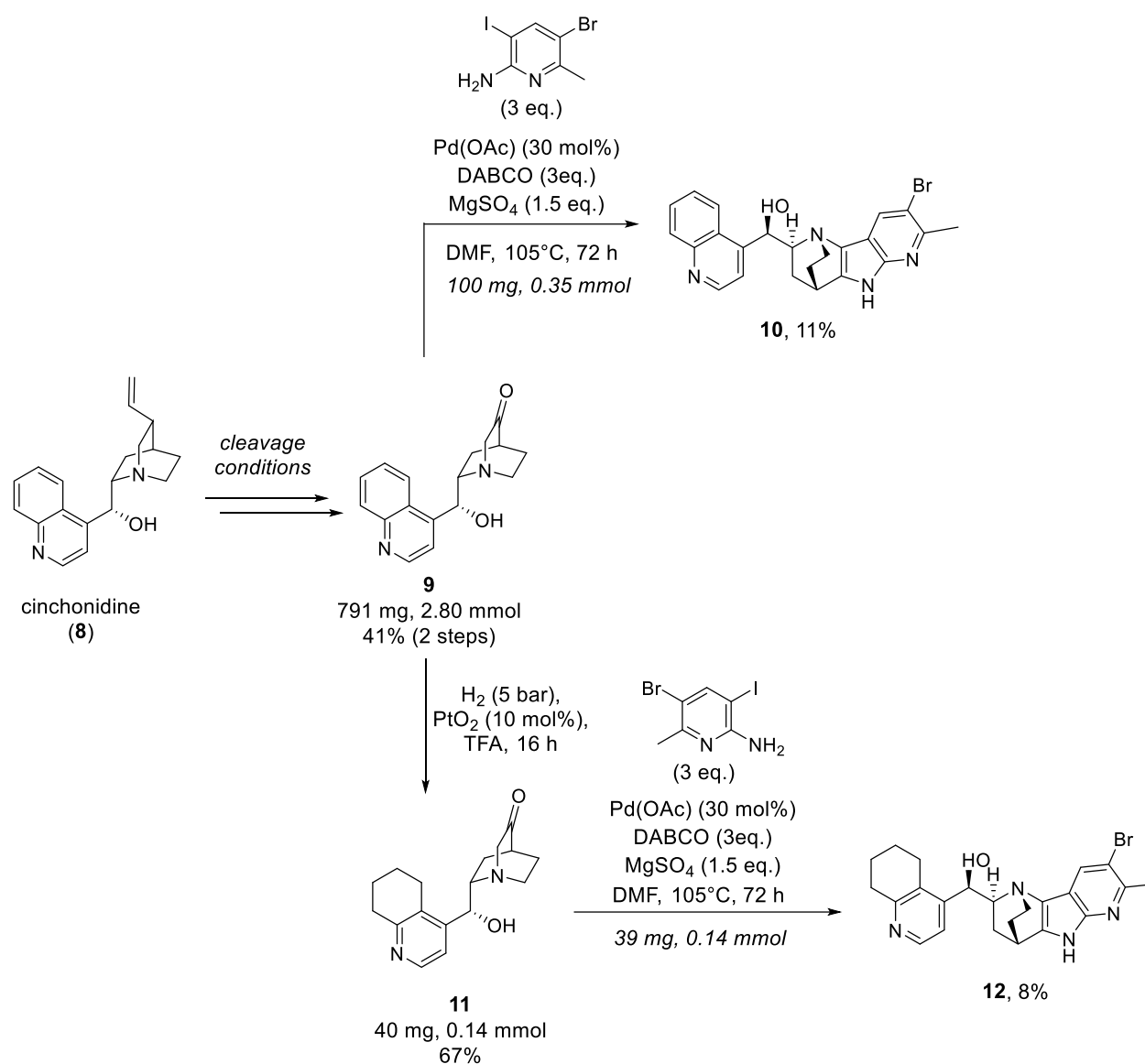
To further evaluate and complete the SAR to identify the minimum pharmacophore, further derivatives were prepared and tested in the course of this work. To gain insight into the molecular features that are crucial for the biological activity, the azaquindole-1's functional groups were truncated or modified.

The first targeted compound (**7**) was the indole derivative of the azaindole-containing lead compound. This compound was derived by the previously mentioned, already established synthetic route, via Rh mediated isomerisation of the double bond, oxidative cleavage and Pd catalysed annulation, changing the 2-iodoaniline to 2-iodo-4-bromo-5-methylaniline (Scheme 2).



Scheme 2: Reaction scheme for the synthesis of the quindole derivative of azaquindole-1.

Further derivatives were synthesised, starting from cinchonidine (**8**), another member of the cinchona alkaloid NP class, that shares the same stereogenic information but not the methoxy group with quinine (Scheme 3). Again, the ketone was derived, utilising the described conditions to give the methoxy-lacking compound (**9**) in 47% yield (2 steps). The cinchonidine ketone then was harnessed to prepare the methoxy lacking derivative of azaquindole-1 (**10**) in the Pd-catalysed annulation to investigate the importance of the quinoline substituent in autophagy activity. Further studies on the quinoline part were accomplished, by starting with the same ketone (**9**) but exposing it to reductive conditions prior to the annulation step, to obtain the partially reduced quinoline moiety (**12**).

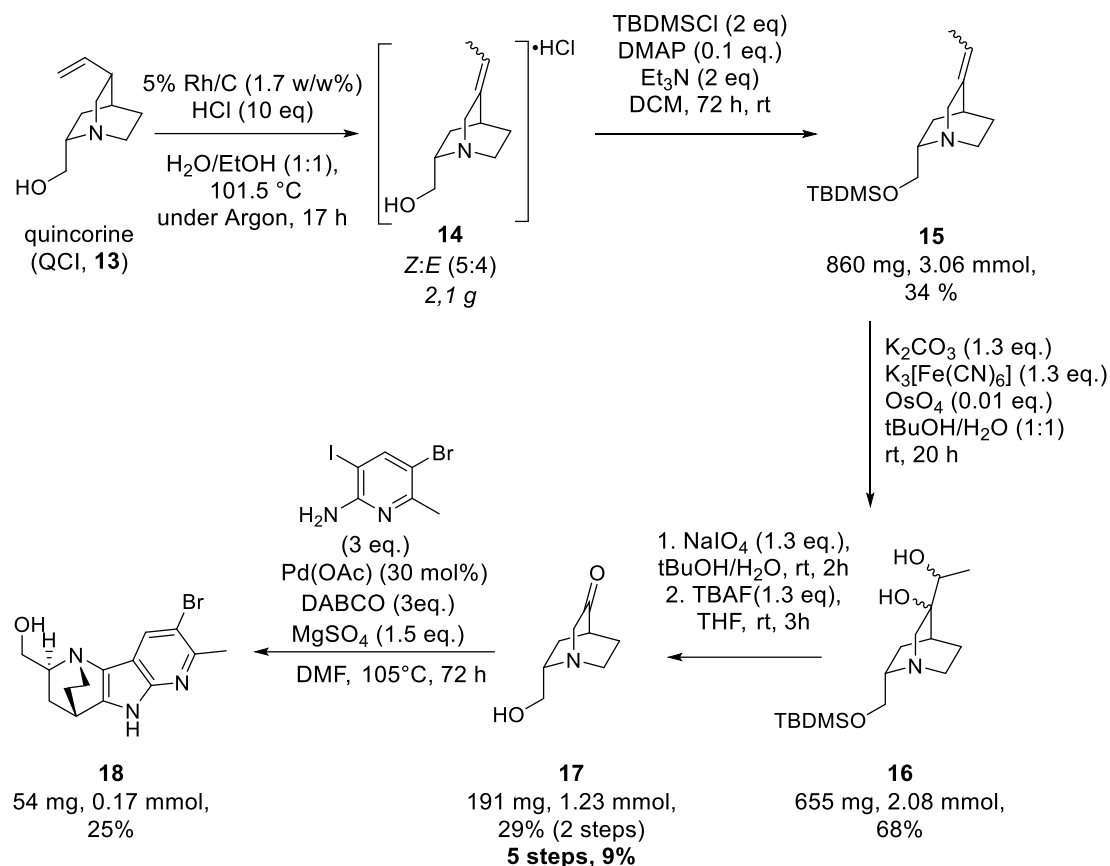


Scheme 3: Reaction scheme for the synthesis of the ‘no methoxy’ derivative and the partially reduced derivative of azaquindole-1.

Since the question arose whether the quinoline moiety was at all important for bioactivity, compound **18** was targeted in a next experiment. Starting from quincorine (QCI, **13**), the terminal double bond was isomerised to gain *iso*-QCI (**14**). Prior to the cleavage procedure, a protection of the primary alcohol as silylether (here: *tert*-butyldimethylsilyl = TBDMS) was mandatory. Following a procedure that was first established by Hoffmann *et al.*<sup>[66]</sup> a two-step cleaving procedure was applied. First, the silylated compound **15** was dihydroxylated under phase separated conditions, using osmium tetroxide as oxidant in the organic layer, while the reoxidation of the catalyst occurs in the aqueous phase by cooxidant potassium ferricyanide.<sup>[66]</sup> Cleavage of the diol with sodium periodate followed by silylether cleavage gave the ketone desired for Pd-catalysed annulation in 9% yield over 5 steps (**17**, Scheme 4). The most limiting

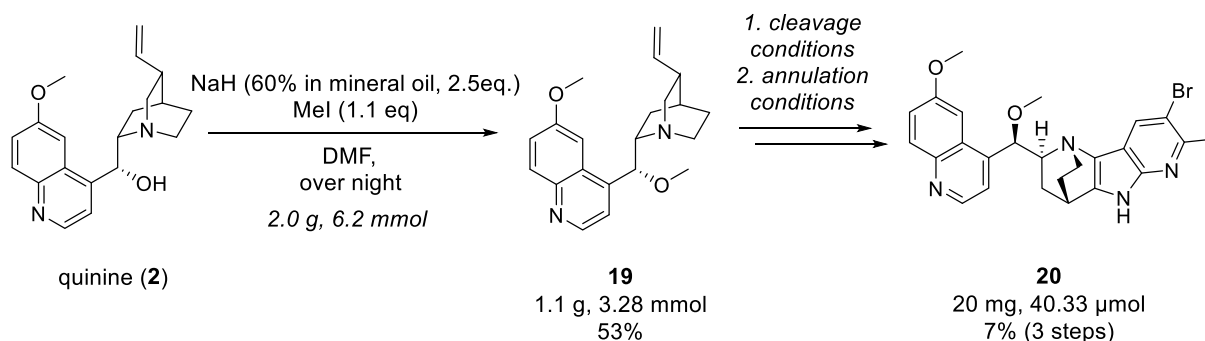


step thereby was the silyl protection (34% yield), maybe due to the high hydrophilicity of the *iso*-QCI hydrochloric acid salt. Attempts to liberate the free amine to improve this step failed.



Scheme 4: Reaction scheme for the synthesis of the quinoline lacking derivative of azaquindole-1.

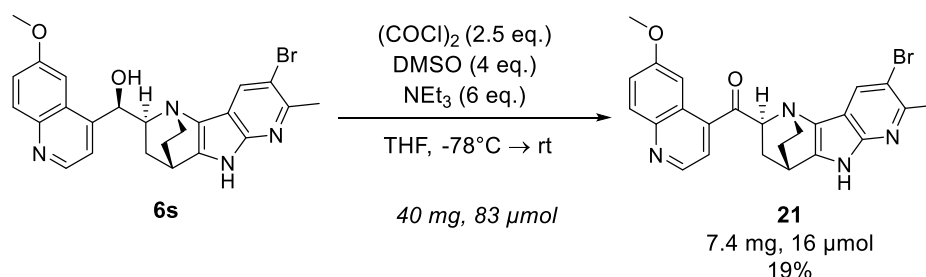
Next, two compounds were targeted, that may give further insights into the role of the azaquindole's alcohol functionality. The methylated compound (**20**) was obtained by alkylation prior to the general azaquindole synthesis procedure. The introduction of the methyl group before indole coupling allowed selective hydroxyl protection over the indole nitrogen (Scheme 5).



Scheme 5: Reaction scheme for the *O*-methylated azaquindole-1 derivative.

## Part I

Oxidation of the azaquinoline-1 hydroxyl group provided a compound not only useful to investigate the effect of the alcohol on the bioactivity but also the impact of the stereocenter. Exposure of azaquinoline-1 to oxidative Swern conditions<sup>[67]</sup> gave the targeted compound **21** in 19% yield (Scheme 6).



Scheme 6: Reaction scheme for the synthesis of the oxidised azaquinoline-1 derivative.

Following their successful synthesis, the modified, truncated, and protected azaquinoline-1 derivatives were subjected to the phenotypic autophagy screening assay. Figure 11 summarises the determined  $\text{IC}_{50}$  values in starvation-induced autophagy (SIA) and rapamycin-induced autophagy (RIA). First, the 7-azaquinoline nitrogen was shown to improve the potency of azaquinoline-1, as removal of the heteroatom (**7**) resulted in a >50-fold increase of the SIA  $\text{IC}_{50}$  value. Additionally, a complete loss of RIA inhibition ( $\text{IC}_{50} > 50 \mu\text{M}$ ) was reported. The quinoline methoxy group was beneficial. After its removal, compound **10** still was capable of inhibiting SIA ( $\text{IC}_{50} 0.08 \pm 0.09 \mu\text{M}$ ) and RIA ( $2.29 \pm 0.4 \mu\text{M}$ ). A reduction and therefore change of 3D shape of the quinoline moiety led to a decrease, but not complete loss in activity compared to azaquinoline-1 or compound **10**. This leads to the suggestion, that the flat shaped quinoline moiety, improves the inhibitory activity. However, the whole quinoline moiety did not seem to be critical for the autophagy inhibitory activity, neither in SIA nor in RIA, but could improve the potency significantly (**18**). Loss of the hydrogen bond donating (HBD) effect, as well as the increased size of the methoxy group does not affect the biological activity, as concluded from comparing the similar  $\text{IC}_{50}$  value measured for azaquinoline-1 and **20**. On the other hand, the oxidation of the hydroxy group in compound **21** not only leads to a structural derivatisation of the hydroxy group, but also the removal of a stereocenter and therefore a change in the 3D shape of this azaquinoline. A complete loss of inhibitory activity, of both SIA and RIA, highlights the importance of the stereochemistry for the activity and most likely the target interaction, which was already reflected by the inactivity of all quinidine-derived compounds.

Overall, these SAR investigations led to the conclusion, that all parts contributing to the azaquindole-1 structure, at least had a positive effect on the potency. Nevertheless, an inhibitory activity was already reached by a truncated version of the molecule only constituted from the combination of quinuclidine and 7-azaindole. During this study, no analogue was identified having an improved activity relative to azaquindole-1. Therefore, azaquindole-1 was chosen for further biological investigations according to the autophagy activity and the related target.

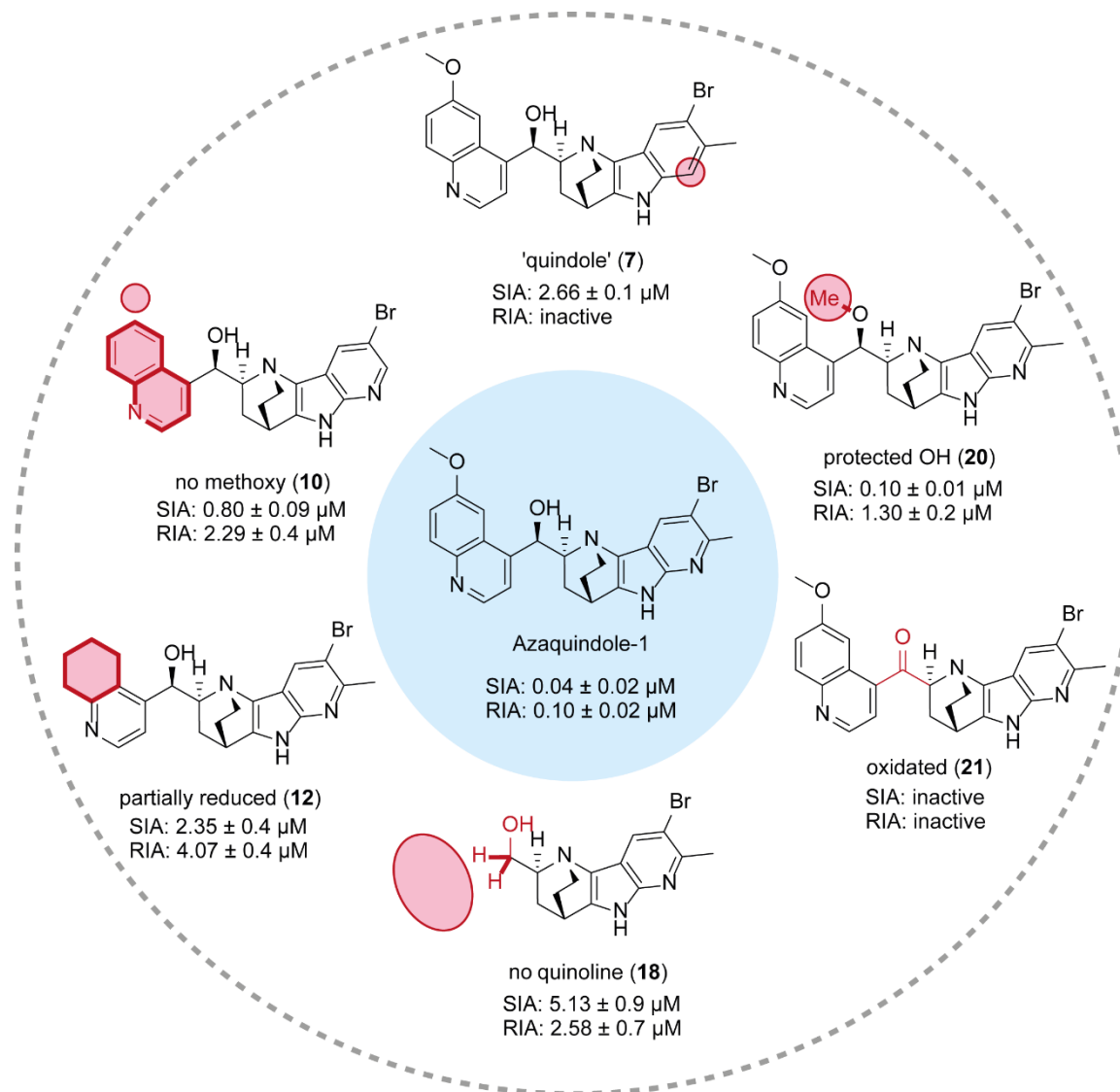


Figure 11: Overview of azaquindole-1 derivatives and their  $IC_{50}$  values in starvation-induced (SIA) and rapamycin-induced (RIA) autophagy.  $IC_{50}$ -values (as mean  $\pm$  SD) were determined in biological triplicates at the COMAS- Center Dortmund (N = 3, n = 3).

### 3.2.2. Validation of Autophagy Inhibition

Figure 12a shows the influence of azaquindole-1 on the LC3 puncta formation in the breast cancer Michigan Cancer Foundation-7 (MCF7) cell line, expressing the LC3 protein tagged with eGFP. Under basal, non-stimulated conditions (cultivation in minimum essential medium = MEM), the fluorescence signal is equally distributed throughout the cells. As expected, activation of autophagy by nutrient starvation, induced through cultivation in Earle's Balanced Salt Solution (EBSS) and simultaneous inhibition of autophagosome lysosome fusion with chloroquine (CQ; 50  $\mu$ M) leads to accumulation of LC3-rich autophagosomes that are visible as green puncta. The same observation was made when autophagy was activated by the mTOR inhibitor rapamycin. Treatment with azaquindole-1 reversed this effect, noticeable in the right row figures. Concentration-dependent experiments and automated counting of puncta per cell applying the MetaMorph software allowed the determination of  $IC_{50}$  values (Figure 12b). The fluorescence-based assay offers many advantages, such as a fast execution time, low cost, and the ease of use, enabling the high throughput setup for preliminary hit identification. However, the use of GFP-conjugates also bears its limitations. GFP-LC3 chimera may behave different than the native LC3 protein, as GFP almost doubles the molecular weight of LC3. Furthermore, GFP is not native in most test systems and might be targeted for degradation, possibly interacting with the desired readout.<sup>[68]</sup> Also, it was shown that GFP-LC3 may associate with aggregates leading to a misinterpretation of results.<sup>[69]</sup> Therefore, the HTS results should be always confirmed in an orthogonal, non-fluorescence-related readout.

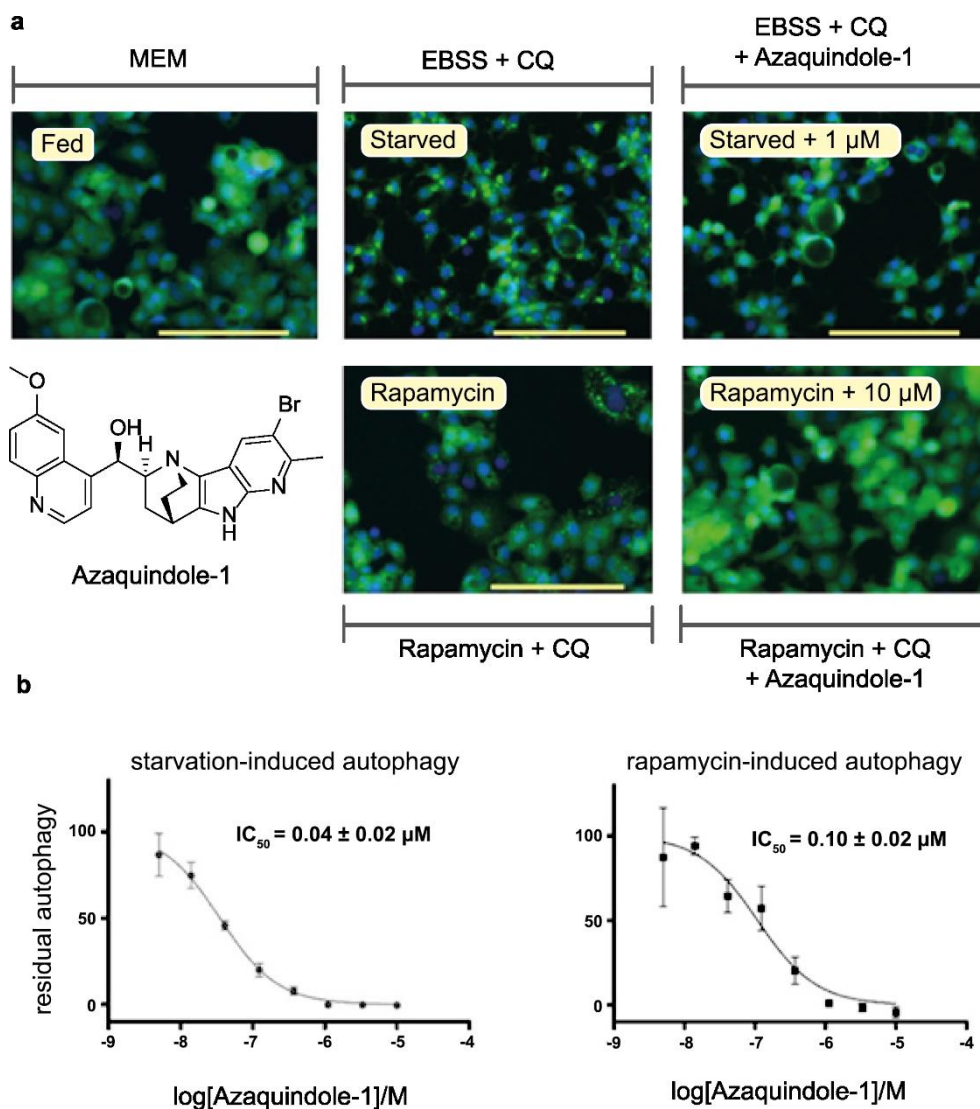


Figure 12: (a) Representative images of the starvation- and rapamycin-induced autophagy screen; green: eGFP-LC3, blue: Hoechst stain (nuclei); Scale bars: 150  $\mu\text{M}$ ; (b) dose-dependent inhibition of starvation- and rapamycin-induced autophagy by azaquindole-1; values are given as mean  $\pm$  SD ( $n \geq 3$ ,  $N = 3$ ).

The LC3 protein abundance was further validated via western blot readout (experiment was performed by a collaboration partner: Dale Corkery). Wild type MCF7 cells were treated with azaquindole-1 (5  $\mu\text{M}$ ) and/or CQ under starvation conditions (EBSS). Control samples (column 1-4) were treated with DMSO and protein levels of LC3-I and LC3-II were investigated at different timepoints (1-4h). The first column in the western blot image shows a control at timepoint 0 and pictures the low basal concentrations of LC3-I and LC3-II. Upon starvation and following autophagy activation, both LC3-I and LC3-II basal concentrations are retained over time (column 2-4). This was expected, as under uninterrupted autophagy signalling, LC3-I is processed to LC3-II which in turn binds to phagophore membranes and is degraded in autolysosomes. Treatment with azaquindole-1 (5  $\mu\text{M}$ ) resulted in an increase of the LC3-I level

## Part I

(column 5-7), which may be due to an impairment in the lipidation process followed by accumulation of LC3-I, while the LC3-II level remained low. Upon treatment with CQ (50  $\mu$ M, column 8-10), the LC3-II concentration increased significantly. This was expected, since CQ inhibits the autophagosome to lysosome fusion and therefore induces an accumulation of LC3-II on the autophagosomal membrane. Subsequent treatment with CQ and azaquindole-1 (column 10-12) showed that the LC3-II accumulation induced by CQ treatment was reversed by azaquindole-1. This finding validated the fluorescence assay outcome, that azaquindole-1 is an inhibitor of the autophagy pathway.

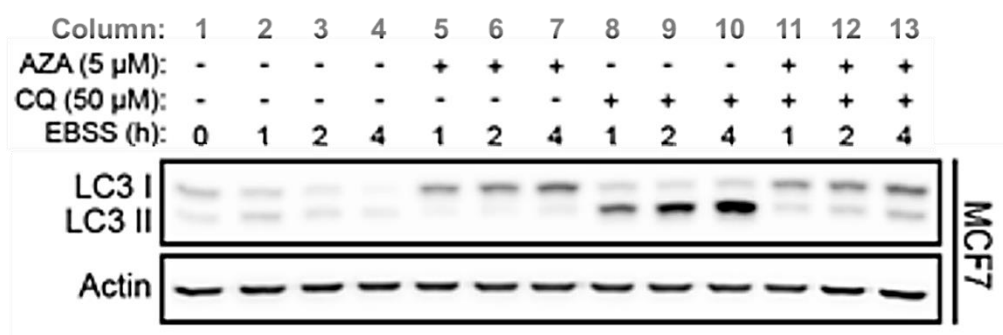


Figure 13: Immunoblot of time-dependent LC3-I and LC3-II accumulation in MCF7 cells upon starvation-induced autophagy; Presence or absence of azaquindole-1 (AZA) and chloroquine (CQ) are indicated above. Experiment was performed by Dale Corkery.

Under cellular stress situations, autophagy inhibitors might show a selective toxic effect, that is not present under common conditions.<sup>[70]</sup> Therefore azaquindole-1 was tested in a selective viability assay under glucose-starved and on the other hand glucose-rich conditions. Cell viability was detected using propidium iodide, a red fluorescent dye that is not capable of passing cell membranes, and therefore selectively stains dead cells after membrane damage.<sup>[71]</sup> Upon treatment with azaquindole-1, MCF7 cells were monitored by fluorescence microscopy for 72 h. DMSO was used as a negative control, while nocodazole<sup>[72]</sup> a small molecule that is inducing cell cycle arrest, was used as a positive control. Fractions of dead cells were calculated by normalising the data on the total amount of viable cells per well, detected by phase contrast microscopy (Figure 14). The azaquindole-1 concentrations are indicated in light blue for low concentrations to dark blue for high concentrations (up to 10  $\mu$ M).

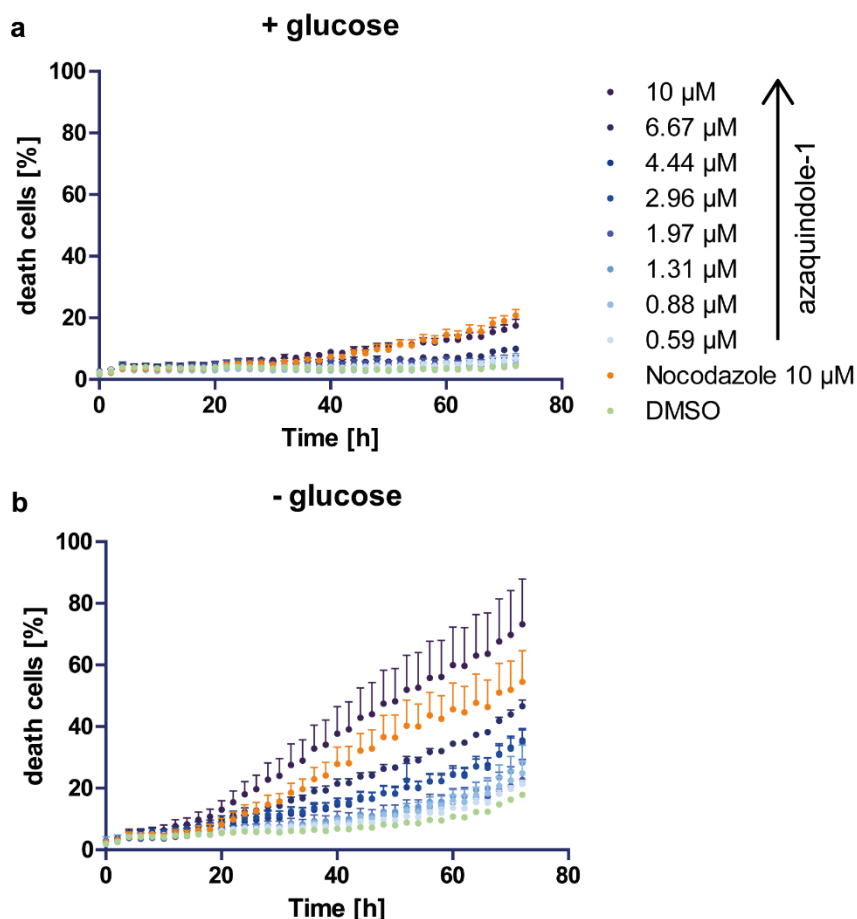


Figure 14: Selective cell viability under autophagy activated or non-activated conditions; values are given as mean  $\pm$  SD ( $n = 3$ ,  $N = 3$ ); (a) non-activated conditions: glucose-rich; (b) autophagy activation: glucose starved.

Under glucose-rich conditions a slight toxicity was measured under treatment with 10  $\mu\text{M}$  azaquindole-1. Nevertheless, after 72 h, only 20% cell death was observed, while at lower concentrations this amount decreased significantly. Under conditions without glucose, an increased amount of cell death was observed, even though the azaquindole-1 showed no increased toxicity at concentrations closer to the  $\text{IC}_{50}$  value in starvation-induced autophagy (0.04  $\mu\text{M}$ ) neither with glucose, nor without. The lowest concentration shown in this measurement is 0.59  $\mu\text{M}$ , at this concentration azaquindole-1-treated cells behaved like the DMSO control under both conditions and suggests that the slightly increased toxicity is not or not only due to the autophagy inhibitory effect.

### 3.2.2 Activity in the Cell-Painting Assay

Besides their activity in the phenotypic autophagy assay, the azaquindoles also were active in the cell painting assay (CPA). Determination of activity in the CPA thereby was set to an induction threshold of 5%, meaning that at least 5% of all measured features (see section 1.2.2.2) were significantly changed compared to the DMSO control. 9 out of 13 synthesised 7-azaindole fused to quinines were identified as CPA active at 10  $\mu$ M concentrations (Table 2). Nevertheless, the induction in the CPA does not seem to parallel the autophagy IC<sub>50</sub> values. This could indicate phenotypic changes that are based on different bioactivities. Especially the indoles functionalised at the 6 positions (Table 2, entries 12 and 13) showed a high induction whereas they were significantly less active in the autophagy screen, than azaquindole-1.

Table 2: Comparison of starvation-induced autophagy IC<sub>50</sub> and CPA induction of azaquindoles.

Entry	R-group and indole position	Nr	Starvation-induced autophagy IC <sub>50</sub> [ $\mu$ M]*	CPA Induction [%]#
1	7-azaindole	6i	4.33 $\pm$ 1.7	inactive
2	4-Cl-7-azaindole	6j	0.52 $\pm$ 0.20	inactive
3	5-Me-7-azaindole	6k	0.31 $\pm$ 0.09	20
4	5-Ar-7-azaindole	6l	9.00 $\pm$ 1.1	55
5	5-CF <sub>3</sub> -7-azaindole	6m	0.12 $\pm$ 0.03	20
6	5-NO <sub>2</sub> -7-azaindole	6n	0.67 $\pm$ 0.13	inactive
7	5-F-7-azaindole	6o	n/a	inactive
8	5-Cl-7-azaindole	6p	0.11 $\pm$ 0.04	43
9	5-Br-7-azaindole	6q	0.08 $\pm$ 0.03	32
10	5-I-7-azaindole	6r	0.08 $\pm$ 0.02	43
11	<b>5-Br-6-Me-7-azaindole</b>	6s	<b>0.04 <math>\pm</math> 0.02</b>	<b>78</b>
12	6-Me-7-azaindole	6t	3.15 $\pm$ 0.5	76
13	6-Cl-7-azaindole	6u	3.09 $\pm$ 0.9	71

\*IC<sub>50</sub>-values (as mean  $\pm$  SD) were determined in biological triplicates at the COMAS- Center Dortmund (N = 3, n = 3). n/a: inactive in starvation-induced autophagy assay (IC<sub>50</sub> > 10  $\mu$ M). #inactive: inactive in CPA at 10  $\mu$ M: induction <5%.

To further investigate this finding, the morphological profiles were compared to each other. It was previously shown that profiles with very high inductions >70% share an overactivation profile. It was suggested that this effect may be due to the interaction with multiple targets



leading to very high inductions and that this overactivity profile is not only related to the compound's primary bioactivity. Lower concentrations of these compounds (preliminary tested at 10  $\mu$ M) in the CPA can lead to lower inductions and may have less convoluted profiles that may reveal the relevant targets. Compounds with inductions >70% therefore should be excluded from analysis and tested at lower concentrations. Likewise, compounds with inductions <5% might be tested at higher concentration to reach meaningful morphological activity for comparison.<sup>[73]</sup>

Comparing lower concentration-induced profiles for the compounds that had a preliminary induction >70%, revealed a high similarity among almost all the previously most active autophagy hits (Figure 15). Generally, profiles sharing a similarity of at least 75%, are considered to be biosimilar. Azaquindoles bearing a methyl (**6k**), iodo (**6r**), chloro (**6p**) or bromo (**6q**) substituent at the indole 5-position (Table 2, entries 3, 8-10), that had a similar activity in the autophagy assay than azaquindole-1, also are biosimilar in the CPA, suggesting a similar mode of action. Compounds bearing a substituent in indole 6-position (**6t** and **6u**, Table 2, entries 12 and 13) showed a lower similarity 72 and 73% respectively, fitting to their weaker autophagy inhibition ability. The trifluoromethyl substituted compound (**6n**, Table 2, entry 5) is the only exception not fitting the trend, which may be a hint to an additional non-autophagy-related activity.

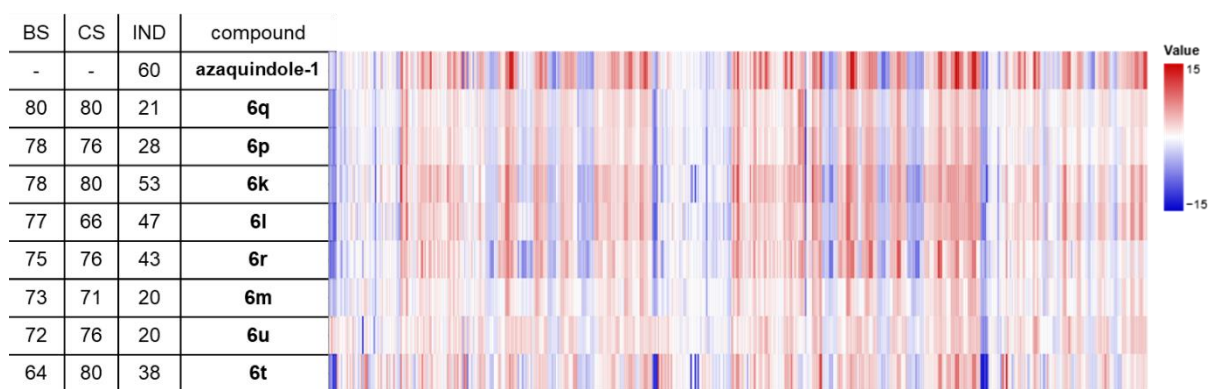


Figure 15: Comparison of morphological fingerprints of azaquindoles; biosimilarities (BS), chemical similarities (CS) and induction (IND) are given as percentages.

Besides the azaquindoles, also five of the truncated and protected derivatives of azaquindole-1 were active in the CPA at 10  $\mu$ M (Table 3). The compound lacking the quinoline moiety, was the only inactive derivative, which parallels its high autophagy  $IC_{50}$  value. However, at 30  $\mu$ M, an induction of 30% could be reached.

Table 3: Comparison of starvation-induced autophagy IC<sub>50</sub> and CPA induction of truncated and modified azaquindole-1 derivatives.

Entry	Truncated derivative	Nr	Starvation-induced autophagy IC <sub>50</sub> [μM]*	CPA Induction [%]#
1	non-aza	7	2.66 ± 0.1	7
2	no methoxy	10	0.80 ± 0.09	64
3	no quinoline	18	5.13 ± 0.9	inactive (30% at 30 μM)
4	partially reduced	12	2.35 ± 0.4	29
5	methyated OH	20	0.10 ± 0.01	54
6	oxidised compound	21	inactive	21

\*IC<sub>50</sub>-values (as mean ± SD) were determined in biological triplicates at the COMAS- Center Dortmund (N = 3, n = 3). n/a: inactive in starvation-induced autophagy assay (IC<sub>50</sub> > 10 μM). #inactive: inactive in CPA at 10 μM: induction <5%.

Within this compound set, the autophagy activity seemed to correlate with the CPA induction. This further indicates that the CPA activity, using the induction as measurement, can hint towards structure-phenotype relationships for the identification of the most active hits if the morphological profiles are similar. Furthermore, the biosimilarity to azaquindole-1 was higher for the derivatives showing a higher activity in the autophagy assay (Figure 16).

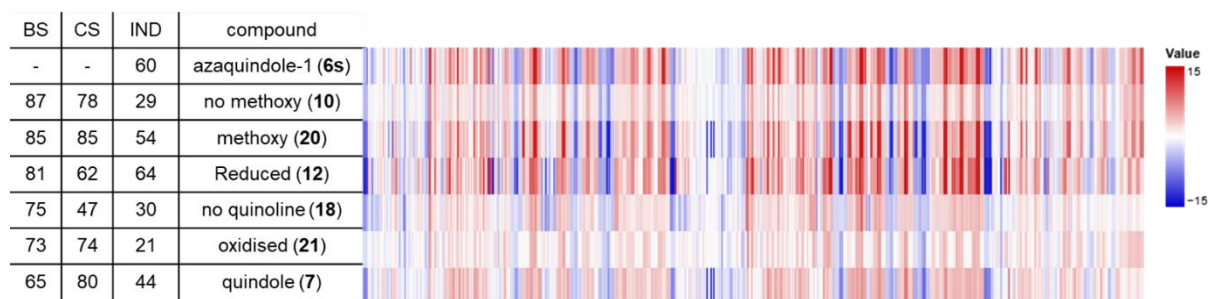


Figure 16: Comparison of morphological fingerprints of azaquindoles-1 derivatives; biosimilarities (BS), chemical similarities (CS) and induction (IND) are given as percentages

### 3.2.3 Cell Painting Guided Target Hypothesis and Target Identification

To further elucidate the azaquindole's mode of action (MOA) in the autophagy pathway, the CPA fingerprint of azaquindole-1 was compared to fingerprints of reference compounds with annotated bioactivities. Several compounds were identified to induce similar morphological changes as azaquindole-1. Interestingly, among the 25 compounds showing the highest profile similarity with azaquindole-1, almost half of the compounds (11) were annotated to be kinase inhibitors. Furthermore, 3 of these kinase inhibitors were annotated as selective VPS34 inhibitors, a PI3K kinase with a known link to autophagy (Figure 9). It was shown before in the rapamycin-induced phenotypic autophagy assay that azaquindole-1 inhibits the autophagy pathway downstream or independent of mTOR. Additionally, the LC3 immunoblot indicated, that azaquindole-1 interferes with the conversion of LC3-I to LC3-II. These previous findings may support the hypothesis of VPS34 as potential autophagy related biological target. Upon autophagy activation, VPS34 is activated and phosphorylates membrane-bound phosphatidyl inositol, which in turn can translocate the ATG-scaffold protein WIPI to the membrane (Figure 9).

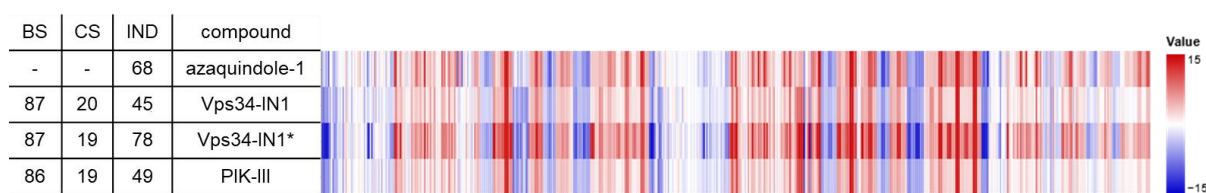


Figure 17: Comparison of morphological fingerprints of azaquindoles-1 to three VPS34 inhibitors from the top 25 biosimilar reference compounds; biosimilarities (BS), chemical similarities (CS) and induction (IND) are given as percentages

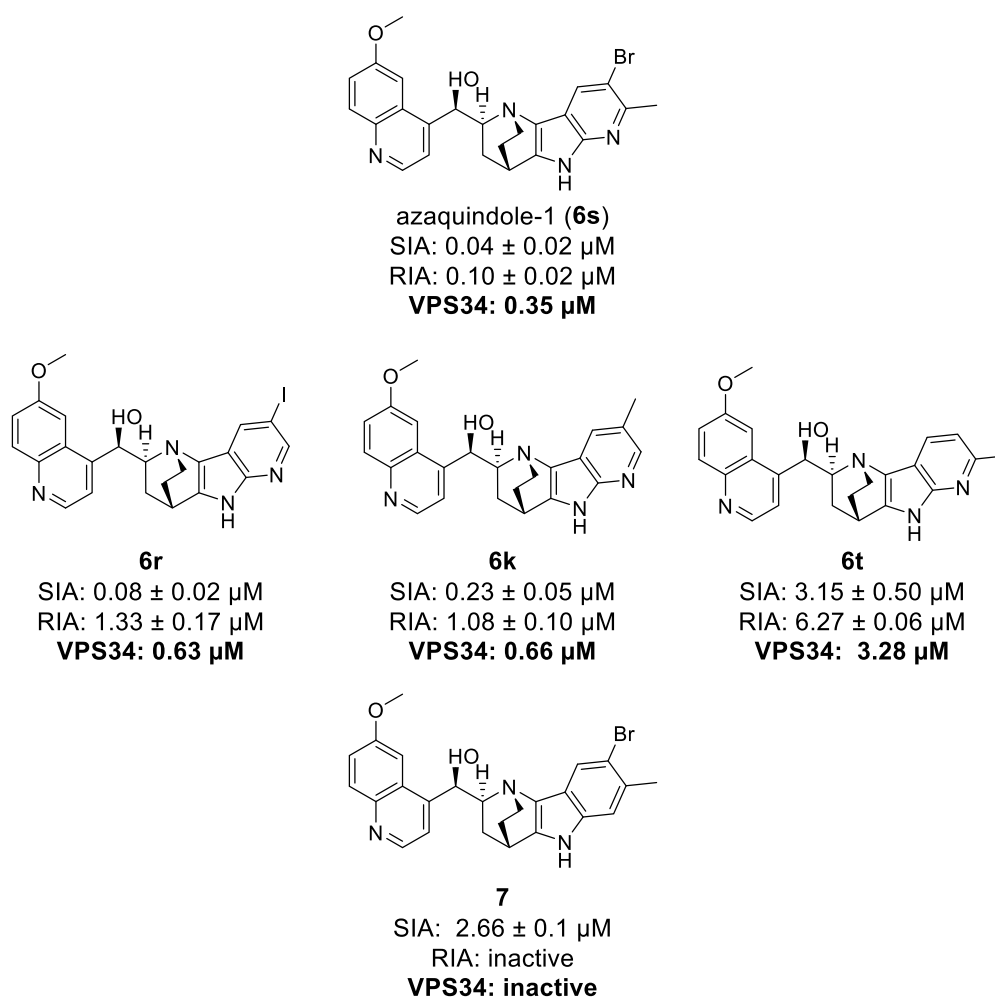
Based on these findings and a strong hint for a kinase target, azaquindole-1 was subjected to an *in-vitro* kinase assay to test its inhibitory effect on VPS34. This experiment was carried out at Thermo Fisher using an Adapta® Universal Kinase Assay, that is based on the ATP to ADP consumption via kinase reaction. Released ADP is detected by a europium-labelled ADP antibody bound to an Alexa Fluor® 647 labelled ADP tracer, which is excited by the Europium via Förster resonance energy transfer (FRET) due to proximity. Upon ADP binding the ADP tracer is released from the antibody, resulting in a decrease in the fluorescent signal associated with kinase activity. Treatment of the kinase with an inhibitor on the other hand leads to a lower tracer displacement and high FRET signal.<sup>[74]</sup> Excitingly, the previous hypothesis proved to be true: Azaquindole-1 inhibits VPS34 with an *in-vitro* IC<sub>50</sub> of 350 nM. Consequently, azaquindole-1 was tested in a broad kinase panel at Thermo Fisher against 485 kinases, to investigate its selectivity. For kinases showing more than 40% inhibition upon treatment with

azaquindole-1 (10  $\mu$ M), an IC<sub>50</sub> value was determined. Depending on the kinase either the Adapta® assay, the Z'-LYTE assay (based on ATP transfer to a synthetic FRET peptide) or the LanthaScreen Eu kinase binding assay (based on an Eu labelled antibody specific for the tested kinase and a quenching tracer specific for the kinase active site).<sup>[75]</sup> Testing of a broad range of kinases delivered 7 further kinases, that were inhibited by azaquindole-1 at concentrations lower than 10  $\mu$ M (Table 4). Based on the sub-micromolar IC<sub>50</sub> value of azaquindole-1, the four most potent kinases (including VPS34) with IC<sub>50</sub> ranging from 93 to 572 nM (Table 4, entries 1-4) were suggested to be the most relevant for further investigation. Interestingly, among others, four additional PI3Ks were identified as targets of azaquindole-1, but only one apart of VPS34 was inhibited with nM potency: PIK3C2G (Table 4, entry 3). Robke *et al.* previously investigated and ruled out the potential role of PIK3CG and PI4KB in autophagy signalling by testing several highly potent inhibitors for their autophagy inhibitory activity.<sup>[76]</sup> Evaluation of the Cdc2 like kinase 2/4 (CLK2/4) inhibitor ML167<sup>[77]</sup> and the CLK2/3/4 inhibitor TG003<sup>[78]</sup> in the autophagy assay revealed, that CLK inhibition is not affecting autophagy. Likewise, selective inhibitors of PIK3CD and sphingosine kinase 2 (SPHK2) were not active in the autophagy assay. Since none of the other kinase targets was shown to be relevant for autophagy signalling VPS34 was the only autophagy-related kinase target of azaquindole-1.

Table 4: Kinases that were inhibited at <10  $\mu$ M azaquindole-1.

Entry	Kinase	Assay type	ATP [ $\mu$ M]	IC50 [nM]
1	CLK4	Lantha	N/A	93.9
2	<b>PIK3C3 (VPS34)</b>	<b>Adapta</b>	<b>Km app</b>	<b>350</b>
3	PIK3C2G (PI3K-C2 gamma)	Adapta	Km app	497
4	CLK2	ZLYTE	Km app	572
5	PIK3C2B (PI3K-C2 beta)	Adapta	100	2160
6	SPHK2	Adapta	10	2770
7	PIK3CD/PIK3R1 (p110 delta/p85 alpha)	Adapta	Km app	4790
8	PI4KB (PI4K beta)	Adapta	Km app	5160

In addition to azaquindole-1, four further selected examples were submitted for testing their inhibitory effects in the *in-vitro* VPS34 assay (Scheme 7). Interestingly, the measured IC<sub>50</sub> values parallel the autophagy IC<sub>50</sub> values. Compounds **6r** and **6k**, that inhibit SIA with nanomolar potency, also were identified to inhibit VPS34 at sub-micromolar concentrations. Moreover, the azaquindole substituted in indole 5-position (**6t**), that was less active in SIA inhibition, also reached a lower potency in VPS34 inhibition (IC<sub>50</sub> 3.28 μM). The indole derivative of azaquindole-1 (**7**), which was slightly active in SIA (IC<sub>50</sub> 2.66 μM) but already differed from the other derivatives by its lack in RIA inhibition at <10 μM, was inactive in the biochemical *in-vitro* assay. This may suggest that the aza-nitrogen is crucial for inhibition of VPS34 and compound **7** has a different MOA in autophagy inhibition.



Scheme 7: Inhibition of VPS34 by selected azaquindole-1 derivatives; values are IC<sub>50</sub> values; SIA: starvation-induced autophagy; RIA: rapamycin-induced autophagy (values are mean ± SD); VPS34 IC<sub>50</sub> were measured in Adapta assay by ThermoFisher.

### 3.2.4 Target Validation

To further validate VPS34 as the target responsible for autophagy inhibition, the effect of azaquindole-1 on different stages of autophagy signalling was investigated. To prove, that the autophagy signalling is not disturbed upstream of VPS34, the phosphorylation status of ULK1 was determined via immunoblotting, using an antibody specifically recognising phosphorylated ULK1 (p-ULK). Under normal, nontreated cellular conditions, the mTOR complex is a key regulator to keep the autophagy level low by phosphorylating the ULK1 protein at serine 757. Phosphorylation at this serine residue prevents ULK1 activation by 5' AMP-activated protein kinase (AMPK). Consequently, the VPS34 complex is not activated and autophagy signalling inhibited. Upon autophagy initiation (e.g., through starvation), mTOR complex formation is inhibited, leading to the activation of the ULK1 kinase activity by Ser317 and Ser777 phosphorylation.<sup>[79]</sup> The activated ULK1 complex then phosphorylates Beclin 1, resulting in ATG14 binding and activation of the VPS34 complex (Figure 18a).<sup>[80]</sup>

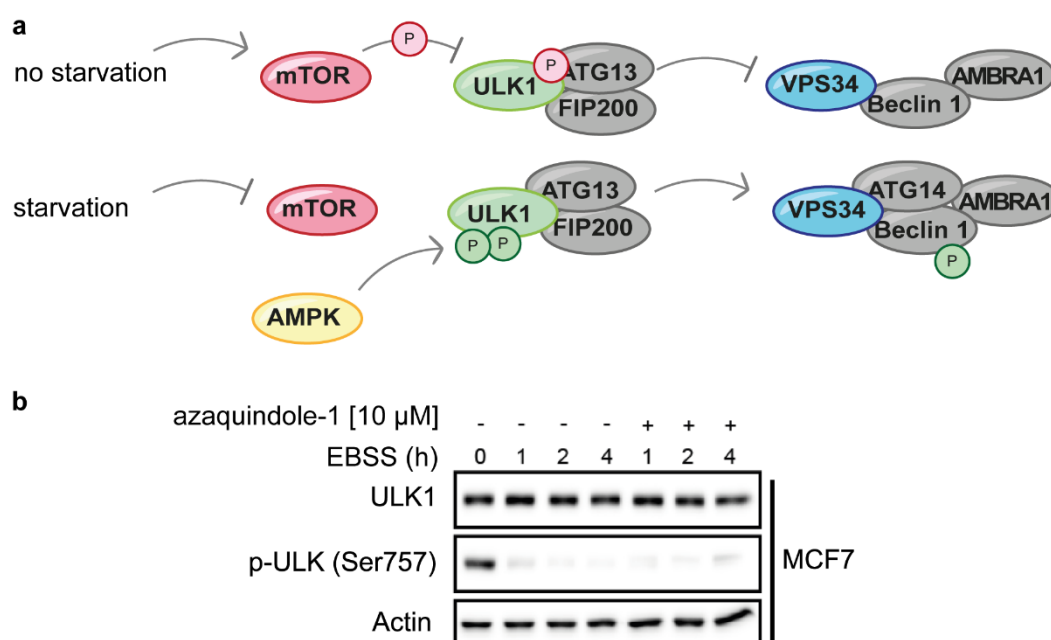


Figure 18: (a) Schematic representation of the ULK1 phosphorylation state in autophagy initiation; deactivating phosphorylation at Ser757 is indicated in red; activating phosphorylations are indicated in green; (b) immunoblot of time-dependent ULK1 phosphorylation (Ser757) upon starvation-induced autophagy; presence or absence of azaquindole-1 are indicated. Experiment was performed by Dale Corkery:

The ULK1 and p-ULK (Ser757) level with and without azaquindole-1 treatment of MCF7 cells was detected over 4 h upon autophagy activation (by EBSS). As expected, the control sample at timepoint 0 (Figure 15b, column 1) shows a high p-ULK (Ser757) level, prior to autophagy activation. After 1 h (Figure 15b, column 2 and 5), the p-ULK (Ser757) concentration in the

cell lysates is significantly reduced, indicating autophagy activation under both azaquindole-1 free and azaquindole-1 treated conditions. Time-dependent observation of the p-ULK (Ser757) level furthermore indicates that there is no time-dependent inhibition of autophagy upstream of ULK1. Immunoblotting of ULK1 (no phosphorylation specific antibody was used), revealed a constant ULK1 level during treatment time, excluding the possibility of low ULK1 expression or ULK1 degradation. The decreased p-ULK (Ser757) level therefore is a result of the inhibited phosphorylation. This finding confirms that azaquindole-1 inhibits autophagy downstream of the ULK1 complex and does not impair autophagy upstream of VPS34.

VPS34 is a kinase that catalyses the phosphorylation of phosphatidylinositol (PI) to phosphatidylinositol-3-phosphate (PI3P) bound to phagophore initiation membranes. Upon PI phosphorylation, the ATG scaffold protein WIPI2b is recruited to the membranes, initiating downstream autophagy signalling (Figure 19).<sup>[81]</sup> Therefore, VPS34 activity can be evaluated by monitoring of WIPI2 protein location in the cell. A HEK293A cell line stably expressing eGFP labelled WIPI2 protein allowed the evaluation of VPS34 activity upon autophagy initiation with and without azaquindole-1 treatment. Accumulation of eGFP-labelled WIPI2 on phagophore membranes upon autophagy activation appears as fluorescent puncta (Figure 19c, VEH). Additional treatment of cells with the known PI3K inhibitor wortmannin resulted in a reversion of this effect. Treatment with azaquindole-1 was also able to disrupt the WIPI2 accumulation, confirming its impairment of VSP34 activity. Additionally, the time-dependent quantification of eGFP-puncta per cell (Figure 19b) clarified the strong inhibition of WIPI2 membrane localisation.

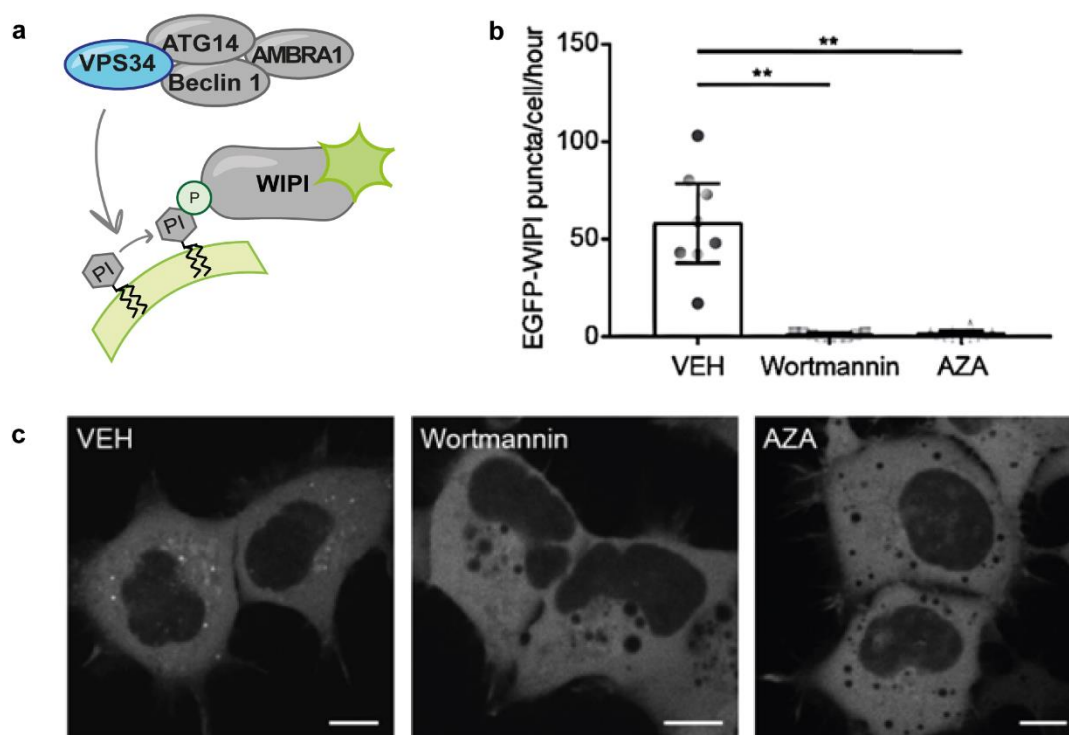


Figure 19: (a) Schematic representation of VPS34 catalysed phosphorylation of phosphatidylinositol (PI) and subsequent membran localization of fluorescence labeled WIPI; (b) quantification of eGFP-WIPI accumulation upon autophagy activation; (c) representative fluorescence figures; VEH: control = DMSO; Wortmannin = known PIK3 inhibitor; AZA= azaquindole-1); Experiment was performed by Dale Corkery.

To validate the binding of azaquindole-1 to VPS34, a cellular thermal shift assay (CETSA) was performed. CETSA is a valuable approach to measure target engagement in complex cellular context that was invented by Nordlund *et al.* in 2013 and is based on the thermal stabilization or destabilization of proteins through ligand binding.<sup>[82]</sup> In CETSA, cellular lysates are treated with either a compound of interest or a control (DMSO). After aliquoting the treated and control samples, the fractions are exposed to different temperatures. Subsequently, denatured proteins are removed by centrifugation. Quantification of the amount of native protein remaining in the individual samples (e.g., by immunoblot) can be used to generate melting curves and determine the melting temperature  $T_m$  (Figure 20).<sup>[82,83]</sup> Since the interaction between a ligand and a protein of interest may induce a change in its thermal stability, the  $T_m$  values of the ligand bound protein and the control may differ.<sup>[84]</sup> Therefore, the detection of such a difference ( $\Delta T_m$ ) is unequivocal evidence for the binding of the compound to the protein.



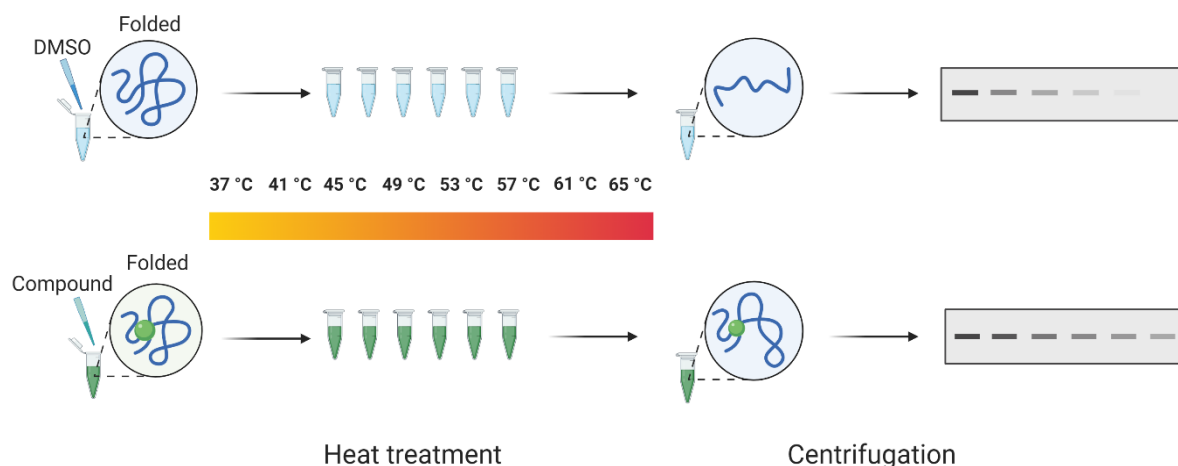


Figure 20: General experimental workflow of the cellular thermal shift assay with an immunoblot readout.

To elucidate the binding of azaquindole-1 to VPS34, two batches of MCF7 cell lysates were treated with either azaquindole-1 (10  $\mu$ M) or DMSO for 10 min. Subsequently, the samples were further fractionised into nine aliquots that were individually heated at different temperatures ranging from 36.9 to 67  $^{\circ}$ C. Removal of denatured proteins was facilitated via ultracentrifugation and the soluble, native protein fraction was analysed by immunoblotting (Figure 21a). As it is already visible by the VPS34 band intensities of the western blot image, quantification revealed a shift of the melting curve of azaquindole-1 treated sample (green) compared to the DMSO control (blue) toward higher temperatures (Figure 21b). Curve fitting and calculation of the melting temperatures from the turning point revealed a significant difference between DMSO and azaquindole-1 of  $\Delta T_m = 4.65$   $^{\circ}$ C. Based on this stabilising effect of azaquindole-1 on VPS34, a binding, even in the complex protein mixture of a lysate, was confirmed.

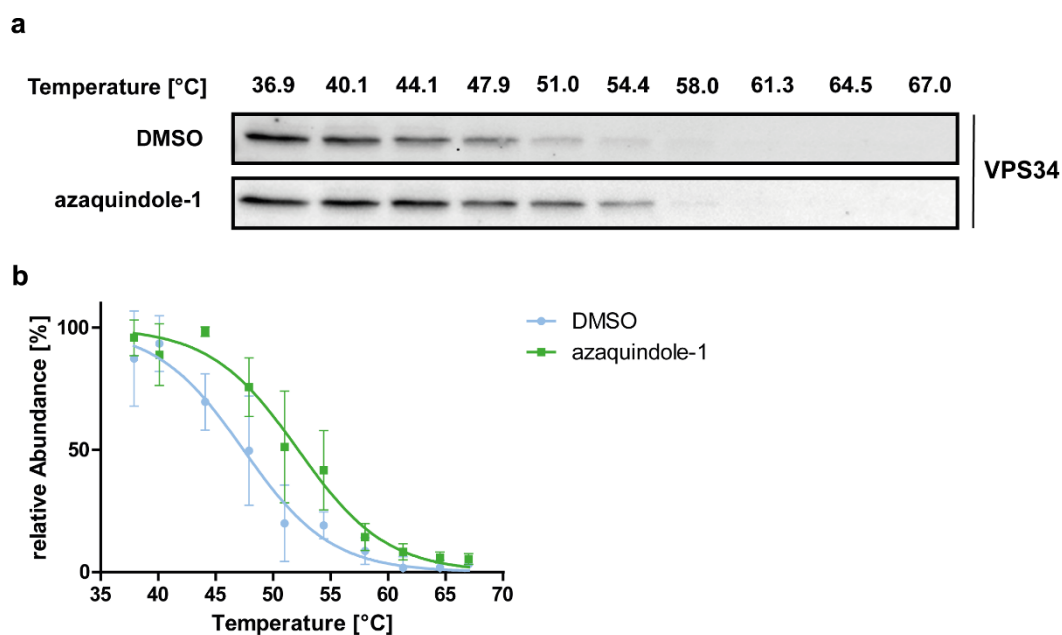


Figure 21: CETSA of azaquindole-1 in MCF7 lysates; **(a)** representative immunoblot of temperature-dependent VPS34 abundance in the presence and absence of azaquindole-1; **(b)** quantification of CETSA immunoblot readout; blue: DMSO, green azaquindole-1 treatment; data are given as mean  $\pm$  SD.

To further test the binding of azaquindole-1 to VPS34 in a cellular context, an in-cell CETSA was performed. Instead of treating MCF7 cell lysates, living cells were treated with the test compound or DMSO in cell culture flasks. After incubation for 1 h at 37 °C, cells were detached and fractionised into individual samples that were heated to different temperatures. After heating the cells, they were lysed and denatured proteins were removed from the samples, prior analysis by immunoblotting (Figure 22a). Quantification of the band intensities again showed a shift of the azaquindole-1-treated sample to higher temperatures (Figure 22b). Even though this shift turned out to be less evident as in the CETSA experiment in lysates, a melting temperature difference of 1.65 °C was calculated. This significant stabilization of VPS34 validated protein binding in a cellular environment. Furthermore, this experiment proves that azaquindole-1 can pass cellular membranes and is taken up into cells in relevant concentrations.

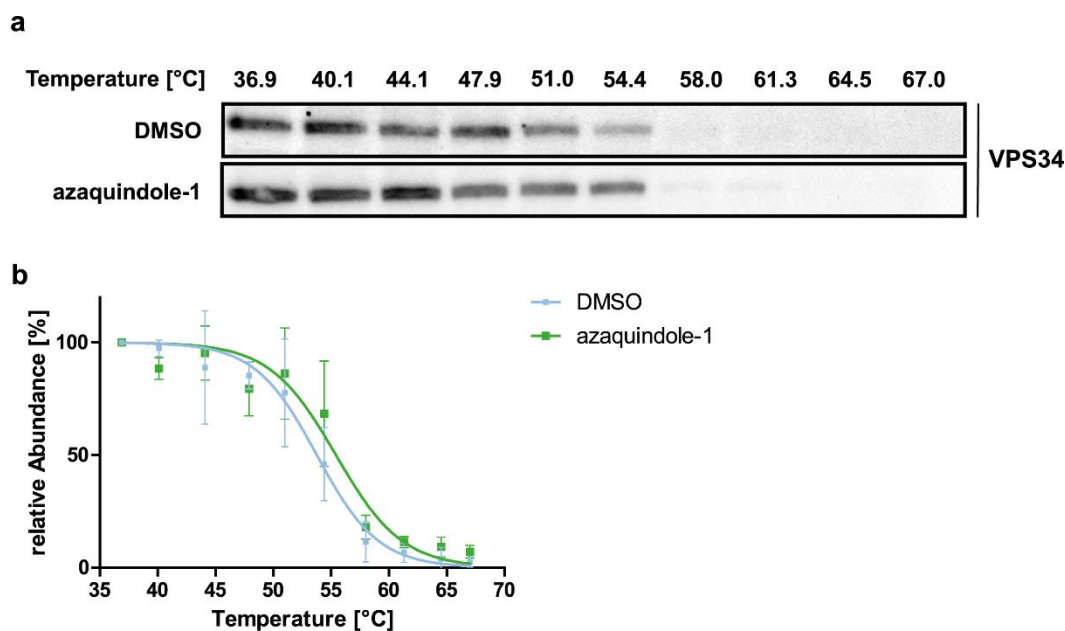


Figure 22: In-cell CETSA of azaquindole-1 in MCF7 cells; (a) representative immunoblot of temperature-dependent VPS34 abundance in presence and absence of azaquindole-1; (b) quantification of CETSA immunoblot readout; blue: DMSO, green azaquindole-1 treatment; data are given as mean  $\pm$  SD.

### 3.2.5 Mode of Inhibition by Enzyme Kinetics

To investigate the mode of VPS34 inhibition an enzyme kinetic study was commissioned from SignalChem. Understanding of the mode of inhibition (MOI) will give insights to the interaction of a compound with the target enzyme, and how the natural enzyme substrate (ATP in the case of kinases) may interfere with its activity.

Generally, there are three main types of enzyme inhibition (competitive, non-competitive, and uncompetitive inhibition) that are classified by their binding affinity to substrate or non-substrate bound state of an enzyme. Competitive inhibitors bind to the free, non-substrate bound enzyme, often to the substrate binding site. It follows, that the natural substrate and inhibitor compete for enzyme binding. Non-competitive, inhibitors can bind to both states, the substrate bound, and non-substrate bound form of the enzyme. Lastly, uncompetitive inhibitors only bind to the enzyme substrate complex.<sup>[85]</sup>

To identify the MOI of an inhibitor, the kinetic of an enzymatic reaction may be evaluated at different substrate concentrations (here: ATP). A quantitative relationship between the velocity of enzyme-catalysed reactions ( $v$ ) and the substrate concentration  $[S]$  was described by Michaelis and Menten (equation 1) under consideration of a single substrate transformation via formation of an enzyme substrate complex.

## Part I

$$v = \frac{V_{max}[S]}{K_M + [S]} \quad (1)$$

Thereby,  $v$  is the starting velocity (experimentally determined),  $V_{max}$  the maximum velocity,  $[S]$  the added substrate concentration (start concentration) and  $K_M$  the Michaelis-Menten constant. The Michaelis-Menten constant can be experimentally determined and describes the substrate concentration that is needed to reach the half maximal velocity of the enzyme reaction ( $v_{max}/2$ ).<sup>[86]</sup>

Consideration of the enzyme inhibitor binding to this equation requires the introduction of a further measurement, the dissociation constant  $K_i$  describing the equilibrium between the enzyme inhibitor complex and the free enzyme and inhibitor. Since the binding of an inhibitor to the enzyme may affect the binding affinity of the substrate, the inhibitor-specific constant  $\alpha$  is introduced (equation 2). The value of this constant represents the mode of inhibitor binding. If  $\alpha$  equals 1, the inhibitor binding does not affect the substrate binding (noncompetitive inhibitors). If the binding of an inhibitor prevents the substrate binding (competitive inhibitors) the  $\alpha$  value will be very high ( $\gg 1$ ). Very small  $\alpha$  values are observed for uncompetitive inhibitors. The advantage of this general equation (2) is its universal applicability to fit velocity curves observed for different modes of inhibition (mixed model).

$$v = \frac{V_{max}[S]}{K_M \left(1 + \frac{[I]}{K_i}\right) + [S] \left(1 + \frac{[I]}{\alpha K_i}\right)} \quad (2)$$

Generally, the MOI can also be determined by considering changes in the variables  $K_M$  and  $V_{max}$  with changing inhibitor concentrations. In competitive enzyme inhibition, the  $V_{max}$  value stays the same with differing inhibitor concentrations, as with an increasing substrate concentration  $[S]$  the maximum velocity still can be achieved. Nevertheless, the  $K_M$  value is increasing with increasing inhibitor concentrations. To reach the same half maximal velocity, a higher  $[S]$  is needed. In uncompetitive inhibition, both values  $K_M$  and  $V_{max}$  are reduced with increasing inhibitor concentration. If an inhibitor prevents substrate binding, both values cannot be reached any more. Last, in non-competitive inhibition, the concentration of active enzyme is reduced by inhibitor binding. Consequently, the  $V_{max}$  value is reduced whereas  $K_M$  stays constant.

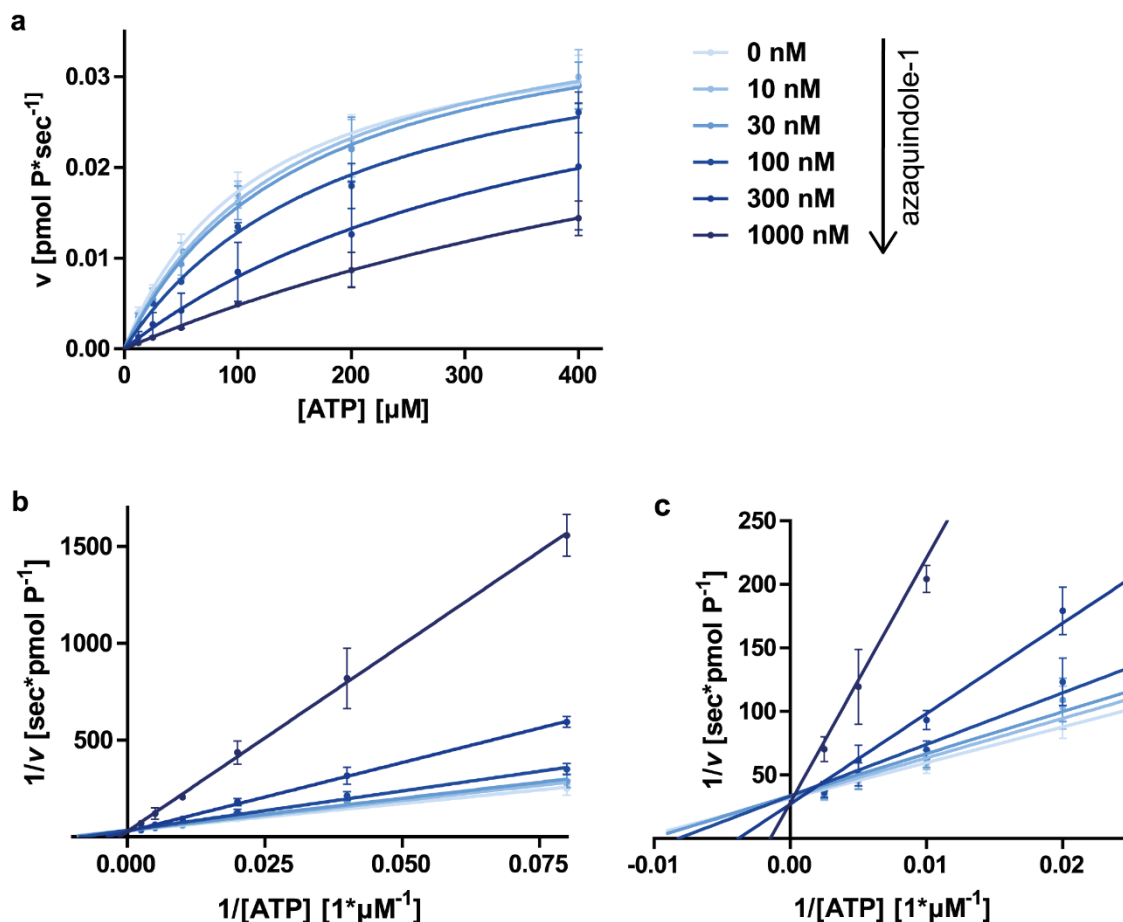


Figure 23: VPS34 kinetic plots in dependency of azaquindole-1 concentrations. Velocities were determined in an ADP-Glo assay, performed by SignalChem ( $n = 3$ ,  $N = 3$ ); (a) Michaelis-Menten plot; (b) Lineweaver-Burk plot (double reciprocal plot); (c) zoom into intersection of graphs with x- and y-axis.

To determine the velocity of the enzymatic reaction in presence and absence of azaquindole-1 at different ATP concentrations, the ADP-Glo assay (Promega) was performed by SignalChem. This assay is based on the detection of ADP, which is produced in the enzyme reaction, by a luciferase-based reaction. The starting velocity  $v$  is determined from the linear range of the substrate consumption saturation curve which is obtained by plotting the signal intensity against the substrate concentration.

The Michaelis-Menten graph (Figure 23a) then was obtained from plotting  $v$  (in pmol transferred phosphate per second) against the ATP concentration for different azaquindole-1 concentrations (0-1000 nM). Fitting of the obtained curves by equation (2) revealed  $K_i = 273.6 \pm 96.3$  nM, and a very high  $\alpha$  value ( $>10^{10}$ ). The high  $\alpha$  suggested a competitive MOI but  $V_{\max}$  was not reached at 400 μM ATP. Double reciprocal plotting in a so-called Lineweaver-Burk plot of velocity data results in a linear correlation that is easier to interpret (b). In this type of plot,  $1/V_{\max}$  corresponds to the intersection of the graph with the y-axis and  $-1/K_M$  to the

## Part I

intersection with the x-axis. Closer inspection of the intersections (Figure 23c) revealed a constant  $1/V_{\max}$  and consequently a constant  $V_{\max}$  at different compound concentrations. Furthermore, with increasing concentrations of azaquindole-1, the  $-1/K_M$  values increased which is equivalent to a decreasing  $K_M$  with increasing inhibitor concentrations. Accordingly, together with the high  $\alpha$  value, these results showed that azaquindole-1 is a competitive inhibitor of VPS34.

### 3.3 Conclusion

Based on a prior identification of azaquindole-1 as potent inhibitor of autophagy, the SAR and the MOA were further investigated. Successful synthesis of 6 truncated or modified azaquindole-1 derivatives facilitated the identification of crucial structural features for autophagy inhibition. Only the secondary alcohol functionality could be modified by protection, without a significant loss in potency. However, neither the whole quinoline part, nor the aza-nitrogen were crucial for autophagy inhibition, even though the efficacy of derivatives lacking the aza-nitrogen or the quinoline part was significantly decreased. Overall, azaquindole-1 was the most active derivative and was utilised for further studies. First, the autophagy activity was validated by immunoblotting of the autophagy marker protein LC3, and a low toxicity was shown under both, autophagy-activated and -non-activated conditions. To investigate the MOA of azaquindole-1, a target hypothesis was generated by comparing its CPA-derived morphological profile to reference profiles. The phenotypic changes were similar to changes induced by kinase inhibitors including the autophagy-related kinase VPS34. Indeed, VPS34 could be inhibited by azaquindole-1 in an *in-vitro* assay. Additionally, kinase profiling showed that azaquindole-1 only inhibits a small subset of kinases at nanomolar concentrations, of which VPS34 turned out to be the only autophagy-related kinase. Further validation experiments, including the investigation of ULK phosphorylation status, investigation of WIPI activity and target engagement via CETSA proved, that VPS34 is the autophagy-related target of azaquindole-1. *In-vitro* kinetic investigation were used to evaluate the MOI: azaquindole-1 is an ATP-competitive inhibitor of VPS34.

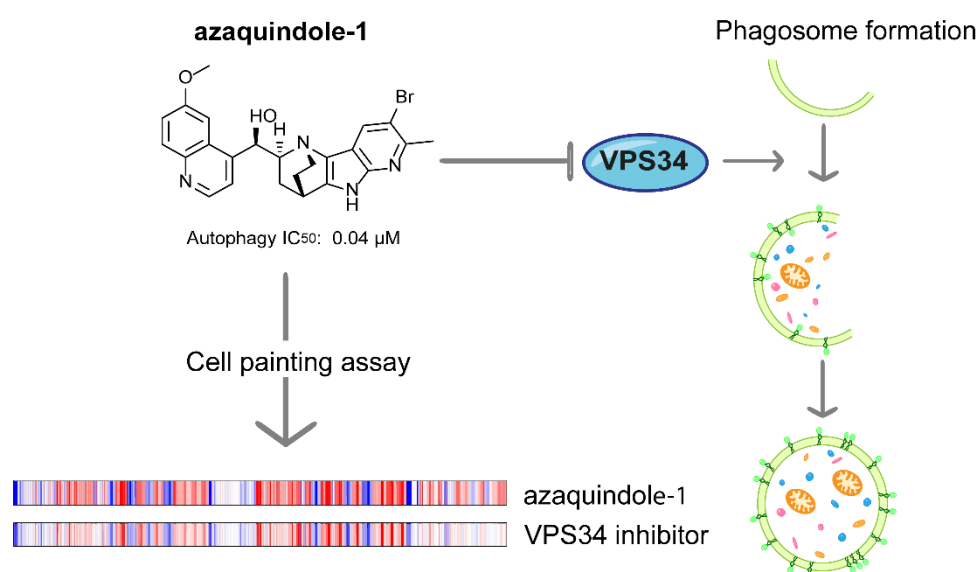


Figure 24: Summary figure. Azaquindole-1 inhibits autophagy by ATP-competitive inhibition of VPS34; CPA identified a first target hypothesis.

## 4. Part II: Cell-painting assay analysis of NP-fragment combinations

### 4.1 Introduction

This work was carried out in collaboration with Dr Annina Burhop and Dr Michael Grigalunas. The results were reported in: M. Grigalunas, A. Burhop, S. Zinken, *et al. Nat. Commun.* **2021**, *12*, 1-11.

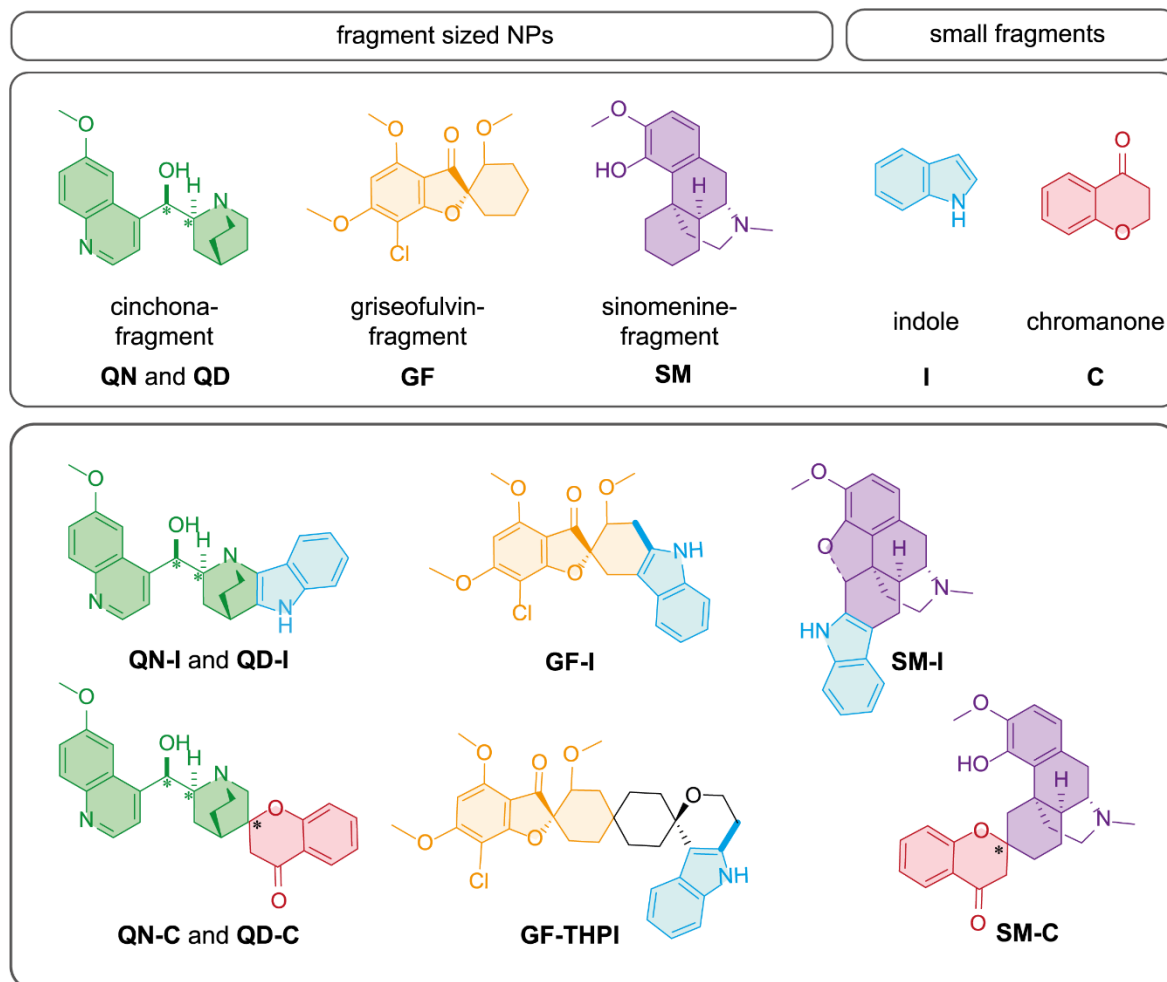


Figure 25: Overview of general PNP structures for comparison in the cell painting assay. Shown PNP compound classes were derived from combination of three fragment-sized NPs with indole or chromanone. Indicated stereocenters and bold highlighted bonds represent the additional existence of stereo- or regio-isomers.

To investigate the influence of individual NP fragments and the influence of their connectivity on the morphological activity of PNPs, the cinchona derived indoles and further PNP classes synthesised in the Waldmann group were investigated in the CPA. The considered PNPs thereby were derived from a small fragment subset comprising four fragment-sized NPs, the cinchona alkaloids quinine (QN) and quinidine (QD), griseofulvin (GF), and sinomenine (SM), that were coupled to the indole (I) or chromanone (C) fragment (Figure 25).



To generate suitable coupling partners, the fragment-sized NPs were all readily transformed to ketones, that then were viable substrates for indole- and chromanone-generating reactions. Utilising a Pd-catalysed annulation, Fischer-indole reaction (M. Grigalunas) and an oxa-Pictet Spengler reaction (A. Burhop) to synthesise indoles and the Kabbe reaction (M. Grigalunas) to synthesise chromanones, eight PNP compound classes could be synthesised. These classes not only differed in the fragment combination, but also in their connectivity. While the Pd-catalysed annulation and the Fischer-indole reaction delivered an edge-fused connection, the oxa-Pictet Spengler and Kabbe reactions gave spiro fused PNPs. Among these PNP classes, also diverse subclasses were synthesised, that differed in their diastereomeric or regioisomeric constellation.

Having established that all classes of compounds showed generally good activity in CPA (induction > 5%), the morphological profiles were compared to investigate the influence of individual fragments on the morphological changes as well as the influence of their various connectivities and stereogenic information.

#### 4.1.1 CPA comparison of compound classes

To compare the morphological profiles of whole compound classes rather than of single compounds, a suitable measure to evaluate similarities had to be identified. A first value, that might be calculated to measure the similarity between compound classes is the median-biosimilarity (MBS). To calculate the MBS, all morphological profiles of one class are compared to all profiles of the compounds of a second class. Figure 26a shows an exemplary comparison table, all morphological profiles of the compounds of class 1 (a-f) are compared to all compounds of class 3 (a-d). The colour scheme indicates similarities and reveals a high similarity within the classes (indicated by green and yellow) but a low similarity between the classes (indicated by red). The exact value for the biosimilarities between each pair of compounds is calculated and the median of these values determined as the final measure for inter- or intra-class MBS.

Another method to generally interpret large data sets is the principal component analysis (PCA). PCA is used to reduce dimensionality of datasets by creating novel uncorrelated variables (principal components) that maximize variance. This allows the simplification of data by retaining most of their information.<sup>[87]</sup> Following this principle, morphological fingerprints that are composed of > 500 different features, are reduced to two to three components ('dimensions'). This allows the representation of each fingerprint as a data point in 2D, or 3D

space (Figure 26b). The distance between these data points represents for similarity between the described compound's morphological profiles. A short distance represents a high similarity between profiles, whereas a long distance represents a low similarity. Compounds with a high profile similarity therefore can form clusters in 2D/3D space. This not only allows a graphical visualization of large sets of morphological profiles but can also hint towards small differences between datasets. Considering both types of analyses, MBS and PCA, the morphological activity of compound classes may be identified as similar or dissimilar.

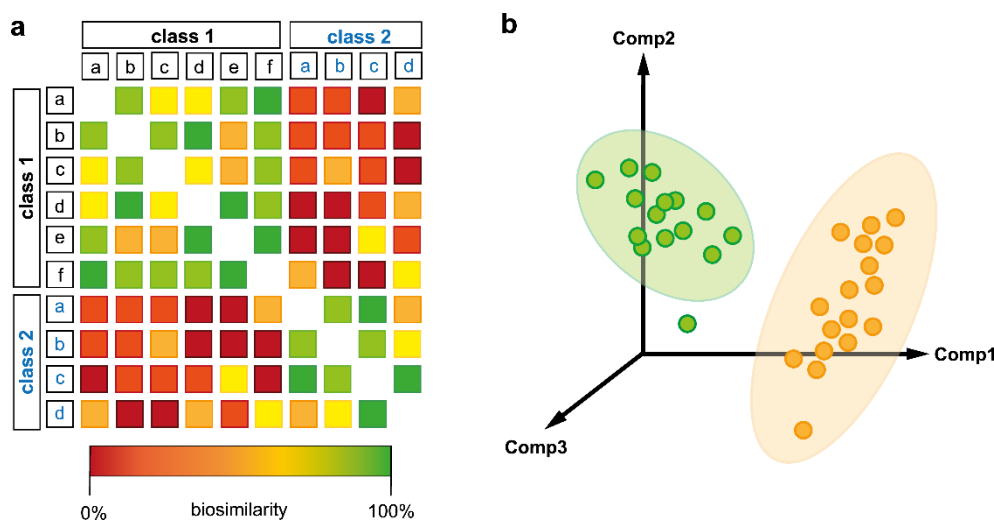


Figure 26: Simplified representation of the biosimilarity of compound classes; (a) example schematic representation of the comparison of two compound classes to calculate the median biosimilarity (MBS); (b) schematic representation for the principal component analysis (PCA) of two compound classes with different bioactivities.

As discussed previously, the induction value (percentage of morphological features that are significantly changed compared to the DMSO control profile) can have an impact on the biosimilarity of compounds. PCA analysis of different compound classes with broad ranges of inductions revealed a high dependency on induction of the first component. Since the induction is a measure of the number of changed features, but not their nature, an analysis mainly based on induction would not give insight into the similarity of morphological changes. The reduction of the induction range to a smaller window can lead to a loss of this dependency, and an induction-based analysis of similarities (Figure 27; example for induction dependency of biosimilarity for azaquindoles) should be done prior to comparison of compound classes. However, the appropriate induction range may vary for each data set and should be investigated before beginning any analysis.

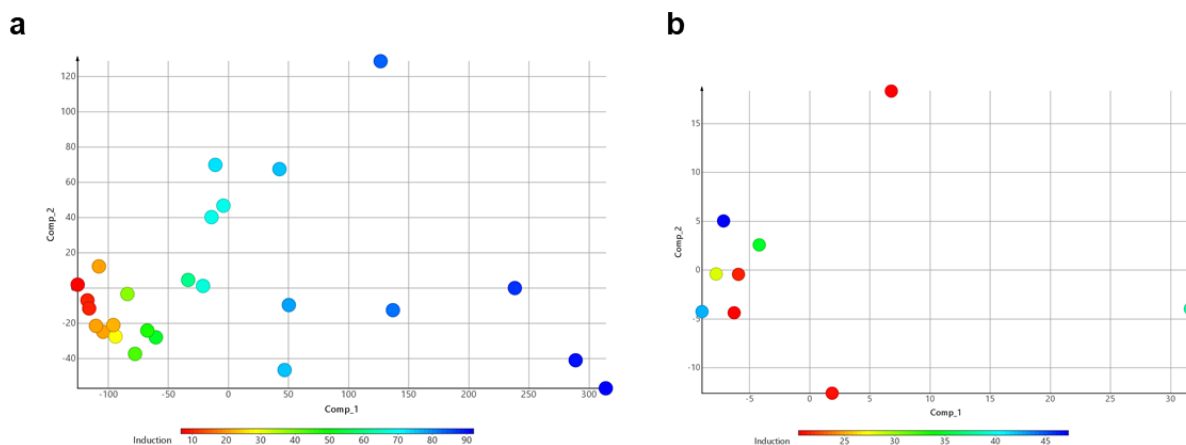


Figure 27: Visualization of the induction influence on the 1<sup>st</sup> component in the PCA of azaquindoles; **(a)** induction: 5-80%; **(b)** induction: 15-40%; data points are stained according to the induction of the corresponding compound, red = low, blue = high.

## 4.2. Results and Discussion

The eight PNP compound classes were proposed to be chemically diverse and cover different areas of chemical space. To investigate the structural diversity of the dataset, the interclass-chemical diversity was calculated by Tanimoto algorithm (0 = no similarity; 1 = identical). The distribution of median similarities between compound classes is shown in Figure 28. The graph shows a high data density around 0.2 that revealed that the majority of comparisons has a rather low inter-class chemical similarity. This suggests a high chemical diversity among the data set.

To get a general insight into the biological diversity of the dataset, the MBS between all

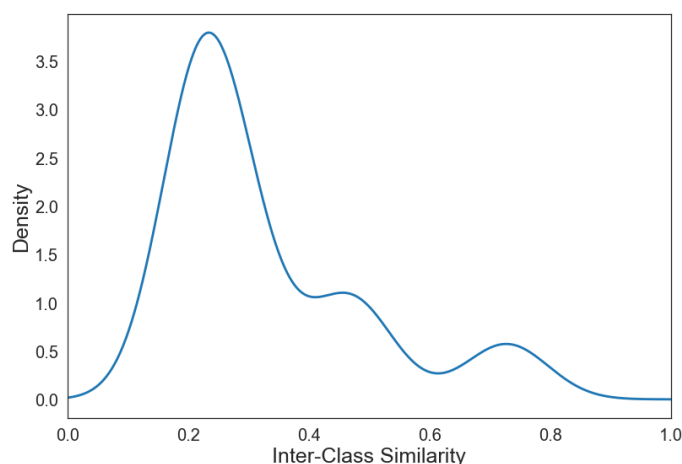


Figure 28: Chemical inter-class similarity of PNP compound classes for CPA investigations. compound classes was determined (Figure 28). Overall, the calculated MBS is relatively low, assuming that compound classes are similar at a similarity of more than 75%. Even though some of the classes are similar to each other, the majority of comparisons revealed significantly

lower MSB. These results parallel the results found for the chemical diversity of the dataset and hints towards a high phenotypical diversity and a broad coverage of biological space by the considered compound classes. Comparing the compounds of one class to themselves could also deliver intra-class similarities (Figure 29, upper diagonal). Generally, although there were exceptions, the intra-class comparisons revealed higher similarity values >70%. This suggests that the dataset consists of homogenous compound classes that are phenotypically diverse.

#### 4.2.1 Influence of the Fusion Pattern on Morphological Activity

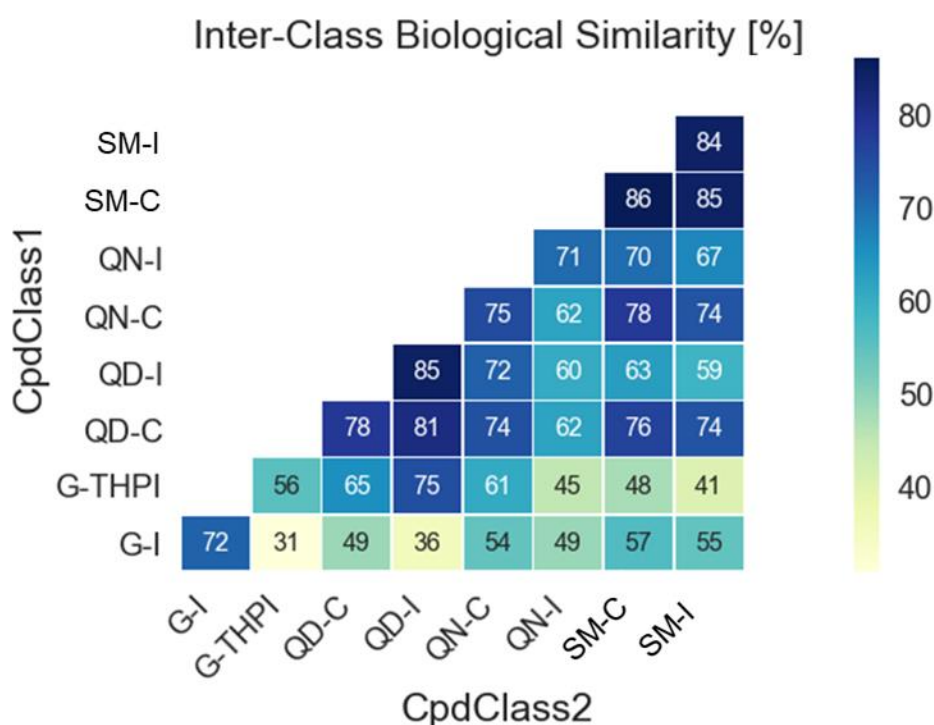


Figure 29: Median biosimilarities (MBS) calculated between PNP compound classes from CPA investigations.

The PNP compound classes GF-I and GF-THPI, that were derived from the griseofulvin and the indole fragment, were identified as two classes suitable for the investigation of different fragment connectivities between two compound classes. While in the GF-I class (two sub classes based on different regioisomers) the two fragments are connected in an edge fused manner, the fragments are connected through a tetrahydropyran (THP) via a spiro fusion in the G-THPI class. Comparison of the compound classes by PCA indicated a clear difference in the morphological profiles between the compound classes but similar morphological changes within each compound class, resulting in the formation of two clusters (Figure 30). The calculated MBS (Figure 29, Section 4.2) also proved this finding. The intra-class similarities are significantly higher than the inter-class similarity (31%). Generally, the finding is fitting

the expectation, considering that the binding of a small molecule to a protein may not only be based on the compound's functionalities, but also its three-dimensional shape.<sup>[9]</sup>

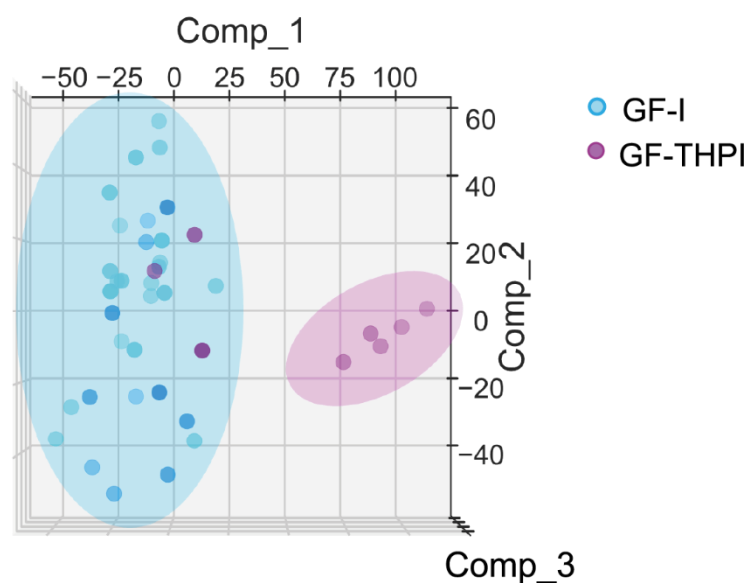


Figure 30: Morphological comparison of griseofulvin-indole classes with different fusion patterns (GF-I (griseofulvin-indoles, blue) vs GF-THPI (griseofulvin-tetrahydropyranoindoles, purple), Expl. Var.: Comp\_1 (39.9%), Comp\_2 (25.8%), Comp\_3 (9.4%); induction: 15-40%). Comp = principal component; PCA = principal component analysis

#### 4.2.2 Influence of Fragment Combinations on Morphological Activity

Furthermore, the composition of the PNP dataset allowed the comparison of fragment combinations. By looking at the individual fragments and their various combinations with other fragments, it was hypothesised that conclusions could be drawn about the influence of that particular fragment on morphological activity. It was assumed, that fragments may either dominate the morphological profile or that their morphological activity can be influenced by another fragment. Comparison of indole-containing compounds by PCA (Figure 31a) led to a defined clustering of these compounds according to the different compound classes. Additionally, the MBS values (Figure 29) were generally low ( $8/10 \leq 60\%$ , median: 52%), also indicating a broad variance between the phenotypic activity of the indole compound classes. This outcome prompted the conclusion that phenotypic change induced by indole-containing PNPs is not exclusively based on the indole structure but influenced by the other fragment. This means, the indole fragment is non-dominating.

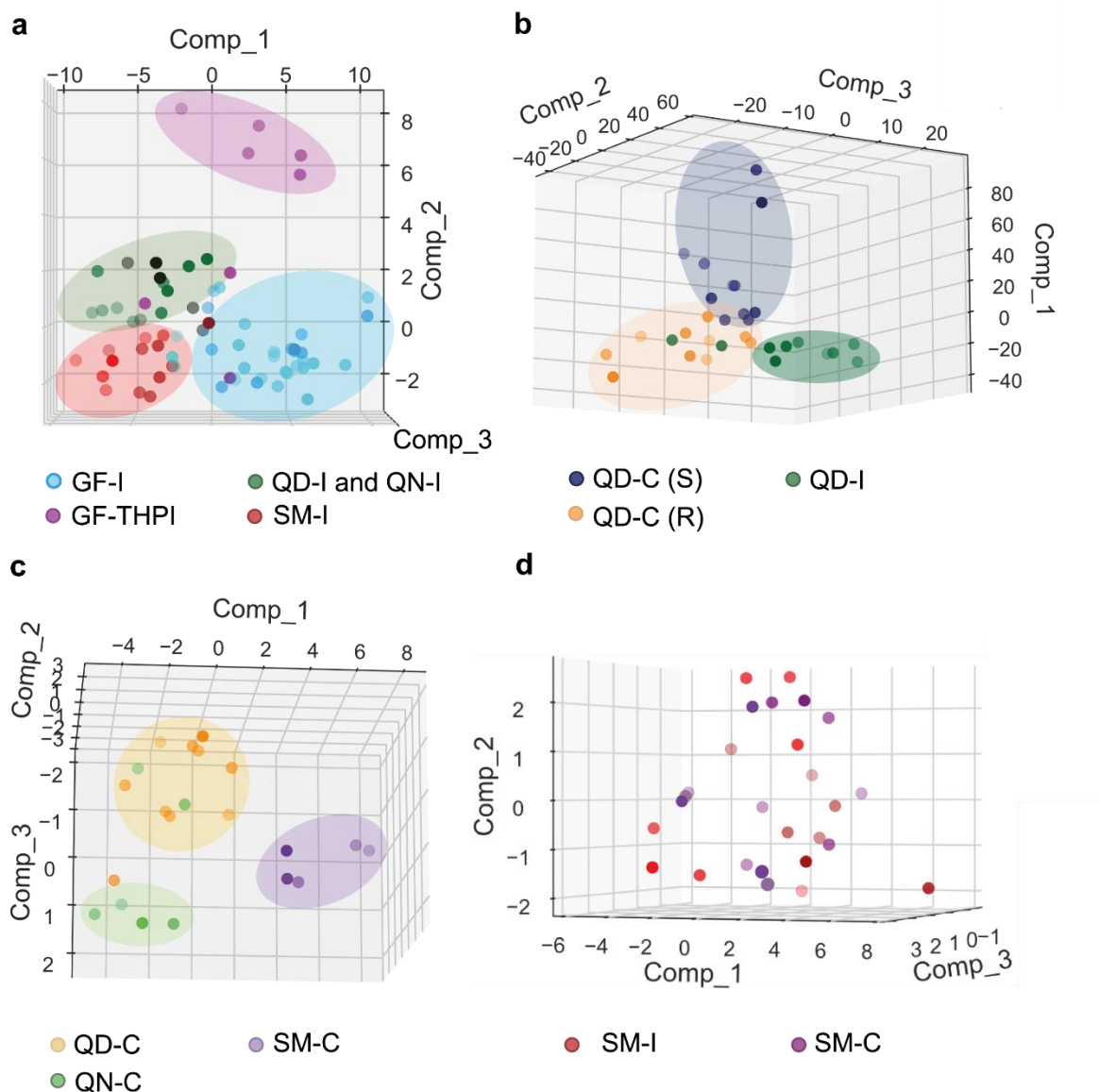


Figure 31: Comparisons of diverse fragment combinations; **(a)** PCA of indole-containing PNPs: GF-I (griseofulvin-indoles, blue), GF-THPI (griseofulvin-tetrahydropyranoindoles, purple), QD-I and QN-I (cinchona alkaloid-indoles, green) and SM-I (sinomenine-indoles (red); Expl. Var.: Comp\_1 (55.1%), Comp\_2 (13.0%), Comp\_3 (8.6%); **(b)** PCA of quinidine-containing PNPs: QD-C (S) (quinidine-chromanone (S-isomer), dark blue), QD-C (R) (quinidine-chromanone (R-isomer), orange) and QD-I (quinidine-indole, green); Expl. Var.: Comp\_1 (45.2%), Comp\_2 (19.6%), Comp\_3 (7.6%); **(c)** PCA of chromanone-containing PNPs: QD-C (quinidine-chromanones, yellow), QN-C (quinine-chromanones) and SM-C (sinomenine-chromanone, purple); Expl. Var.: Comp\_1 (52.4%), Comp\_2 (10.6%), Comp3 (8.2%); **(d)** PCA of sinomenine-containing PNPs: SM-I (sinomenine indoles, red), SM-C (sinomenine chromanones, purple); Expl. Var.: Comp\_1 (54.3%), Comp-2 (13.7%), Comp\_3 (7.0%); all inductions: 15-40%; Comp = principal component; PCA = principal component analysis.

Analysis of quinidine-containing PNPs also showed a clear clustering in the PCA (Figure 31c) and additional MBS values below the similarity cut off (<75%; Figure 29: 63% and 72%), leading to the assumption, that quinidine is a non-dominating fragment as well. An additional interesting finding from this analysis was that the two diastereomeric compound classes QD-C (S) and QD-C (R), that only differ in the configuration of the connecting spiro center, also separated in the PCA. This suggests, that different diastereomers can be identified by the CPA and may have different bioactivities.

Compounds derived from the chromanone fragment were investigated in a similar manner. PCA again revealed a clear clustering of compounds according to the investigated compound classes (Figure 31c). However, in this case the MBS was calculated to be very high (Figure 29:  $5/6 \geq 75\%$ ; median: 77%). Based on profile differences indicated by the PCA result, the chromanones are most likely still non-dominating but that fragments that have a high MBS and no clustering in this type of PNP analysis may be identified as dominating. This definition is true for the sinomenine-derived compounds (Figure 31d). The compounds showed no clustering according to the compound classes in the PCA, but instead an equal distribution of compounds was observed. Furthermore, the comparison of the sinomenine classes resulted in a high MBS (Figure 29: 85%) and led to the assumption, that the sinomenine fragment is dominating.

The PCA and MBS analysis was performed for each of the six different fragments, resulting in the identification of sinomenine as the only dominating fragment in the dataset. Based on the observation, that most of the fragment combinations were built from two non-dominating fragments led to the hypothesis that the phenotypic activity is a result of the combination of fragments rather than of one fragment. As discussed in section 4.2.1, the connectivity patterns and arrangements also seem to influence the bioactivity.

#### 4.2.3 Prediction of Novel Fragment Combinations

Considering the identification of dominating and non-dominating fragments, it was hypothesised that further combination of non-dominating fragments with novel fragments may lead to novel morphological profiles. The combination of dominating fragments on the other hand may lead to PNPs sharing similar profiles. In general, with regard to the design of novel PNP classes that ideally would have novel activities, the use of non-dominating fragments is beneficial. To prove the hypothesis for future PNP design, further compound classes were designed and synthesised.

#### 4.2.3.1 Synthesis of Quinidine Isocoumarins

Since the quinidine fragment was identified as a non-dominating fragment throughout the previous analysis, it was fused to a novel fragment that is not represented in the previous analysis to test the hypothesis. The isocoumarin fragment was identified as a suitable combination partner for quinidine, based on its frequent occurrence in NPs and broad spectrum of bioactivities such as antifungal, antibiotic, anticancer, cytotoxic and anti-inflammatory activities.<sup>[88]</sup> The isocoumarin derivative cytogenine<sup>[89]</sup> showed antidiabetic effects in mice and oospolactone<sup>[90]</sup> has antifungal activities.

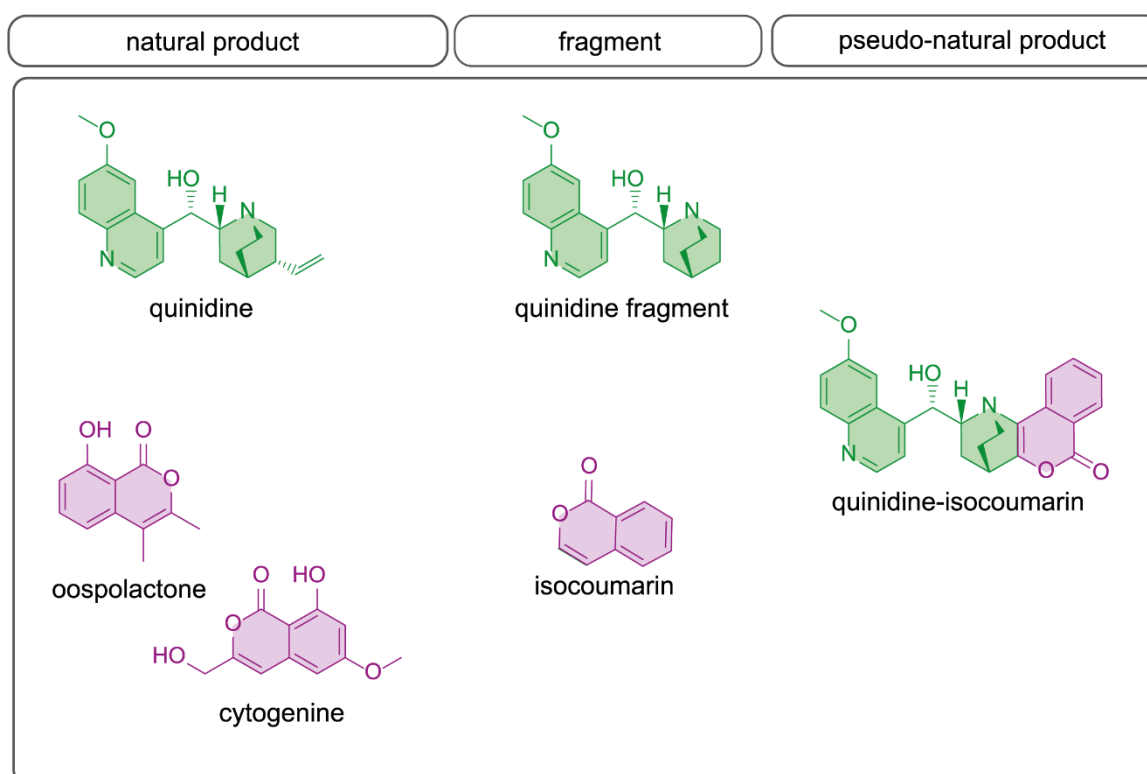


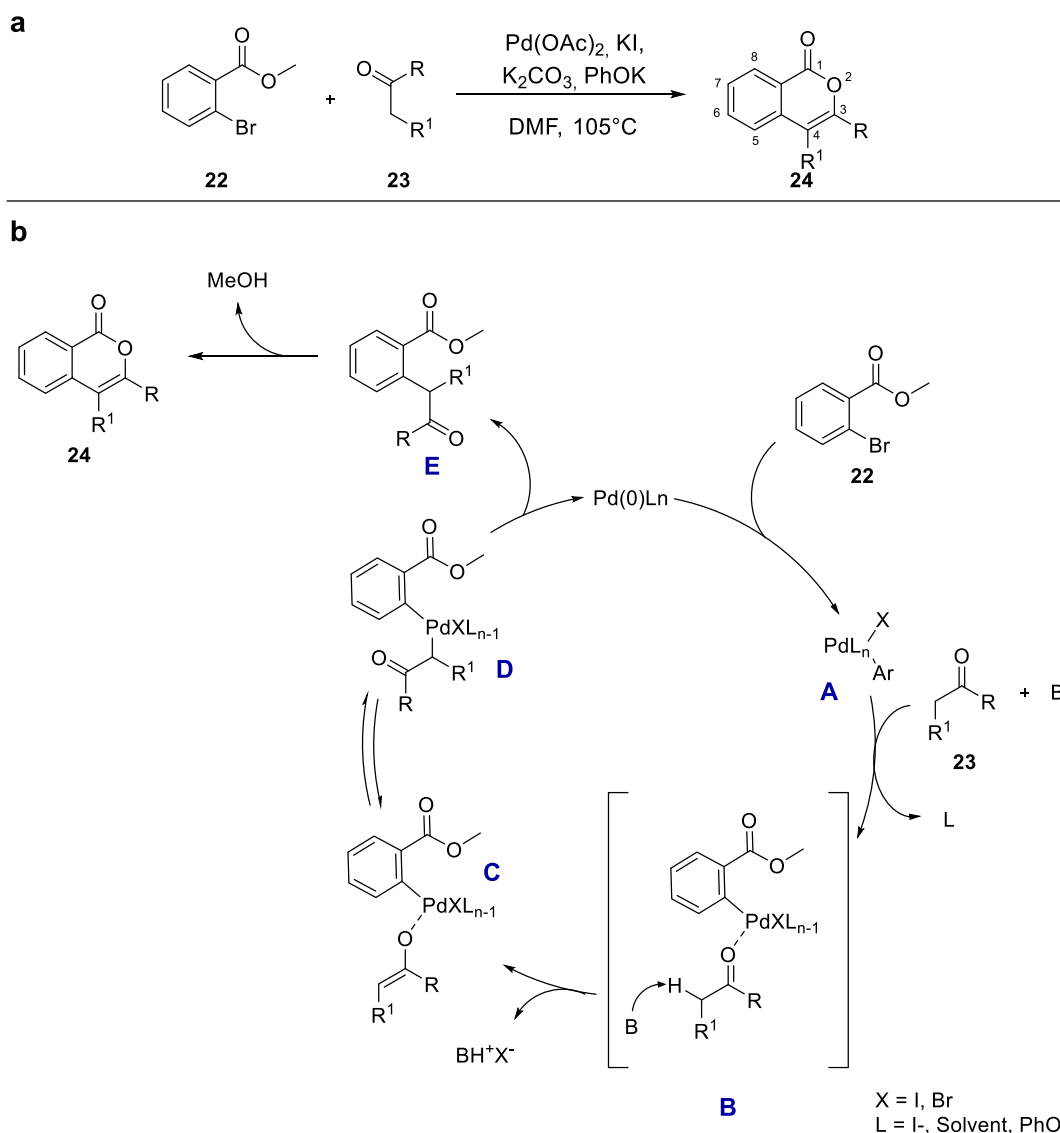
Figure 32: Design principle for of quinidine derived isocoumarins (QD-IC); shown are the parental NPs, derived fragments, and the structure of the novel PNP class.

Another reason to choose this fragment was the availability of an isocoumarin-forming reaction that may be compatible with the previously described ketone functionalised alkaloid. Casnati *et al.* described an intermolecular Pd-catalysed annulation reaction of 2-bromobenzoates with simple  $\alpha$ -saturated ketones to synthesize isocoumarins (Scheme 8a).<sup>[91]</sup>

Most of the previously reported metal-catalysed methods to form isocoumarins are intramolecular reactions of rather complex benzoic acid derivatives bearing an alkyne substituent in the suitable position.<sup>[92]</sup> Also, intermolecular annulation methods starting from benzoic acids and expensive alkynes gained interest; however, many of these methods have regioselectivity issues. Later, the usage of diketones and vinyl acetates as coupling partners moved into focus



and in 2017 Casnati *et al.* reported the first coupling of benzoates with a variety of simple saturated ketones.<sup>[91,93]</sup> Their synthesis was significantly improved by the addition of potassium iodide, and after investigation of its role for the reaction, they hypothesised that iodide may serve as activating ligand on the Pd species. Additionally, they used a combination of two bases ( $K_2CO_3$  and potassium phenolate). The phenolate anion was also suggested to serve as Pd ligand in the annulation reaction. Following their proposed mechanism (Scheme 8b), oxidative addition of  $Pd(0)L_n$  to the bromobenzoate (**A**) is followed by coordination of the carbonyl oxygen to the formed Pd(II) complex (**B**). Subsequent deprotonation by base leads to the formation of a Pd-enolate intermediate, that is in equilibrium between O- and C-bound forms (**C** and **D**). Reductive elimination from the C-bound enolate regenerates the  $Pd(0)L_n$  catalyst and leads to the release of intermediate that (**E**) that cyclises to the desired isocoumarin scaffold (**24**) with the release of methanol.<sup>[91]</sup>



Scheme 8: Pd-catalysed annulation reaction for the synthesis of isocoumarins from ketones and 2-bromobenzoates; **(a)** reaction conditions, optimised by Casnati *et al.*; **(b)** proposed mechanism by Casnati *et al.*<sup>[91]</sup>

Overall, Casnati *et al.* showed a broad substrate scope for their reaction, allowing various substituents (aromatic and aliphatic) in the isocoumarin 3-position and on the phenyl moiety. But what was their most interesting example regarding the use of this synthetic method for the coupling of isocoumarins to quinidine, was the applicability of alicyclic substrates. However, considering the already established synthetic route to access cinchona alkaloid ketones, a way more complex cyclic coupling partner was planned to be introduced. Therefore, a further optimisation of the described reaction conditions was expected.

By applying the reaction conditions optimised by Casnati *et al.* (Table 5, entry 1), the desired PNP could be generated, but in a low yield of 12%. Considering this first successful synthesis of quinidine-isocoumarins, the reaction conditions were subjected to optimisation. Representative optimisation conditions data are summarised in (Table 5).

Table 5: Optimisation of reaction conditions for the Pd-catalysed annulation of quinidine ketone and 2-bromomethylbenzoate.

Reaction scheme: 2-bromomethylbenzoate (22) + quinidine ketone (3)  $\xrightarrow[\text{DMF, 105}^\circ\text{C}]{\text{K}_2\text{CO}_3, \text{PhOK}, \text{Pd(OAc)}_2, \text{KI}}$  quinidine-isocoumarin (25a)

Entry	Pd(OAc) <sub>2</sub> eq.	Ligand	Base (eq.)	Additive	Time [h]	Yield [%]*
1	0.1	-	K <sub>2</sub> CO <sub>3</sub> /PhOK (1.1/0.3)	KI	48	12
1a <sup>#</sup>	0.1	-	K <sub>2</sub> CO <sub>3</sub> /PhOK (1.1/0.3)	KI	48	3
1b <sup>#</sup>	0.1	-	K <sub>2</sub> CO <sub>3</sub> /PhOK (1.1/0.3)	KI	48	traces
2	0.2	-	K <sub>2</sub> CO <sub>3</sub> /PhOK (1.1/0.3)	KI	48	10
3	0.1	-	K <sub>2</sub> CO <sub>3</sub> /PhOK (1.1/2)	KI	24	15
4	0.1	-	K <sub>2</sub> CO <sub>3</sub> /PhOK (1.1/2)	TBAI	24	traces
5	PdCl <sub>2</sub> , 0.1	-	K <sub>2</sub> CO <sub>3</sub> /PhOK (1.1/2)	KI	24	traces
6	0.1	-	KOAc/PhOK (1.1/2)	KI	24	traces
7	0.1	-	K <sub>2</sub> CO <sub>3</sub> /tBuOK (1.1/4)	KI	24	81
8	0.1	CataCXium	K <sub>2</sub> CO <sub>3</sub> /tBuOK (1.1/4)	KI	5	80 (73)
9	0.1	CataCXium	tBuOK (4)	KI	24	44
10	0.1	CataCXium	K <sub>2</sub> CO <sub>3</sub> /tBuOK (1.1/4)	-	5	57

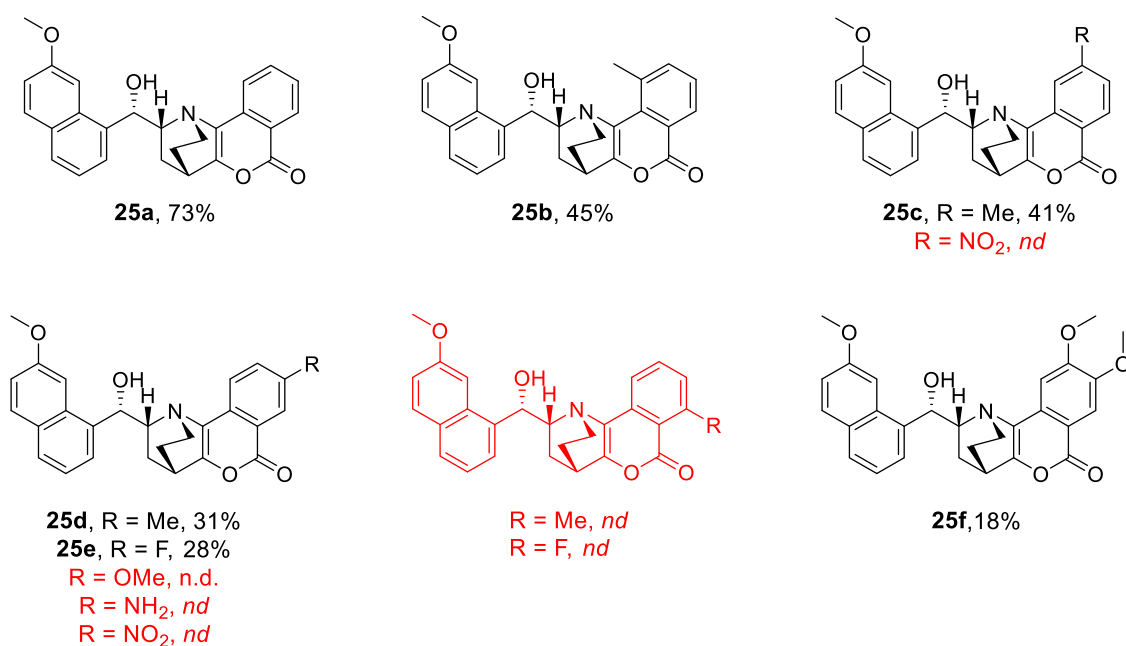
\* Yields determined from crude NMR (isolated yield); constant reaction conditions: T = 105°C (#1a: T = 95°C; 1b: T = 115°C); solvent: DMF.

Changing the temperature to either higher or lower temperatures led to lower reaction yields (entries 1a and 1b). Additionally, an increase in catalyst loading (Table 5, entry 2) did not lead to an improved yield. Increasing the second base (PhOK) concentration (Table 5, entry 3) on the other hand led to a slightly better yield by simultaneous reduction of the reaction time.

## Part II

Changing of either the iodine source, the Pd source or the first base ( $K_2CO_3$ ), did not improve the reactions success. Interestingly, the exchange of the second base to another alcoholate (tBuOK) lead to a significant increase of the yield to 81%. Considering the previously described role of the alcoholate as potential Pd ligands, this increase in yield might be due to different sterical and electronic properties of the two alcoholates.

Furthermore, it was shown that the addition of the Pd ligand CataCXium decreased the reaction time to 5 h while retaining a yield of 80% (Table 5, entry 8). Even though, a stronger base was substituted for PhOK, the addition of the first base ( $K_2CO_3$ ) was important for the reaction performance. Conducting the experiment without addition of potassium carbonate led to a significant decrease in yield (Table 5, entry 9). Last, performing the reaction with optimised conditions, but without iodine source, proved the importance of KI for the reaction (Table 5, entry 10).



Scheme 9: Quinidine-isocoumarins (QD-IC) for CPA investigations; failed couplings are indicated in red.

For the generation of a compound subset suitable for the CPA comparison, the quinidine ketone was fused to 2-bromobenzoates bearing substituents in different positions. Overall, only the benzoate substitution in ortho-position to the carboxylic ester did not afford the desired isocoumarin products under the optimised reaction conditions. Introducing a methyl group was possible in all positions except this one. Furthermore, a fluorine group (**25e**) or two methoxy groups (**25f**) were introduced to the isocoumarin moiety in a moderate yield. Based on the collection of a rather small compound set, it is difficult to assume any effects of different

functional groups on the reactivity. However, it is notable that the benzoate ortho-position was not suitable for substitution, and that the nitro group which is characterised by a strong -M and -I effect could not lead to any product formation in meta or para position.

In total, 6 derivatives were subjected to the CPA, of which 4 were active (induction >5%) at 10  $\mu$ M. To generate phenotypic profiles in an induction range that was suitable to compare quinidine-derived PNPs (20-40%), some of the isocoumarins were tested at higher concentrations (30 or 50  $\mu$ M). Following this general procedure, 5 morphological profiles in an appropriate induction range (19-40%) were identified for further investigations.

#### 4.2.3.2 CPA Analysis of Predicted Compounds

To validate the hypothesis that it is possible to predict whether a novel PNP compound class will either have a unique or a similar phenotypic activity, the newly synthesised compounds were compared to the existing PNP classes. The quinidine-isocoumarins (QD-IC) were hypothesised to induce a unique phenotypic profile in the CPA, since the quinidine fragment was previously identified to be non-dominating. PCA of the quinidine indoles (QD-I) and the quinidine chromanones (QD-C) together with the novel quinidine compound class gave an overall less clear picture than in some of the previous cluster formations. Generally, the members QD-IC class showed a wide distribution over the 3D space (Figure 33a). However, most of the compounds were falling in a space different from the previous compounds. Together with overall low MBS values (Figure 33b, 64-74%), it was at least possible to prove that the phenotypic activity of the quinidine fragment can be influenced by other fragments.

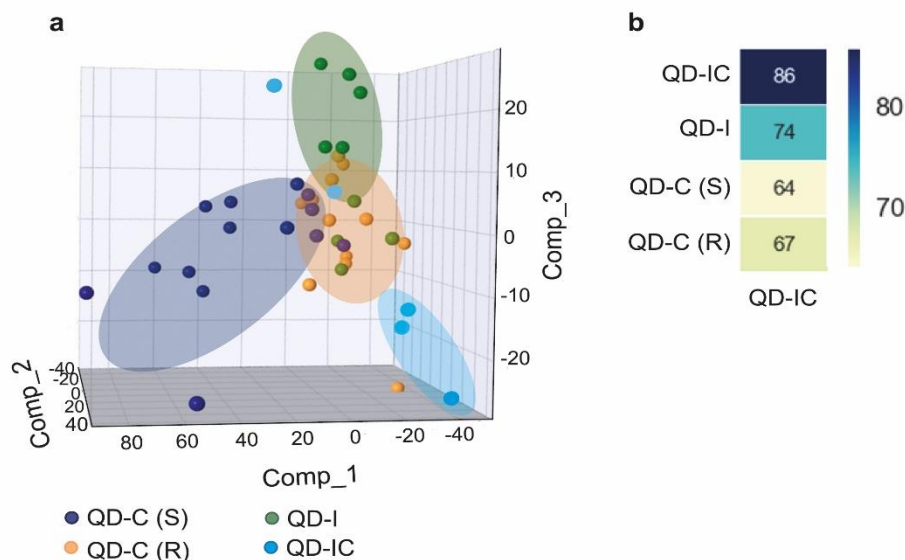


Figure 33: Comparison of QD-IC (quinidine isocoumarins) to previous quinidine PNPs; **(a)** PCA of QD-C (S) (quinidine-chromanone (S-isomer), dark blue), QD-C (R) (quinidine-chromanone (R-isomer), orange), QD-I (quinidine-indole, green) and QD-IC (quinidine-isocoumarin, light blue), Expl. Var.: Comp\_1 (42.7%), Comp\_2 (16.7%), Comp\_3 (8.7%); all inductions: 15-40%; Comp = component; PCA = principal component analysis; **(b)** MBS values calculated between QD-IC and previous quinidine derived PNPs.

A clearer picture was obtained for the chromane-indoles (C-I, Figure 34a), a PNP compound class that was derived from two non-dominating fragments and therefore hypothesised to induce a unique phenotype in the CPA. Since the C-I class was obtained by combination of two previously investigated fragments, it was possible to compare it to both, the indole-derived PNPs and the chromanone PNPs. The C-I cluster highlighted in purple clearly separated from previously found clusters for both, indole- and chromanone-derived PNPs (Figure 34b and Figure 34d). Furthermore, the MBS values obtained from comparison of the C-I class with both indole- and chromanone-subclasses, are below the 75% biosimilarity threshold (Figure 34c and Figure 34e). These findings proved the hypothesis: the C-I compound class showed a unique phenotypic activity.

Proof of the non-dominating phenotypic behaviour of quinidine as well as indole and chromanone suggests that these fragments are suitable combination partners for future PNP projects. Combination with distinct fragments has a high potential to not only explore unknown areas of chemical, but also biological space.

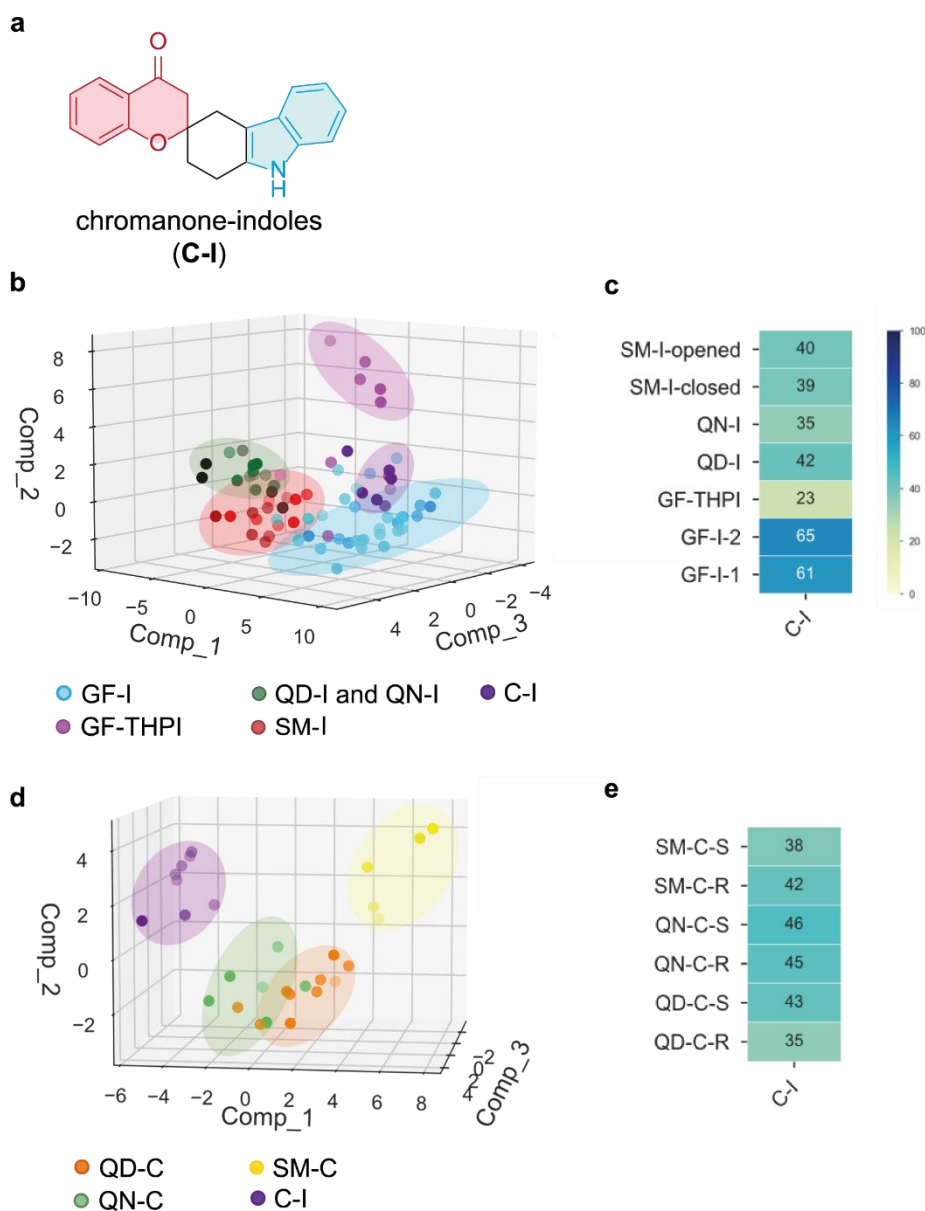


Figure 34: Comparison of C-I (chromanone-indoles) to previous indole- and chromanone-derived PNPs; (a) general structure of C-Is; (b) PCA of indole containing PNPs: GF-I (griseofulvin-indoles, blue), GF-THPI (griseofulvin-tetrahydropyranoindoles, violet), QD-I and QN-I (cinchona alkaloid-indoles, green), SM-I (sinomenine-indoles, red) and C-I (chromanone-indole, purple); Expl. Var.: Comp\_1 (52.3%), Comp\_2 (12.4%), Comp\_3 9.1%); (c) MBS values calculated between C-I and previous indole derived PNPs; (d) PCA of chromanone-containing PNPs; QD-C (quinidine-chromanones, yellow), QN-C (quinine-chromanones, green) S-C (sinomenine-chromanone, yellow) and C-I (chromanone-indoles, purple); Expl. Var.: Comp\_1 (49.7%), Comp\_2 (19.6%), Comp\_3 (6.6%); (e) MBS values calculated between C-I and previous chromanone-derived PNPs; b and d: all inductions: 15-40%; Comp = principal component; PCA = principal component analysis.

## Part II

To prove, that it is also possible to predict a dominating phenotypic behavior, another sinomenine containing PNP class was investigated by means of the CPA. Sinomenine-pyrimidines (SM-P, Figure 35a) were compared with the previously described sinomenine-derived PNPs in a PCA. This led to the observation that the new SM-P compound class also fits the behaviour of the previous classes in which no defined cluster of SM-P could be found (Figure 35b). Additionally, the MBS values were high (>80%) for the comparisons with all other sinomenine-derived PNPs (Figure 35c). This led to the conclusion that the prediction was right, and that the sinomenine fragment is not suitable for the design of novel PNP compound classes. Combinations with further fragments will likely lead to a similar phenotypic behaviour.

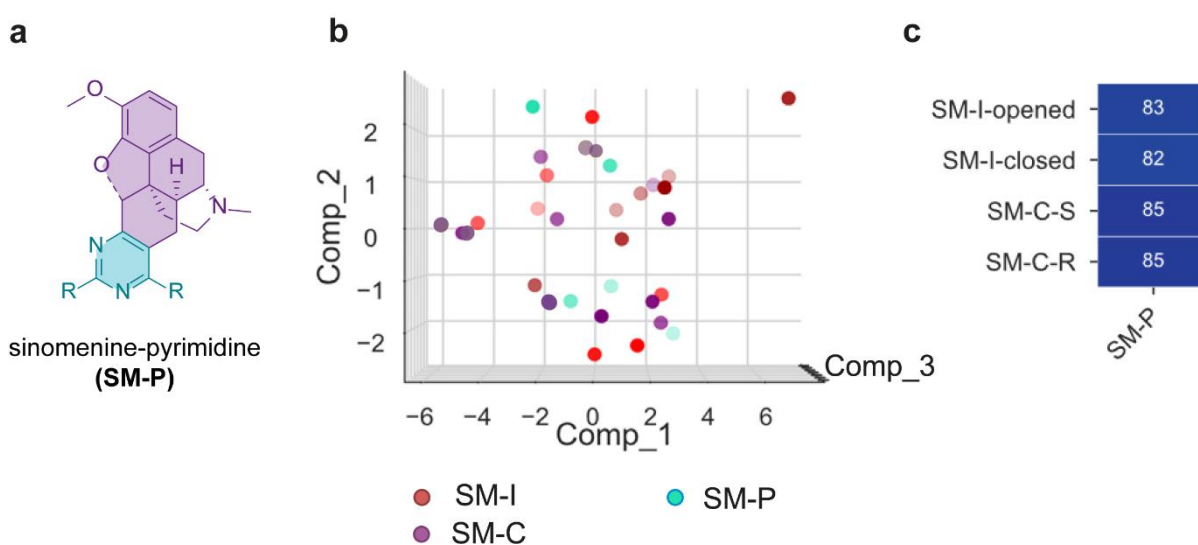


Figure 35: Comparison of SM-P (sinomenine-pyrimidines) to previous indole and chromanone derived PNPs; (a) general structure of SM-Ps; (b) PCA of sinomenine containing PNPs: SM-I (sinomenine indoles, red), SM-C (sinomenine chromanones, purple) and SM-P (sinomenine-pyrimidines, turquoise); Expl. Var.: Comp\_1 (50.0%), Comp\_22 (14.0%), Comp\_3 (9.4%); all inductions: 15-40%; PC = principal component; Comp = component; PCA = principal component analysis; (c) MBS between SM-P and previous sinomenine containing compound classes.



### 4.3 Conclusion

Comparing the morphological profiles that were obtained for diverse PNPs in the CPA gave insights into the influence of fragments and their combination on the PNP phenotypic activity. Investigation of a compound collection that was based on the combination of a small subset of fragments (indole, chromanone, quinine, quinidine, griseofulvin, sinomenine) revealed, that the combination of different fragments can lead to diverse morphological profiles. Furthermore, the connectivity of fragments in different arrangements led to diverse profiles. Nevertheless, one of the fragments in the dataset (sinomenine) proved to dominate the bioactivity. A fusion of various fragments to sinomenine led to similar morphological profiles.

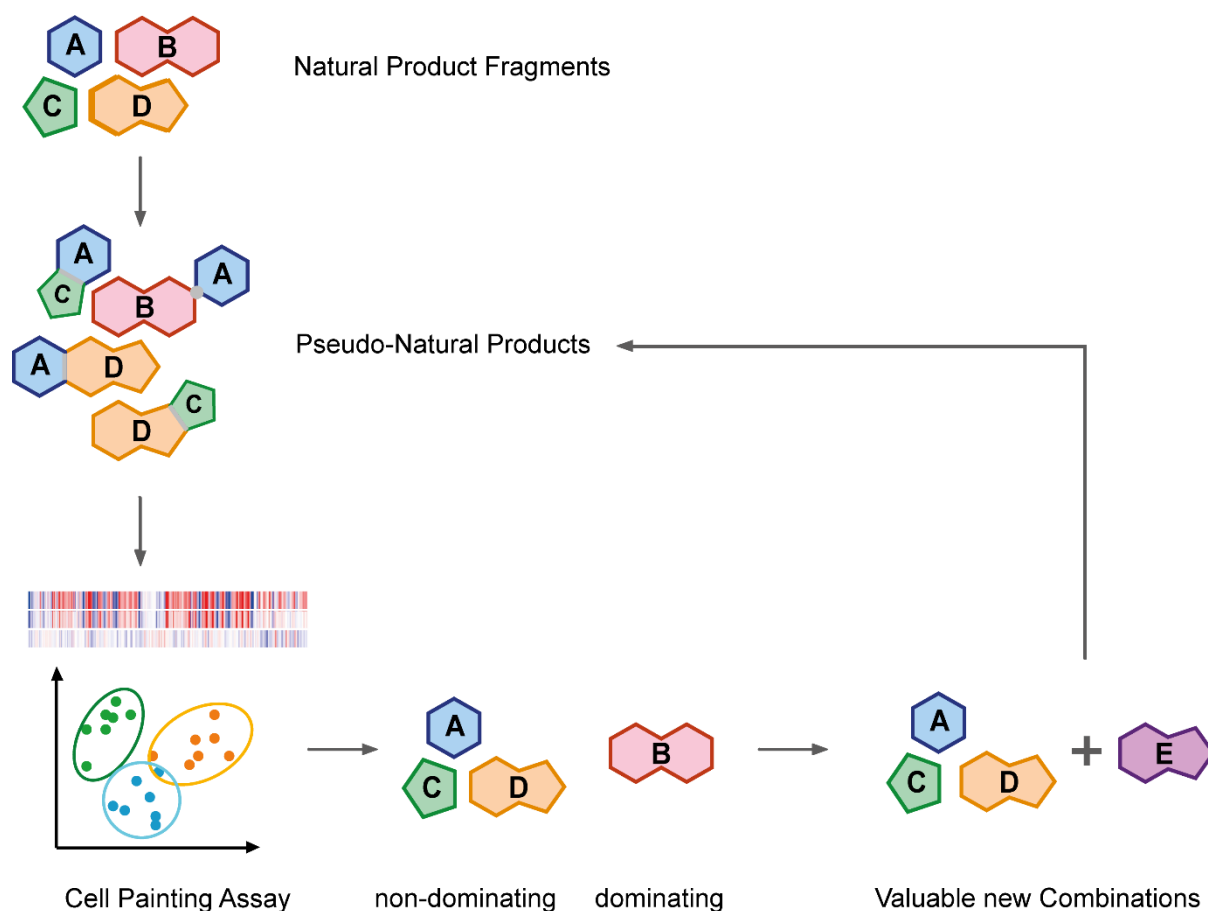


Figure 36: General principle for the application of the CPA for the design of novel PNP compound classes.

Based on the assumption, that non-dominating fragments are more suitable for the design of novel and unique PNP classes, the morphological behaviour of further PNPs was predicted. For the quinidine-isocoumarins and chromanone-indoles a unique phenotypic outcome was expected, while the sinomenine-pyrimidines were thought to show a similar phenotypic profile as previous sinomenine PNPs. Both hypotheses were true, leading to the suggestion to

## Part II

incorporate morphological profiling to the design process of novel PNP classes. The classification in dominating and non-dominating fragments may improve the biological diversity of PNP classes by focusing on the combination of non-dominating fragments (Figure 36).

## 5. Part III: Chromalines – Cell Painting-Aided Design of a Novel PNP Compound Class

### 5.1 Introduction

In previous CPA-based investigations, the PNP classes used for comparisons not only differed in their fragment combination, but also in their fragment connectivity (Part 2; Figure 25). Furthermore, it was shown that the connectivity can have a crucial influence on the morphological profiles (see Part 2; Figure 30)<sup>[14]</sup>. Based on this context, PNP classes should now be compared with each other, which share a fragment but also have the same connectivity. This study may provide a further insight to the role of the connection type and the combination of different fragments. Compounds sharing the same connection type could, based on their similar 3D structure, have similar morphological profiles. However, different fragments may also still result in diverse bioactivities. Additionally, this study may give further insights into the role of substituent pattern on the bioactivity of molecules.

To facilitate this analysis, previous PNP classes designed and synthesised by the Waldmann group were examined for PNP classes sharing the same connectivity pattern. Besides this, the compound classes had to have activity in the CPA. Two classes, that met these requirements are the chromopyrones<sup>[24]</sup> and the pyrroquinolines<sup>[14]</sup> (Figure 37a). Both classes combined two NP fragments by a bridged fusion, whereby the fragments shared three atoms with each other.

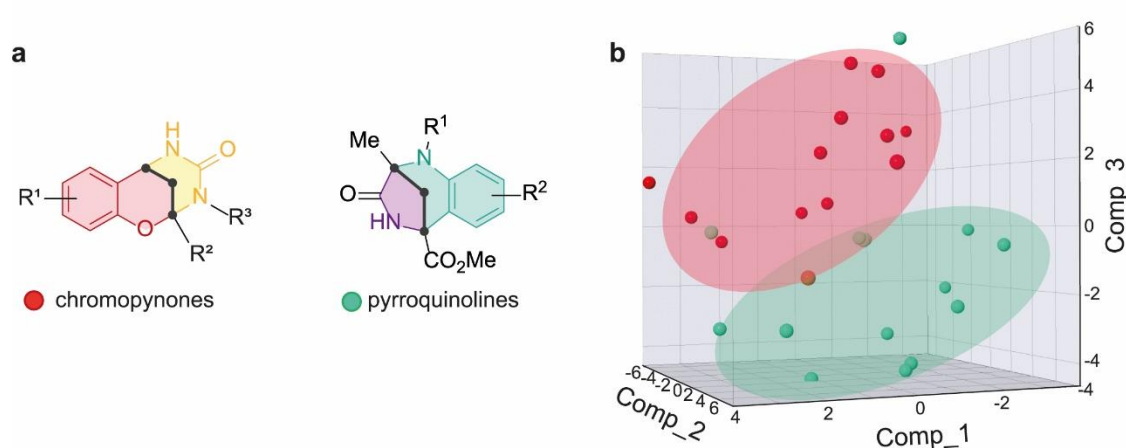


Figure 37: (a) General structures of chromopyrones and pyrroquinolines; (b) PCA of chromopyrones (red) and pyrroquinolines (green); Expl Var: Comp\_1 37.5%, Comp\_2: 21.9%, Comp\_3: 11.1%, induction 15-40%; PCA = principal component analysis; Comp = principal component.

### Part III

The chromopyrones were derived from the chromane and the tetrahydropyrimidinone fragments by a multicomponent reaction (see also general introduction 1.1.2.3, Figure 5I). Both fragments are represented in NPs which have diverse bioactivities. Investigation of the chromopyrone class in cell-based assays revealed their activity as glucose uptake inhibitors. Further biological investigation showed a selectivity for the glucose transporters GLUT-1 and GLUT-3. Besides this activity, chromopyrones also induced significant morphological changes in the CPA. Furthermore, the closely related chromanone fragment was proven to be non-dominating in different previous examples (Part II), leading to the conclusion that the chosen chromane fragment most likely is non-dominating.

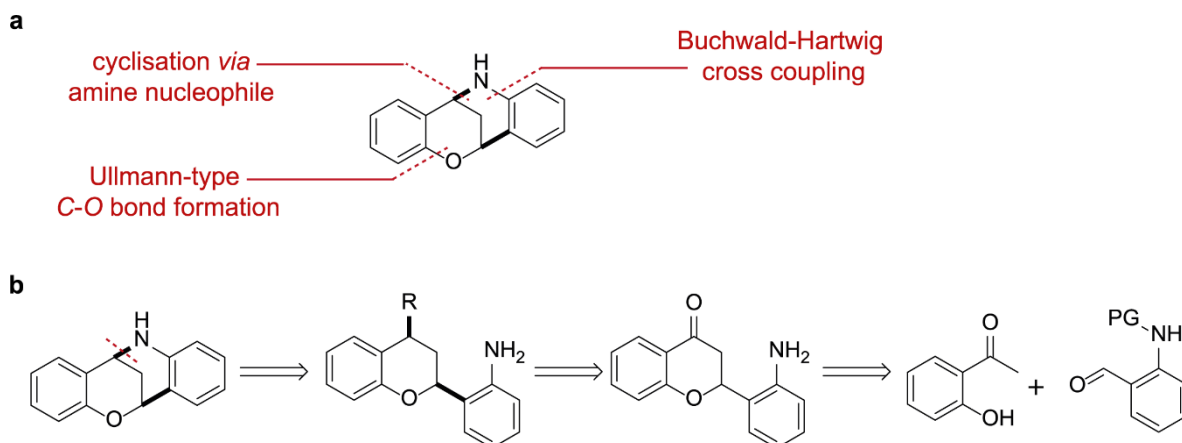
The pyrroquinolines were derived from the NP fragments pyrrolidine and tetrahydroquinolines and were synthesised to investigate the influence of the orientation of fragments to each other. Besides the PNPs that were derived by bridged fused fragment combinations, other compounds with different connectivities and orientations of these fragments were submitted to the CPA. Comparison of the induced morphological changes revealed that the connection and the orientation of the pyrrolidine fragment to the tetrahydroquinoline fragment had a significant influence on the obtained morphological profiles. PCA of the diverse pyrroquinoline subclasses showed a clear clustering according to the connection type. This study not only proved the CPA activity of the bridged compound class, but also was a clear hint towards the non-dominating behaviour of the tetrahydroquinoline (THQ) fragment. Even a different orientation of one incipient fragment could significantly influence the morphological activity.

PCA of the chromopyrones and the pyrroquinolines demonstrated that these PNPs were endowed with different morphological activities. Formation of two distinct clusters for the two PNP classes was observed (Figure 37).

## 5.2 Results and Discussion

### 5.2.1 Synthesis of Chromalines

To build up a chromaline compound set suitable for PCA comparisons a synthetic route had to be developed. From a retrosynthetic point of view, three different main disconnections were identified (Scheme 10a).



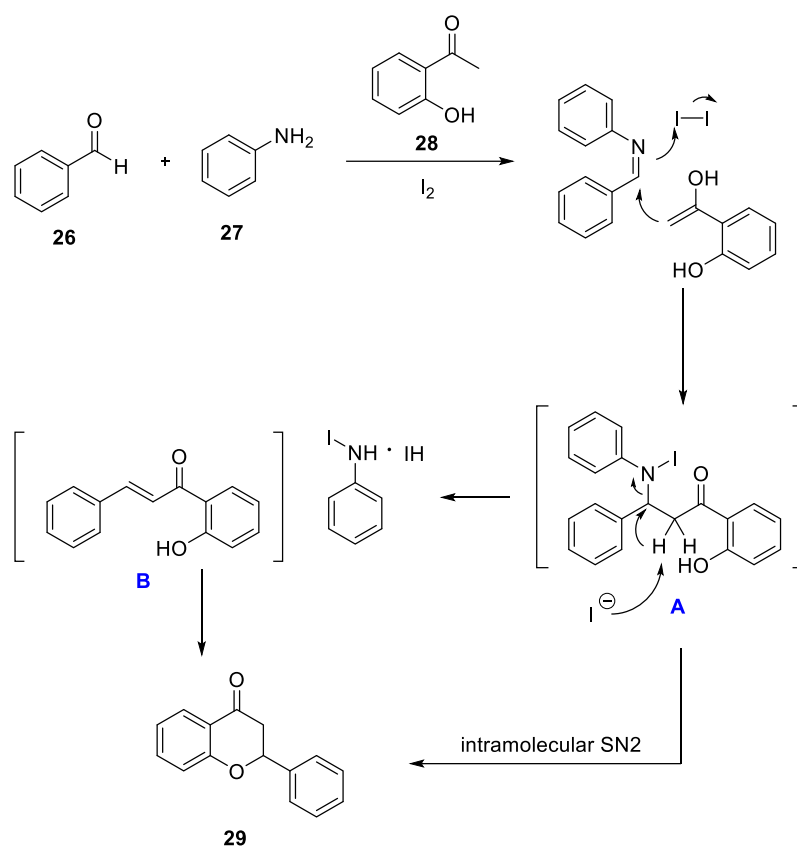
Scheme 10: (a) Retrosynthetic analysis of chromaline; (b) suggested chromaline retrosynthesis starting from flavanone.

Ullmann-type C-O bond formation could give the desired chromaline from 2-(2-halophenyl)-tetrahydroquinolinol. Buchwald-Hartwig cross coupling might allow cyclisation by intramolecular C-N bond formation. Furthermore, the formation of the second C-N bond was suggested to be a promising key step to synthesize the bridged compounds. Potential strategies for a cyclisation might be the introduction of a leaving group or the introduction of a Michael-acceptor. Generally, these starting points may be obtained from flavanones, whose synthesis has been well studied. Based on the starting material availability the flavanone route (Scheme 10b) was further investigated.

#### 5.2.1.1 Synthesis of a Flavanone Starting Material

Due to its occurrence in many NPs with diverse bioactivities and its importance as intermediate in the synthesis of biologically relevant small molecules, a broad range of flavanone generating reactions have been developed. Commonly, flavanones are generated via the cyclisation of substituted 2'-hydroxychalcones that can be derived from 2-hydroxyacetophenones and aldehydes. However, many reported cyclisation reactions require the use of corrosive reagents, high catalyst loadings and/or harsh reaction conditions and show further drawbacks such as low yields, long reaction times and limited synthetic scopes.<sup>[97]</sup>

In 2014 Kavala *et al.* reported an iodine-catalysed, multicomponent Mannich type reaction to synthesise flavanones in one-pot.<sup>[98]</sup> Due to its availability, low cost and high tolerance to air and moisture, iodine was suggested to be a well applicable catalyst.<sup>[99]</sup> Also, the generally used simple setup was suitable for chromaline starting material synthesis. The use of simple and commercially available aldehyde and 2-hydroxyacetophenone starting materials under mild temperature (40 °C) in methanol, were appropriate conditions. Furthermore, they reported a broad scope, containing a nitro-group functionalised flavanone, that was identified as suitable starting point for the chromaline synthesis.<sup>[98]</sup>



Scheme 11: Mechanism of an iodine-catalysed, multicomponent Mannich type reaction to synthesise flavanones.

Kavala *et al.* reported a plausible mechanism for the iodine catalysed reaction (Scheme 11). According to their proposal, imine formation is followed by coordination of the highly polarizable iodine. The activated imine is subsequently attacked by the enol form of the 2'-hydroxyacetophenone to form a novel carbon-carbon bond (intermediate A). Then, intermediate A undergoes an elimination of the N-iodoaniline upon deprotonation facilitated by deprotonation through the iodine anion to form the chalcone intermediate B. Intramolecular 1,4-Michael addition, which may be catalysed by the N-iodoaniline-HI complex, leads to formation of the cyclised flavanone product. Alternatively, intermediate A might undergo an

intramolecular S<sub>N</sub>2 reaction to directly form the flavanone product, by release of N-iodoaniline as leaving group.<sup>[98]</sup>

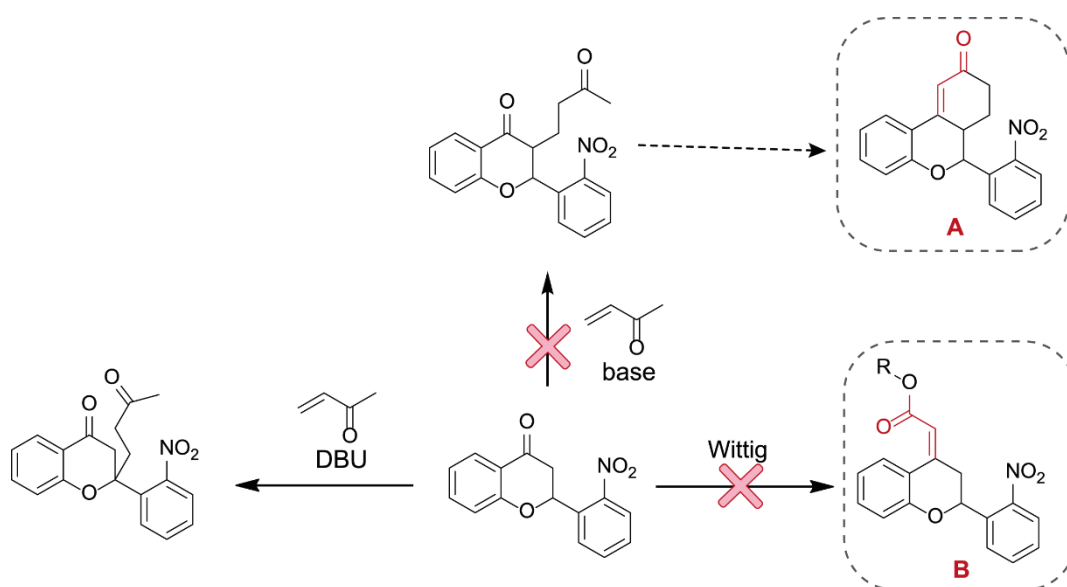
The reported reaction was used to synthesize a subset of nitro-functionalised flavanones from further substituted 2-hydroxyacetophenones and 2-nitrobenzaldehyde. Up-scaling of the reaction by maintaining the described reaction conditions led to a significant drop in the yield, as previously described by Kavala *et al.* Nevertheless, 22 derivatives were successfully synthesised in acceptable amounts for following syntheses (Table 6). Generally, the reaction was found to cover a broad scope, ~85% (22/26) of all tried examples were successful in a 2 g scale. It was possible to introduce substituents to almost all positions of the acetophenone and the aldehyde moiety. Only the R<sup>8</sup> position (ortho to the nitro group) could not be explored, due to the lack in commercially available 2-nitrobenzaldehydes bearing a substituent in this position.

The introduction of a methoxy group bearing a -I effect, to the R<sup>1</sup> position failed, and only traces of the desired product were obtained (Table 6, entry 2). Nevertheless, the reaction of the bulky 1-acetyl-2-naphthol with the benzaldehyde was successful and showed the accessibility of that position. (Table 6, entry 17). 2-Hydroxyacetophenones bearing substituents with an electron-withdrawing effect (such as: F, Br, Cl) generally resulted in similar yields as the unsubstituted starting material. Similarly, the introduction of electron-donating groups (such as NH<sub>2</sub>, OMe, NHCOMe) was possible. Introduction of the methoxy group and the amine functionality to the R<sup>2</sup> position improved the reaction yield (Table 6, entries 6, 7). This might be due to an increased electron density on the hydroxy functionality in its para position, leading to an increased nucleophilicity for cyclisation (see also Scheme 11). Only the introduction of the methoxy group position to the R<sup>3</sup> position (hydroxy meta-position) failed, as it was also observed for the R<sup>1</sup> position. Introduction of electron donating groups (OMe, Me) generally was unfavoured in these positions. Finally, the introduction of two substituents was possible.

All tested 2-nitrobenzaldehydes bearing one or two substituents with either electron-withdrawing or electron-donating groups successfully formed the desired flavanone derivatives. Generally, introduction of electron-withdrawing groups (F, Br, Cl) resulted in lower yield compared to the unsubstituted compound (Table 6, entry 1), while introduction of electron-donating groups (NR<sub>2</sub>, OMe) led to a significant increase in yield.

### 5.2.1.2 Synthesis of Flavan-4-ol from Flavanone

With these diverse flavanone derivatives in hand, a next step was thought to be the activation of the carbonyl carbon, to later allow a cyclisation by nucleophilic attack of the deprotected (reduced) amine. First, different reaction conditions were employed to install a Michael acceptor. HWE reaction could be used to transform the ketone to a suitable  $\alpha,\beta$ -unsaturated ester (Scheme 12, target molecule B).<sup>[100]</sup> However, several attempts applying harsh, high temperature and  $\mu W$ -assisted conditions and using different phosphonates did not give the desired compound in an acceptable yield. Applying strong bases to facilitate the reaction resulted in a decomposition of the flavanone starting material and the use of stable ylids did not lead to product formation. Furthermore, applying Robinson annulation conditions<sup>[101]</sup>, that first introduce a methylvinylketone (MVK) to the ketone  $\alpha$ -position followed by cyclisation to an  $\alpha,\beta$ -unsaturated ketone, were not successful (Scheme 12, target molecule A). Interestingly, the MVK reacted at the  $\beta$ -position instead.



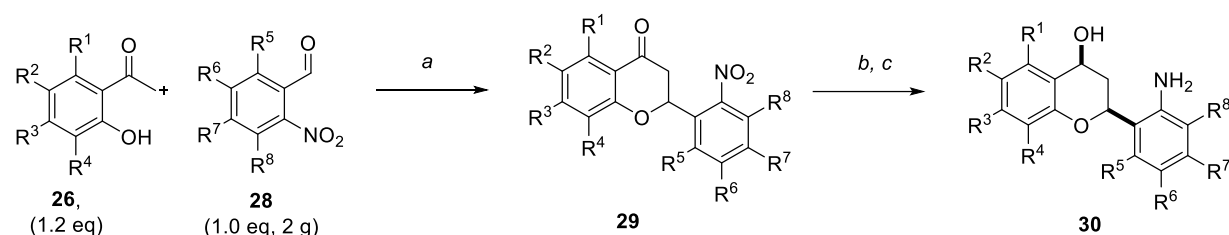
Scheme 12: Failed attempts to introduce a Michael acceptor to the flavanone core-structure.

An alternative approach was to reduce the ketone functionality to an alcohol, to either use it for elimination and cyclisation, or to facilitate a substitution reaction with the free amine (Scheme 10b, R = OH). A straightforward and simple method for the flavanone ketone reduction was established by using sodium borohydride as reducing agent. Interestingly, the reaction was diastereoselective as confirmed by  $^1\text{H}$  NMR spectroscopy (> 95:5 dr) and resulted in the *cis*-isomer. Investigation of previous literature revealed that this observation was made for a similar scaffold.<sup>[102]</sup> Unfortunately, the *cis* configuration is not suitable to apply  $\text{S}_{\text{N}}2$  reaction conditions for cyclisation.



The obtained flavan-4-ol derivatives could be directly reduced in the next step without further purification. The reduction of the nitro-group was facilitated by a Béchamp reduction using molecular iron and hydrochloric acid in acetic acid, ethanol, and water. Overall, an efficient two-step reduction procedure was developed to synthesize the amine functionalised flavan-4-ols (**30**) in moderate to good yields over two steps (Table 6). The critical reduction step, leading to some comparatively low yields, was the nitro-reduction step. With longer reaction times, but also for a couple of substrates, a side product was formed. Isolation and structural elucidation of this side product led to the identification of an aromatised quinoline bearing a phenol substituent in 2-position (Table 7, B (**32**)). To form this side product, it was suggested that a previous formation of the chromaline scaffold (Table 7 (**31**)) might be necessary. A subsequent protonation of the chromane oxygen under acidic conditions, followed by ring cleavage and aromatisation of the quinoline may be a potential path to derive the quinoline compound. Based on this observation, the acid mediated cyclisation to form the final chromaline compound class was further investigated.

Table 6: Reaction scheme to access flavan-4-ols via flavanone; scope and yields of the shown reactions.



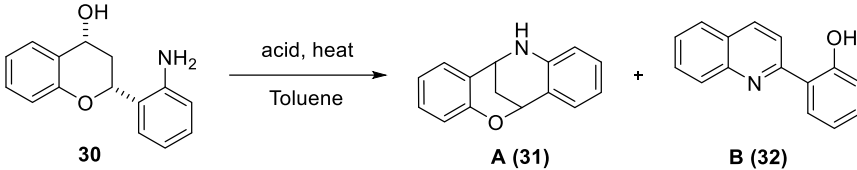
Entry	R <sup>1</sup>	R <sup>2</sup>	R <sup>3</sup>	R <sup>4</sup>	R <sup>5</sup>	R <sup>6</sup>	R <sup>7</sup>	Nr	Yield [%]	Nr	Yield [%]
1	H	H	H	H	H	H	H	29a	35	30a	84
2	OMe	H	H	H	H	H	H	29b	traces	-	-
3	H	Me	H	H	H	H	H	29c	19	30c	80
4	H	Cl	H	H	H	H	H	29d	38	30d	62
5	H	F	H	H	H	H	H	29e	32	30e	60
6	H	NH <sub>2</sub>	H	H	H	H	H	29f	91	30f	13
7	H	OMe	H	H	H	H	H	29g	39	30g	65
8	H	NCOCH <sub>3</sub>	H	H	H	H	H	29h	17	30h	23
9	H	H	Me	H	H	H	H	29i	5	30i	83
10	H	H	Br	H	H	H	H	29j	21	30j	49
11	H	H	F	H	H	H	H	29k	14	30k	73
12	H	H	OMe	H	H	H	H	29l	nd	-	-
13	H	Me	Me	H	H	H	H	29m	31	30m	30
14	H	Cl	Me	H	H	H	H	29n	8	30n	74
15	H	Cl	H	Cl	H	H	H	29o	17	30o	52
16	H	Me	H	Me	H	H	H	29p	nd	-	-
17		C <sub>4</sub> H <sub>4</sub>	H	H	H	H	H	29q	28	30q	11
18	H	H	C <sub>4</sub> H <sub>4</sub>	H	H	H	H	29r	nd	-	-
19	H	H	H	H	Cl	H	H	29s	14	30s	41
20	H	H	H	H	H	Br	H	29t	29	30t	58
21	H	H	H	H	H	F	H	29u	27	30u	56
22	H	H	H	H	H	H	CF <sub>3</sub>	29v	22	30v	51
23	H	H	H	H	H	H	CO <sub>2</sub> Me	29w	23	30w	30
24	H	H	H	H	H	H	NMe <sub>2</sub>	29x	71	30x	traces
25	H	H	H	H	H	OMe	OMe	29x	75	30y	75
26	H	H	H	H	H	OCH <sub>2</sub> O		29z	63	30z	46

a) Aniline (1.5 eq.), I<sub>2</sub> (0.3 eq.), MeOH (1 M), 40 °C, 10-18 h; b) NaBH<sub>4</sub> (1.5 eq.), MeOH (0.1 M), rt, 1 h; c) Fe (6 eq.), HCl (1.4 eq.), EtOH:AcOH:H<sub>2</sub>O (2:2:1, 0.15 M), 80 °C, 1 h.

### 5.2.1.3 Development of an Intramolecular Flavanol Cyclisation Reaction

To potentially favour the formation of the chromaline scaffold (A) instead of the aromatic quinoline compound (B), diverse reaction conditions were investigated. In a first attempt different Brønsted acids were tested. While sulfuric acid in catalytic amounts (Table 7, entry 1) led to a decomposition of the starting material and the observation of traces of compound B (identified by HPLC-MS and crude NMR), the use of acetic acid as solvent (0.05 M, Table 7, entry 2) only gave traces of both products. Changing the acid to trifluoroacetic acid (TFA) allowed the isolation and structural elucidation of the chromaline product. Increasing the TFA concentration (Table 7, entry 4) led to a significant increase of the yield for product A (25%), but also of the undesired product B (20%). Also, the usage of Lewis acids (Table 7, entries 5-7) could not improve the formation of product A and prevent the ring opening to form the undesired side product B.

Table 7: Optimisation of the intramolecular flavanol cyclisation reaction.



The reaction scheme shows the conversion of compound 30 to products A (31) and B (32). Compound 30 is a flavanol derivative with a hydroxyl group and an amino group. The reaction conditions are acid and heat in toluene. Product A (31) is a chromaline scaffold, and product B (32) is an aromatic quinoline compound.

Entry	Acid (eq.)	T [°C]	additives	time	Yield A*	Yield B*
1	H <sub>2</sub> SO <sub>4</sub> (0.2)	100	-	5 h	-	traces
2	AcOH (solvent)	rt-70°C	-	7 d	traces	traces
3	TFA (0.5)	100	-	5 h	14% (10%)	7%
4	TFA (1.0)	100	-	5 h	25%	20%
5	AgOTf (0.2)	100	-	5 h	6%	3%
6	FeCl <sub>3</sub> (0.2)	100	-	5 h	18%	6%
7	Bi(OTf) <sub>3</sub> (0.2)	100	-	5 h	13%	4%
8	TFA (1.0)	150 (μw)	-	1 h	35% (36%)	22% (24)
9	1.5	150 (μw)	-	1 h	41%	22%
10	2.0	150 (μw)	-	1 h	42%	30%
11	3.0	150 (μw)	-	1 h	29%	40%
12	5.0	150 (μw)	-	1 h	8%	30%
13	1.5	150 (μw)	-	5 min	50%	24%
14	1.5	130 (μw)	-	5 min	61%	23%
15	1.5	100 (μw)	-	5 min	25%	7%
16	1.5	130 (μw)	water (1 eq)	5 min	58%	23%
17	1.5	130 (μw)	Mol sieves	5 min	36%	8%

### Part III

Further investigation of the TFA-mediated cyclisation could improve the yield of the desired chromaline product to ~60%. Employing a microwave-assisted reaction and an increase in reaction temperature led to a first improvement (Table 7, entry 8). Adjustment of the TFA concentration under these conditions led to the observation of a defined concentration window that showed improved product formation (Table 7, entries 8-12). By plotting of the NMR yields of product A and B against the TFA concentration (Figure 40), the optimal concentration was determined to be between 1.5 and 2 equivalents. Using 1.5 equivalents of TFA led to the observation of a high A to B ratio and was used for further investigations. While lower TFA concentrations led to a decrease in conversion of starting material, higher TFA concentrations led to the observation of an increase in product B formation and furthermore a decomposition (at 5 equivalents).

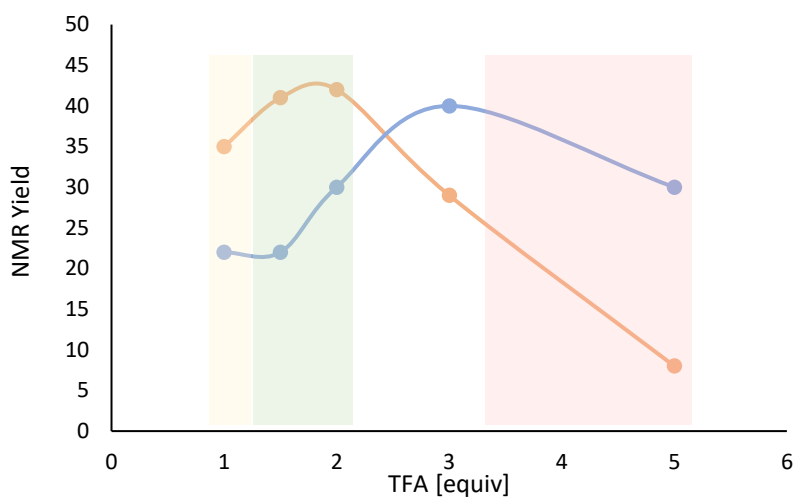


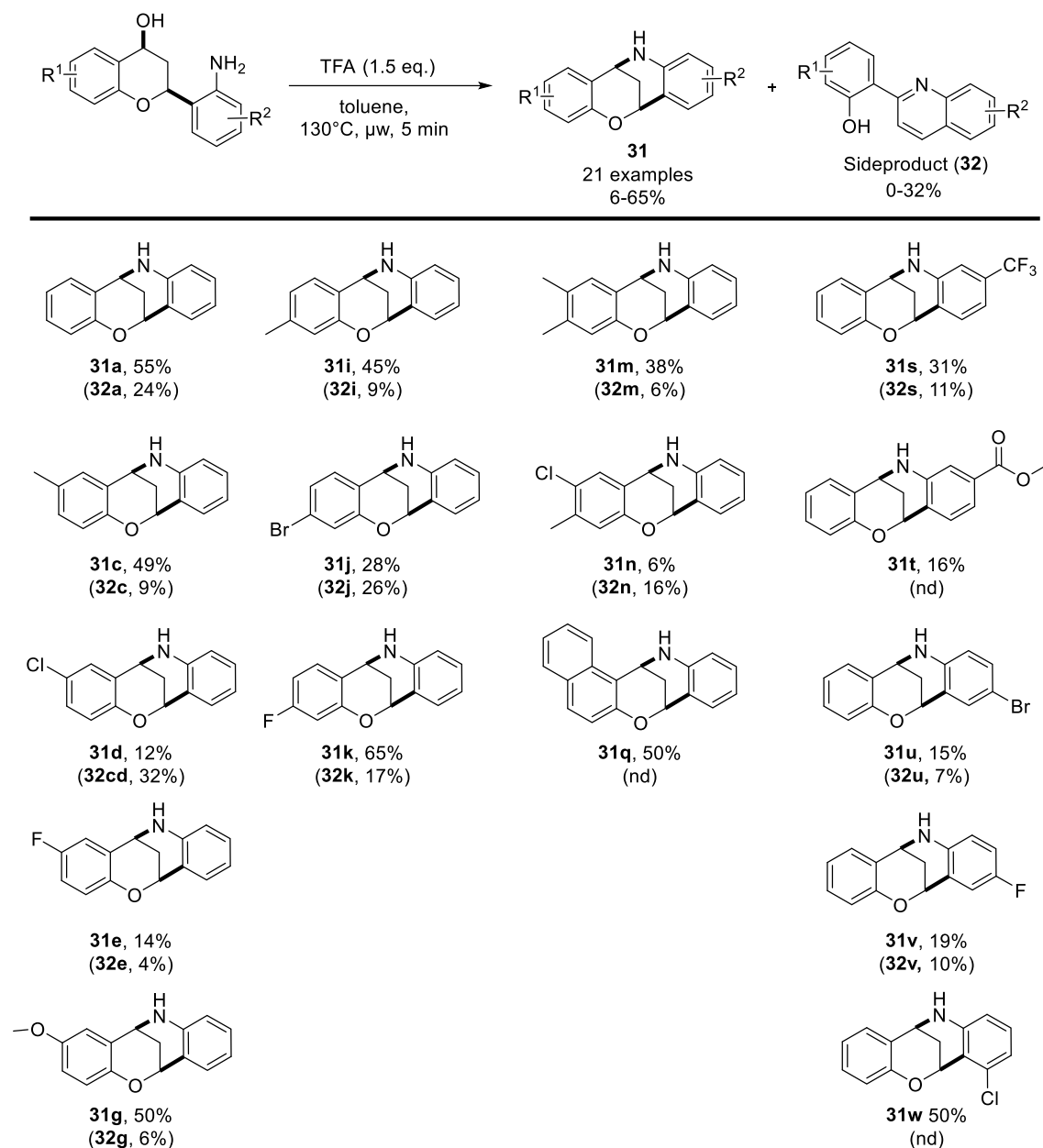
Figure 38: Plotting of NMR Yields of product A (orange) and product B (blue) against the used TFA concentration.

To further optimise the reaction conditions, the reaction temperature and reaction time were examined. It could be shown, that reducing the reaction time to 5 minutes and reducing the temperature to 130 °C could improve the chromaline formation (Table 7, entries 13-15).

Furthermore, it was shown that a removal of water from the reaction vessel could not improve the reaction yield or A/B ratio (Table 7, entry 16). Addition of water to the reaction did not lead to a change in reaction success (Table 7, entry 17).

With optimised conditions in hand (1.5 equivalents TFA, 130°C ( $\mu$ w), 5 min), the previously synthesised amine functionalised flavanols should be cyclised to generate chromaline derivatives for CPA analysis. In total 16 out of 21 flavanols could be cyclised with yields up

to 65% (Scheme 133). In almost all cases, the previously described side product was isolated as well.



Scheme 133: Optimised reaction conditions for the intramolecular cyclisation of flavanols and overview of synthesised chromaline derivatives. Sideproduct yields are given in brackets.

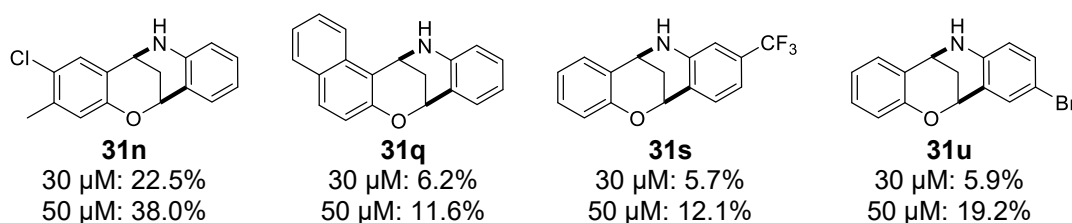
Substitution in all previous explored positions was possible. Methyl functionalization in general led to a similar yield as the unsubstituted chromaline in various substitution positions, while the side product formation was decreased (**31a**, **31i**, **31m**). Flavanols bearing further halosubstitution in chromane 6-position were cyclised less efficiently (**31d**, **31e**, **31n**), the double chlorinated chromaline could not be isolated at all. The electron donating methoxy group at chromane 6 position had no effect on the cyclisation. However, chromalines bearing

either a free amine or amide in this position could not be isolated. Chromane 7-position functionalisation led to generally moderate yields. The derivative bearing the electron withdrawing fluorine in this position could be cyclised in the overall highest yield (**31k**, 65%) with a good product to side product ratio (65/16%).

Functionalisation of the quinoline part of the molecule with electron withdrawing substituents (Cl, Br, F, CF<sub>3</sub>, CO<sub>2</sub>Me) was generally allowed. Increasing the electron density of the aromatic system by electron donating groups prevented the cyclisation reaction. In total 16 diverse chromaline compounds were synthesised and subjected to the CPA.

### 5.2.2 A Preliminary CPA Analysis

Four of the 16 synthesised chromaline derivatives induced morphological changes and were active in the CPA (induction > 5%) at a 30 μM concentration. The most CPA active molecule was the chromaline derivative **31n**, bearing a methyl and chlorine substituent on the chromane moiety, but also introducing a bromine substituent on the quinoline moiety (**31u**) led to the significant induction of morphological changes at 50 μM. Lower CPA activities were reached by the treatment of cells with compound **31q** and **31s** (Scheme 14).



Scheme 14: Structures and induction values of chromalines that showed CPA activity.

To allow a valid comparison of the obtained morphological profile, profiles with an induction range of 10-25% were considered (Figure 40). Intra-class comparison revealed an overall low similarity between the chromaline compounds. Not only the biosimilarity between the four considered compounds was below the similarity threshold (MBS = 73%, Figure 40), but also the chemical similarity between the compounds was low.

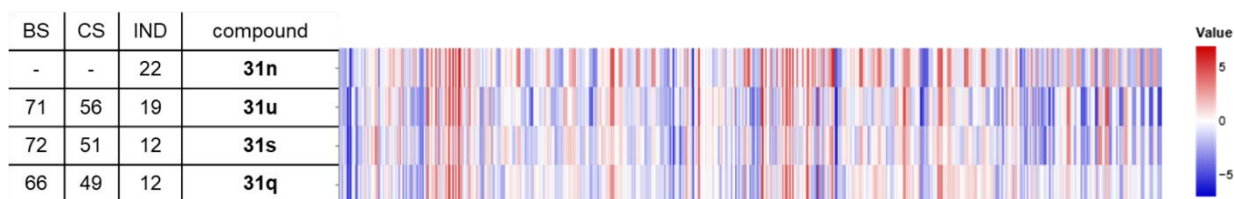


Figure 40: Comparison of morphological fingerprints of CPA active chromalines from a preliminary compound library; biosimilarities (BS), chemical similarities (CS) and induction (IND) are given as percentages.

To gain insight into the phenotypic behaviour of the chromane and the quinoline fragment, a PCA analysis was performed. The morphological profiles of chromalines separated from both compound classes, the chromopyrones and the pyrroquinolines. Furthermore, the MBS values between the chromalines and the other classes were low (27 and 40%, Figure 39). These observations led to the conclusion and proof of the previous hypothesis, that both fragments the tetrahydroquinoline, but also the chromane are non-dominating and that their morphological activity can be influenced by fusion to another fragment. Additionally, it was shown that the way of connectivity is not dominating the activity. Consequently, the chromaline compound class was endowed with a unique morphological activity.

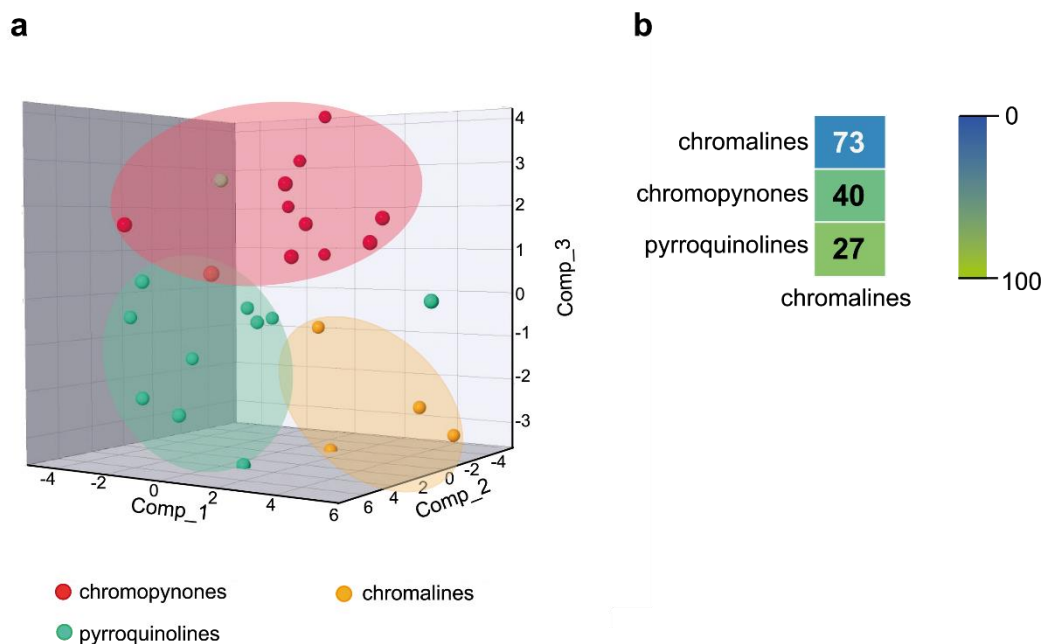
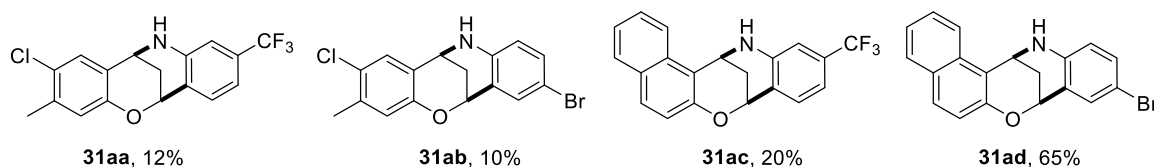


Figure 39: (a) Preliminary PCA of chromalines (orange), chromopyrones (red) and pyrroquinolines (green); Expl Var: Comp\_1 39.5%, Comp\_2: 22.2%, Comp\_3: 12.4%, induction 15-40%; PCA = principal component analysis; Comp = principal component; (b) MBS values calculated between chromalines and chromopyrones and pyrroquinoline.

To verify these conclusions from the behaviour of a rather small compound subset (4 CPA active compounds), further chromaline derivatives were synthesised.

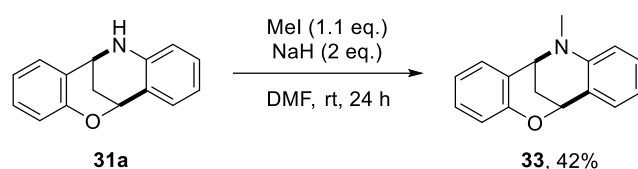
### 5.2.3 Synthesis of Chromaline Derivatives

A first expansion of the chromaline scope was facilitated by the combination of the chromane and quinoline substituents that were decorating the initial found hits in the CPA (Scheme 15). Combining these substituents led to four novel chromalines that were predicted to be active in the CPA. Synthesis of these derivatives followed the previously discussed four step procedure.



Scheme 15: Combination of substituents from CPA active chromalines.

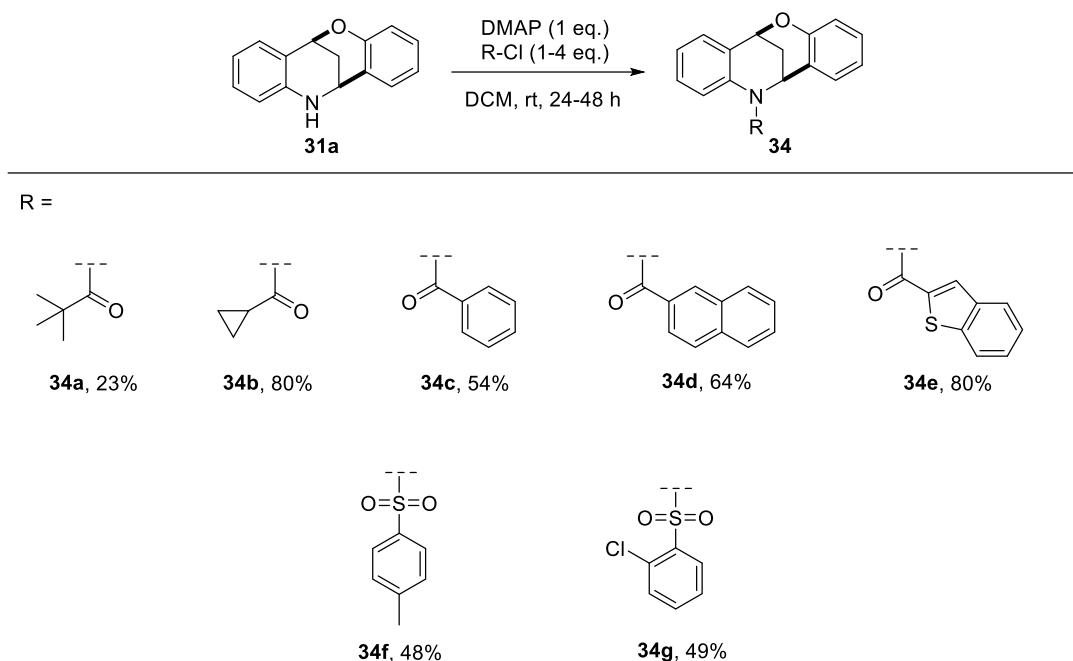
Additional derivatives were accessible by amine functionalization of the unsubstituted chromaline. Reaction with methyl iodide under basic conditions gave access to the methylated compound **33** in moderate yield (Scheme 16).



Scheme 16: Reaction scheme for the methyl functionalisation of the chromaline amine.

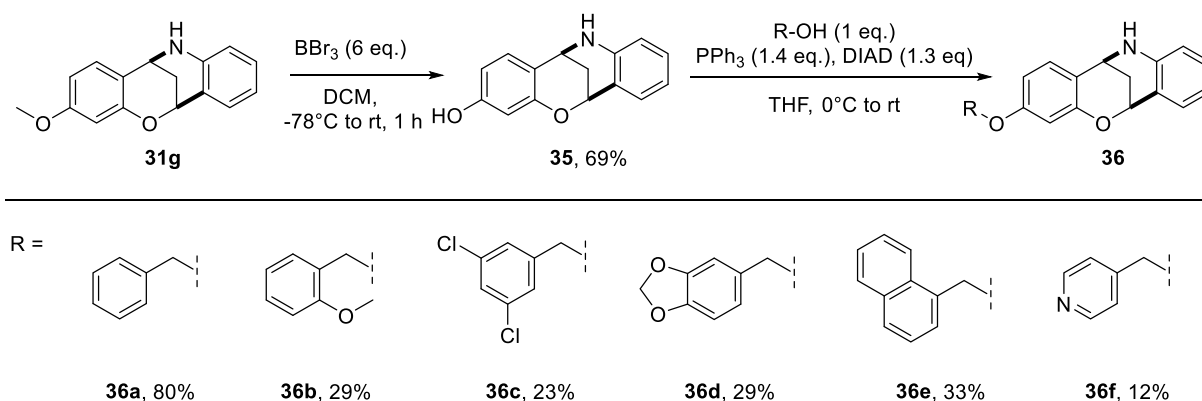
To further expand the scope at the amine position, it was reacted with diverse acid chlorides. In total 5 amide derivatives were synthesised bearing aliphatic or (hetero)aromatic residues. Generally, a low reactivity of the free amine was observed, and excess amounts of acid chloride were added to the reaction for a full conversion of the starting material. Besides the amide-functionalised compounds, two sulfonamides were synthesised by reaction of chromaline (**31a**) with sulfonyl chlorides (Scheme 17).





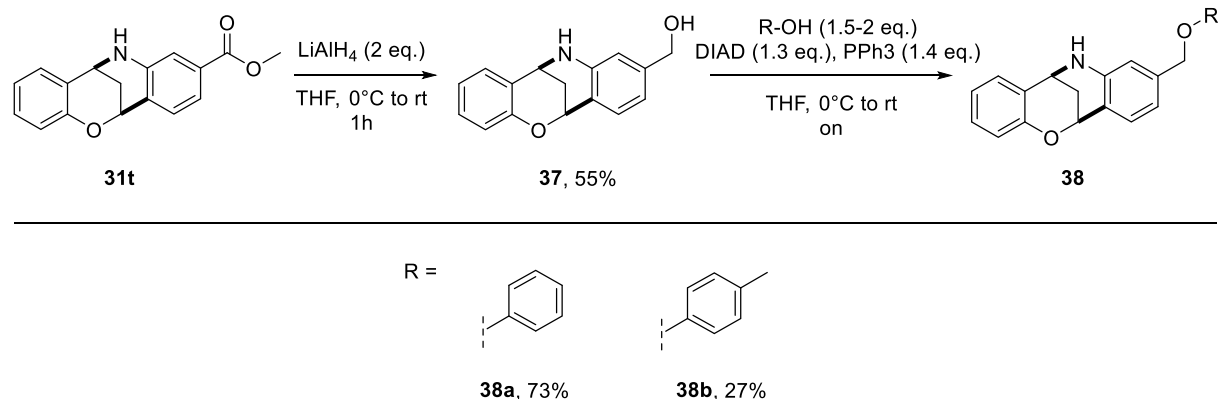
Scheme 18: Reaction scheme for the functionalisation of the chromaline amine

To further expand the scope on either the chromane or the quinoline moiety, previously synthesised derivatives bearing a handle for functionalisation were further modified. A free hydroxy group in chromane 7-position was derived from demethylation of the chromaline derivative **31g** (Scheme 18). The free hydroxy group was subsequently modified with a subset of primary alcohols by applying Mitsunobu conditions. This procedure allowed the introduction of further (hetero)aromatics bearing different substituents.

Scheme 17: Reaction scheme for the derivatisation of chromaline **31g**.

Last, the ester functionality of chromaline **31t** was reduced to the corresponding alcohol (**37**). Functionalization of the hydroxygroup following a Mitsunobu reaction gave access to two

derivatives bearing a substitution at the quinoline moiety. Introduction of other nucleophiles (amides, sulfonamides) to this position failed.



Scheme 19: Reaction scheme for the derivatisation of chromaline **31t**.

### 5.2.4 Cheminformatic Analysis of the Chromaline Compound Class

The further expanded chromaline compound class, containing in total 39 derivatives, was analysed by cheminformatic methods to further investigate their structural features (calculations were performed by Dr. Axel Pahl).

In order to compare the cheminformatic results, three different reference sets were included into all analyses. The selected Enamine<sup>[103]</sup> dataset (blue) is representative of a typical screening collection while the DrugBank<sup>[104]</sup> dataset (orange) represents experimental and marketed drugs. The ChEMBL<sup>[105]</sup> NP dataset (green) represents bioactive NPs.

To evaluate the three-dimensionality of the chromaline library members, a principal moment of inertia (PMI) plot was created. Generally, the shape of a molecule is important for the binding to a molecular target.<sup>[4,9]</sup> One widely used possibility to describe the shape of compounds are the PMI descriptors. These descriptors can give insights into the geometry of molecules, and how strongly it is influenced by a rod-like, disc-like, or sphere-like shape. In the triangular PMI plot molecules that have a rod-like shape are found in the top left corner, disc-like shapes in the bottom corner and sphere-like molecules in the upper right corner of the graph.<sup>[106,107]</sup> Plotting of the chromaline compounds in a PMI plot (Figure 41a, red points) revealed a high structural distribution of molecular shapes. While some of the compounds are condensed to an area close to the rod-like space, some are shifted towards the sphere-like area, and some are distributed to the center of the plot. Some of the compounds even seem to have a shape that is highly influenced by disc-like and sphere-like component. Comparison to the reference dataset revealed a similar distribution as it can be found for NPs from the ChEMBL database (green lines). NPs are generally endowed with a high molecular complexity, and

therefore their shapes can cover more sphere-like areas in the PMI plot. Based on the linear design approaches used in the development of drug-like molecules, these molecules have a higher potential to cover rod to disc like areas.<sup>[106]</sup>

Overall, the high distribution of molecular shapes within the chromaline compound class may suggest a coverage of diverse biological space. Considering that a compound must structurally fit a binding site to have a biological effect, diverse compound collections may bind diverse targets.

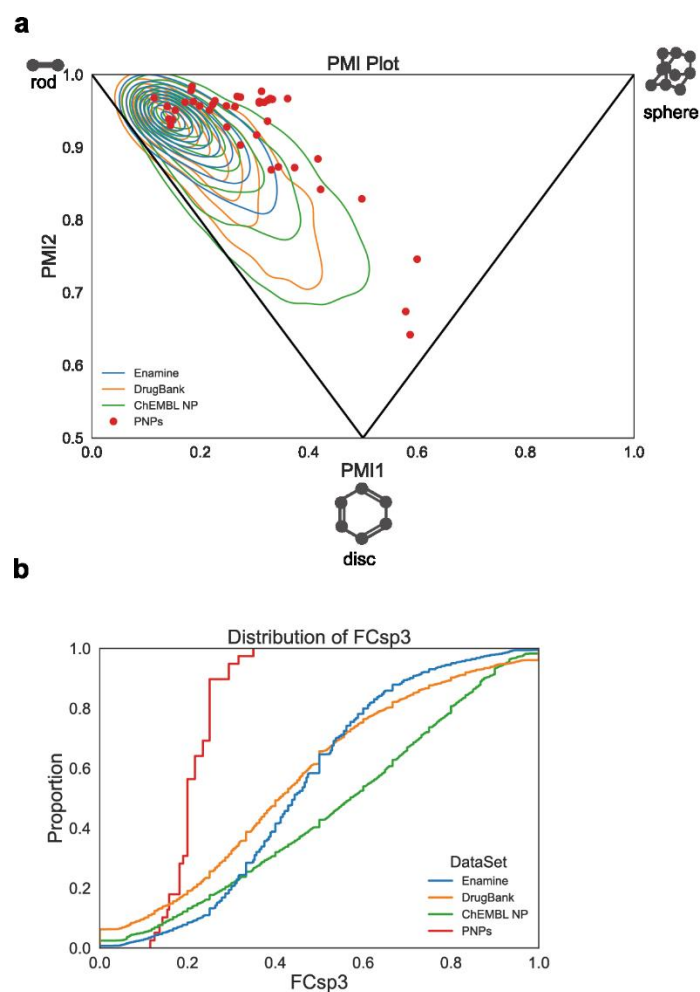


Figure 41: Three-dimensionality evaluation of the chromaline library (red); (a) pincipal moment of inertia (PMI) plot; (b) distribution of FCsp<sup>3</sup>; reference sets: Enamine (blue), DrugBank (orange), ChEMBL NP (green).

A parameter that is commonly used to determine the complexity of compounds is the fraction of sp<sup>3</sup> carbons (FCsp<sup>3</sup>). This parameter is calculated form the proportion of sp<sup>3</sup>-hybridised carbons to the total number of carbon atoms. Generally, a suitable value representing a beneficial tridimensionality for bioactivity-likeness (drug-likeness) is FCsp<sup>3</sup>  $\geq$  0.42.<sup>[108,109]</sup> Calculation of the FCsp<sup>3</sup> for the chromaline class revealed that all the PNP compounds had a lower value (0.2 to 0.3, Figure 41b). This observation was not too surprising, considering that

most of the library members contained two  $sp^3$ -hybridised carbons. However, based on the bridged connectivity and a resulting V-shape of the NP fragments, the compounds have a three-dimensional structure (as shown by the PMI plot).

To gain further insights into the NP- and drug-likeness of the chromaline compound class, the NP-likeness score and the quantitative estimate of drug-likeness (QED) were calculated (Figure 42). The NP-likeness score is a measure for the similarity of a molecule to the structural space that is occupied by NPs. Positive NP-likeness values indicate a high degree of NP-likeness, whereas more negative NP-likeness values indicate that the compounds are less NP-like.<sup>[110,111]</sup> Considering the underlying PNP design principle that was applied in the development of the chromaline compound class, it was assumed that chromalines share some NP properties. On the other hand, the chromane and THQ fragment were combined in an arrangement that is not found in nature, leading to the expectation that chromalines, or PNPs in general, are characterised by an NP-likeness score distinct from known drugs but also from NPs. Indeed, plotting of the NP-likeness distribution of chromalines (red line, Figure 42a) showed that the NP-likeness (highest distribution around 0) of the PNP class falls in between the distribution of the Enamine (blue line) and the ChEMBL-NP (green line) compounds but most closely correlates to DrugBank compounds. The distribution of the Enamine data set is similarly narrow as that of the chromaline but strongly shifted into the negative range, which indicates a high deviation from NPs, while the NP datasets distribution is shifted to positive values, indicating high NP similarity, as expected.

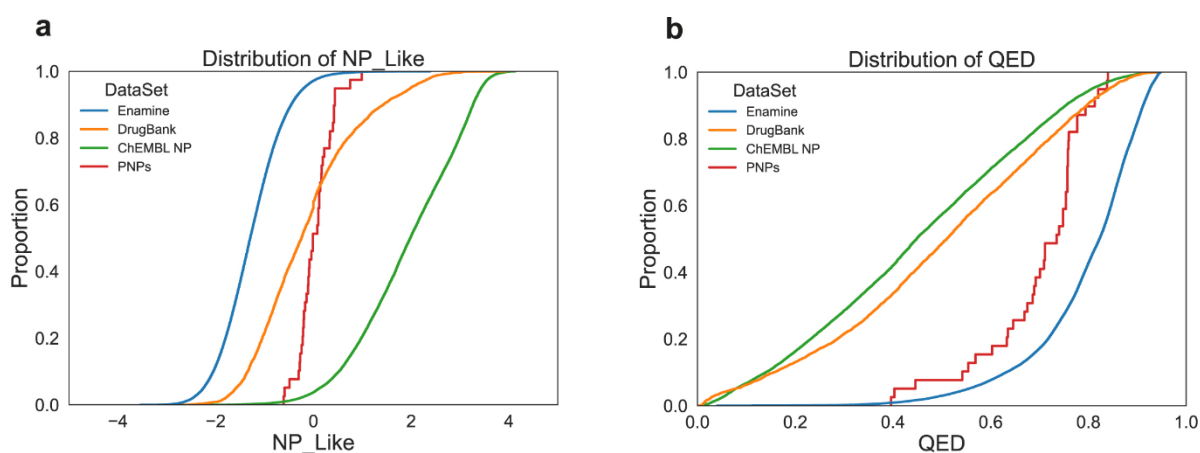


Figure 42: NP- and drug-likeness of the chromaline library (red); (a) Distribution of the NP-likeness; (b) Distribution of the quantitative estimated drug-likeness; reference sets: Enamine (blue), DrugBank (orange), ChEMBL NP (green).

The QED was introduced to quantify and rank molecules for the drug-likeness of their physicochemical properties, whereby a QED value of zero indicates that all properties are unfavourable and a value of one that all properties are favourable. Compared to rule-based approaches (*e.g.* Lipinski's rule of 5 (Ro5)<sup>[112]</sup>) the QED is not based on yes or no answers that are determined by clear defined thresholds. The Ro5 was originally implemented as a guideline but has been used to set up screening filters leading to the discrimination of many compounds that may have had favourable properties. QED rather investigates how well the sum of a compounds physicochemical properties fits the property distribution of marketed drugs. This leads to the fact that compounds are still classified as drug-like even if one (or more) of its properties is unfavourable.<sup>[113,114]</sup>

The distribution of the QED of chromalines is favourable for drug-development. The obtained distribution (Figure 42b, red line) is close to the distribution found for the Enamine reference set that was implemented because of its overall good coverage of drug-like properties.

A PCA of 17 different physiochemical and structural descriptors was used to further investigate the chromaline library in comparison to the NP- and drug-like reference sets (Figure 43). In the PCA, the 17 regarded features were differently valued on the principal components PC1, PC2 and PC3. Reducing these values to the 3 components could give a clearer insight into the structural variance and distribution in the chromaline dataset but also its physiochemical properties compared to the reference datasets.

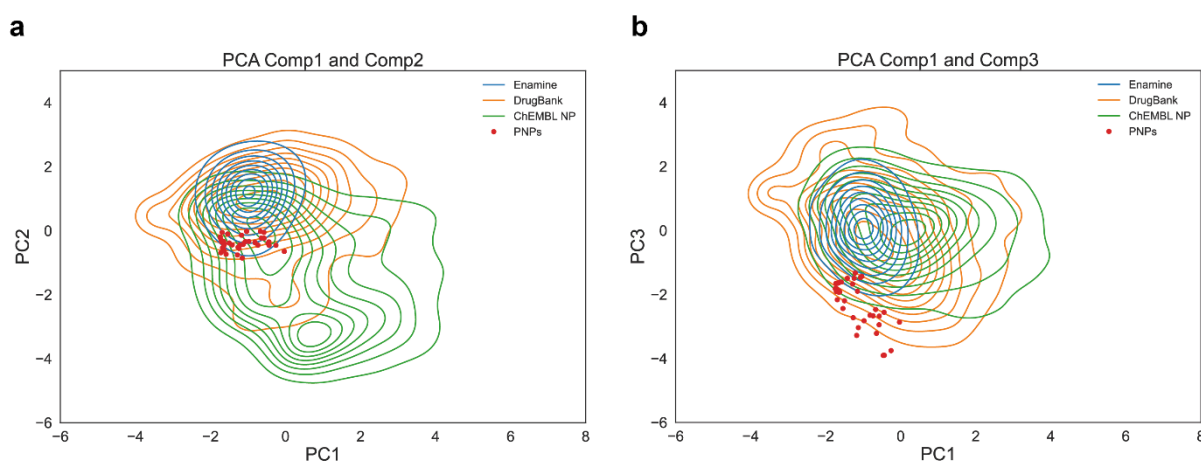


Figure 43: PCA of 17 different physiochemical and structural descriptors to describe the chromaline library (red); (a) plot of Comp1 against Comp2; (b) plot of Comp1 against Comp3; reference sets: Enamine (blue), DrugBank (orange), ChEMBL NP (green).

Considering the PCA between component 1 and 2 revealed a high feature similarity of the chromalines (red points) to the enamine database (blue) but a shift towards the area occupied

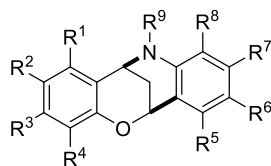
by the NP references (green). Charting component 1 vs. component 3 resulted in an overlap of most of the reference sets densities. The chromaline PNPs thereby were located at the edge or outside of this density. This may reveal novel molecular properties and the potential coverage of novel chemical and biological space.

Overall, it was assumed, that the chromaline PNP class shares some drug-like structural and physicochemical properties as well as features that can be found in NPs. This observation proves the success of the PNP design principle in terms of bringing together structural features of NPs and the physicochemical advantages of drug-like molecules.

### 5.2.5 Cell Painting Assay Analysis of Chromalines

Analysis of the CPA data that were obtained for the full chromaline dataset revealed a generally high potential to change the cellular morphology. Of the 39 compounds submitted, 20 were active in the CPA (induction  $\geq 5\%$ ) at a concentration of 50  $\mu\text{M}$  (Table 8) and 19 of these compounds still showed activity at 30  $\mu\text{M}$ .

Table 8: CPA inductions of compounds active in the CPA (induction  $>5\%$ ) at 30 and 50  $\mu\text{M}$  concentrations.



Entry	R <sup>1</sup>	R <sup>2</sup>	R <sup>3</sup>	R <sup>6</sup>	R <sup>7</sup>	R <sup>9</sup>	Nr	CPA Induction at 50 $\mu\text{M}$ [%]	CPA Induction at 30 $\mu\text{M}$ [%]
1	H	H	OCH <sub>2</sub> Ph	H	H	H	<b>36a</b>	53.5	22.1
2	H	H	H	H	CH <sub>2</sub> O-4-MePh	H	<b>38b</b>	40.9	12.3
3	H	H	H	H	CH <sub>2</sub> OPh	H	<b>38a</b>	40.2	6.4
4	C <sub>4</sub> H <sub>4</sub>		H	Br	H	H	<b>31ad</b>	38.3	11.4
5	H	H	OH	H	H	H	<b>35</b>	38.0	22.5
6	H	H	OCH <sub>2</sub> -3,5-Cl-Ph	H	H	H	<b>36c</b>	37.8	22.3
7	H	H	OCH <sub>2</sub> -BDO*	H	H	H	<b>36d</b>	37.0	24.4
8	H	H	H	H	H	SO <sub>2</sub> -2-Cl-Ph	<b>34g</b>	36.3	31.6
9	H	H	OCH <sub>2</sub> -2-OMe-Ph	H	H	H	<b>36b</b>	35.4	16.4
10	H	Me	Cl	Br	H	H	<b>31ab</b>	32.6	7.1
11	H	H	OCH <sub>2</sub> -4-Py	H	H	H	<b>36f</b>	32.3	11.9

Entry	R <sup>1</sup>	R <sup>2</sup>	R <sup>3</sup>	R <sup>6</sup>	R <sup>7</sup>	R <sup>9</sup>	Nr	CPA	CPA
								Induction at 50 $\mu$ M [%]	Induction at 30 $\mu$ M [%]
12	C <sub>4</sub> H <sub>4</sub>		H	H	H	H	31ac	32.1	5.7
13	H	H	H	H	H	SO <sup>2</sup> -4- Me-Ph	34f	24.9	18.1
14	H	H	H	Br	H	H	31u	19.2	5.9
15	H	H	H	H	H	(CO)-2- Napht <sup>#</sup>	34d	19.0	14.2
16	H	H	Br	H	H	H	31j	16.1	<5
17	H	H	H	H	CF <sub>3</sub>	H	31s	12.1	5.7
18	C <sub>4</sub> H <sub>4</sub>		H	H	H	H	31q	11.6	6.2
19	H	H	H	H	H	(CO)-Ph	34c	10.4	5.4
20	H	H	H	H	H	(CO)-2- BTh <sup>++</sup>	34e	9.8	13.5

\*BDO = benzo[3,4]dioxole; <sup>#</sup>Napht = naphtyl; <sup>++</sup>BTh = Benzothiophene

Interestingly, 3 out of the 4 chromalines, that were derived by the substituent combination of the initial hit compounds (**31n**, **31u**, **31s**, **31q**) were active in the CPA as well (**31ab**, **31ac**, **31ad**). Only the combination of the trifluoromethyl-functionalisation at the quinoline moiety and the chlorine- and methyl-functionalisation at the chromane moiety was not active at 50  $\mu$ M (**31aa**). Comparison of the morphological profiles of the initial hit compounds (**31n**, **31u**, **31s**, **31q**) and the combination products (**31ab**, **31ac**, **31ad**) revealed a high similarity between most of the seven compounds. Merely two compounds bearing a trifluoromethyl group (**31s** and **31ac**) showed a different phenotypic behaviour than the other compounds.

Besides the biosimilarity, also a comparably high induction of two of the combination compounds was observed (**31ab** and **31ad**). This may be a first hint towards a chromaline structure phenotype relationship, as it was also observed for the azaquinole class (Part 1).

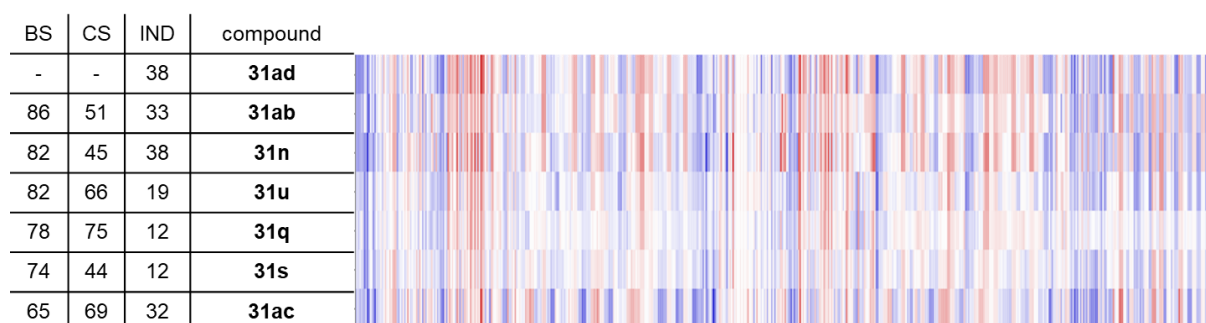


Figure 44: Comparison of morphological fingerprints of preliminary CPA active chromalines and their combinations; biosimilarities (BS), chemical similarities (CS) and induction (IND) are given as percentages.

Evaluation of the chromaline derivatives that were derived by functionalisation of previous chromaline compounds (**34**, **35**, **36**, **38**, see 5.2.3) led to the observation of further CPA active compounds (Table 8, entries 1-3, 5-9, 11, 13, 15, 19, 20). The introduction of aromatic substituents on the chromane (C-R, **36**, Table 8, entries 1, 6, 7, 9, 11) or the quinoline moiety (Q-R, **38**, Table 8: entries 2 and 3) as well as on the free amine (N-R, **34**, Table 8: entries 8, 13, 15, 19, 20) could improve the previously measured induction values. Introduction of alkyl amides or a methyl group to the free amine of the chromaline PNP on the other hand led to inactive derivatives.

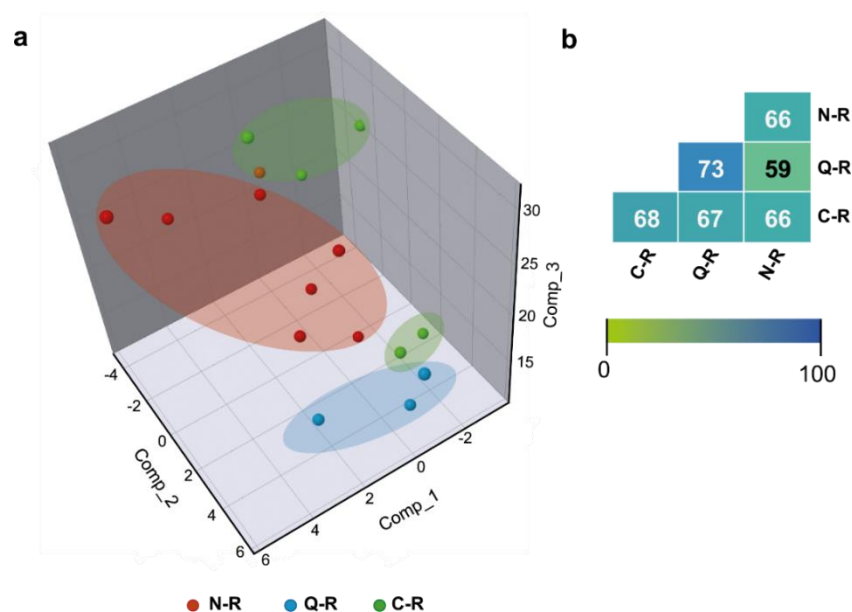


Figure 45: Comparison of different substituent pattern on the chromalines: substituent on the amine (N-R), substituent on the quinoline moiety (Q-R) and substituent on the chromane moiety (C-R); (a) PCA of the substituent pattern, N-R (red), Q-R (blue) and C-R (green); Expl Var: Comp\_1 40.9%, Comp\_2: 23.4%, Comp\_3: 8.4%, induction 10-30%; PCA = principal component analysis; Comp = principal component; (b) MBS values (%) calculated between the different substituent pattern.

The biosimilarity of compounds bearing differently positioned substituents was investigated. A PCA of the phenotypic profiles of compounds bearing either a substituent on the chromane moiety (C-R (green), **36**), on the quinoline moiety (Q-R (blue), **38**) or at the amine position (N-R (red), **34**) was applied to compounds in a suitable induction window (10-30%; Figure 45a). This led to the observation that the substitution of the chromaline quinoline (Q-R (blue), **38**) part may lead to distinct phenotypic changes. On the other hand, compounds bearing a substituent on the chromane moiety (C-R (green), **36**), or the amine (N-R (red), **34**) showed very diverse phenotypic changes as indicated by the broad distribution of the compound profiles in the PCA. This observation is also reflected by the calculated MBS (Figure 45b). A



generally low MBS (59-73%) was calculated for both, the inter- and intra-class comparison of the different substituent pattern. It was concluded, that the chromalines bioactivities are highly dependent on the substituents decorating the scaffold, whereby the direction of the molecule extension is not necessarily inducing specific phenotypic profiles. The chemical similarity, median intra-class similarity (Figure 46c) including all chromalines was 0.44 which also indicates a high chemical diversity of the library.

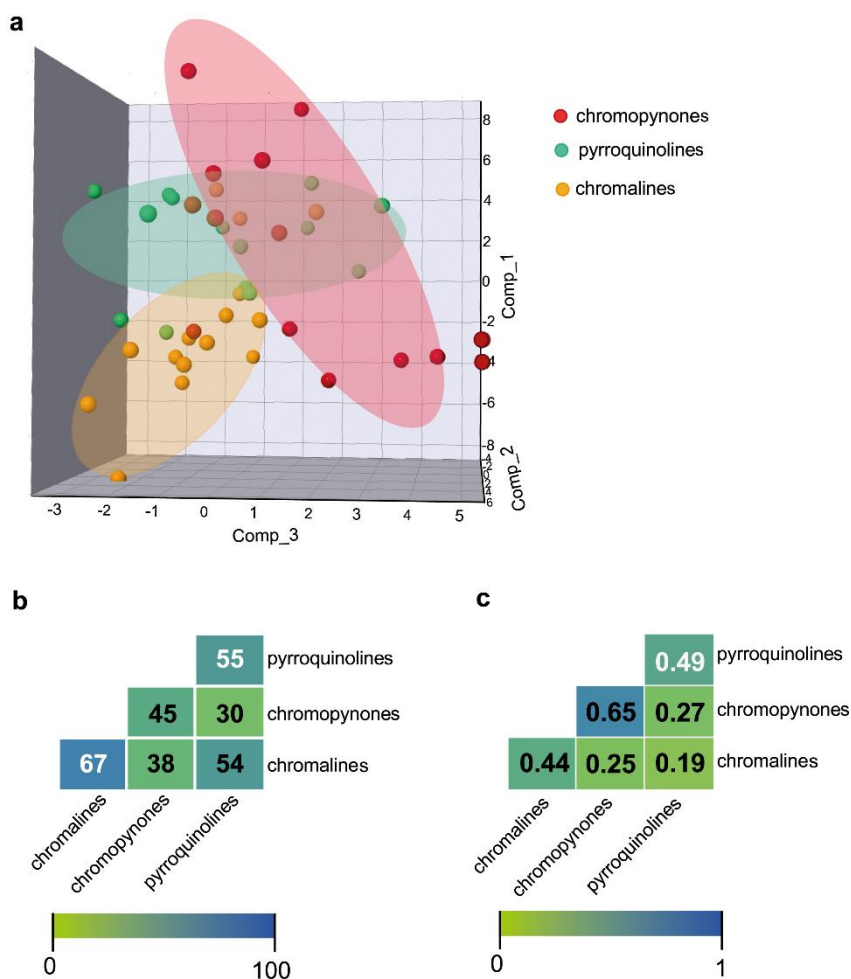


Figure 46: Comparison of chromalines to the previous PNP compound classes; **(a)** PCA of chromalines (orange), chromopynones (red) and pyrroquinolines (green); Expl Var: Comp\_1 38.2%, Comp\_2: 17.6%, Comp\_3: 11.3%, induction 15-40%; PCA = principal component analysis; Comp = principal component; **(b)** MBS values (%) calculated between chromalines, chromopynones and pyrroquinolines; **(c)** Chemical similarities of the analysed PNP compound classes.

To finally clarify the questions of whether the chromane fragment is dominating and whether the chromaline compound class shows a novel and unique phenotypic activity, the final dataset was compared to the previous PNP compound classes (Figure 46). Although the PCA (Figure 46a) showed overlaps and high distributions of the compound classes, still distinct areas were

covered by the chromalines, the chromopyrones and the pyrroquinolines. The chromopyrones showed a wide coverage of morphologies which was also reflected in a low intra-class MBS value (45%, Figure 46b). The chromaline compound class was shown to cover some similar areas as the other two PNPs, but generally was shifted to a novel area of the PCA. Furthermore the inter-class MBS values reflected a low similarity between all of the compound classes. This led to the conclusion that the chromalines were endowed with a novel and unique bioactivity. Consequently, it was hypothesised that the chromane and pyrroquinoline fragments are both non-dominating and suitable coupling partners for future PNP projects.

### 5.3 Conclusion

Inspired by previous PNP examples that are active in the CPA, a novel compound class was designed and synthesised for further CPA analyses. To further investigate the design principle that was discussed in part two of this thesis, these novel PNPs were supposed to share the same connectivity of fragments as the inspiring PNPs. To facilitate this, the chromalines were designed to share the chromane part with the chromopyrones and the quinoline part with the pyrroquinolines. In all three compound classes, the NP fragments were connected via the same bridged fusion pattern. To synthesise the novel PNP class, a four-step procedure was established, starting from simple 2-nitrobenzaldehyde and 2-hydroxyacetophenone starting materials. Synthesis of flavanones, followed by a two-step reduction procedure and an acid-mediated cyclisation as a key step gave access to 20 chromalines bearing diverse substituents. Further modification of some of the described derivatives further expanded the scope on the chromane and quinoline part of the molecule. Cheminformatic analysis of the structural and physicochemical features of the novel PNPs revealed a high diversity in the chromalaine library. The compounds shared both drug-like properties but also NP-like structural features.

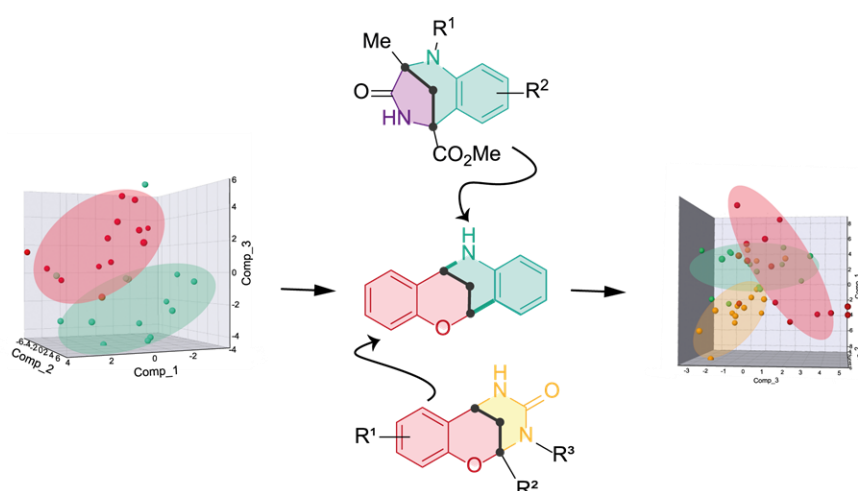


Figure 47: Schematic representation of the CPA guided design of chromalines and the PCA analysis showing the a novel and unique bioactivity of the PNP compound class compared to chromopyrones and pyrroquinolines.

CPA analysis of the new chromaline compound class revealed a generally high potential to induce morphological changes (51% of all compounds were active). Comparison of compounds with differently positioned substituents showed, that substitution on the quinoline part may induce distinct morphological changes. Generally, it was shown that the morphological profiles are highly influenced by different substituents. Furthermore, comparison to the two previous PNP classes revealed a distinct coverage in the PCA and a low

### Part III

MBS. This observation led to the conclusion that the structurally and bioactivity diverse chromaline compound class has a unique bioactivity. These findings highlight the advantages of the CPA-guided design principle but also of the PNP approach in general to identify small molecules covering novel areas in chemical and biological space.

## 6. Experimental

### 6.1 Materials and Methods for Organic Synthesis

All commercially available compounds were used as provided without further purification. Reactions with air or moisture sensitive reagents or intermediates were carried out under inert atmosphere (argon) and glassware was dried by heat gun under vacuum prior to use. Dry solvents were received from Acros, Sigma Aldrich or VWR in anhydrous quality and used without further purification. All other solvents were used in laboratory grade, solvents for chromatography were technical grade. In all experiments Milli-Q grade water was used.

Thin layer chromatography (TLC) was performed on Merck silica gel aluminium plate with F 254 indicator (Merck 60 F254). Visualisation of compounds was achieved by UV or KMnO<sub>4</sub> staining (1.5 g, 10 g K<sub>2</sub>CO<sub>3</sub> in, 1.5 mL 10% aqueous NaOH, 200 mL H<sub>2</sub>O). For flash column chromatography silica gel from Acros Organics (particle size 40-60 µm, 230-400 mesh) was used. Solvents for column chromatography were laboratory grade. Solvent mixtures are given in volume/volume.

<sup>1</sup>H NMR and <sup>13</sup>C NMR spectra were recorded on Bruker Avance III HD NanoBay (400 MHz), Bruker Avance NEO (500 MHz), Bruker Avance III HD (600 MHz) and Bruker AV Avance III HD (700 MHz) spectrometers. All spectra were referenced to the proton and carbon shift of the used solvent (CDCl<sub>3</sub>: δ = 7.26, 77.16 ppm, CD<sub>2</sub>Cl<sub>2</sub>: δ = 5.32, 54.00 ppm, DMSO-d<sub>6</sub>: δ = 2.50, 39.52 ppm, MeOD: δ = 3.31, 49.00 ppm). Multiplicities are indicated by s (broad singlet), s (singlet), d (doublet), t (triplet), q (quartet), m (multiplet); coupling constants (*J*) are given in Hertz (Hz). For structural assignments 2D NMR correlations, including <sup>1</sup>H/<sup>1</sup>H COSY, <sup>1</sup>H/<sup>1</sup>H NOESY, <sup>1</sup>H/<sup>13</sup>C HSQC, <sup>1</sup>H/<sup>13</sup>C HMBC, were applied.

Fourier transform infrared spectroscopy (FT-IR) spectra were measured with a Bruker Tensor 27 spectrometer (ATR, neat) and are reported in terms of frequency of absorption (cm<sup>-1</sup>).

Preparative mass-directed HPLC (Agilent Series, 1100/LC/MSD VL, Agilent Series) with a reversed-phase C<sub>18</sub> column (flow 20.0 mL/min, solvent A: 0.1% TFA in water, solvent B: 0.1% TFA in acetonitrile) was used for separation.

Analytical uHPLC-MS was performed on an Agilent 1290 Infinity system (column: Zorbax Eclipse C<sub>18</sub> Rapid Resolution 2.1x50 mm 1.8 µm). High resolution mass spectra were recorded on a LTQ Orbitrap mass spectrometer coupled to an Accela HPLC-System (HPLC column:

## Experimental

Hypersyl GOLD, 50 mm x 1 mm, particle size 1.9  $\mu\text{m}$ , ionization method: electron spray ionization). Optical rotations were measured in a Schmitd + Hansch Polartronic HH8 at a concentration  $c = 0.001\text{g mL}^{-1}$  in MeOH.  $[\alpha]_{\text{D}}^{20}$  values are given in  $[\text{° mL g}^{-1} \text{dm}^{-1}]$ .



## 6.2 Chemical Synthesis

### 6.2.1 Azaquindole-1 Derivatives

#### General procedure A: Preparation of the ketones

##### *Step I: Isomerisation of the Cinchona alkaloid double bond:*

In two batches, the cinchona alkaloid starting material ( $2 \times 6.0$  g,  $2 \times 18.4$  mmol [18.4 mmol in each batch, 36.8 mmol over 2 batches], 1.0 eq.) was dissolved in 1:1 H<sub>2</sub>O/EtOH ( $2 \times 120$  mL, [120 mL in each batch, 240 mL overall]) and concentrated HCl ( $2 \times 15.6$  mL, 181 mmol [181 mmol in each batch, 362 mmol over 2 batches], 10 eq.) was added. Rh/C (5 wt%,  $2 \times 100$  mg [100 mg in each batch, 200 mg overall], 1.7 w/w%) was added and the reaction mixtures were heated at reflux (101.5°C) under Ar for 17 h. The reaction mixtures were cooled to rt and the two batches were combined and filtered through celite, flushing through with MeOH. The filtrate was concentrated *in vacuo*. To the resulting oil was added H<sub>2</sub>O (100 mL). Lyophilisation (72 h) gave the internal alkenes as the hydrochloride salts, which were carried forward to the next step without further purification.

##### *Step II: Oxidative cleavage of the alkene to the ketone:*

The relevant hydrochloride salt (5.0 mmol) was dissolved in 8:2 AcOH/H<sub>2</sub>O (24 mL) and K<sub>2</sub>OsO<sub>4</sub>•2H<sub>2</sub>O (18 mg, 0.05 mmol, 1.0 mol%) was added. The reaction mixture was stirred at rt for 10 min, then cooled to 0 °C. NaIO<sub>4</sub> (2.14 g, 10.0 mmol, 2.0 eq.) was added. The mixture was warmed to rt and stirred for 17 h. The mixture obtained was quenched with aqueous NaOH (10 M, ~50 mL) at 0°C until it was basic (tested with pH indicator paper). Sat. aq. Na<sub>2</sub>SO<sub>3</sub> solution (10 mL) was added to destroy OsO<sub>4</sub>. The resulting solution was extracted with 9:1 CHCl<sub>3</sub>/MeOH (4 x 50 mL) and 8:2 CHCl<sub>3</sub>/MeOH (2 x 50 mL). The combined organic fractions were dried over Na<sub>2</sub>SO<sub>4</sub>, filtered, and concentrated *in vacuo*. Flash column chromatography gave the ketones.

#### General Procedure B: Pd-catalysed indole formation

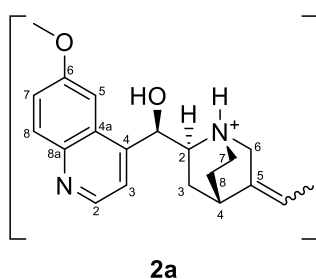
The ketone (100 mg, 0.32 mmol, 1 eq.), *o*-iodoaniline (0.96 mmol, 3 eq.), DABCO (108 mg, 0.96 mmol, 3 eq.) and Pd(OAc)<sub>2</sub> (7 mg, 10 mol%) were added to a 7 mL reaction tube and dissolved in 1 mL anhydrous DMF. The vial was sealed with a screw cap bearing a PTFE/silicone septum and degassed under a stream of Argon for 20 min. The reaction vial was further sealed with parafilm and transferred to a pre-heated heating block at 105 °C (the solvent level in the vial was submerged below the heating block level). The conversion of starting



material was monitored every 24 h (HPLC-MS). In case of incomplete conversion, the reaction mixture was cooled to rt, added with additional Pd(OAc)<sub>2</sub> (7 mg, 10 mol%), degassed under a steam of argon for 20 min and returned to the heating block for additional 24 h. After complete conversion of starting material (usually 24-72h) the reaction mixture was cooled to room temperature, diluted in MeOH (5 mL) and passed through a syringe filter. After removal of the solvents *in vacuo* the desired product was purified by flash column chromatography ({50:80:1 DCM:EtOH:NH<sub>4</sub>OH}/DCM) and/or preparative HPLC (ACN+0.1% TFA/H<sub>2</sub>O+0.1%TFA).

### Preparation of compound 7

#### (1*S*,2*S*,4*S*)-5-Ethylidene-2-[(*R*)-hydroxy(6-methoxyquinolin-4-yl)methyl]-1-azabicyclo[2.2.2]octan-1-ium chloride (2a)

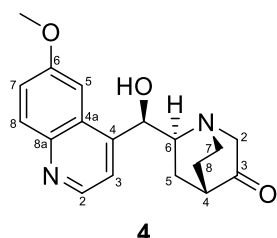


General procedure A, Part I, was followed using quinine in two batches (2 × 6.0 g, 2 × 18.4 mmol [18.4 mmol in each batch, 36.8 mmol over 2 batches]) to give the title product **4** (14.9 g) as a pale yellow solid which was carried forward to the next step without further purification. <sup>1</sup>H NMR (500 MHz, CD<sub>3</sub>OD, 2:1 mixture of *Z/E* alkenes, NH<sup>+</sup> and OH not observed): δ 9.08 (1H, d, *J* 3.4, quinoline 2-H), 8.38 (1H, d, *J* 3.4, quinoline 3-H), 8.26 (1H, d, *J* 8.8, quinoline 8-H), 7.90 (0.67H, s, major quinoline 5-H), 7.88 (0.33H, s, minor quinoline 5-H), 7.83 (1H, d, *J* 8.8, quinoline 7-H), 6.71 (1H, s, CH(OH)), 5.56-5.49 (0.67H, m, major C=CHCH<sub>3</sub>), 5.49-5.43 (0.33H, m, minor C=CHCH<sub>3</sub>), 4.47-4.39 (1H, m, 7-H<sub>A</sub>), 4.23 (1H, d, *J* 16.1, 6-H<sub>A</sub>), 4.14-4.01 (1H, m, 6-H<sub>B</sub>), 3.85-3.77 (0.67H, m, major 2-H), 3.77-3.67 (0.33H, s, minor 2-H), 3.47-3.38 (1H, m, 7-H<sub>B</sub>), 3.17 (0.33H, s, minor 4-H), 2.71 (0.67H, s, major 4-H), 2.52-2.41 (1H, m, 3-H<sub>A</sub>), 2.31-2.21 (1H, m, 8-H<sub>A</sub>), 2.02-1.91 (1H, m, 8-H<sub>B</sub>), 1.63 (1H, d, *J* 4.8, minor C=CHCH<sub>3</sub>), 1.57 (2H, d, *J* 5.9, major C=CHCH<sub>3</sub>), 1.53-1.41 (1H, m, 3-H<sub>B</sub>). <sup>13</sup>C NMR (125 MHz, CD<sub>3</sub>OD, 2:1 mixture of *Z/E* alkenes): δ 162.5 (Ar-C<sub>q</sub>), 158.3 (major Ar-C<sub>q</sub>), 158.2 (minor Ar-C<sub>q</sub>), 141.7 (2 peaks, quinoline 2-C), 134.8 (2 peaks, Ar-C<sub>q</sub>), 131.9 (major 5-C), 131.0 (minor 5-C), 129.6 (major Ar-C<sub>q</sub>), 129.5 (minor Ar-C<sub>q</sub>), 129.1 (quinoline 7-C), 124.0 (minor quinoline 8-C), 123.9 (major quinoline 8-C), 121.4 (quinoline 3-C), 121.2 (minor C=CHCH<sub>3</sub>), 120.9 (major C=CHCH<sub>3</sub>), 103.6 (major quinoline 5-C), 103.5 (minor quinoline 5-C), 68.1 (minor CH(OH)), 68.0 (major CH(OH)), 61.7 (major 2-C), 61.5 (minor 2-C), 58.7 (major OCH<sub>3</sub>), 58.6 (minor OCH<sub>3</sub>), 58.2 (minor 6-C), 56.5 (major 6-C), 46.0 (major 7-C), 45.8

## Experimental

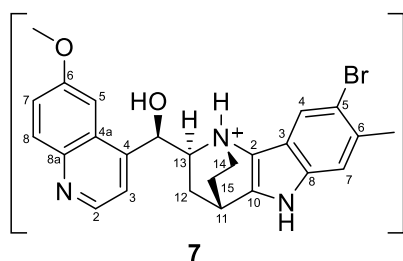
(minor 7-C), 32.6 (major 4-C), 25.8 (minor 4-C), 25.6 (major 8-C), 24.7 (major 3-C), 24.5 (minor 8-C), 23.9 (minor 3-C), 13.0 (minor C=CHCH<sub>3</sub>), 12.8 (major C=CHCH<sub>3</sub>).

### (1*S*,4*S*,6*S*)-6-[(*R*)-Hydroxy(6-methoxyquinolin-4-yl)methyl]-1-azabicyclo[2.2.2]octan-3-one (4)



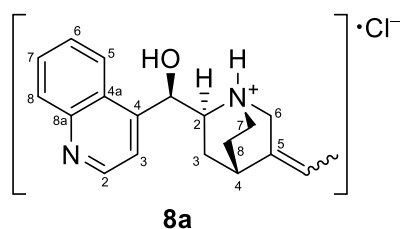
General Procedure A, Part II, was followed using compound **8** (2.0 g, assume 5.1 mmol). Flash column chromatography eluting with 5-35% {50:80:1 CH<sub>2</sub>Cl<sub>2</sub>:EtOH:NH<sub>4</sub>OH<sub>(sat. aq.)</sub>} in CH<sub>2</sub>Cl<sub>2</sub> gave the title product **6** (788 mg, 2.52 mmol, 50%) as a colourless solid. <sup>1</sup>H NMR (500 MHz, CD<sub>3</sub>OD, OH not observed): δ 8.67 (1H, d, *J* 4.6, quinoline 2-H), 7.94 (1H, d, *J* 9.2, quinoline 8-H), 7.71 (1H, d, *J* 4.6, quinoline 3-H), 7.46 (1H, d, *J* 2.7, quinoline 5-H), 7.42 (1H, dd, *J* 9.2, 2.7, quinoline 7-H), 5.69 (1H, d, *J* 3.7, CH(OH)), 3.98 (3H, s, OCH<sub>3</sub>), 3.90-3.82 (1H, m, quinuclidine 7-H<sub>A</sub>), 3.37-3.23 (3H, m, quinuclidine 2-H<sub>A</sub> and 2-H<sub>B</sub> and quinuclidine 6-H), 2.88-2.80 (1H, m, quinuclidine 7-H<sub>B</sub>), 2.49-2.38 (2 H, m, quinuclidine 4-H and quinuclidine 5-H<sub>A</sub>), 2.27-2.19 (1H, m, quinuclidine 8-H<sub>A</sub>), 1.97-1.86 (1H, m, quinuclidine 8-H<sub>B</sub>), 1.74-1.65 (1H, m, quinuclidine 5-H<sub>B</sub>). <sup>13</sup>C NMR (125 MHz, CD<sub>3</sub>OD): δ 220.2 (quinuclidine 3-C), 159.7 (quinoline 6-C), 150.5 (Ar-C<sub>q</sub>), 148.2 (quinoline 2-C), 144.8 (Ar-C<sub>q</sub>), 131.3 (quinoline 8-C), 128.2 (Ar-C<sub>q</sub>), 123.4 (quinoline 7-C), 120.0 (quinoline 3-C), 102.6 (quinoline 5-C), 71.9 (CH(OH)), 65.5 (2-C), 61.4 (quinuclidine 6-C), 56.4 (OCH<sub>3</sub>), 43.6 (quinuclidine 7-C), 41.9 (quinuclidine 4-C), 26.1 (quinuclidine 5-C), 25.8 (quinuclidine 8-C). HRMS (ESI): C<sub>18</sub>H<sub>21</sub>N<sub>2</sub>O<sub>3</sub> [M+H]<sup>+</sup>; calculated: 313.1547, found: 313.1548. [α]<sub>D</sub><sup>20</sup> = -147 (c. 0.1, MeOH).

**(R)-[(13S)-5-Bromo-6-methyl-1,9-diazatetracyclo[9.2.2.0<sup>2,10</sup>.0<sup>3,8</sup>]pentadeca-2(10),3,5,7-tetraen-13-yl](6-methoxyquinolin-4-yl)methyl (7)**

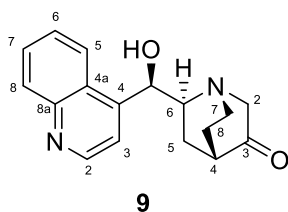


Prepared according to General Procedure B using ketone **4** and 20 mol% Pd(OAc)<sub>2</sub> (48 h). Flash column chromatography eluting with 20% {50:80:1 CH<sub>2</sub>Cl<sub>2</sub>:EtOH:NH<sub>4</sub>OH} in CH<sub>2</sub>Cl<sub>2</sub> followed by mass-directed preparative HPLC (MeCN in H<sub>2</sub>O + 0.1% TFA; Rt = 15.0 min) gave the *title compound S-1* (36 mg, 75 μmol, 23%) as a yellow solid. <sup>1</sup>H NMR (700 MHz, CD<sub>3</sub>OD, NH<sup>+</sup>, NH and OH not observed) δ 8.89 (d, *J* 5.4, 1H, quinoline 2-H), 8.16 (d, *J* 5.4, 1H, quinoline 3-H), 8.05 (d, *J* 9.3, 1H, quinoline 8-H), 8.00 (s, 1H, indole 4-H), 7.66 (d, *J* 2.3, 1H, quinoline 5-H), 7.61 (dd, *J* 9.3, 2.3, 1H, quinoline 7-H), 7.36 (s, 1H, indole 7-H), 6.60 (s, 1H, app. s, CH(OH)), 4.82-4.77 (m, 1H, 14-H<sub>A</sub>), 4.09 (s, 3H, OCH<sub>3</sub>), 3.75 (s, 1H, app. s, 11-H), 3.70-3.65 (m, 1H, 13-H), 3.30-3.27 (m, 1H, 14-H<sub>B</sub>), 2.64-2.60 (m, 1H, 12-H<sub>A</sub>), 2.50-2.43 (m, 4H, CH<sub>3</sub> and 15-H<sub>A</sub>), 2.00-1.93 (m, 1H, 15-H<sub>B</sub>), 1.44-1.39 (m, 1H, 12-H<sub>B</sub>). <sup>13</sup>C NMR (176 MHz, CD<sub>3</sub>OD, CF<sub>3</sub>CO<sub>2</sub><sup>-</sup> not observed) δ 162.9 (q, *J*<sub>CF</sub> 35.8, CF<sub>3</sub>CO<sub>2</sub><sup>-</sup>), 161.6 (quinoline 6-C), 154.4 (Ar-C<sub>q</sub>), 144.3 (quinoline 2-C), 141.0 (Ar-C<sub>q</sub>), 138.7 (Ar-C<sub>q</sub>), 135.2 (Ar-C<sub>q</sub>), 132.3 (Ar-C<sub>q</sub>), 128.4 (Ar-C<sub>q</sub>), 127.4 (quinoline 7-C), 127.0 (quinoline 8-C), 120.4 (indole 4-C or quinoline 3-C), 120.3 (indole 4-C or quinoline 3-C), 118.5 (Ar-C<sub>q</sub>), 118.3 (Ar-C<sub>q</sub>), 117.1 (Ar-C<sub>q</sub>), 114.9 (indole 7-C), 102.3 (quinoline 5-C), 69.8 (13-C), 68.0 (CH(OH)), 57.2 (OCH<sub>3</sub>), 51.3 (14-C), 28.9 (11-C), 27.1 (15-C), 24.8 (12-C), 23.6 (CH<sub>3</sub>). HRMS (ESI); C<sub>25</sub>H<sub>24</sub>O<sub>2</sub>N<sub>3</sub><sup>79</sup>Br [M+H]<sup>+</sup>; calculated: 478.1125, found: 478.1122; C<sub>25</sub>H<sub>24</sub>O<sub>2</sub>N<sub>3</sub><sup>81</sup>Br [M+H]<sup>+</sup>; calculated: 480.1104, found: 478.1100. [α]<sub>D</sub><sup>20</sup> -10 (c. 0.1, MeOH).

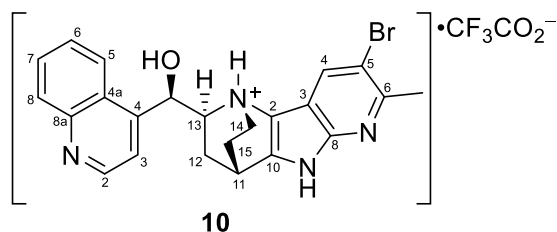
## Preparation of compound 10 and 12

**(1*S*,2*S*,4*S*)-5-Ethylidene-2-[(*R*)-hydroxy(quinolin-4-yl)methyl]-1-azabicyclo[2.2.2]octan-1-ium chloride 8a**

General procedure A, Part I, was followed using cinchonidine (6.0 g, 20.4 mmol) to give the title product **8a** (8.1 g) as a pale yellow solid which was carried forward to the next step without further purification. <sup>1</sup>H NMR (700 MHz, CD<sub>3</sub>OD, 2:1 mixture of *Z/E* alkenes, NH<sup>+</sup> and OH not observed) δ 9.28 (1H, app. s, quinoline 2-H), 8.91 (0.66H, d, *J* 8.0, major quinoline 8-H), 8.88 (0.33H, d, *J* 8.0, minor quinoline 8-H), 8.42 (1H, app. s, quinoline 3-H), 8.36 (1H, d, *J* 8.0, quinoline 5-H), 8.24 (1H, app. s, quinoline 6-H), 8.13-8.06 (1H, m, quinoline 7-H), 6.62 (1H, d, *J* 5.4, CH(OH)), 5.50 (0.66H, d, *J* 5.6, major C=CHCH<sub>3</sub>), 5.44 (0.33H, d, *J* 4.9, minor C=CHCH<sub>3</sub>), 4.40 (1H, app. s, quinuclidine 7-H<sub>A</sub>), 4.28-3.99 (2H, m, quinuclidine 6-H<sub>A</sub> and quinuclidine 6-H<sub>B</sub>), 3.82 (0.66H, app. s, major quinuclidine 2-H), 3.76 (0.33H, app. s, minor quinuclidine 2-H), 3.43 (1H, d, *J* 9.3, quinuclidine 7-H<sub>B</sub>), 3.15 (0.66H, s, minor quinuclidine 4-H), 2.70 (0.33H, s, major quinuclidine 4-H), 2.45 (1H, s, quinuclidine 3-H<sub>A</sub>), 2.25 (1H, d, *J* 12.0, quinuclidine 8-H<sub>A</sub>), 1.96 (1H, d, *J* 12.0, quinuclidine 8-H<sub>B</sub>), 1.61 (2H, d, *J* 4.9, minor CH<sub>3</sub>), 1.54 (1H, d, *J* 5.6, major CH<sub>3</sub>), 1.48 (1H, app. s, quinuclidine 3-H<sub>B</sub>). <sup>13</sup>C NMR (176 MHz, CD<sub>3</sub>OD, 2:1 mixture of *Z/E* alkenes): δ 160.7 (Ar-C<sub>q</sub>), 160.6 (Ar-C<sub>q</sub>), 145.6 (quinoline 2-C), 138.9 (Ar-C<sub>q</sub>), 138.9 (Ar-C<sub>q</sub>), 136.3 (quinoline 6-C), 132.1 (quinoline 7-C), 131.8 (Ar-C<sub>q</sub>), 130.9 (Ar-C<sub>q</sub>), 127.2 (major quinoline 8-C), 127.2 (minor quinoline 8-C), 126.3 (Ar-C<sub>q</sub>), 126.2 (Ar-C<sub>q</sub>), 122.5 (minor quinoline 5-C), 122.5 (major quinoline 5-C), 121.3 (minor quinoline 3-C), 121.2 (major quinoline 3-C), 120.9 (C=CHCH<sub>3</sub>), 68.4 (minor CH(OH)), 68.4 (major CH(OH)), 62.4 (major quinuclidine 2-C), 62.2 (minor quinuclidine 2-C), 58.4 (minor quinuclidine 6-C), 56.7 (major quinuclidine 6-C), 46.2 (major quinuclidine 7-C), 46.1 (minor quinuclidine 7-C), 32.6 (major quinuclidine 4-C), 25.8 (minor quinuclidine 4-C), 25.5 (minor quinuclidine 8-C), 24.8 (major quinuclidine 8-C), 24.5 (minor quinuclidine 3-C), 24.1 (major quinuclidine 3-C), 13.0 (minor CH<sub>3</sub>), 12.8 (major CH<sub>3</sub>). HRMS (ESI): calc. for [M+H]<sup>+</sup> C<sub>19</sub>H<sub>23</sub>ON<sub>2</sub>: 295.1849 found 295.18039.

**(1*S*,4*S*,6*S*)-6-[(1*R*)-1-(Quinolin-4-yl)ethyl]-1-azabicyclo[2.2.2]octan-3-one (9)**

General Procedure A, Part II, was followed using compound **8a** (2.0 g, 6.1 mmol). Flash column chromatography eluting with 5-20% {50:80:1 CH<sub>2</sub>Cl<sub>2</sub>:EtOH:NH<sub>4</sub>OH<sub>(sat. aq.)</sub>} in CH<sub>2</sub>Cl<sub>2</sub> gave the *title product* **9** (791 mg, 2.80 mmol, 41%) as a yellow solid. <sup>1</sup>H NMR (600 MHz, CD<sub>3</sub>OD, OH not observed): δ 8.83 (1H, d, *J* 4.6, quinoline 2-H), 8.27 (1H, d, *J* 8.4, quinoline 8-H), 8.06 (1H, d, *J* 8.7, quinoline 5-H), 7.80-7.76 (1H, m, quinoline 6-H), 7.75 (1H, d, *J* 4.6, quinoline 3-H), 7.68-7.65 (1H, m, quinoline 7-H), 5.74 (1H, d, *J* 4.3, CH(OH)), 3.82-3.76 (1H, m, quinuclidine 7-H<sub>A</sub>), 3.29-3.21 (3H, m, quinuclidine 6-H, quinuclidine 2-H<sub>A</sub> and quinuclidine 2-H<sub>B</sub>), 2.84-2.78 (1H, m, quinuclidine 7-H<sub>B</sub>), 2.46-2.41 (2H, m, quinuclidine 4-H and quinuclidine 5-H<sub>A</sub>), 2.25-2.18 (1H, m, quinuclidine 8-H<sub>A</sub>), 1.95-1.88 (1H, m, quinuclidine 8-H<sub>B</sub>), 1.80-1.74 (1H, m, quinoline 5-H<sub>B</sub>). <sup>13</sup>C NMR (151 MHz, CD<sub>3</sub>OD): δ 220.3 (quinuclidine 3-C), 152.1 (Ar-C<sub>q</sub>), 151.0 (quinoline 2-C), 148.8 (Ar-C<sub>q</sub>), 130.7 (quinoline 6-C), 130.0 (quinoline 5-C), 128.2 (quinoline 7-C), 127.2 (Ar-C<sub>q</sub>), 124.6 (quinolone 8-C), 119.9 (quinoline 3-C), 71.9 (CH(OH)), 65.5 (quinuclidine 2-C), 61.9 (quinuclidine 6-C), 43.4 (quinuclidine 7-C), 41.8 (quinuclidine 4-C), 26.6 (quinuclidine 5-C), 25.8 (quinuclidine 8-C). HRMS (ESI): calc. for [M+H]<sup>+</sup> C<sub>17</sub>H<sub>19</sub>O<sub>2</sub>N<sub>2</sub>: 283.1441, found: 283.1440. [α]<sub>D</sub><sup>20</sup> = -128 (MeOH).

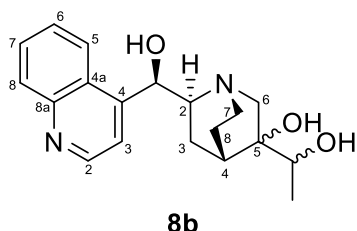
**(1*R*,11*S*,13*S*)-5-Bromo-13-[(*R*)-hydroxy(quinolin-4-yl)methyl]-6-methyl-1,7,9-triazatetracyclo[9.2.2.0<sub>2,10</sub>.0<sub>3,8</sub>]pentadeca-2(10),3,5,7-tetraen-1-ium trifluoroacetate (10)**

Prepared according to General Procedure B using ketone **9** (100 mg, 0.35 mmol, 1.0 eq.) and 20 mol% Pd(OAc)<sub>2</sub> (24 h). Flash column chromatography eluting with 5-20% {50:80:1 CH<sub>2</sub>Cl<sub>2</sub>:EtOH:NH<sub>4</sub>OH} in CH<sub>2</sub>Cl<sub>2</sub> followed by mass-directed preparative HPLC (MeCN in H<sub>2</sub>O + 0.1% TFA; Rt = 11.4 min) gave the *title compound* **10** (18.3 mg, 40.7 μmol, 11%) as a yellow solid. <sup>1</sup>H NMR (700 MHz, CD<sub>3</sub>OD, NH<sup>+</sup>, NH, and OH not observed): δ 9.04 (1H, d, *J* 5.2, quinoline 2-H), 8.49 (1H, d, app. *J* 8.5, quinoline 8-H), 8.34 (1H, s, indole 4-H), 8.16-8.13 (2H, m, quinoline 3-H and quinoline 5-H), 7.96 (1H, app. t, *J* 7.7, quinoline 6-H), 7.86 (1H, app. t, *J* 7.7, quinoline 7-H), 6.52 (1H, app. s, CH(OH)), 4.84-4.81 (1H, m, 14-H<sub>A</sub>) 3.81-3.75 (2H, m, 11-H and 13-H), 3.25 (1H, td, *J* 11.3,

## Experimental

5.0, 14-H<sub>B</sub>), 2.69 (1H, ddd, *J* 12.3, 6.4, 2.0, 12-H<sub>A</sub>), 2.54-2.48 (1H, m, 15-H<sub>A</sub>), 2.67 (3H, s, CH<sub>3</sub>), 1.97-1.91 (1H, m, 15-H<sub>B</sub>), 1.56-1.50 (1H, m, 12-H<sub>B</sub>). <sup>13</sup>C NMR (176 MHz, CD<sub>3</sub>OD, CF<sub>3</sub>CO<sub>2</sub><sup>-</sup> not observed): δ 162.5 (q, *J*<sub>CF</sub> 35.6, CF<sub>3</sub>CO<sub>2</sub><sup>-</sup>), 154.2 (Ar-C<sub>q</sub>), 151.1 (Ar-C<sub>q</sub>), 148.7 (quinoline 2-C), 145.5 (Ar-C<sub>q</sub>), 144.5 (Ar-C<sub>q</sub>), 141.9 (Ar-C<sub>q</sub>), 133.4 (quinolone 6-C), 130.3 (quinoline 7-C), 129.6 (indole 4-C), 126.9 (quinoline 3-C), 126.7 (Ar-C<sub>q</sub>), 124.5 (quinoline 8-C), 120.4 (quinoline 5-C), 115.6 (Ar-C<sub>q</sub>), 114.8 (Ar-C<sub>q</sub>), 111.5 (Ar-C<sub>q</sub>), 69.7 (13-C), 68.0 (CH(OH)), 52.1 (14-C), 28.6 (11-C), 26.9 (15-C), 25.2 (12-C), 25.1 (CH<sub>3</sub>). HRMS (ESI): C<sub>23</sub>H<sub>22</sub>ON<sub>4</sub><sup>79</sup>Br [M+H]<sup>+</sup>; calculated: 449.0972, found 449.09675; C<sub>23</sub>H<sub>22</sub>ON<sub>4</sub><sup>81</sup>Br [M+H]<sup>+</sup>; calculated: 451.0951, found 451.0943. [α]<sub>D</sub><sup>20</sup> = +123 (c. 0.1, MeOH).

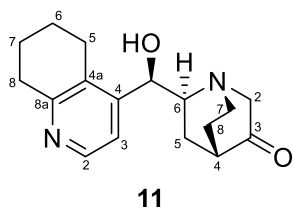
### (1*S*,4*S*,6*S*)-6-[(*R*)-Hydroxy(quinolin-4-yl)methyl]-3-(1-hydroxyethyl)-1-azabicyclo[2.2.2]octan-3-ol (**8b**)



To a stirred solution of compound **8a** (free base form, 2.0 g, 6.8 mmol) in *t*BuOH/H<sub>2</sub>O (36 mL, 0.2 M) was added was K<sub>2</sub>CO<sub>3</sub> (2.9 g, 20.4 mmol, 3.0 eq.) and K<sub>3</sub>Fe(CN)<sub>6</sub> (6.7 g, 20.4 mmol, 3.0 eq.) The mixture was stirred for 45 min, then OsO<sub>4</sub> (4.0% in H<sub>2</sub>O, 432 μL, 68 μmol, 1.0 mol%) was added. The reaction mixture was stirred for 6 h. Due to the poor conversion observed, K<sub>2</sub>O<sub>8</sub>O<sub>4</sub> (75 mg, 0.20 mmol, 4.0 mol%) was added. The reaction mixture was stirred for an additional 3 days. The reaction mixture was quenched by the addition of Na<sub>2</sub>S<sub>2</sub>O<sub>5</sub> (1.0 g). Sat. aq. NaHCO<sub>3</sub> solution (100 mL) was added and the reaction mixture was extracted with 9:1 CHCl<sub>3</sub>/MeOH (4 × 100 mL). The combined organics were dried, filtered, and concentrated *in vacuo*. Flash column chromatography eluting with 50-100% {50:8:1 CH<sub>2</sub>Cl<sub>2</sub>:EtOH:NH<sub>4</sub>OH} in CH<sub>2</sub>Cl<sub>2</sub> gave the *title compound 8b* (97 mg, 0.30 mmol, 4%, mixture of 4 diastereomers) as a pale brown oil. <sup>1</sup>H NMR (700 MHz, CD<sub>3</sub>OD, characteristic peaks given, see Section Fehler! Verweisquelle konnte nicht gefunden werden. for the processed NMR): δ 8.78-8.73 (1H, m, Ar-H), 8.17 (1H, d, *J* 8.4, Ar-H), 7.99 (1H, d, *J* 8.4, Ar-H), 7.73-7.65 (2H, m, Ar-H), 7.61-7.54 (1H, m, Ar-H), 5.67-5.60 (1H, m, ArCH(OH)), 1.05 (0.33H, d, *J* 6.4, diastereomer-1, CH<sub>3</sub>), 1.01 (0.33H, d, *J* 6.3, diastereomer-2, CH<sub>3</sub>), 1.00 (0.17H, d, *J* 6.3, diastereomer-3, CH<sub>3</sub>), 0.99 (0.17H, d, *J* 6.4, diastereomer-4, CH<sub>3</sub>). <sup>13</sup>C NMR (175 MHz, CD<sub>3</sub>OD): δ 152.4 (2 peaks), 152.3 (2 peaks), 150.90 (2 peaks), 150.8 (2 peaks), 148.8, 148.7 (2 peaks), 130.6 (3 peaks), 130.0 (2 peaks), 129.9 (2 peaks), 128.1 (2 peaks), 128.0, 127.1 (3 peaks), 124.6 (2 peaks), 124.5, 119.9 (2 peaks), 119.8 (2 peaks), 74.4, 74.2, 74.1, 73.9, 72.7, 72.6, 72.1, 72.3, 72.1, 72.0, 71.5, 71.3, 70.9, 69.8, 65.9, 65.1, 63.5, 63.1, 61.4, 61.1, 60.5, 60.4, 43.8, 43.7 (2 peaks), 43.5, 31.7, 31.3,

30.5, 30.1, 23.7, 23.6, 23.5, 23.4, 22.8, 22.6, 22.2 (2 peaks), 17.6, 17.5, 16.2, 16.0. **HRMS** (ESI): C<sub>19</sub>H<sub>25</sub>O<sub>3</sub>N<sub>2</sub> [M+H]<sup>+</sup>; calculated: 329.1860, found: 329.1860.

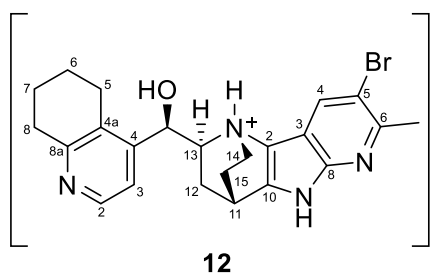
**(1*S*,4*S*,6*S*)-6-[(*R*)-Hydroxy(5,6,7,8-tetrahydroquinolin-4-yl)methyl]-1-azabicyclo[2.2.2]octan-3-one (11)**



Compound **8a** (70 mg, 0.21 mmol) was dissolved in TFA (2.0 mL) and PtO<sub>2</sub> (5 mg, 21 μmol, 10 mol%) was added. The reaction mixture was stirred under an atmosphere of H<sub>2</sub> (5 bar) for 17 h. The reaction mixture was filtered through celite, flushing through with CH<sub>2</sub>Cl<sub>2</sub>, and concentrated *in vacuo*. The crude reaction product was diluted in 8:2 AcOH/H<sub>2</sub>O (1.0 mL). NaIO<sub>4</sub> (90 mg, 0.42 mmol, 2.0 eq.) was added at 0 °C. The reaction mixture was warmed to rt, then stirred overnight. The reaction mixture was cooled to 0 °C, then quenched with 10 M solution NaOH (~1.5 mL) until it was basic. The reaction mixture was transferred to a separating funnel and extracted with 9:1 CHCl<sub>3</sub>/MeOH (5 x 10 mL). The combined organics were dried over Na<sub>2</sub>SO<sub>4</sub>, filtered, and concentrated *in vacuo*. Flash column chromatography eluting with 40% {50:8:1 CH<sub>2</sub>Cl<sub>2</sub>:EtOH:NH<sub>4</sub>OH} in CH<sub>2</sub>Cl<sub>2</sub> gave the *title product* **11** (40 mg, 0.14 mmol, 67% over 2 steps) as a colourless amorphous solid. **<sup>1</sup>H NMR** (500 MHz, CD<sub>3</sub>OD, OH not observed, spectrum complicated by deuterium exchange: only 1 of 2 protons at 2-C observed): δ 8.25 (1H, d, *J* 5.2, pyridine 2-H), 7.39 (1H, d, *J* 5.2, pyridine 3-H), 5.14 (1H, d, *J* 4.9, CH(OH)), 3.67-3.60 (1H, m, quinuclidine 7-H<sub>A</sub>), 3.30-3.25 (1H, m, 2-H), 3.11-3.04 (1H, m, quinuclidine 6-H), 2.96-2.88 (3H, m, CH<sub>A</sub>H<sub>B</sub> and CH<sub>2</sub>), 2.84-2.73 (2H, m, CH<sub>A</sub>H<sub>B</sub> and quinuclidine 7-H<sub>B</sub>), 2.46-2.42 (1H, m, quinuclidine 4-H), 2.37 (1H, ddd, *J* 13.4, 8.0, 2.2, quinuclidine 5-H<sub>A</sub>), 2.19-2.12 (1H, m, quinuclidine 8-H<sub>A</sub>), 1.97-1.80 (6H, m, includes 5-H<sub>B</sub>, 8-H<sub>B</sub> and 2 × CH<sub>2</sub>). **<sup>13</sup>C NMR** (125 MHz, CD<sub>3</sub>OD): complicated by deuterium exchange at 2-C. **HRMS** (ESI): C<sub>17</sub>H<sub>23</sub>O<sub>2</sub>N<sub>2</sub> [M+H]<sup>+</sup>; calculated: 287.1754, found: 287.1751. [ $\alpha$ ]<sub>20</sub><sup>D</sup> = -79 (c. 0.1, MeOH).

## Experimental

### (1*R*,11*S*,13*S*)-5-Bromo-13-[(*R*)-hydroxy(5,6,7,8-tetrahydroquinolin-4-yl)methyl]-6-methyl-1,7,9-triazatetracyclo[9.2.2.0<sup>2,10</sup>.0<sup>3,8</sup>]pentadeca-2(10),3(8),4,6-tetraen-1-ium trifluoroacetate (**12**)

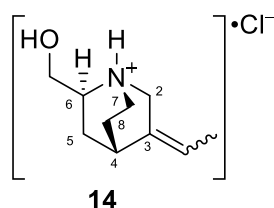


•CF<sub>3</sub>CO<sub>2</sub><sup>-</sup> Prepared according to General Procedure B using ketone **11** (39 mg, 0.14 mmol), MgSO<sub>4</sub> (1.5 eq.) and 30 mol% Pd(OAc)<sub>2</sub> (72 h). Flash column chromatography eluting with 5-20% {50:80:1 CH<sub>2</sub>Cl<sub>2</sub>:EtOH:NH<sub>4</sub>OH} in CH<sub>2</sub>Cl<sub>2</sub> gave the *title compound* **12** (7 mg, 12 μmol, 9%)

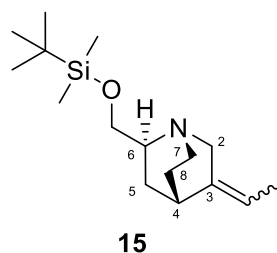
as a brown oil. <sup>1</sup>H NMR (500 MHz, CD<sub>3</sub>OD, OH not observed): δ 8.52 (1H, d, *J* 6.2, Py 2-H), 8.34 (1H, s, indole 4-H), 8.08 (1H, d, *J* 6.2, Py 3-H), 5.96 (1H, app. s, CH(OH)), 4.65 (1H, ddd, *J* 11.7, 9.2, 4.1, 14-H<sub>A</sub>), 3.80-3.76 (1H, m, 11-H), 3.59 (1H, dd, *J* 10.3, 6.6, 13-H), 3.21-3.14 (1H, m, 14-H<sub>B</sub>), 3.12-2.96 (3H, m, CH<sub>A</sub>H<sub>B</sub> and CH<sub>2</sub>), 2.81-2.73 (1H, m, CH<sub>A</sub>H<sub>B</sub>), 2.68-2.62 (4H, m, includes 12-H<sub>A</sub>, and at δ 2.65: 3H, s, CH<sub>3</sub>), 2.47-2.39 (1H, m, 15-H<sub>A</sub>), 1.99-1.80 (5H, m, 15-H<sub>B</sub> and 2 × CH<sub>2</sub>), 1.58-1.50 (1H, m, 12-H<sub>B</sub>). <sup>13</sup>C NMR (125 MHz, CD<sub>3</sub>OD): δ 160.7 (Ar-C<sub>q</sub>), 154.1 (Ar-C<sub>q</sub>), 151.2 (Ar-C<sub>q</sub>), 145.5 (Ar-C<sub>q</sub>), 141.8 (Ar-C<sub>q</sub>), 139.7 (Py 2-C), 136.1 (Ar-C<sub>q</sub>), 129.8 (indole 4-C), 123.2 (Py 3-C), 115.4 (Ar-C<sub>q</sub>), 114.9 (Ar-C<sub>q</sub>), 111.6 (Ar-C<sub>q</sub>), 67.8 (13-C), 67.5 (CH(OH)), 51.7 (14-C), 29.0 (CH<sub>2</sub>), 28.5 (11-C), 26.8 (15-C), 25.7 (CH<sub>2</sub>), 25.1 (CH<sub>3</sub>), 24.7 (12-C), 22.1 (CH<sub>2</sub>), 21.3 (CH<sub>2</sub>). HRMS (ESI): C<sub>2</sub>H<sub>26</sub>ON<sub>4</sub><sup>79</sup>Br [M+H]<sup>+</sup>; calculated: 453.1285, found: 453.1282; C<sub>2</sub>H<sub>26</sub>ON<sub>4</sub><sup>81</sup>Br [M+H]<sup>+</sup>; calculated: 455.1264, found: 455.1262.



## Preparation of compound 18

**(1*S*,2*S*,4*S*)-5-Ethylidene-2-(hydroxymethyl)-1-azabicyclo[2.2.2]octan-1-ium chloride (14)**

General procedure A, Part I, was followed using quincorine (1.52 g, 9.1 mmol). Flash column chromatography eluting with 1:4 ({50:80:1 DCM:EtOH:NH<sub>4</sub>OH}/DCM) gave the *title compound* **14** (2.1 g) as yellow oil. <sup>1</sup>H NMR (500 MHz, CD<sub>3</sub>OD, 55:45 mixture of *Z/E* alkenes, NH<sup>+</sup> and OH not observed): δ 5.48 (0.55H, d, *J* 6.8, major C=CHCH<sub>3</sub>), 5.42 (0.45H, d, *J* 6.8, minor C=CHCH<sub>3</sub>), 4.09-3.91 (2H, m, 2-H<sub>A</sub> and 2-H<sub>B</sub>), 3.84-3.78 (1H, m, CH<sub>A</sub>H<sub>B</sub>OH), 3.77-3.69 (1H, m, CH<sub>A</sub>H<sub>B</sub>OH), 3.67-3.56 (2H, 6-H, 7-H<sub>A</sub>), 3.29-3.21 (1H, m, 7-H<sub>B</sub>), 3.09 (0.45H, s, minor 4-H), 2.63 (0.55H, s, major 4-H), 2.07-1.95 (2H, m, 5-H<sub>A</sub> and 8-H<sub>A</sub>), 1.95-1.86 (1H, m, 5-H<sub>B</sub>), 1.71 (1.35H, d, *J* 6.8, minor CH<sub>3</sub>), 1.61 (1.65H, d, *J* 6.8, major CH<sub>3</sub>), 1.58-1.51 (1H, m, 8-H<sub>B</sub>). <sup>13</sup>C NMR (126 MHz, CD<sub>3</sub>OD): δ 132.2 (minor 3-C), 131.4 (major 3-C), 120.8 (minor C=CHCH<sub>3</sub>), 120.6 (major C=CHCH<sub>3</sub>), 61.6 (minor 6-C), 61.4 (major 6-C), 61.6 (minor CH<sub>2</sub>OH), 61.2 (major CH<sub>2</sub>OH), 56.9 (minor 2-C), 55.1 (major 2-C), 42.8 (minor 7-C), 42.6 (major 7-C), 31.9 (minor 4-C), 28.4 (minor 8-C), 27.5 (major 8-C), 25.4 (minor 5-C), 25.1 (major 4-C), 24.5 (major 5-C), 12.9 (minor CH<sub>3</sub>), 12.8 (major CH<sub>3</sub>). HRMS (ESI): C<sub>10</sub>H<sub>18</sub>ON [M+H]<sup>+</sup>; calculated: 168.1383, found 168.1379.

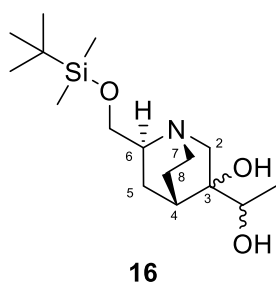
**(1*S*,2*S*,4*S*)-2-[(*tert*-Butyldimethylsilyl)oxy]methyl}-5-ethylidene-1-azabicyclo[2.2.2]octane (15)**

To a stirred solution of compound **14** (1.52 g, 9.1 mmol) in CH<sub>2</sub>Cl<sub>2</sub> (30 mL, 0.3 M) was added Et<sub>3</sub>N (3.8 mL, 27.2 mmol, 3.0 eq.). After the solution was stirred under Ar for 15 min, DMAP (111 mg, 0.9 mmol, 0.1 eq.) and TBDMSCl (4.11 g, 27.2 mmol, 3.0 eq.) were added at 0 °C. The reaction mixture was stirred for 48 h at rt until the reaction showed complete consumption of the starting material (monitored by LCMS). The reaction mixture was washed with saturated aqueous NaHCO<sub>3</sub> (50 mL) and the resulting solution was extracted with CH<sub>2</sub>Cl<sub>2</sub> (4 x 50 mL). The combined organic layers were dried over MgSO<sub>4</sub>, filtered and concentrated *in vacuo*. The crude product was purified by flash column chromatography eluting with 1:9 ({50:80:1 CH<sub>2</sub>Cl<sub>2</sub>:EtOH:NH<sub>4</sub>OH}/ CH<sub>2</sub>Cl<sub>2</sub>) followed by removal of solvents under reduced pressure to give the *title compound* **15** (860 mg, 3.06 mmol, 34%) as yellow oil. <sup>1</sup>H NMR (700 MHz, CD<sub>3</sub>OD, 1:1 mixture of *Z/E* alkenes): δ 5.31-5.19 (1H, m, C=CHCH<sub>3</sub>), 3.76-3.68 (2H, m, CH<sub>2</sub>OTBDMS), 3.51-3.36 (2H, m, 2-H<sub>A</sub> and 2-H<sub>B</sub>), 3.22-

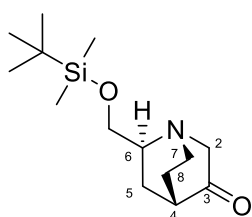
## Experimental

3.14 (1H, m, 7-H<sub>A</sub>), 2.88-2.82 (1H, m, 6-H), 2.81 (0.5H, s, 4-H<sup>a</sup>), 2.72-2.63 (1H, m, 7-H<sub>B</sub>), 2.32 (0.5H, s, 4-H<sup>b</sup>), 1.78-1.66 (2H, m, 5-H<sub>A</sub> and 8-H<sub>A</sub>), 1.64-1.52 (5H, m, 5-H<sub>B</sub>, 8-H<sub>B</sub> and C=CHCH<sub>3</sub>), 0.92 (9H, s, Si(CH<sub>3</sub>)<sub>2</sub>C(CH<sub>3</sub>)<sub>3</sub>), 0.10 (3H, app, d, *J* 1.3, Si(CH<sup>a</sup>)<sub>2</sub>C(CH<sub>3</sub>)<sub>3</sub>), 0.08 (3H, app, d, *J* 1.3, Si(CH<sup>b</sup>)<sub>2</sub>C(CH<sub>3</sub>)<sub>3</sub>). <sup>13</sup>C NMR (176 MHz, CD<sub>3</sub>OD): δ 141.6 (3-C<sup>a</sup>), 140.5 (3-C<sup>b</sup>), 115.7 (C<sup>a</sup>HCH<sub>3</sub>), 115.4 (C<sup>b</sup>HCH<sub>3</sub>), 66.5 (C<sup>a</sup>H<sub>2</sub>OTBDMS), 66.4 (C<sup>b</sup>H<sub>2</sub>OTBDMS), 59.5 (6-C<sup>a</sup>), 59.2 (6-C<sup>b</sup>), 58.9 (2-C<sup>a</sup>), 56.6 (2-C<sup>b</sup>), 43.7 (7-C<sup>a</sup>), 43.6 (7-C<sup>b</sup>), 34.4 (4-C<sup>a</sup>), 32.0 (8-C<sup>a</sup>), 31.1 (8-C<sup>b</sup>), 28.7 (5-C<sup>a</sup>), 27.5 (5-C<sup>b</sup>), 26.8 (4-C<sup>b</sup>), 26.4 (Si(CH<sub>3</sub>)<sub>2</sub>C(C<sup>a</sup>H<sub>3</sub>)<sub>3</sub>), 26.4 (Si(CH<sub>3</sub>)<sub>2</sub>C(C<sup>b</sup>H<sub>3</sub>)<sub>3</sub>), 19.2 (Si(CH<sub>3</sub>)<sub>2</sub>C<sup>a</sup>(CH<sub>3</sub>)<sub>3</sub>), 19.2 (Si(CH<sub>3</sub>)<sub>2</sub>C<sup>b</sup>(CH<sub>3</sub>)<sub>3</sub>), 12.8 (C=CHC<sup>a</sup>H<sub>3</sub>), 12.4 (C=CHC<sup>b</sup>H<sub>3</sub>), -5.3 (Si(CH<sub>3</sub>)<sub>2</sub>C(CH<sub>3</sub>)<sub>3</sub>). HRMS (ESI): C<sub>16</sub>H<sub>32</sub>ONSi [M+H]<sup>+</sup>; calculated: 282.2248 found 282.2247.

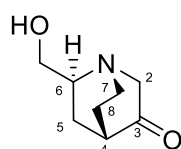
### (1*S*,4*S*,6*S*)-6-{{*tert*-Butyldimethylsilyloxy}methyl}-3-(1-hydroxyethyl)-1-azabicyclo[2.2.2]octan-3-ol (16)



Compound **15** (860 mg, 3.05 mmol) was added to a two phase system of K<sub>2</sub>CO<sub>3</sub> (1.28 g, 9.15 mmol, 3.0 eq.) and K<sub>3</sub>Fe(CN)<sub>6</sub> (3.01 g, 9.15 mmol, 3.0 eq.) in 1:1 *t*BuOH/H<sub>2</sub>O (0.3 M, 10.2 mL). The reaction mixture was stirred for 45 min, then 4% OsO<sub>4</sub> in H<sub>2</sub>O (194 μL, 30.6 μmol, 1.0 mol%) was added at rt. After 20 h the reaction mixture was quenched with a saturated aqueous solution Na<sub>2</sub>S<sub>2</sub>O<sub>3</sub> (2 mL) and washed with saturated aqueous NaHCO<sub>3</sub> (50 mL) and the resulting solution was extracted with CH<sub>2</sub>Cl<sub>2</sub> (4 x 50 mL). The combined organic layers were dried over MgSO<sub>4</sub>, filtered and concentrated *in vacuo*. The obtained crude was purified by flash column chromatography eluting with 1:9 ({50:80:1 CH<sub>2</sub>Cl<sub>2</sub>:EtOH:NH<sub>4</sub>OH}/CH<sub>2</sub>Cl<sub>2</sub>) followed by removal of solvents under reduced pressure gave the *title compound 16* (655 mg, 2.08 mmol, 68 %) as white solid. <sup>1</sup>H NMR (700 MHz, CD<sub>3</sub>OD, characteristic peaks given): δ 3.92-3.78 (1H, m, CH(OH)CH<sub>3</sub>), 3.75-3.67 (2H, m), 3.19-2.98 (2H, m), 2.81-2.42 (3H, m), 2.23-1.98 (1H, m), 1.88-1.47 (2H, m), 1.41-1.18 (2H, m), 1.17-1.10 (3H, m, CH(OH)CH<sub>3</sub>), 0.93 (9H, s, Si(CH<sub>3</sub>)<sub>2</sub>C(CH<sub>3</sub>)<sub>3</sub>), 0.12-0.04 (6H, m, Si(CH<sub>3</sub>)<sub>2</sub>C(CH<sub>3</sub>)<sub>3</sub>). <sup>13</sup>C NMR (176 MHz, CD<sub>3</sub>OD): δ 74.5, 74.4, 74.1, 74.0, 73.8, 72.9, 72.6, 70.8, 70.0, 66.6, 66.5, 66.4, 65.1, 64.5, 62.7, 62.4, 58.3, 58.0, 57.8, 57.7, 42.7, 42.6, 42.4, 31.3, 31.0, 30.1, 29.8, 27.0, 26.9, 26.4, 26.4, 26.3, 26.2, 23.6, 23.5, 22.5, 22.4, 19.2, 17.6, 16.2, 16.0, -5.3. HRMS (ESI): C<sub>16</sub>H<sub>34</sub>O<sub>3</sub>NSi [M+H]<sup>+</sup>; calculated: 316.2302, found: 316.2301.

**(1*S*,4*S*,6*S*)-6-[(*tert*-Butyldimethylsilyloxy)methyl]-1-azabicyclo[2.2.2]octan-3-one (17, protected)****17, protected**

Compound **16** (655 mg, 2.08 mmol) was dissolved in *t*BuOH (7 mL, 0.3 M). A saturated solution of NaIO<sub>4</sub> (578 mg, 2.70 mmol, 1.3 eq.) in H<sub>2</sub>O (6.35 mL) was added. The reaction mixture was stirred at rt for 2 h, treated with aqueous NaHCO<sub>3</sub> (50 mL) and extracted with CH<sub>2</sub>Cl<sub>2</sub> (4 x 50 mL). The combined organic layers were dried over MgSO<sub>4</sub>, filtered and concentrated *in vacuo*. Flash column chromatography eluting with 1:9 ({50:80:1 CH<sub>2</sub>Cl<sub>2</sub>:EtOH:NH<sub>4</sub>OH}/CH<sub>2</sub>Cl<sub>2</sub>) gave the *title product* **17, protected** (412 mg, 1.53 mmol, 73%) as white solid. <sup>1</sup>H NMR (600 MHz, CD<sub>3</sub>OD): δ 3.82 (1H, s, CH<sub>A</sub>H<sub>B</sub>OTBDMS), 3.81 (1H, s, CH<sub>A</sub>H<sub>B</sub>OTBDMS), 3.38-3.32 (1H, m, 7-H<sub>A</sub>), 3.08-2.95 (1H, m, 6-H), 2.84-2.73 (1H, m, 7-H<sub>B</sub>), 2.44-2.36 (1H, m, 4-H), 2.11-1.96 (2H, m, 5-H<sub>A</sub> and 8-H<sub>A</sub>), 1.95-1.80 (2H, m, 5-H<sub>B</sub> and 8-H<sub>B</sub>), 0.94 (9H, s, Si(CH<sub>3</sub>)<sub>2</sub>C(CH<sub>3</sub>)<sub>3</sub>), 0.12 (6H, d, *J* 3.5, Si(CH<sub>3</sub>)<sub>2</sub>C(CH<sub>3</sub>)<sub>3</sub>). <sup>13</sup>C NMR (151 MHz, CD<sub>3</sub>OD): δ 220.2 (3-C), 66.1 (CH<sub>2</sub>OTBDMS), 58.8 (6-C), 42.5 (7-C), 41.6 (4-C), 29.1 (8-C), 26.4 (Si(CH<sub>3</sub>)<sub>2</sub>C(CH<sub>3</sub>)<sub>3</sub>), 25.9 (5-C), 19.2 (Si(CH<sub>3</sub>)<sub>2</sub>C(CH<sub>3</sub>)<sub>3</sub>), -5.4 (Si(CH<sub>3</sub>)<sub>2</sub>C(CH<sub>3</sub>)<sub>3</sub>). HRMS (ESI): C<sub>14</sub>H<sub>28</sub>O<sub>2</sub>NSi [M+H]<sup>+</sup>; calculated: 270.1884, found 270.1884. [α]<sub>D</sub><sup>20</sup> = -21 (c. 0.1, MeOH).

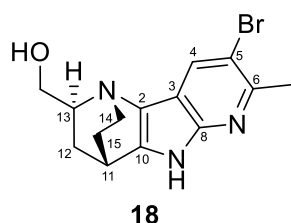
**(1*S*,4*S*,6*S*)-6-(Hydroxymethyl)-1-azabicyclo[2.2.2]octan-3-one (17)****17**

TBAF (1.0 M in THF, 2.9 mL, 1.3 eq.) was added to compound **17, protected** (600 mg, 2.23 mmol, 1.0 eq.) in THF (4.5 mL) at 0 °C. The resulting mixture was stirred at rt for 20 h, then a 1:1 sat aq. brine / sat. aq. NaHCO<sub>3</sub> mixture was added (10 mL). The mixture was extracted with CHCl<sub>3</sub> (1 × 20 mL), CHCl<sub>3</sub>:MeOH (9:1, 3 × 20 mL), and CHCl<sub>3</sub>:MeOH (8:2, 3 × 20 mL). The combined organics were dried over MgSO<sub>4</sub>, filtrated and concentrated *in vacuo*. Flash column chromatography eluting with 5% to 10% {50:80:1 CH<sub>2</sub>Cl<sub>2</sub>:EtOH:NH<sub>4</sub>OH} in CH<sub>2</sub>Cl<sub>2</sub>, gave the *title compound* **18** as white solid (191 mg, 1.23 mmol, 55%). <sup>1</sup>H NMR (600 MHz, CD<sub>3</sub>OD, OH, 2-H not observed): δ 3.71 (dd, *J* 11.5, 8.2 Hz, 1H, CH<sub>A</sub>H<sub>B</sub>OH), 3.61 (dd, *J* 11.5, 6.0 Hz, 1H, CH<sub>A</sub>H<sub>B</sub>OH), 3.23 (ddd, *J* 14.3, 10.2, 5.5 Hz, 1H, quinuclidine 7-H<sub>A</sub>), 3.07-2.98 (m, 1H, quinuclidine 6-H), 2.84-2.74 (m, 1H, quinuclidine 7-H<sub>B</sub>), 2.39-2.35 (m, 1H, quinuclidine 4-H), 2.11-2.03 (m, 1H, quinuclidine 5-H<sub>A</sub>), 2.00-1.94 (m, 1H, quinuclidine 8-H<sub>A</sub>), 1.94-1.88 (m, 1H, quinuclidine 8-H<sub>B</sub>), 1.62 (ddd, *J* 13.5, 7.5, 2.3 Hz, 1H, quinuclidine 5-H<sub>B</sub>). <sup>13</sup>C NMR (151 MHz, CD<sub>3</sub>OD): δ 220.5 (quinuclidine 3-C), 98.2 (quinuclidine 2-C), 64.0 (CH<sub>2</sub>OH), 58.8

## Experimental

(quinuclidine 6-C), 41.5 (quinuclidine 4-C), 41.2 (quinuclidine 7-C), 29.7 (quinuclidine 5-C), 26.0 (quinuclidine 8-C). **HRMS** (ESI): C<sub>8</sub>H<sub>14</sub>O<sub>2</sub>N [M+H]<sup>+</sup>; calculated: 156.1019, found: 156.1016.  $[\alpha]_{\text{D}}^{20} = -27$  (c. 0.1, MeOH).

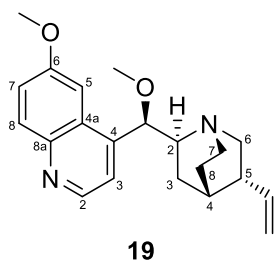
### [(11*S*,13*S*)-5-Bromo-6-methyl-1,7,9-triazatetracyclo[9.2.2.02,10.03,8]pentadeca-2(10),3,5,7-tetraen-13-yl]methanol (**18**)



Prepared according to General Procedure B using ketone **18** (100 mg, 0.35 mmol, 1.0 eq.) and 20 mol% Pd(OAc)<sub>2</sub>. Flash column chromatography eluting with 5-15% {50:80:1 CH<sub>2</sub>Cl<sub>2</sub>:EtOH:NH<sub>4</sub>OH} in CH<sub>2</sub>Cl<sub>2</sub> gave the *title compound 18* (53 mg, 0.17 mmol, 26%) as a yellow solid. **<sup>1</sup>H NMR** (600 MHz, CD<sub>3</sub>OD, NH and OH not observed): δ 8.16 (1H, s, 4-H), 3.85 (1H, dd, *J* 11.4, 8.1, CH<sub>A</sub>H<sub>B</sub>OH), 3.77 (1H, dd, *J* 11.4, 6.1 Hz, CH<sub>A</sub>H<sub>B</sub>OH), 3.50-3.44 (1H, m, 14-H<sub>A</sub>), 3.42-3.39 (1H, m, 11-H), 2.89-2.82 (1H, m, 13-H), 2.65 (3H, s, CH<sub>3</sub>), 2.53-2.44 (1H, m, 14-H<sub>B</sub>), 1.96-1.90 (1H, m, 15-H<sub>A</sub>), 1.84-1.77 (1H, m, 12-H<sub>A</sub>), 1.62-1.55 (1H, m, 15-H<sub>B</sub>), 1.55-1.50 (1H, m, 12-H<sub>B</sub>). **<sup>13</sup>C NMR** (151 MHz, CD<sub>3</sub>OD): δ 148.0 (Ar-C<sub>q</sub>), 145.8 (Ar-C<sub>q</sub>), 145.4 (Ar-C<sub>q</sub>), 129.2 (4-C), 125.1 (Ar-C<sub>q</sub>), 115.6 (Ar-C<sub>q</sub>), 113.6 (Ar-C<sub>q</sub>), 64.6 (CH<sub>2</sub>OH), 64.4 (13-H), 45.7 (14-C), 33.5 (12-C), 30.3 (15-C), 28.9 (11-C), 24.7 (CH<sub>3</sub>). **HRMS** (ESI): C<sub>14</sub>H<sub>17</sub>ON<sub>3</sub><sup>79</sup>Br [M+H]<sup>+</sup>; calculated: 322.0549, found: 322.0554; C<sub>14</sub>H<sub>17</sub>ON<sub>3</sub><sup>81</sup>Br [M+H]<sup>+</sup>; calculated: 324.0529, found: 324.0527.  $[\alpha]_{\text{D}}^{20} = -36$  (c. 0.1, MeOH).

## Preparation of compound 20

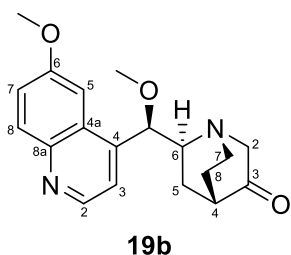
## 4-[(R)-[(1S,2S,4S,5R)-5-Ethenyl-1-azabicyclo[2.2.2]octan-2-yl](methoxy)methyl]-6-methoxyquinoline (19)



To a stirred solution of quinine (2.0 g, 6.2 mmol, 1.0 eq.) in anhydrous DMF (20 mL) was added portionwise NaH (60% dispersion in mineral oil, 618 mg, 15.5 mmol, 2.5 eq.) at rt. The reaction mixture was stirred for 1 h, then MeI (430  $\mu$ l, 6.9 mmol, 1.1 eq.) was added dropwise. The reaction mixture was stirred for 17 h, then quenched with sat. aq. brine solution (20 mL). The resulting solution was extracted with EtOAc (3  $\times$  50 mL), then the combined organics were dried over MgSO<sub>4</sub>, filtered, and concentrated *in vacuo*. Flash column chromatography eluting with 9:1 EtOAc–MeOH gave the title product as an off-white solid (1.11 g, 3.3 mmol, 53%). **<sup>1</sup>H NMR** (500 MHz, CD<sub>3</sub>OD):  $\delta$  8.65 (1H, d, *J* 4.6, quinoline 2-H), 7.94 (1H, d, *J* 9.8, quinoline 8-H), 7.54 (1H, d, *J* 4.6, quinoline 3-H), 7.44–7.38 (2H, m, quinoline 5-H and 7-H), 5.70 (1H, ddd, *J* 17.1, 10.4, 7.5, CHCH=CH<sub>2</sub>), 5.10 (1H, d, *J* 3.0, CH(OCH<sub>3</sub>)), 4.93 (1H, dt, *J* 17.2, 1.5, CHCH=CH<sub>cis</sub>H<sub>trans</sub>), 4.88–4.83 (1H, m, CHCH=CH<sub>cis</sub>H<sub>trans</sub>), 3.95 (3H, s, OCH<sub>3</sub>), 3.52–3.45 (1H, m, 6-H<sub>A</sub>), 3.31 (OCH<sub>3</sub>), 3.13–3.04 (2H, m, 2-H and 7-H<sub>A</sub>), 2.78–2.69 (1H, m, 6-H<sub>B</sub>), 2.64 (1H, ddd, *J* 13.6, 5.0, 2.6, 7-H<sub>B</sub>), 2.36–2.29 (1H, m, 5-H), 1.87–1.74 (3H, m, 3-H<sub>A</sub>, 4-H, and 8-H<sub>A</sub>), 1.62–1.54 (1H, m, 8-H<sub>B</sub>), 1.51–1.44 (1H, m, 3-H<sub>B</sub>). **<sup>13</sup>C NMR** (125 MHz, CD<sub>3</sub>OD):  $\delta$  159.9 (quinoline 6-C), 148.2 (quinoline 2-C), 146.4 (Ar-C<sub>q</sub>), 145.1 (Ar-C<sub>q</sub>), 142.5 (CH=CH<sub>2</sub>), 131.6 (quinoline 8-C), 128.9 (Ar-C<sub>q</sub>), 123.6 (quinoline 7-C), 120.3 (quinoline 3-C), 115.1 (CH=CH<sub>2</sub>), 102.3 (quinoline 5-C), 83.2 (CH(OCH<sub>3</sub>)), 61.0 (2-C), 57.5 (7-C or OCH<sub>3</sub>), 57.4 (7-C or OCH<sub>3</sub>), 56.5 (OCH<sub>3</sub>), 44.2 (6-C), 40.8 (5-C), 29.1 (4-C), 28.1 (8-C), 22.3 (3-C). **HRMS** (ESI): C<sub>21</sub>H<sub>27</sub>O<sub>2</sub>N<sub>2</sub> [M+H]<sup>+</sup>; calculated: 339.2067, found: 339.2067.  $[\alpha]_{20}^D = -209$  (c. 0.1, MeOH).

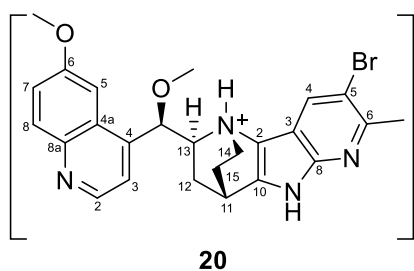
## Experimental

### (1*S*,4*S*,6*S*)-6-[(*R*)-Methoxy(6-methoxyquinolin-4-yl)methyl]-1-azabicyclo[2.2.2]octan-3-one **19b**



General procedure A, Part I, was followed using compound **19** (1.10 g, 3.25 mmol, 1.0 eq.) to give **19a** (1.3 g) as a pale yellow solid which was carried forward to the next step without further purification. General Procedure A, Part II, was followed using compound **19a** (1.3 g, assume 3.25 mmol). Flash column chromatography eluting with 5-35% {50:80:1 CH<sub>2</sub>Cl<sub>2</sub>:EtOH:NH<sub>4</sub>OH<sub>(sat. aq.)</sub>} in CH<sub>2</sub>Cl<sub>2</sub> gave the *title product* **19b** (568 mg, 1.74 mmol, 54%) as a yellow solid. <sup>1</sup>H NMR (500 MHz, CD<sub>3</sub>OD, not observed): δ 8.62 (1H, d, *J* 4.6, quinoline 2-H), 7.89 (1H, d, *J* 9.2, quinoline 8-H), 7.50 (1H, d, *J* 4.6, quinoline 3-H), 7.41 (1H, d, *J* 2.7, quinoline 5-H), 7.34 (1H, dd, *J* 9.3, 2.7, quinoline 7-H), 5.14 (1H, d, *J* 4.1, CH(OCH<sub>3</sub>)), 3.92 (3H, s, OCH<sub>3</sub>), 3.61-3.53 (1H, m, 7-H<sub>A</sub>), 3.29 (3H, s, OCH<sub>3</sub>), 3.22-3.10 (2H, m, 2-H<sub>A</sub> and 6-H), 2.84-2.58 (2H, m, 2-H<sub>B</sub> and 7-H<sub>B</sub>), 2.31-2.23 (2H, m, 4-H and 5-H<sub>A</sub>), 2.12-2.02 (1H, m, 8-H<sub>A</sub>), 1.89-1.71 (1H, m, 8-H<sub>B</sub>), 1.69-1.57 (1H, m, 5-H<sub>B</sub>). <sup>13</sup>C NMR (125 MHz, CD<sub>3</sub>OD, 3-C not observed): δ 159.7 (quinoline 6-C), 148.2 (quinoline 2-C), 146.5 (Ar-C<sub>q</sub>), 145.0 (Ar-C<sub>q</sub>), 131.5 (quinoline 8-C), 128.9 (Ar-C<sub>q</sub>), 123.6 (quinoline 7-C), 120.2 (quinoline 3-C), 102.5 (quinoline 5-C), 82.9 (CH(OCH<sub>3</sub>)), 65.3 (2-C), 61.1 (6-C), 57.5 (OCH<sub>3</sub>), 56.4 (OCH<sub>3</sub>), 43.4 (7-C), 41.6 (4-C), 26.8 (5-C), 25.7 (8-C). HRMS (ESI): C<sub>19</sub>H<sub>23</sub>O<sub>3</sub>N<sub>2</sub> [M+H]<sup>+</sup>; calculated: 327.1703, found: 327.1700. [α]<sub>20</sub><sup>D</sup> = -125 (c. 0.1, MeOH).

**(1*R*,11*S*,13*S*)-5-Bromo-13-[(*R*)-methoxy(6-methoxyquinolin-4-yl)methyl]-6-methyl-1,7,9-triazatetracyclo[9.2.2.0<sup>2,10</sup>.0<sup>3,8</sup>]pentadeca-2(10),3(8),4,6-tetraen-1-ium trifluoroacetate **20****



•CF<sub>3</sub>CO<sub>2</sub><sup>-</sup> Prepared according to General Procedure B using ketone **19b** and 30 mol% Pd(OAc)<sub>2</sub> (72h). Flash column chromatography eluting with 1:19 to 1:4 ({50:80:1 CH<sub>2</sub>Cl<sub>2</sub>:EtOH:NH<sub>4</sub>OH}/CH<sub>2</sub>Cl<sub>2</sub>), followed by mass-directed preparative HPLC (MeCN in H<sub>2</sub>O + 0.1% TFA; Rt = 14 min) gave

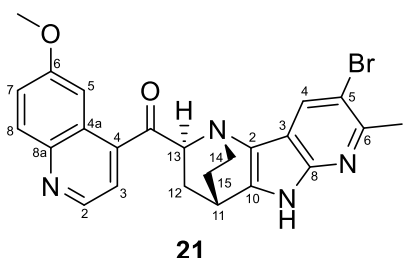
the *title compound* **20** (20 mg, 40 μmol, 13%) as a yellow solid. <sup>1</sup>H NMR (700 MHz, CD<sub>3</sub>OD, NH and NH<sup>+</sup> not observed) δ 8.93 (1H, d, *J* 5.4, quinoline 2-H), 8.41 (1H, indole 4-H), 8.08 (1H, d, *J* 9.2, quinoline 8-H), 8.06 (1H, d, *J* 5.4, quinoline 3-H), 7.71 (1H, d, 2.3, quinoline 5-H), 7.67 (1H, dd, *J* 9.2, 2.3, quinoline 7-H), 6.30 (1H, app. s, CH(OCH<sub>3</sub>)), 4.54-4.46 (1H, m, 14-H<sub>A</sub>), 4.10 (3H, s, OCH<sub>3</sub>), 3.77 (1H, app. s, 11-H), 3.72-3.68 (1H, m, 13-H), 3.62 (3H, s, OCH<sub>3</sub>), 3.30-3.24 (1H, m, 14-H<sub>B</sub>), 2.66 (3H, s, CH<sub>3</sub>), 2.65-2.61 (1H, m, 12-H<sub>A</sub>), 2.48-2.42 (1H, m, 15-H<sub>A</sub>), 2.37-2.33 (1H, m, 15-H<sub>B</sub>), 1.98 (1H, d, *J* 11.7, 12-H<sub>B</sub>). <sup>13</sup>C NMR (176 MHz, CD<sub>3</sub>OD, CF<sub>3</sub>CO<sub>2</sub><sup>-</sup> not observed) δ 162.5 (q, *J*<sub>CF</sub> 35.6, CF<sub>3</sub>CO<sub>2</sub><sup>-</sup>), 161.9 (quinoline 6-C), 151.1 (Ar-C<sub>q</sub>), 145.7 (Ar-C<sub>q</sub>), 144.1 (quinoline 2-C), 141.9 (Ar-C<sub>q</sub>), 138.6 (Ar-C<sub>q</sub>), 129.6 (indole 4-C), 127.8 (quinoline 7-C), 126.7 (quinoline 8-C), 120.4 (quinoline 3-C), 116.9 (Ar-C<sub>q</sub>), 114.8 (Ar-C<sub>q</sub>), 111.7 (Ar-C<sub>q</sub>), 109.1 (Ar-C<sub>q</sub>), 102.6 (quinoline 5-C), 93.6 (Ar-C<sub>q</sub>), 78.16 (CH(OCH<sub>3</sub>)), 68.7 (13-C), 58.1 (OCH<sub>3</sub>), 57.5 (OCH<sub>3</sub>), 51.1, (14-C), 28.6 (11-C), 27.1 (15-C), 25.5 (12-C), 25.1 (CH<sub>3</sub>). HRMS (ESI): C<sub>25</sub>H<sub>26</sub>O<sub>2</sub>N<sub>4</sub><sup>79</sup>Br [M+H]<sup>+</sup>; calculated: 493.1234, found: 493.1229; C<sub>25</sub>H<sub>26</sub>O<sub>2</sub>N<sub>4</sub><sup>81</sup>Br [M+H]<sup>+</sup>; calculated: 495.1213, found: 495.1208. [α]<sub>D</sub><sup>20</sup> -10 (c. 0.1, MeOH).

## Experimental

### Preparation of compound 21

#### (13*S*)-5-Bromo-13-(6-methoxyquinoline-4-carbonyl)-6-methyl-1,9-diazatetracyclo

#### [9.2.2.0<sup>2,10</sup>.0<sup>3,8</sup>]pentadeca-2(10),3,5,7-tetraene (21)



DMSO (22.2  $\mu\text{L}$ , 313  $\mu\text{mol}$ , 3 eq.) in THF (800  $\mu\text{L}$ ) was cooled to  $-78^\circ\text{C}$ . Oxalylchloride (17.9  $\mu\text{L}$  0.21 mmol, 2.5 eq.) was added slowly and the mixture was stirred for 0.5 h at  $-78^\circ\text{C}$ . Compound **6s** (azaquinole-1, 40 mg, 83  $\mu\text{mol}$ ) was dissolved in THF (0.1 M, 800  $\mu\text{L}$ ) and added dropwise.

The mixture was stirred for 0.5 h at  $-78^\circ\text{C}$ , then  $\text{Et}_3\text{N}$  (69.8  $\mu\text{L}$ , 0.50 mmol, 6.0 eq.) was added dropwise. The mixture was stirred at  $-78^\circ\text{C}$  for 0.5 h, at  $0^\circ\text{C}$  for 0.5 h and at rt for 2 h. Purification by mass-directed preparative HPLC (MeCN in  $\text{H}_2\text{O}$  + 0.1% TFA;  $R_t$  = 14 min) followed by column chromatography eluting with 10-50% {50:80:1  $\text{CH}_2\text{Cl}_2$ :EtOH: $\text{NH}_4\text{OH}$ } in  $\text{CH}_2\text{Cl}_2$  gave the *title compound* **21** as an orange solid (7.4 mg, 15.5  $\mu\text{mol}$ , 19%).  $^1\text{H NMR}$  (600 MHz,  $\text{Cl}_3\text{CD}$ ):  $\delta$  8.95 (1H, d,  $J$  4.4, quinoline 2-H), 8.87 (1H, s, NH), 8.04 (1H, d,  $J$  9.2, quinoline 8-H), 7.69 (1H, d,  $J$  4.4, quinoline 3-H), 7.31 (1H, dd,  $J$  9.2, 2.8, quinolone 7-H), 6.55 (1H, s, indole 4-H), 6.30 (1H, d,  $J$  2.9, quinoline 5-H), 4.66 (1H, dd,  $J$  8.4, 4.2, 13-H), 3.60-3.57 (1H, m, 11-H), 3.44-3.38 (1H, m, 14- $\text{H}_\text{A}$ ), 3.24 (3H, s,  $\text{OCH}_3$ ), 2.73-2.67 (1H, m, 14- $\text{H}_\text{B}$ ), 2.66-2.62 (1H, m, 12- $\text{H}_\text{A}$ ), 2.61 (3H, s,  $\text{CH}_3$ ), 2.22-2.17 (1H, m, 12- $\text{H}_\text{B}$ ), 2.09-2.03 (1H, m, 15- $\text{H}_\text{A}$ ), 1.66-1.59 (1H, m, 15- $\text{H}_\text{B}$ ).  $^{13}\text{C NMR}$  (126 MHz,  $\text{Cl}_3\text{CD}$ ):  $\delta$  202.2 (C=O), 158.5 (quinoline 6-C), 148.0 (Ar- $\text{C}_\text{q}$ ), 146.8 (quinoline 2-C), 145.6 (Ar- $\text{C}_\text{q}$ ), 144.5 (Ar- $\text{C}_\text{q}$ ), 143.6 (Ar- $\text{C}_\text{q}$ ), 142.0 (Ar- $\text{C}_\text{q}$ ), 131.3 (quinolone 8-C), 128.4 (indole 4-C), 125.4 (Ar- $\text{C}_\text{q}$ ), 123.1 (quinoline 7-C), 120.8 (Ar- $\text{C}_\text{q}$ ), 119.5 (quinoline 3-C), 115.2 (Ar- $\text{C}_\text{q}$ ), 113.5 (Ar- $\text{C}_\text{q}$ ), 102.2 (quinoline 5-C), 67.6 (13-C), 54.8 ( $\text{OCH}_3$ ), 51.7 (14-C), 31.0 (12-C), 29.6 (15-C), 28.2 (11-C), 24.9 ( $\text{CH}_3$ ). **HRMS** (ESI):  $\text{C}_{24}\text{H}_{22}\text{O}_2\text{N}_4^{79}\text{Br}$  [ $\text{M}+\text{H}$ ] $^+$ ; calculated: 477.0921; found: 477.0907;  $\text{C}_{24}\text{H}_{22}\text{O}_2\text{N}_4^{81}\text{Br}$  [ $\text{M}+\text{H}$ ] $^+$ ; calculated: 479.0900, found: 479.0887.  $[\alpha]_{\text{D}}^{20}$  +48 (c 0.1, MeCN).



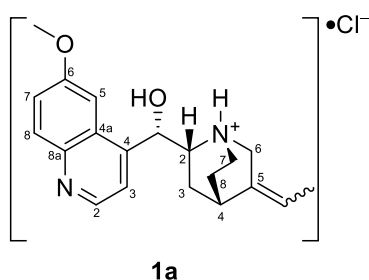
## 6.2.2 Synthesis of Isocoumarin-Quinidines

### General Procedure C: Preparation of Isocoumarins

A 5 mL screwcap vial with septum, equipped with a stirring bar was flushed with Argon for 10 min. Then ketone **3**, 2-Bromobenzoate,  $K_2CO_3$ , KI and tBuOK were subsequently added and dissolved in DMF (0.5 M). The mixture was flushed with Ar for 15 min and the vial closed with parafilm. Then the reaction was transferred to a preheated heating block (105°C; solvent-level below 'heating-block level') and heated for 24 h. The reaction progress was monitored via TLC until full completion of starting material. Subsequently, the reaction mixture was cooled to ambient temperature, filtrated through a syringe filter (pore size: 0.45  $\mu$ M) and the solvent was removed *in vacuo*. Flash column chromatography eluting with 5-50% {50:80:1 DCM:EtOH:NH<sub>4</sub>OH}/DCM gave the desired compound

### Synthesis of the quinidine ketone (**3**)

#### (1*S*,2*R*,4*S*)-5-Ethylidene-2-[(*S*)-hydroxy(6-methoxyquinolin-4-yl)methyl]-1-azabicyclo[2.2.2]octan-1-ium chloride (**1a**)

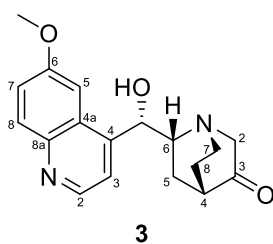


General procedure A, Part I, was followed using quinidine in two batches (2  $\times$  6.0 g, 2  $\times$  18.4 mmol [18.4 mmol in each batch, 36.8 mmol over 2 batches]) to give the title product **1a** (15.2 g) as a pale yellow solid which was carried forward to the next step without further purification. <sup>1</sup>H NMR (500 MHz, CD<sub>3</sub>OD, 2:1 mixture of Z/E alkenes, NH<sup>+</sup> and OH not observed):  $\delta$  9.05-9.01 (1H, m, quinoline 2-H), 8.31-8.28 (1H, m, quinoline 3-H), 8.22 (1H, d, *J* 9.3, quinoline 8-H), 7.91-7.84 (2H, m, quinoline 5-H and 7-H), 6.67 (0.67H, s, major CH(OH)), 6.65 (0.33H, s, minor CH(OH)), 5.58-5.52 (0.67H, m, major C=CHCH<sub>3</sub>), 5.51-5.44 (0.33H, m, minor C=CHCH<sub>3</sub>), 5.01-4.95 (1H, m, 6-H<sub>A</sub>), 4.19 (2H, s, major OCH<sub>3</sub>), 4.18 (1H, s, minor OCH<sub>3</sub>), 4.09 (0.67H, d, *J* 15.9, major 6-H<sub>B</sub>), 3.98-3.86 (1.33H, m, 2-H and minor 6-H<sub>B</sub>), 3.64-3.56 (1H, m, 7-H<sub>A</sub>), 3.37-3.25 (1H, m, 7-H<sub>B</sub>), 3.13 (0.33H, s, minor 4-H), 2.68 (0.67H, s, major 4-H), 2.35 (1H, app. t, *J* 9.7, 3-H<sub>A</sub>), 1.99-1.84 (2H, m, 8-H<sub>A</sub> and 8-H<sub>B</sub>), 1.72 (1H, d, *J* 6.9, minor C=CHCH<sub>3</sub>), 1.63 (2H, d, *J* 6.9, major C=CHCH<sub>3</sub>), 1.60-1.49 (1H, m, 3-H<sub>B</sub>). <sup>13</sup>C NMR (125 MHz, CD<sub>3</sub>OD, 2:1 mixture of Z/E alkenes):  $\delta$  162.6 (2 peaks, Ar-C<sub>q</sub>), 158.2 (2 peaks, Ar-C<sub>q</sub>), 141.8 (quinoline 2-C), 134.9 (2 peaks, Ar-C<sub>q</sub>), 132.6 (major 5-C), 131.7 (minor 5-C), 129.6 (quinoline 7-C), 129.2 (2 peaks, Ar-C<sub>q</sub>), 123.9 (quinoline 8-C), 121.3 (quinoline 3-C), 119.5 (minor C=CHCH<sub>3</sub>), 119.4 (major C=CHCH<sub>3</sub>), 103.6 (2 peaks, quinoline 5-C), 68.3 (CH(OH)),

## Experimental

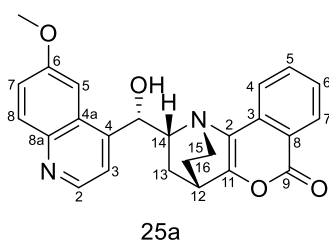
60.7 (major 2-C), 60.5 (minor 2-C), 58.5 (major OCH<sub>3</sub>), 58.4 (minor OCH<sub>3</sub>), 53.1 (minor 6-C), 51.7 (7-C), 51.4 (major 6-C), 32.9 (major 4-C), 26.0 (minor 4-C), 24.6 (2 peaks, major 3-C or major 8-C), 23.9 (minor 3-C or minor 8-C), 23.6 (minor 3-C or minor 8-C), 12.8 (minor C=CHCH<sub>3</sub>), 12.7 (major C=CHCH<sub>3</sub>).

### (1*S*,4*S*,6*R*)-6-[(*S*)-Hydroxy(6-methoxyquinolin-4-yl)methyl]-1-azabicyclo[2.2.2]octan-3-one (**3**)



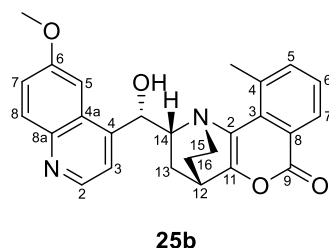
General Procedure A, Part II, was followed using compound **8** (2.0 g, assume 4.9 mmol). Flash column chromatography eluting with 5-35% (50:80:1 CH<sub>2</sub>Cl<sub>2</sub>:EtOH:NH<sub>4</sub>OH<sub>(sat. aq.)</sub>) in CH<sub>2</sub>Cl<sub>2</sub> gave the title product **3** (591 mg, 1.89 mmol, 38%) as a colourless solid. <sup>1</sup>H NMR (500 MHz, CD<sub>3</sub>OD, OH not observed): δ 8.71 (1H, d, *J* 4.6, quinoline 2-H), 8.00 (1H, d, *J* 9.0, quinoline 8-H), 7.72 (1H, d, *J* 4.6, quinoline 3-H), 7.50-7.44 (2H, m, quinoline 5-H and 7-H), 5.76 (1H, d, *J* 2.4, CH(OH)), 4.37 (1H, app. dd, *J* 18.7, 1.9, quinuclidine 2-H<sub>A</sub>), 4.04 (3H, s, OCH<sub>3</sub>), 3.41-3.36 (1H, m, quinuclidine 6-H), 3.26 (1H, d, *J* 18.7, quinuclidine 2-H<sub>B</sub>), 3.20-3.10 (1H, m, quinuclidine 7-H<sub>A</sub>), 2.99 (1H, ddd, *J* 13.9, 10.2, 6.8, quinuclidine 7-H<sub>B</sub>), 2.50-2.38 (2H, m, quinuclidine 4-H and 5-H<sub>A</sub>), 2.06-1.89 (2H, m, quinuclidine 8-H), 1.74-1.65 (1H, m, quinuclidine 5-H<sub>B</sub>). <sup>13</sup>C NMR (125 MHz, CD<sub>3</sub>OD, quinuclidine 2-C not observed due to deuterium exchange): δ 220.5 (quinuclidine 3-C), 159.8 (quinoline 6-C), 150.0 (Ar-C<sub>q</sub>), 148.2 (quinoline 2-C), 144.7 (Ar-C<sub>q</sub>), 131.4 (quinoline 8-C), 127.9 (Ar-C<sub>q</sub>), 123.4 (quinoline 7-C), 119.8 (quinoline 3-C), 102.2 (quinoline 5-C), 71.8 (CH(OH)), 59.6 (6-C), 56.4 (OCH<sub>3</sub>), 50.9 (quinuclidine 7-C), 42.2 (quinuclidine 4-C), 25.3 (quinuclidine 5-C or 8-C), 25.2 (quinuclidine 5-C or 8-C). HRMS (ESI): C<sub>18</sub>H<sub>21</sub>N<sub>2</sub>O<sub>3</sub> [M+H]<sup>+</sup>; calculated: 313.1549, found: 313.1547. [α]<sub>D</sub><sup>20</sup> = +122 (c. 1.0, MeOH).

**(1*R*,12*S*,14*S*)-14-[(*R*)-hydroxy(6-methoxyquinolin-4-yl)methyl]-10-oxatetracyclo[10.2.2.0<sup>2,11</sup>.0<sup>3,8</sup>]hexadeca-2(11),3,5,7-tetraen-9-one (25a)**



Prepared according to the general procedure C. Flash column chromatography eluting with 1:9 to 1:1 ({50:80:1 DCM:EtOH:NH<sub>4</sub>OH}/DCM) gave the desired product as white solid (30.40 mg, 73.0 μmol, 73%). <sup>1</sup>H NMR (700 MHz, Methanol-*d*<sub>4</sub>) δ 8.62 (d, *J* 4.6, 1H), 8.24 (d, *J* 6.6, 1H), 7.94 (d, *J* 9.3, 1H), 7.79 (t, *J* 7.1, 1H), 7.68 (d, *J* 8.4, 1H), 7.57 (d, *J* 2.6, 1H), 7.52-7.48 (m, 2H), 7.43 (dd, *J* 9.3, 2.6, 1H), 5.55 (d, *J* 3.2, 1H), 4.02 (s, 3H), 3.62-3.58 (m, 0H), 3.26-3.20 (m, 1H), 2.69-2.63 (m, 1H), 2.16-2.11 (m, 1H), 1.95-1.89 (m, 1H), 1.81 (s, 1H), 1.76-1.69 (m, 1H). <sup>13</sup>C NMR (176 MHz, Methanol-*d*<sub>4</sub>) δ 174.5, 174.2, 159.7, 157.5, 150.2, 148.1, 144.7, 134.6, 131.3, 130.0, 128.1, 126.9, 126.6, 126.2, 123.5, 120.2, 119.6, 102.8, 72.2, 63.4, 56.5, 52.6, 33.1, 30.4, 27.5. [α]<sub>D</sub><sup>20</sup> -35 (MeOH; c = 1). HR-MS: calc. for [M+H]<sup>+</sup> C<sub>25</sub>H<sub>23</sub>O<sub>4</sub>N<sub>2</sub>: 415.1652 found 415.1643.

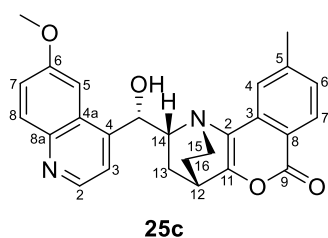
**(1*R*,12*S*,14*S*)-14-[(*R*)-hydroxy(6-methoxyquinolin-4-yl)methyl]-4-methyl-10-oxatetracyclo[10.2.2.0<sup>2,11</sup>.0<sup>3,8</sup>]hexadeca-2(11),3,5,7-tetraen-9-one (25b)**



Prepared according to the general procedure C. Flash column chromatography eluting with 1:9 to 1:1 ({50:80:1 DCM:EtOH:NH<sub>4</sub>OH}/DCM) gave the desired product as white solid (23.4 mg, 54.6 μmol, 57%). <sup>1</sup>H NMR (700 MHz, Methanol-*d*<sub>4</sub>) δ 8.62 (d, *J* 4.6, 1H), 8.07 (d, *J* 7.6, 1H), 7.95 (d, *J* 9.2, 1H), 7.64 (d, *J* 7.6, 1H), 7.57 (d, *J* 2.7, 1H), 7.52 (d, *J* 4.6, 1H), 7.43 (dd, *J* 9.2, 2.7, 1H), 7.38 (t, *J* 7.6, 1H), 5.55 (d, *J* 3.3, 1H), 4.02 (s, 3H), 3.63-3.55 (m, 1H), 3.28-3.19 (m, 2H), 2.70-2.63 (m, 1H), 2.59 (s, 3H), 2.20-2.14 (m, 1H), 1.95-1.88 (m, 1H), 1.86-1.79 (m, 1H), 1.78-1.72 (m, 1H). <sup>13</sup>C NMR (176 MHz, Methanol-*d*<sub>4</sub>) δ 174.8, 173.9, 159.7, 155.9, 150.2, 148.1, 144.7, 135.5, 131.3, 129.8, 129.2, 128.1, 126.6, 125.8, 124.6, 123.5, 120.2, 102.8, 72.2, 63.4, 56.5, 52.7, 33.1, 30.5, 27.6, 15.7. [α]<sub>D</sub><sup>20</sup> -52 (MeOH; c = 1). HR-MS: calc. for [M+H]<sup>+</sup> C<sub>26</sub>H<sub>25</sub>O<sub>4</sub>N<sub>2</sub>: 429.1801 found 429.1808.

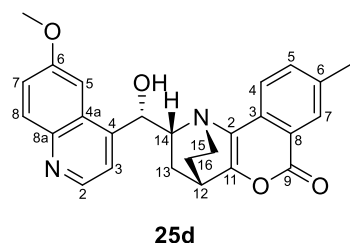
## Experimental

### (1*R*,12*S*,14*S*)-14-[(*R*)-hydroxy(6-methoxyquinolin-4-yl)methyl]-5-methyl-10-oxatetracyclo[10.2.2.0<sup>2,11</sup>.0<sup>3,8</sup>]hexadeca-2(11),3,5,7-tetraen-9-one (25c)



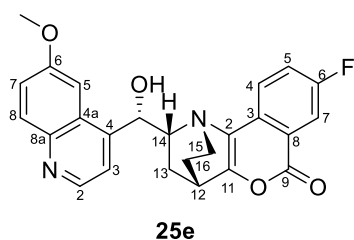
Prepared according to the general procedure C. Flash column chromatography eluting with 1:9 to 1:1 ({50:80:1 DCM:EtOH:NH<sub>4</sub>OH}/DCM) gave the desired product as yellow solid (16.7 mg, 38.9 μmol, 41%). <sup>1</sup>H NMR (700 MHz, Methanol-*d*<sub>4</sub>, OH not observed) δ 8.62 (d, *J* 4.6, 1H), 8.11 (d, *J* 8.2, 1H), 7.94 (d, *J* 9.2, 1H), 7.57 (d, *J* 2.6, 1H), 7.52 (d, *J* 4.6, 1H), 7.49 (s, 1H), 7.43 (dd, *J* 9.2, 2.6, 1H), 7.33 (d, *J* 8.2, 1H), 5.53 (d, *J* 3.3, 1H), 4.01 (s, 3H), 3.62-3.56 (m, 1H), 3.25-3.15 (m, 2H), 2.69-2.60 (m, 1H), 2.54 (s, 3H), 2.18-2.12 (m, 1H), 1.93-1.86 (m, 1H), 1.82-1.77 (m, 1H), 1.75-1.70 (m, 1H). <sup>13</sup>C NMR (176 MHz, Methanol-*d*<sub>4</sub>) δ 174.6, 173.9, 159.7, 157.6, 150.2, 148.1, 146.3, 144.8, 131.2, 129.8, 128.1, 127.6, 126.7, 124.3, 123.4, 120.2, 119.2, 102.8, 72.2, 63.4, 56.4, 52.7, 49.5, 33.0, 30.5, 27.6, 21.7. [ $\alpha$ ]<sub>D</sub><sup>20</sup> -70 (MeOH; c = 1). HR-MS: calc. for [M+H]<sup>+</sup> C<sub>25</sub>H<sub>23</sub>O<sub>4</sub>N<sub>2</sub>: 429.1809 found 429.1799.

### (1*R*,12*S*,14*S*)-14-[(*R*)-hydroxy(6-methoxyquinolin-4-yl)methyl]-6-methyl-10-oxatetracyclo[10.2.2.0<sup>2,11</sup>.0<sup>3,8</sup>]hexadeca-2(11),3,5,7-tetraen-9-one (25d)



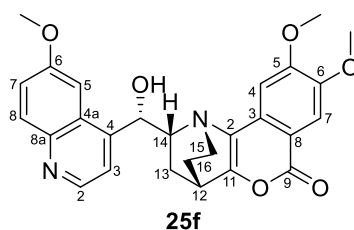
(Prepared according to the general procedure C. Flash column chromatography eluting with 1:9 to 1:1 ({50:80:1 DCM:EtOH:NH<sub>4</sub>OH}/DCM) gave the desired product as white solid (13.00 mg, 30.3 μmol, 32%). <sup>1</sup>H NMR (700 MHz, Methanol-*d*<sub>4</sub>) δ 8.88 (d, *J* 5.4, 1H), 8.13 (d, *J* 9.1, 1H), 8.00 (s, 1H), 7.95 (d, *J* 5.4, 1H), 7.78-7.72 (m, 2H), 7.69 (dd, *J* 8.6, 2.2, 1H), 7.63 (d, *J* 8.6, 1H), 5.57 (d, *J* 4.6, 1H), 4.01 (s, 3H), 4.01-3.95 (m, 1H), 3.49-3.38 (m, 2H), 2.92-2.85 (m, 1H), 2.51 (s, 3H), 2.26-2.20 (m, 1H), 2.09-1.98 (m, 2H), 1.96-1.89 (m, 1H). <sup>13</sup>C NMR (176 MHz, Methanol-*d*<sub>4</sub>, 1 Ar-C<sub>q</sub> not observed) δ 161.4, 155.8, 143.4, 137.3, 136.5, 129.2, 127.6, 127.5, 126.5, 126.1, 125.8, 125.8, 121.4, 119.6, 118.3, 116.7, 103.7, 71.5, 64.9, 56.9, 53.5, 32.7, 30.0, 25.8, 21.0. [ $\alpha$ ]<sub>D</sub><sup>20</sup> -34 (MeOH; c = 1). HR-MS: calc. for [M+H]<sup>+</sup> C<sub>26</sub>H<sub>25</sub>O<sub>4</sub>N<sub>2</sub>: 429.1801 found 429.1850.

**1*R*,12*S*,14*S*)-6-fluoro-14-[(*R*)-hydroxy(6-ethoxyquinolin-4-yl)methyl]-10-oxatetracyclo[10.2.2.0<sup>2,11</sup>.0<sup>3,8</sup>]hexadeca-2(11),3,5,7-tetraen-9-one (25e)**



Prepared according to the general procedure C. Flash column chromatography eluting with 1:9 to 1:1 ({50:80:1 DCM:EtOH:NH<sub>4</sub>OH}/DCM) gave the desired product as pale yellow solid (11.7 mg, 27.1 μmol, 28%). <sup>1</sup>H NMR (700 MHz, Methanol-*d*<sub>4</sub>, OH not observed) δ 8.62 (d, *J* 4.6, 1H), 7.95 (d, *J* 9.2, 1H), 7.87 (dd, *J* 8.4, 3.1, 1H), 7.74 (dd, *J* 9.2, 4.1, 1H), 7.60-7.54 (m, 2H), 7.51 (d, *J* 4.6, 1H), 7.43 (dd, *J* 9.2, 2.6, 1H), 5.57 (d, *J* 3.0, 1H), 4.03 (s, 3H), 3.61-3.57 (m, 1H), 3.35 (s, 1H), 3.25-3.22 (m, 2H), 2.69-2.63 (m, 1H), 2.17-2.10 (m, 2H), 1.94-1.88 (m, 1H), 1.85-1.78 (m, 1H). <sup>13</sup>C NMR (176 MHz, Methanol-*d*<sub>4</sub>) δ 174.4, 173.6, 160.9 (d, *J*<sub>CF</sub> 244.9), 159.8, 153.7, 150.1, 148.1, 144.7, 131.3, 129.6, 128.1, 128.0 (d, *J*<sub>CF</sub> 7.2), 123.5, 122.6, 122.4, 122.1 (d, *J*<sub>CF</sub> 7.2), 111.5 (d, *J*<sub>CF</sub> 24.1), 102.7, 72.1, 63.4, 56.5, 52.6, 33.1, 30.3, 27.5. [ $\alpha$ ]<sub>D</sub><sup>20</sup> -62 (MeOH; c = 1). HR-MS: calc. for [M+H]<sup>+</sup> C<sub>25</sub>H<sub>23</sub>O<sub>4</sub>N<sub>2</sub>F: 433.1558 found 433.1547.

**(1*R*,12*S*,14*S*)-14-[(*R*)-hydroxy(6-methoxyquinolin-4-yl)methyl]-5,6-dimethoxy-10-oxatetracyclo[10.2.2.0<sup>2,11</sup>.0<sup>3,8</sup>]hexadeca-2(11),3,5,7-tetraen-9-one (25f)**

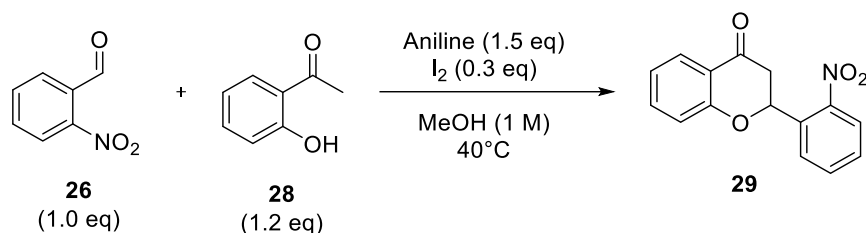


Prepared according to the general procedure C. Flash column chromatography eluting with 1:9 to 1:1 ({50:80:1 DCM:EtOH:NH<sub>4</sub>OH}/DCM) gave the desired product as white solid (8.5 mg, 17.9 μmol, 19%). <sup>1</sup>H NMR (700 MHz, Methanol-*d*<sub>4</sub>) δ 8.86 (d, *J* 5.4, 1H), 8.12 (d, *J* 8.6, 1H), 7.92 (d, *J* 5.4, 1H), 7.74-7.71 (m, 2H), 7.55 (s, 1H), 7.28 (s, 1H), 5.51 (*app.* s, 1H), 4.01 (s, 3H), 3.99 (s, 3H), 3.95 (s, 3H), 3.43-3.39 (m, 2H), 3.25-3.19 (m, 1H), 2.90-2.80 (m, 1H), 2.26-2.15 (m, 1H), 2.10-1.99 (m, 3H), 1.95-1.86 (m, 1H). <sup>13</sup>C NMR (176 MHz, Methanol-*d*<sub>4</sub>) δ 170.3, 169.6, 160.0, 155.1, 152.3, 148.2, 142.1, 136.3, 127.8, 126.1, 124.5, 124.2, 120.0, 117.6, 104.1, 102.2, 100.3, 69.8, 63.6, 55.7, 55.5, 55.3, 52.3, 46.5, 31.1, 24.2, 7.8. [ $\alpha$ ]<sub>D</sub><sup>20</sup> -41 (MeOH; c = 1). HR-MS: calc. for [M+H]<sup>+</sup> C<sub>27</sub>H<sub>27</sub>O<sub>6</sub>N<sub>2</sub>: 475.1864 found 475.1858.

## Experimental

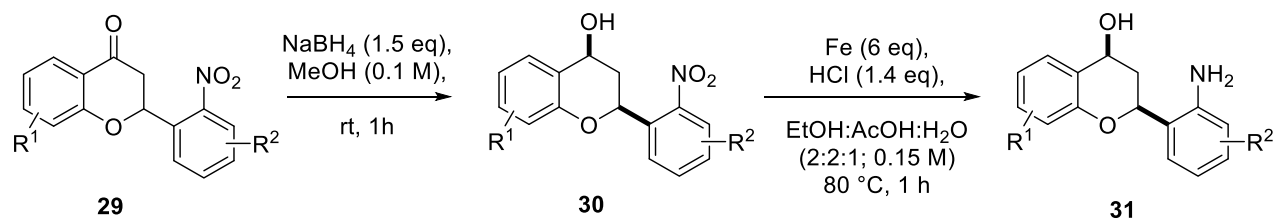
### 6.2.3 Synthesis of Chromalines

#### General procedure D: Flavanone synthesis:



A round-bottom flask was equipped with a magnetic stirring bar and heat dried under reduced pressure. The 2'-nitroaldehyde (1.0 eq.) was dissolved in anhydrous methanol (0.1 M), and 2-hydroxyacetophenone (1.2 eq), aniline (1.5 eq.) and iodine were added sequentially. The mixture was stirred at 40 °C for 10-18 h. After full conversion of the starting material (monitored by TLC), saturated Na<sub>2</sub>S<sub>2</sub>O<sub>3</sub> (aq) solution was added and extracted with CH<sub>2</sub>Cl<sub>2</sub> (3×). The combined organic phases were dried over anhydrous Mg<sub>2</sub>SO<sub>4</sub>, filtrated and solvents were removed under reduced pressure. The crude products, were purified by short silica column and/or recrystallization from *n*-pentane:ethyl acetate (8:2).

#### General procedure E: Two-step reduction of flavanone



##### Part1:

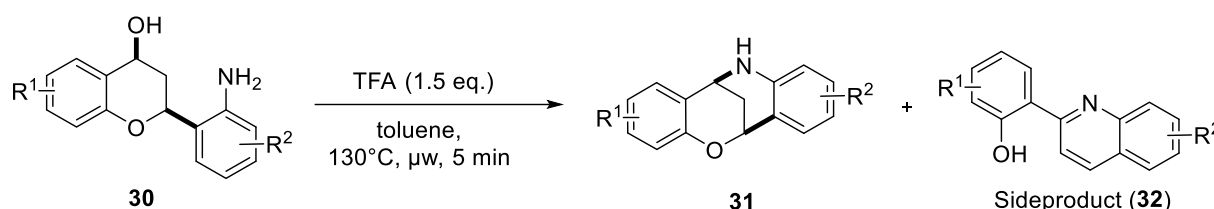
The ketone (**29**) was dissolved in anhydrous Methanol (0.1 M) and the solution cooled to 0 °C. Then NaBH<sub>4</sub> (1.5 eq.) was added, and the reaction stirred for 1 h at room temperature. The solvent was removed under reduced pressure and the solid redissolved in DCM (15 mL) and H<sub>2</sub>O (7.5 mL). The aqueous phase was extracted with DCM (3x20 mL) and the organic phases were combined and dried over MgSO<sub>4</sub>. Filtration and removal of the solvent under reduced pressure afforded the crude product, which was directly used in the next step.

##### Part2:

The alcohol was redissolved in a previously prepared solvent mixture containing acetic acid, ethanol and water (2:2:1; 0.15 M). Iron (6 eq.) and 32% HCl (1.4 eq.) were added subsequently, and the reaction heated to 80 °C for 1 h until full completion of the reaction (monitored via

TLC). The reaction then was allowed to cool to room temperature and quenched by careful addition of saturated  $\text{Na}_2\text{CO}_3$  solution (aq.). The aqueous phase was extracted with DCM (3x 25 mL), the combined organic phases were dried over  $\text{MgSO}_4$  and filtered. Evaporation of the solvent afforded the crude product **31**, which was purified by flash column chromatography eluting with 10 to 50% [DCM:EtOH: $\text{NH}_4\text{OH}$  (50:8:1)] in DCM.

**General procedure F: Cyclisation of Flavanols to synthesise Chromalines**



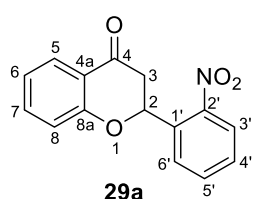
A microwave tube was equipped with a magnetic stirring bar and flavan-4-ol (**30**) was added and dissolved in toluene (0.04 M). TFA (1.5 eq.) was added and the tube carefully sealed with an appropriate microwave lid containing a septum seal. The reaction vial was then placed in the reaction microwave and heated to 130°C for 5 min (ramping time was set to 20 min). After completion of the reaction solvents and TFA were removed under reduced pressure and the crude purified by flash column chromatography eluting with 2.5% to 10 % EtOAc in pentane. In all purified reaction, the product (**31**) was the second fraction, while the first fraction generally was identified as side product **32**.

Product is the second fraction.

## Experimental

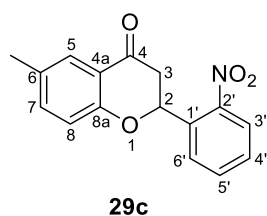
### Preparation of Flavanones

#### 2-(2-nitrophenyl)-3,4-dihydro-2H-1-benzopyran-4-one (29a)



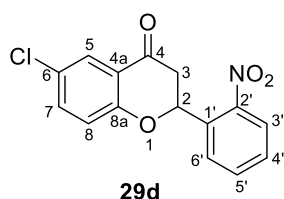
Prepared according to general procedure D. Flash column chromatography eluting with 5-20% EtOAc in *n*-pentane, followed by recrystallisation from pentane:EtOAc (8:2) afforded the desired product **29a** (905 mg, 3.36 mmol, 34%) as yellow solid. **<sup>1</sup>H-NMR** (500 MHz, CDCl<sub>3</sub>): δ 8.06 (1H, dd, *J* 8.2, 1.2 Hz, 3'-H), 8.02 (1H, dd, *J* 7.9, 1.2 Hz, 6'-H), 7.96 (1H, dd, *J* 7.9, 1.7 Hz, 5-H), 7.77 (1H, td, *J* 7.6, 1.1 Hz, 5'-H), 7.60-7.53 (1H, m, 4'-H), 7.56-7.49 (1H, m, 6-H), 7.13-7.06 (1H, m, 7-H), 7.03 (1H, d, *J* 8.3 Hz, 8-H), 6.11 (1H, dd, *J* 13.2, 2.7 Hz, 2-H), 3.22 (1H, dd, *J* 16.9, 2.7 Hz, 3-H<sub>a</sub>), 2.94 (1H, dd, *J* 16.9, 13.2 Hz, 3-H<sub>b</sub>). **<sup>13</sup>C NMR** (126 MHz, CDCl<sub>3</sub>): δ 191.0 (4-C), 161.2 (8a-C), 147.4 (2'-C), 136.4 (6-C), 134.9 (1'-C), 134.2 (4'-C), 129.5 (5'-C), 128.3 (6'-C), 127.4 (5-C), 125.0 (3'-C), 122.3 (7-C), 121.1 (4a-C), 118.1 (8-C), 75.7 (2-C), 44.6 (3-C). **FT-IR**: 2870, 1686, 1603, 1580, 1520, 1475, 1463, 1410, 1358, 1342, 1304, 1234, 1223, 1179 cm<sup>-1</sup> **HR-MS**: calc. for [M+H]<sup>+</sup> C<sub>15</sub>H<sub>11</sub>O<sub>4</sub>N: 270.0608 found: 270.0758.

#### 2-(2-nitrophenyl)-6-methyl-3,4-dihydro-2H-1-benzopyran-4-one (29c)

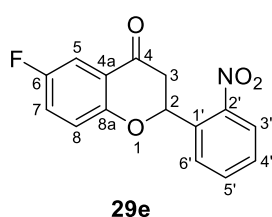


Prepared according to general procedure D. Flash column chromatography eluting with 5-20% EtOAc in *n*-pentane, followed by recrystallisation from pentane:EtOAc (8:2) afforded the desired product **29c** (367.4 mg, 1.30 mmol, 19%) as yellow solid. **<sup>1</sup>H-NMR** (500 MHz, CDCl<sub>3</sub>): δ 8.05 (1H, dd, *J* 8.2, 1.2 Hz, 3'-H), 8.01 (1H, dd, *J* 7.9, 1.2 Hz, 6'-H), 7.79-7.74 (2H, m, 5-H and 5'-H), 7.58-7.53 (1H, m, 4'-H), 7.33 (1H, dd, *J* 8.4, 2.1 Hz, 7-H), 6.93 (1H, d, *J* 8.4 Hz, 8-H), 6.06 (1H, dd, *J* 13.1, 2.6 Hz, 2-H), 3.19 (1H, dd, *J* 16.9, 2.6 Hz, 3-H<sub>a</sub>), 2.92 (1H, dd, *J* 16.9, 13.1 Hz, 3-H<sub>b</sub>), 2.06 (3H, s, CH<sub>3</sub>). **<sup>13</sup>C NMR** (126 MHz, CDCl<sub>3</sub>): δ 191.2 (4-C), 159.3 (8a-C), 147.4 (2'-C), 137.5 (7-C), 135.0 (1'-C), 134.2 (5'-C), 131.8 (6-C), 129.4 (4'-C), 128.3 (6'-C), 126.9 (5-C), 124.9 (3'-C), 120.8 (4a-C), 117.9 (8-C), 75.7 (2-C), 44.6 (3-C), 20.6 (CH<sub>3</sub>). **FT-IR**: 1576, 1521, 1488, 1422, 1399, 1349, 1289, 1214, 1194, 1174, 1129. **HR-MS**: calc. for [M+H]<sup>+</sup> C<sub>16</sub>H<sub>14</sub>O<sub>4</sub>N: 284.0917 found: 284.0915.



**2-(2-nitrophenyl)-6-chloro-3,4-dihydro-2H-1-benzopyran-4-one (29d)**

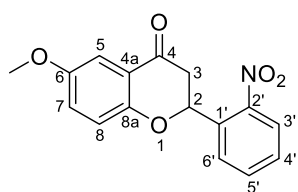
Prepared according to general procedure D. Flash column chromatography eluting with 5-20% EtOAc in *n*-pentane, followed by recrystallisation from pentane:EtOAc (8:2) afforded the desired product **29d** (767.50 mg, 2.53 mmol, 38%) as yellow solid. **<sup>1</sup>H-NMR** (600 MHz, CDCl<sub>3</sub>): δ 8.07 (dd, *J* 8.3, 1.2 Hz, 1H, 3'-H), 7.98 (dd, *J* 7.8, 1.2 Hz, 1H, 6'-H), 7.92 (d, *J* 2.8 Hz, 1H, 5-H), 7.78 (td, *J* 7.8, 1.1 Hz, 1H, 5'-H), 7.60-7.55 (m, 1H, 4'-H), 7.46 (dd, *J* 8.8, 2.8 Hz, 1H, 7-H), 7.00 (d, *J* 8.8 Hz, 1H, 8-H), 6.10 (dd, *J* 13.2, 2.7 Hz, 1H, 2-H), 3.23 (dd, *J* 17.0, 2.7 Hz, 1H, 3-H<sub>a</sub>), 2.93 (dd, *J* 17.0, 13.2 Hz, 1H, 3-H<sub>b</sub>). **<sup>13</sup>C NMR** (151 MHz, CDCl<sub>3</sub>): δ 189.8 (4-C), 159.7 (8a-C), 147.4 (2'-C), 136.2 (7-C), 134.4 (1'-C), 134.2 (5'-C), 129.6 (4'-C), 128.2 (6'-C), 127.9 (6-C), 126.8 (5-C), 125.1 (3'-C), 122.0 (4a-C), 119.9 (8-C), 76.0 (2-C), 44.2 (3-C). **FT-IR**: 3082, 1689, 1602, 1578, 1522, 1466, 1446, 1421, 1398, 1376, 1348, 1312, 1285, 1273, 1253, 1213 1179, 1145. **HR-MS**: not stable under MS conditions; identity confirmed by NMR and the next reaction steps.

**2-(2-nitrophenyl)-7-fluoro-3,4-dihydro-2H-1-benzopyran-4-one (29e)**

Prepared according to general procedure D. Flash column chromatography eluting with 5-20% EtOAc in *n*-pentane, followed by recrystallisation from pentane:EtOAc (8:2) afforded the desired product **xx** (608.01 mg, 2.12 mmol, 32%) as yellow solid. **<sup>1</sup>H-NMR** (600 MHz, CDCl<sub>3</sub>): δ 8.07 (1H, dd, *J* 8.2, 1.4 Hz, 3'-H), 7.99 (1H, dd, *J* 7.8, 1.4 Hz (6'-H), 7.78 (1H, td, *J* 7.8f, 1.4 Hz, 5'-H), 7.61 (1H, dd, *J* 8.2, 3.2 Hz, 5-H), 7.59-7.55 (1H, m, 4'-H), 7.26-7.23 (1H, m, 7-H), 7.02 (1H, dd, *J* 9.0, 4.1 Hz, 8-H), 6.08 (1H, dd, *J* 13.2, 2.6 Hz, 2-H), 3.23 (1H, dd, *J* 17.1, 2.6 Hz, 2-H<sub>a</sub>), 2.93 (1H, dd, *J* 17.1, 13.2 Hz, 2-H<sub>b</sub>). **<sup>13</sup>C NMR** (151 MHz, CDCl<sub>3</sub>): δ 190.3 (d, *J*<sub>CF</sub> 1.9 Hz, 4-C), 157.8 (d, *J*<sub>CF</sub> 243.2 Hz, 6-C), 157.5 (d, *J*<sub>CF</sub> 1.9 Hz, 8a-C), 147.5 (2'-C), 134.6 (1'-C), 134.3 (5'-C), 129.7 (4'-C), 128.3 (6'-C), 125.1 (3'-C), 124.0 (d, *J*<sub>CF</sub> 24.7 Hz, 7-C), 121.8 (d, *J*<sub>CF</sub> 6.6 Hz, 4a-C), 119.9 (d, *J*<sub>CF</sub> 7.5 Hz, 8-C), 112.5 (d, *J*<sub>CF</sub> 23.4 Hz, 5-C), 76.1 (2-C), 44.4 (3-C). **<sup>19</sup>F NMR** (565 MHz, CDCl<sub>3</sub>): δ -120.16 - -120.22 (m). **FT-IR**: 2361, 2159, 1792, 1772, 1734, 1717, 1700, 1695, 1684, 1653, 1646, 1635 1616, 1558, 1539, 1521, 1506, 1457. **HR-MS**: calc. for [M+H]<sup>+</sup> C<sub>15</sub>H<sub>11</sub>O<sub>4</sub>NF: 288.0667 found: 288.0583.

## Experimental

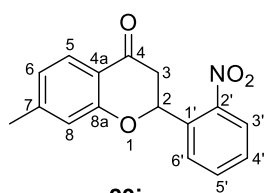
### 2-(2-nitrophenyl)-6-methoxy-3,4-dihydro-2H-1-benzopyran-4-one (29g)



**29g**

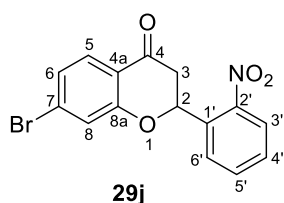
Prepared according to general procedure D. Flash column chromatography eluting with 5-20% EtOAc in *n*-pentane, followed by recrystallisation from pentane:EtOAc (8:2) afforded the desired product **xx** (767 mg, 2.57 mmol, 39%) as yellow solid. **<sup>1</sup>H-NMR** (500 MHz, CDCl<sub>3</sub>): δ 8.05 (1H, dd, *J* 8.0, 1.1 Hz, 3'-H), 8.01 (1H, dd, *J* 7.7, 1.4 Hz, 6'-H), 7.77 (1H, td, *J* 7.7, 1.1 Hz, 5'-H), 7.55 (1H, td, *J* 8.0, 1.4 Hz, 4'-H), 7.38 (1H, d, *J* 3.2 Hz, 5-H), 7.13 (1H, dd, *J* 9.0, 3.2 Hz, 7-H), 6.96 (1H, d, *J* 9.0 Hz, 8-H), 6.05 (1H, dd, *J* 13.3, 2.6 Hz, 2-H), 3.83 (3H, s, OCH<sub>3</sub>), 3.20 (1H, dd, *J* 17.0, 2.6 Hz, 3-H<sub>a</sub>), 2.91 (1H, dd, *J* 17.0, 13.3 Hz, 3-H<sub>b</sub>). **<sup>13</sup>C NMR** (126 MHz, CDCl<sub>3</sub>): δ 191.1 (4-C), 155.9 (8a-C), 154.7 (6-C), 147.4 (2'-C), 135.0 (1'-C), 134.2 (5'-C), 129.4 (4'-C), 128.3 (6'-C), 125.5 (7-C), 125.0 (3'-C), 121.1 (4a-C), 119.4 (8-C), 107.6 (5-C), 75.8 (2-C), 56.0 (OCH<sub>3</sub>), 44.5 (3-C). **FT-IR**: 1681, 1615, 1522, 1485, 1460, 1427, 1407, 1361, 1341, 1278, 1217, 1162, 1141. **HR-MS**: calc. for [M+H]<sup>+</sup> C<sub>16</sub>H<sub>14</sub>O<sub>5</sub>N: 300.0867 found: 300.0865.

### 2-(2-nitrophenyl)-7-methyl-3,4-dihydro-2H-1-benzopyran-4-one (29i)

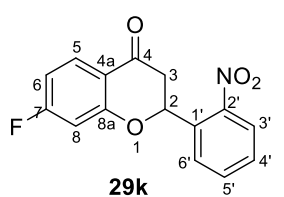


**29i**

Prepared according general procedure D. Flash column chromatography eluting with 5-20% EtOAc in *n*-pentane, followed by recrystallisation from pentane:EtOAc (8:2) afforded the desired product **29i** (88.10 mg, 0.31 mmol, 5%) as yellow solid. **<sup>1</sup>H-NMR** (500 MHz, CDCl<sub>3</sub>): δ 8.05 (1H, dd, *J* 8.2, 1.3 Hz, 3'-H), 7.98 (1H, dd, *J* 7.9, 1.4 Hz, 6'-H), 7.85 (1H, d, *J* 8.1 Hz, 5-H), 7.76 (1H, td, *J* 7.7, 1.3 Hz, 5'-H), 7.56 (1H, t, *J* 7.7 Hz, 4'-H), 6.91 (1H, d, *J* 8.1 Hz, 6-H), 6.84 (1H, s, 8-H), 6.08 (1H, dd, *J* 13.1, 2.7 Hz, 2-H), 3.18 (1H, dd, *J* 16.9, 2.7 Hz, 3-H<sub>a</sub>), 2.91 (1H, dd, *J* 16.9, 13.1 Hz, 3-H<sub>b</sub>), 2.38 (3H, s, CH<sub>3</sub>). **<sup>13</sup>C NMR** (126 MHz, CDCl<sub>3</sub>): δ 190.7 (4-C), 161.3 (8a-C or 7-C), 148.1 (8a-C or 7-C), 147.5 (2'-C), 134.9 (1'-C), 134.1 (5'-C), 129.4 (4'-C), 128.3 (6'-C), 127.2 (5-C), 125.0 (3'-C), 123.6 (6-C), 118.9 (4a-C), 118.1 (8-C), 75.7 (2-C), 44.4 (3-C), 22.1 (CH<sub>3</sub>). **FT-IR**: 1682, 1620, 1569, 1521 1491, 1449, 1371, 1349, 1297, 1245, 1222, 1151. **HR-MS**: calc. for [M+H]<sup>+</sup> C<sub>16</sub>H<sub>14</sub>O<sub>4</sub>N: 284.0917 found: 284.0916.

**2-(2-nitrophenyl)-7-chloro-3,4-dihydro-2H-1-benzopyran-4-one (29j)**

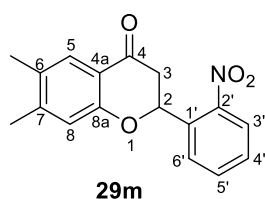
Prepared according to general procedure D. Flash column chromatography eluting with 5-20% EtOAc in *n*-pentane, followed by recrystallisation from pentane:EtOAc (8:2) afforded the desired product **29j** (240.00 mg, 0.69 mmol, 21%) as yellow solid. **<sup>1</sup>H-NMR** (600 MHz, CDCl<sub>3</sub>): δ 8.07 (1H, dd, *J* 8.3, 1.2 Hz, 3'-H), 7.96 (1H, dd, *J* 7.8, 1.2 Hz, 6'-H), 7.82 (1H, d, *J* 8.3 Hz, 5-H), 7.78 (1H, td, *J* 7.8, 1.1 Hz, 5'-H), 7.60-7.56 (1H, m, 4'-H), 7.26-7.23 (2H, m, 6-H and 8-H), 6.12 (1H, dd, *J* 13.1, 2.7 Hz, 2-H), 3.22 (1H, dd, *J* 17.0, 2.7 Hz, 3-H<sub>a</sub>), 2.93 (1H, dd, *J* 17.0, 13.1 Hz, 3-H<sub>b</sub>). **<sup>13</sup>C NMR** (151 MHz, CDCl<sub>3</sub>): δ 190.0 (4-C), 161.4 (8a-C), 147.4 (2'-C), 134.4 (1'-C), 134.3 (5'-C), 130.8, 129.7, 128.6 (5-C), 128.2 (6'-C), 126.0 (6-C or 8-C), 125.1 (3'-C), 121.4 (6-C or 8-C), 120.1 (4a-C), 76.2 (2-C), 44.4 (3-C). **FT-IR**: 3085, 1688, 1652, 1596, 1562, 1521, 1468, 1446, 1423, 1400, 1368, 1348, 1310, 1286, 1254, 1216. **HR-MS**: not stable under MS conditions; identity confirmed by NMR, next reaction steps.

**2-(2-nitrophenyl)-7-fluoro-3,4-dihydro-2H-1-benzopyran-4-one (29k)**

Prepared according to general procedure D. Flash column chromatography eluting with 5-20% EtOAc in *n*-pentane, followed by recrystallisation from pentane:EtOAc (8:2) afforded the desired product **29k** (270.90 mg, 0.94 mmol, 14%) as yellow solid. **<sup>1</sup>H-NMR** (400 MHz, CDCl<sub>3</sub>): δ 8.07 (1H, dd, *J* 8.2, 1.4 Hz, 3'-H), 8.02-7.95 (2H, m, 5-H and 6'-H), 7.82-7.72 (1H, m, 5'-H), 7.61-7.54 (1H, m, 4'-H), 6.82 (1H, td, *J* 8.4, 2.3 Hz, 6-H), 6.73 (1H, dd, *J* 9.6, 2.4 Hz, 8-H), 6.13 (1H, dd, *J* 13.0, 2.7 Hz, 2-H), 3.21 (1H, dd, *J* 17.0, 2.7 Hz, 3-H<sub>a</sub>), 2.93 (1H, dd, *J* 17.0, 13.0 Hz, 3-H<sub>b</sub>). **<sup>13</sup>C NMR** (151 MHz, CDCl<sub>3</sub>): δ 189.5 (4-C), 167.7 (d, *J*<sub>CF</sub> 256.9 Hz, 7-H), 162.9 (d, *J*<sub>CF</sub> 13.2 Hz, 8a-C), 147.4 (2'-C), 134.4 (1'-C), 134.2 (5'-C), 130.0 (d, *J*<sub>CF</sub> 11.6 Hz, 5-C), 129.6 (4'-C), 128.2 (6'-C), 125.1 (3'-C), 118.1 (d, *J*<sub>CF</sub> 2.2 Hz, 4a-C), 110.7 (d, *J*<sub>CF</sub> 22.6 Hz, 6-C), 105.1 (d, *J*<sub>CF</sub> 24.8 Hz, 8-C), 76.3 (2-C), 44.2 (3-C). **<sup>19</sup>F-NMR** (565 MHz, CDCl<sub>3</sub>) δ -99.72 (m, 1F). **FT-IR**: 1689, 1615, 1586, 1524, 1489, 1440, 1403, 1371, 1350, 1292, 1259, 1249, 1217. **HR-MS**: calc. for [M+H]<sup>+</sup> C<sub>15</sub>H<sub>11</sub>O<sub>4</sub>NF: 288.0667 found: 288.0663.

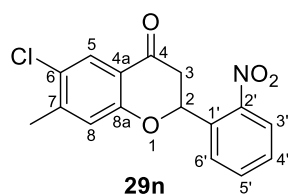
## Experimental

### 2-(2-nitrophenyl)-7-methyl-3,4-dihydro-2H-1-benzopyran-4-one (29m)



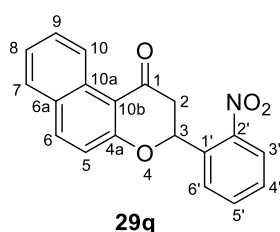
Prepared according to general procedure D. Flash column chromatography eluting with 5-20% EtOAc in *n*-pentane, followed by recrystallisation from pentane:EtOAc (8:2) afforded the desired product **29m** (611.20 mg, 2.06 mmol, 31%) as yellow solid. **<sup>1</sup>H-NMR** (400 MHz, CDCl<sub>3</sub>): δ 8.04 (dd, *J* 8.2, 1.3 Hz, 1H, 3'-H), 8.00-7.96 (m, 1H, 6'-H), 7.77-7.72 (m, 1H, 5'-H), 7.70 (s, 1H, 5-H), 7.57-7.52 (m, 1H, 4'-H), 6.82 (s, 1H, 8-H), 6.05 (dd, *J* 13.0, 2.8 Hz, 1H, 2-H), 3.15 (dd, *J* 16.9, 2.8 Hz, 1H), 2.90 (dd, *J* 16.9, 13.0 Hz, 1H), 2.29 (s, 3H, CH<sub>3</sub>), 2.25 (s, 3H, CH<sub>3</sub>). **<sup>13</sup>C NMR** (176 MHz, CDCl<sub>3</sub>): δ 190.9 (4-C), 159.6 (8a-C), 147.6 (2'-C), 147.0 (6-C or 7-C), 135.1 (1'-C), 134.1 (4'-C), 131.0 (6-C or 7-C), 129.4 (4'-C), 128.3 (6'-C), 127.3 (5-C), 124.9 (3'-C), 119.0 (4a-C), 118.6 (8-C), 75.7 (2-C), 44.5 (3-C), 20.7 (CH<sub>3</sub>), 19.0 (CH<sub>3</sub>). **FT-IR**: 1684, 1617, 1522, 1485, 1459, 1418, 1343, 1254, 1228. **HR-MS**: calc. for [M+H]<sup>+</sup> C<sub>17</sub>H<sub>16</sub>O<sub>4</sub>N: 298.1074 found: 298.1076.

### 2-(2-nitrophenyl)-6-chloro-7-methyl-3,4-dihydro-2H-1-benzopyran-4-one (29n)



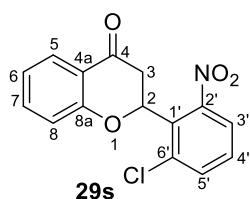
Prepared according to general procedure D. Flash column chromatography eluting with 5-20% EtOAc in *n*-pentane, followed by recrystallisation from pentane:EtOAc (8:2) afforded the desired product **29n** (164.00 mg, 0.52 mmol, 8%) as yellow solid. **<sup>1</sup>H-NMR** (600 MHz, CDCl<sub>3</sub>): δ 8.05 (1H, dd, *J* 8.3, 1.2 Hz, 3'-H), 7.95 (1H, dd, *J* 7.7, 1.2 Hz, 6'-H), 7.90 (1H, s, 5-H), 7.76 (1H, td, *J* 7.7, 1.2 Hz, 5'-H), 7.58-7.55 (1H, m, 4'-H), 6.93 (1H, s, 8-H), 6.07 (1H, dd, *J* 13.0, 2.7 Hz, 2-H), 3.19 (1H, dd, *J* 17.0, 2.7 Hz, 3-H<sub>a</sub>), 2.91 (1H, dd, *J* 17.0, 13.0 Hz, 3-H<sub>b</sub>), 2.39 (3H, s, CH<sub>3</sub>). **<sup>13</sup>C NMR** (151 MHz, CDCl<sub>3</sub>): δ 189.7 (4-C), 159.5 (8a-C), 147.5 (2'-C), 145.6 (6-C or 7-C), 134.5 (1'-C), 134.2 (5'-C), 129.6 (4'-C), 128.6 (6-C or 7-C), 128.2 (6'-C), 127.1 (5-C), 125.0 (3'-C), 120.2 (4a-C), 120.1 (8-C), 75.9 (2-C), 44.2 (CH<sub>3</sub>), 21.0 (3-C). **FT-IR**: 2112 1691, 1611, 1520, 1469, 1451, 1405, 1380, 1358, 1340, 1279, 1226. **HR-MS**: calc. for [M+H]<sup>+</sup> C<sub>16</sub>H<sub>13</sub>O<sub>4</sub>NCl: 318.0527, found: 318.0529, calc. for [M+H]<sup>+</sup> C<sub>16</sub>H<sub>13</sub>O<sub>4</sub>N<sup>37</sup>Cl: 320.0498, found: 320.0498.

### 3-(2-nitrophenyl)-1H,2H,3H-naphtho[2,1-b]pyran-1-one (29q)



Prepared according to general procedure D. Flash column chromatography eluting with 5-20% EtOAc in *n*-pentane, followed by recrystallisation from pentane:EtOAc **29q** (8:2) afforded the desired product (594.70 mg, 1.86 mmol, 28%) as yellow solid. **<sup>1</sup>H-NMR** (500 MHz, CDCl<sub>3</sub>): δ 9.49 (1H, d, *J* 7.6 Hz, 10-H), 8.09 (2H, dd, *J* 8.2, 1.2 Hz, 3'-H), 8.05 (1H, d, *J* 6.6 Hz, 6'-H), 7.98 (1H, d, *J* 9.0 Hz, 6-H), 7.82-7.76 (2H, m, 5'-H and 7-H), 7.70-7.66 (1H, m, 9-H), 7.61-7.55 (1H, m, 4'-H), 7.50-7.45 (m, 1H, 8-H), 7.17 (1H, d, *J* 9.0 Hz, 5-H), 6.24 (2H, dd, *J* 13.4, 2.8 Hz), 3.32 (1H, dd, *J* 16.7, 3.0 Hz, 3-H<sub>a</sub>), 3.09 (1H, dd, *J* 16.6, 13.4 Hz, 3-H<sub>b</sub>). **<sup>13</sup>C NMR** (126 MHz, CDCl<sub>3</sub>): δ 191.9 (1-C), 163.4 (4a-C), 147.5 (2'-C), 137.9 (6-C), 134.7 (1'-C), 134.2 (5'-C), 131.5 (10a-C), 130.0 (9-C), 129.6 (4'-C), 129.5 (6a-C), 129.4 (10-C), 128.6 (7-C), 128.3 (6'-C), 126.2 (10-C), 125.3 (8-C), 125.1 (3'-C), 118.6 (5-C), 75.8 (3-C), 45.6 (2-C). **FT-IR**: 1668, 1613, 1594, 1566, 1519, 1485, 1458, 1436, 1412, 1394, 1343, 1277, 1232, 1206, 1165, 1141, 1123, 1071. **HR-MS**: calc. for [M+H]<sup>+</sup> C<sub>19</sub>H<sub>14</sub>O<sub>4</sub>N: 320.0917 found: 320.1918.

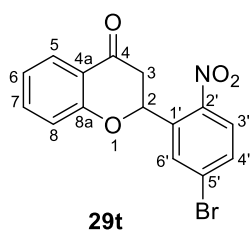
### 2-(2-nitrophenyl-6-chloro)-7-methyl-3,4-dihydro-2H-1-benzopyran-4-one (29s)



Prepared according to general procedure D. Flash column chromatography eluting with 5-20% EtOAc in *n*-pentane, afforded the desired product **29s** (233.80 mg, 0.77 mmol, 14%) as yellow solid, containing an aniline impurity. **<sup>1</sup>H-NMR** (700 MHz, CDCl<sub>3</sub>): δ 7.94 (1H, dd, *J* 7.9, 1.8 Hz, 5-H), 7.64 (1H, dd, *J* 8.1, 1.1 Hz, 3'-H or 5'-H), 7.60 (1H, dd, *J* 8.2, 1.1 Hz, 3'-H or 5'-H), 7.52-7.46 (2H, m, 4'-H and 7-H), 7.42-7.39 (1H, m, aniline impurity), 7.11-7.06 (1H, m, 6-H), 6.96-6.93 (1H, m, 8-H), 6.48-6.45 (0H, m, aniline impurity), 6.04 (1H, dd, *J* 14.3, 3.2 Hz, 2-H), 3.64 (1H, dd, *J* 17.0, 14.3 Hz, 3-H<sub>a</sub>), 3.03 (1H, dd, *J* 17.0, 3.2 Hz, 3-H<sub>b</sub>). **<sup>13</sup>C NMR** (176 MHz, CDCl<sub>3</sub>): δ 190.7 (4-C), 160.3 (8a-C), 151.2 (2'-C), 146.2 (aniline impurity), 138.0 (aniline impurity), 136.5 (7-C), 133.8 (6'-C), 133.2 (3'-C or 5'-C), 130.1 (4'-C), 129.5 (1'-C), 127.3 (5-C), 123.2 (3'-C or 5'-C), 122.3 (6-C), 120.7 (4a-C), 118.0 (8-C), 117.4 (aniline impurity), 75.7 (2-C), 40.9 (3-C). **FT-IR**: 1689, 1605, 1534, 1486, 1473, 1463, 1444, 1368, 1303, 1229. **HR-MS**: calc. for [M+H]<sup>+</sup> C<sub>15</sub>H<sub>11</sub>O<sub>4</sub>NCl: 304.0371 found: 304.0374; calc. for [M+H]<sup>+</sup> C<sub>15</sub>H<sub>11</sub>O<sub>4</sub>N<sup>37</sup>Cl: 306.0341 found: 304.0343.

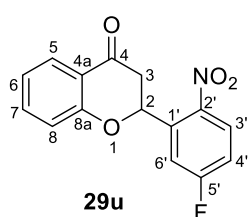
## Experimental

### 2-(2-nitrophenyl-5-bromo)-7-methyl-3,4-dihydro-2H-1-benzopyran-4-one (29t)

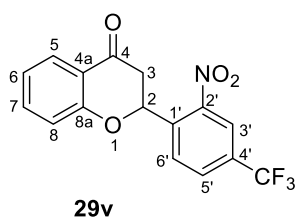


Prepared according to general procedure D. Flash column chromatography eluting with 5-20% EtOAc in *n*-pentane, followed by recrystallisation from pentane:EtOAc (8:2) afforded the desired product **29t** (444.80 mg, 1.28 mmol, 29%) as yellow solid. **<sup>1</sup>H-NMR** (700 MHz, CDCl<sub>3</sub>): δ 8.20 (1H, d, *J* 2.2 Hz, 6'-H), 7.99-7.96 (2H, m, 3'-H and 5-H), 7.70 (1H, dd, *J* 8.7, 2.2 Hz, 4'-H), 7.57-7.53 (1H, m, 7-H), 7.14-7.11 (1H, m, 6-H), 7.07 (1H, d, *J* 8.4 Hz, 8-H), 6.11 (1H, dd, *J* 13.3, 2.5 Hz, 2-H), 3.21 (1H, dd, *J* 16.9, 2.5 Hz, 3-H<sub>a</sub>), 2.90 (1H, dd, *J* 16.9, 13.3 Hz, 3-H<sub>b</sub>). **<sup>13</sup>C NMR** (176 MHz, CDCl<sub>3</sub>): δ 190.4 (4-C), 161.0 (4a-C), 145.9 (2'-C), 137.0 (1'-C), 136.5 (7-C), 132.6 (4'-C), 131.6 (6'-C), 129.5 (5'-C), 127.5 (3'-C or 5-C), 126.6 (3'-C or 5-C), 122.6 (6-C), 121.1 (8a-C), 118.1 (8-C), 75.4 (2-C), 44.6 (3-C). **FT-IR**: 1682, 1605, 1581, 1562, 1518, 1461, 1340, 1301, 1221, 1175. **HR-MS**: calc. for [M+H]<sup>+</sup> C<sub>15</sub>H<sub>11</sub>O<sub>4</sub>NBr: 347.9866 found: 347.9869; calc. for [M+H]<sup>+</sup> C<sub>15</sub>H<sub>11</sub>O<sub>4</sub>N<sup>81</sup>Br: 349.9845, found: 349.9848.

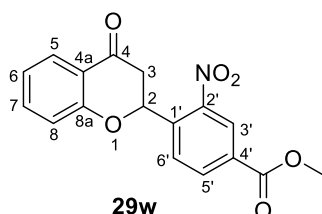
### 2-(2-nitrophenyl-5-fluoro)-3,4-dihydro-2H-1-benzopyran-4-one (29u)



Prepared according to general procedure D. Flash column chromatography eluting with 5-20% EtOAc in *n*-pentane, followed by recrystallisation from pentane:EtOAc (8:2) afforded the desired product **29u** (462,50 mg, 1.61 mmol, 27%) as yellow solid. **<sup>1</sup>H-NMR** (600 MHz, CDCl<sub>3</sub>): δ 8.19 (1H, dd, *J* 9.1, 5.0 Hz, 3'-H), 7.97 (1H, dd, *J* 7.8, 1.6 Hz, 5-H), 7.76 (1H, dd, *J* 9.4, 2.8 Hz, 6'-H), 7.57-7.52 (1H, m, 6-H), 7.25-7.22 (1H, m, 4'-H), 7.14-7.10 (1H, m, 7-H), 7.06 (1H, dd, *J* 8.3, 0.6 Hz, 8-H), 6.16 (1H, dd, *J* 13.2, 2.5 Hz, 2-H), 3.23 (1H, dd, *J* 16.9, 2.5 Hz, 3-H<sub>a</sub>), 2.87 (1H, dd, *J* 16.9, 13.2 Hz, 3-H<sub>b</sub>). **<sup>13</sup>C NMR** (151 MHz, CDCl<sub>3</sub>): δ 190.5 (4-C), 165.7 (d, *J*<sub>CF</sub> 258.0 Hz, 5'-C), 160.9 (4a-C), 143.1 (2'-C), 138.9 (d, *J*<sub>CF</sub> 8.8 Hz, 3'-C), 136.5 (6-C), 128.2 (d, *J*<sub>CF</sub> 9.9 Hz, 1'-C), 127.4 (5-C), 122.5 (7-C), 121.1 (8a-C), 118.1 (8-C), 116.5 (d, *J*<sub>CF</sub> 23.1 Hz, 4'-C), 115.7 (d, *J*<sub>CF</sub> 25.9 Hz, 6'-C), 75.6 (2-C), 44.5 (3-C). **<sup>19</sup>F-NMR** (565 MHz, CDCl<sub>3</sub>) δ -100.8 (1F, m). **FT-IR**: 1684, 1606, 1580, 1526, 1480, 1462, 1410, 1364, 1345, 1322, 1302, 1276, 1256, 1220. **HR-MS**: calc. for [M+H]<sup>+</sup> C<sub>15</sub>H<sub>11</sub>O<sub>4</sub>NF: 288.0667 found 288.0663.

**2-(2-nitrophenyl)-4-trifluoromethyl-3,4-dihydro-2H-1-benzopyran-4-one (29v)**

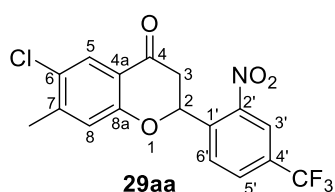
Prepared according to general procedure D. Flash column chromatography eluting with 5-20% EtOAc in *n*-pentane, followed by recrystallisation from pentane:EtOAc (8:2) afforded the desired product **29v** (332.20 mg, 0.99 mmol, 22%) as yellow solid.  $^1\text{H-NMR}$  (600 MHz,  $\text{CDCl}_3$ ):  $\delta$  8.35 (1H, s, 3'-H), 8.22 (1H, d,  $J$  8.3 Hz, 6'-H), 8.03 (1H, dd,  $J$  8.3, 1.7 Hz, 5'-H), 7.98 (1H, dd,  $J$  7.9, 1.7 Hz, 5-H), 7.59-7.52 (1H, m, 7-H), 7.16-7.11 (1H, m, 6-H), 7.05 (1H, dd,  $J$  8.3, 0.6 Hz, 8-H), 6.16 (1H, dd,  $J$  13.1, 2.6 Hz, 2-H), 3.23 (1H, dd,  $J$  16.9, 2.6 Hz, 3-H<sub>a</sub>), 2.93 (1H, dd,  $J$  16.9, 13.1 Hz, 3-H<sub>b</sub>).  $^{13}\text{C NMR}$  (151 MHz,  $\text{CDCl}_3$ ):  $\delta$  190.1 (4-C), 160.9 (8a-C), 147.3 (2'-C), 138.7 (f1'-C), 136.6 (7-C), 132.2 (q,  $J_{\text{CF}}$  34.7 Hz, 4'-C), 130.7 (q,  $J_{\text{CF}}$  3.3 Hz, 5'-C), 129.6 (6'-C), 127.5 (5-C), 122.7 (6-C), 122.4 (q,  $J_{\text{CF}}$  3.9 Hz, 3'-C), 121.1 (4a-C), 118.1 (8-C), 75.5 (2-C), 44.4 (3-C).  $^{19}\text{F NMR}$  (Chloroform-*d*, 565 MHz)  $\delta$  -63.00. **FT-IR**: 1687, 1160, 1581, 1534, 1474, 1463, 1347, 1318, 1304, 1275, 1222. **HR-MS**: calc. for  $[\text{M}+\text{H}]^+$   $\text{C}_{16}\text{H}_{11}\text{O}_4\text{NF}_3$ : 338.0634 found 338.0635.

**[5-(methoxycarbonyl)-2-(4-oxo-3,4-dihydro-2H-1-benzopyran-2-yl)phenyl]azinic acid (29w)**

Prepared according to general procedure D. Flash column chromatography eluting with 5-20% EtOAc in *n*-pentane, followed by recrystallisation from pentane:EtOAc (8:2) afforded the desired product **29w** (368.10 mg, 1.12 mmol, 23%) as yellow solid.  $^1\text{H-NMR}$  (600 MHz,  $\text{CDCl}_3$ ):  $\delta$  8.70 (1H, d,  $J$  1.7 Hz, 3'-H), 8.40 (1H, dd,  $J$  8.2, 1.7 Hz, 5'-H), 8.13 (1H, d,  $J$  8.2 Hz, 6'-H), 7.97 (1H, dd,  $J$  7.9, 1.7 Hz, 5-H), 7.56-7.53 (1H, m, 7-H), 7.12 (1H, t,  $J$  7.5 Hz, 6-H), 7.05 (1H, dd,  $J$  8.3, 1.0 Hz, 8-H), 6.15 (1H, dd,  $J$  13.2, 2.6 Hz, 2'-H), 4.00 (3H, s), 3.22 (1H, dd,  $J$  16.9, 2.7 Hz, 3-H<sub>a</sub>), 2.93 (1H, dd,  $J$  16.9, 13.2 Hz, 3-H<sub>b</sub>).  $^{13}\text{C NMR}$  (151 MHz,  $\text{CDCl}_3$ ):  $\delta$  190.4 (4-C), 164.7 ( $\text{CO}_2\text{Me}$ ), 161.1 (8a-C), 147.4 (2'-C), 139.2 (1'-C), 136.6 (7-C), 134.7 (5'-C), 131.8 (4'-C), 128.9 (6'-C), 127.5 (5-C), 126.2 (3'-C), 122.6 (6-H), 121.2 (4a-C), 118.2 (8-C), 75.7 (2-C), 53.1 ( $\text{CO}_2\text{CH}_3$ ), 44.5 (3-C). **FT-IR**: 2323, 2080, 1727, 1690, 1606, 1533, 1462, 1436, 1345, 1290, 1266. **HR-MS**: calc. for  $[\text{M}+\text{H}]^+$   $\text{C}_{17}\text{H}_{14}\text{O}_6\text{N}$ : 328.0816 found 328.0817.

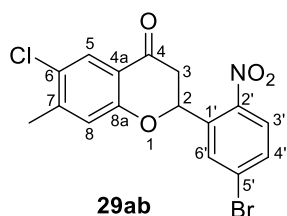
## Experimental

### 2-(2-nitrophenyl-4-trifluoromethyl)-6-chloro-7-methyl-3,4-dihydro-2H-1-benzopyran-4-one (29aa)



Prepared according to general procedure D. Flash column chromatography eluting with 5-20% EtOAc in *n*-pentane, afforded the desired product **29aa** (103.20 mg, 0.27 mmol, 12%) as yellow solid. <sup>1</sup>H-NMR (500 MHz, CDCl<sub>3</sub>): δ 8.35 (1H, s, 3'-H), 8.17 (1H, d, *J* 8.2 Hz, 6'-H), 8.02 (1H, d, *J* 8.2 Hz, 5'-H), 7.92 (1H, s, 5-H), 6.94 (1H, s, 8-H), 6.12 (1H, dd, *J* 13.0, 2.6 Hz), 3.21 (1H, dd, *J* 16.9, 2.7 Hz), 2.89 (1H, dd, *J* 16.9, 13.1 Hz), 2.41 (3H, s, CH<sub>3</sub>). <sup>13</sup>C NMR (126 MHz, CDCl<sub>3</sub>): δ 188.9 (4-C), 159.1 (8a-C), 147.3 (2'-C), 145.9 (6-C), 138.3 (1'-C), 132.3 (q, *J*<sub>CF</sub> 34.7 Hz, 4'-C) 130.7 (q, *J*<sub>CF</sub> 3.7 Hz, 5'-C), 129.5 (6'-C), 128.9 (7-C), 127.2 (5-C), 123.8 (q, *J*<sub>CF</sub> 139.0 Hz, CF<sub>3</sub>), 122.5 (q, *J*<sub>CF</sub> 3.9 Hz, 3'-C), 120.1 (8-H), 120.1 (4a-C), 75.6 (2-C), 44.0 (3-C), 21.1 (CH<sub>3</sub>). FT-IR: 2349, 2114, 1690, 1632, 1614, 1540, 1509, 1469, 1454, 1434, 1409, 1371, 1353, 1326, 1248, 1225. HR-MS: not stable under MS conditions; identity confirmed by NMR, next reaction steps.

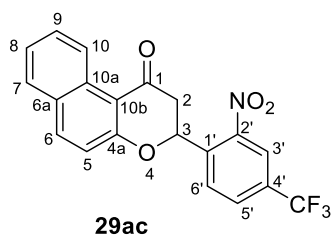
### 2-(2-nitrophenyl-4-bromo)-6-chloro-7-methyl-3,4-dihydro-2H-1-benzopyran-4-one (29ab)



Prepared according to general procedure D. Flash column chromatography eluting with 5-20% EtOAc in *n*-pentane, afforded the desired product **29ab** (245 mg, 0.62 mmol, 14%) as yellow solid, containing an aniline impurity. <sup>1</sup>H-NMR (500 MHz, CDCl<sub>3</sub>): δ 8.15 (1H, d, *J* 2.1 Hz, 6'-H), 7.98 (1H, d, *J* 8.7 Hz, 3'-H), 7.91 (1H, s, 5-H), 7.70 (1H, dd, *J* 8.7, 2.1 Hz, 4'-H), 6.97 (1H, s, 8-H), 6.07 (1H, dd, *J* 13.2, 2.4 Hz, 2-H), 3.18 (1H, dd, *J* 17.0, 2.5 Hz, 3-H<sub>a</sub>), 2.86 (1H, dd, *J* 17.0, 13.2 Hz, 3-H<sub>b</sub>), 2.41 (3H, s, CH<sub>3</sub>). <sup>13</sup>C NMR (126 MHz, CDCl<sub>3</sub>): δ 189.2 (4-C), 159.2 (8a-C), 145.8 (2'-C), 145.7 (6-C), 136.7 (5'-C), 132.7 (4'-C), 131.5 (6'-C), 129.6 (1'-C), 128.8 (7-C), 127.1 (5-C), 126.7 (3'-C), 120.2 (8-C), 120.1 (4a-C), 75.5 (2-C), 44.1 (3-C), 21.1 (CH<sub>3</sub>). FT-IR: 3107, 2161, 1691, 1604, 1568, 1522 1468, 1451, 1405, 1392, 1370, 1359, 1344, 1330, 1298, 1272, 1251, 1233, 1224, 1207. HR-MS: not stable under MS conditions; identity confirmed by NMR, next reaction steps.

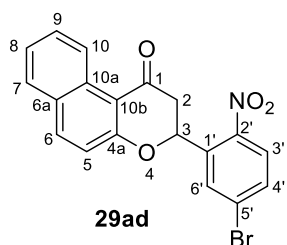
### 3-(2-nitro-4-trifluoromethyl-phenyl)-1H,2H,3H-naphtho[2,1-b]pyran-1-one (29ac)





Prepared according general procedure D. Flash column chromatography eluting with 5-20% EtOAc in *n*-pentane, followed by recrystallisation from pentane:EtOAc (8:2) afforded the desired product **29ac** (88.40 mg, 0.22 mmol, 10%) as yellow solid. **<sup>1</sup>H-NMR** (600 MHz, CDCl<sub>3</sub>): δ 9.48 (1H, d, *J* 8.4 Hz, 10-H), 8.37 (1H, d, *J* 1.5 Hz, 3'-H), 8.25 (1H, d, *J* 8.3 Hz, 6'-H), 8.04 (1H, dd, *J* 8.3, 1.5 Hz, 5'-H), 8.00 (1H, d, *J* 9.0 Hz, 6-H), 7.80 (1H, d, *J* 8.1 Hz, 7-H), 7.69 (1H, ddd, *J* 8.4, 7.0, 1.4 Hz, 9-H), 7.49 (1H, ddd, *J* 8.1, 7.0, 1.1 Hz, 8-H), 7.17 (1H, d, *J* 9.0 Hz, 5-H), 6.29 (1H, dd, *J* 13.4, 2.9 Hz, 3-H), 3.32 (1H, dd, *J* 16.6, 2.9 Hz, 2-H<sub>a</sub>), 3.06 (1H, dd, *J* 16.6, 13.4 Hz, 2-H<sub>b</sub>). **<sup>13</sup>C NMR** (151 MHz, CDCl<sub>3</sub>): δ 191.1 (1-C), 163.0 (4a-C), 147.4 (2'-C), 138.5 (1'-C), 138.1 (6-C), 132.2 (q, *J*<sub>CF</sub> 34.6 Hz, 4'-C), 131.5 (10a-C), 130.7 (q, *J*<sub>CF</sub> 3.3 Hz, 5'-C), 130.2 (9-C), 129.8 (6a-C), 129.6 (6'-C), 128.6 (7-C), 126.2 (10-C), 125.5 (8-C), 122.7 (q, *J*<sub>CF</sub> 272.9 Hz, CF<sub>3</sub>), 122.5 (q, *J*<sub>CF</sub> 3.7 Hz, 3'-C), 118.4 (5-C), 113.1 (10b-C), 75.6 (3-C), 45.4 (2-C). **FT-IR**: 3107, 1667, 1617, 1594, 1567, 1538, 1511, 1460, 1436, 1404, 1395, 1370, 1323, 1277, 1252, 1233, 1208, **HR-MS**: calc. for [M+H]<sup>+</sup> C<sub>20</sub>H<sub>13</sub>O<sub>4</sub>NF<sub>3</sub>: 388.0791 found 388.0792.

### 3-(2-nitro-5-bromophenyl)- 1H,2H,3H-naphtho[2,1-b]pyran-1-one (29ad)

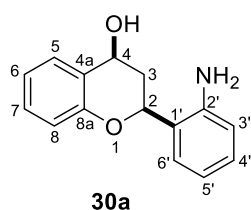


Prepared according to general procedure D. Flash column chromatography eluting with 5-20% EtOAc in *n*-pentane, followed by recrystallisation from pentane:EtOAc (8:2) afforded the desired product **29ad** (270.80 mg, 0.68 mmol, 19%) as yellow solid. **<sup>1</sup>H-NMR** (500 MHz, CDCl<sub>3</sub>): δ 9.48 (1H, d, *J* 8.7 Hz, 10-H), 8.23 (1H, d, *J* 2.1 Hz, 6'-H), 8.03-7.97 (2H, 3'-H and 6-H), 7.80 (1H, d, *J* 8.1 Hz, 7-H), 7.74-7.67 (2H, m, 4'-H and 9-H), 7.51-7.46 (1H, m, 8-H), 7.19 (1H, d, *J* 8.9 Hz, 5-H), 6.23 (1H, dd, *J* 13.7, 2.8 Hz, 3-H), 3.29 (1H, dd, *J* 16.6, 2.8 Hz, 2-H<sub>a</sub>), 3.03 (1H, dd, *J* 16.6, 13.7 Hz, 2-H<sub>b</sub>). **<sup>13</sup>C NMR** (126 MHz, CDCl<sub>3</sub>): δ 191.4 (1-C), 163.1 (4a-C), 145.9 (2'-C), 138.0 (6-C), 136.8 (1'-C), 132.7 (4'-C), 131.6 (6'-C), 131.5 (10a-C), 130.1 (9-C), 129.7 (6a-C or 5'-C), 129.6 (6a-C or 5'-C), 128.6 (7-C), 126.7 (3'-C), 126.2 (10-C), 125.5 (8-C), 118.5 (5-C), 113.1 (10b-C), 75.5 (3-C), 45.6 (2-C). **FT-IR**: 3107, 2157, 1691, 1665, 1616, 1596, 1568, 1513, 1467, 1458, 1436, 1405, 1392, 1370, 1332, 1298, 1279, 1249, 1225, 1206. **HR-MS**: calc. for [M+H]<sup>+</sup> C<sub>19</sub>H<sub>12</sub>O<sub>4</sub>NBr: 398.0023 found:398.001, calc. for [M+H]<sup>+</sup> C<sub>19</sub>H<sub>12</sub>O<sub>4</sub>N<sup>81</sup>Br: 400.0002, found: 400.0000.

## Experimental

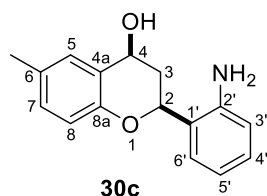
### Preparation of Flavan-4-ols

#### 2-(2-aminophenyl)-3,4-dihydro-2H-1-benzopyran-4-ol (30a)

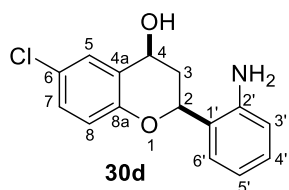


Prepared according to general procedure E. Flash column chromatography eluting with 10-50% [DCM:EtOH:NH<sub>4</sub>OH (50:8:1)] in DCM afforded the desired product **30a** (37.80 mg, 0.16 mmol, 84%) as pale yellow solid (dr. 20:1). **<sup>1</sup>H-NMR** (500 MHz, CDCl<sub>3</sub>, OH not observed): δ 7.54 (1H, d, *J* 7.6 Hz, 5-H), 7.22-7.16 (3H, m, 7-H, 4'-H and 7'-H), 7.00 (1H, td, *J* 7.6, 1.0 Hz, 6-H), 6.86 (1H, d, *J* 8.2 Hz, 8-H), 6.82 (1H, t, *J* 7.5 Hz, 5'-H), 6.75 (1H, d, *J* 7.8 Hz, 3-H), 5.21 (1H, dd, *J* 11.7, 2.1 Hz), 5.11 (1H, dd, *J* 10.5, 6.7 Hz), 3.41 (2H, br. s, NH<sub>2</sub>), 2.55-2.42 (2H, m, 3-H<sub>a</sub> and 3-H<sub>b</sub>). **<sup>13</sup>C NMR** (126 MHz, CDCl<sub>3</sub>): δ 154.2 (8a-C), 145.2 (2'-C), 129.6 (5-C), 129.2 (7-C, 4'-C or 7'-C), 127.4 (7-C, 4'-C or 7'-C), 127.3 (7-C, 4'-C or 7'-C), 126.2 (4a-C), 124.0 (1'-C), 121.4 (6-C), 119.0 (5'-C), 117.2 (3'-C), 116.7 (8-C), 75.9 (2-C), 66.1 (4-C), 35.9 (3-C). **FT-IR**: 3373, 2349, 2112, 1985, 1806, 1611, 1582, 1499, 1484, 1455, 1300, 1271. **HR-MS**: calc. for [M+H]<sup>+</sup> C<sub>15</sub>H<sub>16</sub>O<sub>2</sub>N: 242.1175, found 242.1172.

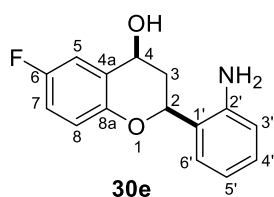
#### 2-(2-aminophenyl)-3,4-dihydro-6-methyl-2H-1-benzopyran-4-ol (30c)



Prepared according to general procedure E. Flash column chromatography eluting with 10-50% [DCM:EtOH:NH<sub>4</sub>OH (50:8:1)] in DCM afforded the desired product (367.40 mg, 1.30 mmol, 19%) as pale yellow solid (dr. 15:1). **<sup>1</sup>H-NMR** (700 MHz, CDCl<sub>3</sub>, OH and NH<sub>2</sub> not observed): δ 7.34 (1H, s, 5-H), 7.23-7.16 (2H, m, 6'-H and 4'-H), 6.92 (1H, d, *J* 8.2 Hz, 7H), 6.88-6.80 (2H, m, 3'-H and 5'-H), 6.77 (1H, d, *J* 8.2 Hz, 8H), 5.18 (1H, dd, *J* 11.9, 1.8 Hz, 2-H), 5.09 (1H, dd, *J* 10.4, 6.7 Hz, 4-H), 2.52-2.47 (1H, m, 3-H<sub>a</sub>), 2.46-2.40 (1H, m, 3-H<sub>b</sub>), 2.29 (3H, s, CH<sub>3</sub>). **<sup>13</sup>C NMR** (176 MHz, CDCl<sub>3</sub>): δ 152.0 (8a-C), 143.7 (2'-C), 130.8 (6-C), 129.9 (7-C), 129.6 (4'-C), 127.5 (5-C), 127.5 (6'-C), 125.8 (4a-C), 125.1 (1'-C), 119.9 (5'-C), 118.0 (3'-C), 116.6 (8-C), 75.9 (2-C), 66.1 (4-C), 36.4 (3-C), 20.8 (CH<sub>3</sub>). **FT-IR**: 3381, 1711, 1609, 1585, 1494, 1459, 1330, 1275. **HR-MS**: calc. for [M+H]<sup>+</sup> C<sub>16</sub>H<sub>18</sub>O<sub>2</sub>N: 256.1332 found: 256.1329.

**2-(2-aminophenyl)-3,4-dihydro-6-chloro-2H-1-benzopyran-4-ol (30d)**

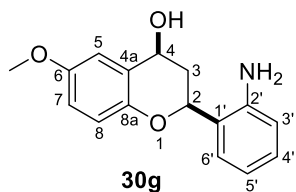
Prepared according to general procedure E. Flash column chromatography eluting with 10-50% [DCM:EtOH:NH<sub>4</sub>OH (50:8:1)] in DCM afforded the desired product **30d** (422.70 mg, 1.53 mmol, 62%) as pale yellow solid (dr. >10:1), NMR assignments belong to the major isomer. <sup>1</sup>H-NMR (600 MHz, CDCl<sub>3</sub>, OH and NH<sub>2</sub> not observed): 7.53 (1H, dd, *J* 2.6, 0.9 Hz, 5-H), 7.21-7.16 (2H, m, 4'-H and 6'-H), 7.10 (1H, dd, *J* 8.7, 2.4 Hz, 7-H), 6.84 (1H, td, *J* 7.5, 1.0 Hz, 5'-H), 6.80-6.77 (2H, m, 3'-H and 8-H), 5.20 (1H, dd, *J* 11.9, 1.9 Hz, 2-H), 5.08 (1H, dd, *J* 10.6, 6.5 Hz, 4-H), 2.56-2.49 (1H, m, 3-H<sub>b</sub>), 2.48-2.39 (1H, m, 3-H<sub>a</sub>). <sup>13</sup>C NMR (151 MHz, CDCl<sub>3</sub>): δ 152.8 (8a-C), 144.7 (2'-C), 129.8 (4'-C), 129.2 (7-C), 127.6 (6-C), 127.4 (6'-C), 127.2 (5-C), 126.4 (4a-C), 123.9 (1'-C), 119.3 (5'-C), 118.1 (8-C), 117.5 (3'-C), 76.1 (2-C), 65.9 (4-C), 35.7 (3-C). **FT-IR**: 3436, 3349, 2968, 2862, 2324, 2064, 1978, 1698, 1624, 1596, 1574, 1501, 1478, 1457, 1409, 1385, 1315, 1295, 1269, 1259.

**2-(2-aminophenyl)-3,4-dihydro-6-fluoro-2H-1-benzopyran-4-ol (30e)**

Prepared according to general procedure E. Flash column chromatography eluting with 10-50% [DCM:EtOH:NH<sub>4</sub>OH (50:8:1)] in DCM afforded the desired product **30e** (290.70 mg, 1.12 mmol, 59%) as pale yellow solid (dr. 10:1), NMR assignments belong to the major isomer. <sup>1</sup>H-NMR (500 MHz, CDCl<sub>3</sub>, OH not observed): 7.23 (1H, dd, *J* 9.0, 3.0 Hz, 5-H), 7.20-7.15 (2H, m, 4'-H and 6'-H), 6.89-6.84 (1H, m, 7-H), 6.82 (1H, td, *J* 7.5, 1.2 Hz, 5'-H), 6.78 (1H, dd, *J* 9.0, 4.7 Hz, 8-H), 6.74 (1H, d, *J* 7.8 Hz, 3'-H), 5.16 (1H, dd, *J* 11.4, 2.4 Hz, 2-H), 5.07-5.01 (1H, m, 4-H), 3.54 (2H, bs, NH<sub>2</sub>), 2.53-2.34 (2H, m, 3-H<sub>a</sub> and 3-H<sub>b</sub>). <sup>13</sup>C NMR (126 MHz, CDCl<sub>3</sub>): δ 157.6 (d, *J*<sub>CF</sub> 239.3 Hz, 6-C), 150.1 (d, *J*<sub>CF</sub> 2.0 Hz, 8a-C), 145.1 (2'-C), 129.7 (6'-C or 4'-H), 127.4 (6'-C or 4'-H), 127.3 (d, *J*<sub>CF</sub> 6.7 Hz, 4a-C), 123.8 (1'-C), 119.0 (6'-C), 117.7 (d, *J*<sub>CF</sub> 7.9 Hz, 8-C), 117.3 (3'-C), 116.0 (d, *J*<sub>CF</sub> 23.5 Hz, 7-C), 113.4 (d, *J*<sub>CF</sub> 23.6 Hz, 5-C), 77.4 (2-C), 65.9 (4-C), 35.6 (3-C). <sup>19</sup>F NMR (565 MHz, CDCl<sub>3</sub>) δ -110.90- -111.00 (m, minor isomer), -112.51- -112.61 (m, major isomer). **FT-IR**: 3372, 1874, 1619, 1485, 1459, 1432, 1252. **HR-MS**: calc. for [M+H]<sup>+</sup> C<sub>15</sub>H<sub>15</sub>O<sub>2</sub>NF: 260.1081 found: 260.1079.

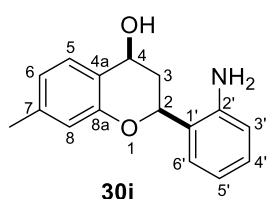
## Experimental

### 2-(2-aminophenyl)-3,4-dihydro-6-methoxy-2H-1-benzopyran-4-ol (**30g**)

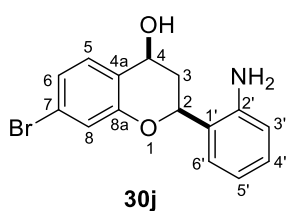


Prepared according to general procedure E. Flash column chromatography eluting with 10-50% [DCM:EtOH:NH<sub>4</sub>OH (50:8:1)] in DCM afforded the desired product **30g** (422.70 mg, 1.53 mmol, 62%) as pale yellow solid (dr. >10:1), NMR assignments belong to the major isomer. **<sup>1</sup>H-NMR** (600 MHz, CDCl<sub>3</sub>, OH and NH<sub>2</sub> not observed): 7.21-7.15 (2H, m, 4'-H and 6'-H), 7.08 (1H, d, *J* 2.7 Hz, 5-H), 6.85 (1H, t, *J* 7.6 Hz, 5'-H), 6.82-6.77 (2H, m, 3'-H and 8-H), 6.70 (1H, dd, *J* 8.8, 2.6 Hz, 7-H), 5.15 (1H, dd, *J* 11.9, 1.8 Hz, 2-H), 5.08 (1H, dd, *J* 10.5, 6.6 Hz, 4-H), 3.78 (3H, s, OCH<sub>3</sub>), 2.53-2.47 (1H, m, 3H<sub>a</sub>), 2.47-2.38 (1H, m, 3-H<sub>b</sub>). **<sup>13</sup>C NMR** (151 MHz, CDCl<sub>3</sub>): δ 154.3 (6-C), 148.2 (2'-C), 129.6 (4'-H or 6'-H), 127.5 (4'-H or 6'-H), 126.6 (4a-C), 124.8 (1'-C), 119.6 (5'-C), 117.8 (3'-H or 8-H), 117.6 (3'-H or 8-H), 115.8 (7-C), 111.3 (5-C), 76.0 (2-C), 66.3 (4-C), 55.9 (OCH<sub>3</sub>), 36.3 (3-C). **FT-IR**: 3384, 1738, 1610, 1489, 1458, 1365, 1267, 1217. **HR-MS**: calc. for [M+H]<sup>+</sup> C<sub>16</sub>H<sub>18</sub>O<sub>3</sub>N: 272.1281 found: 272.1279.

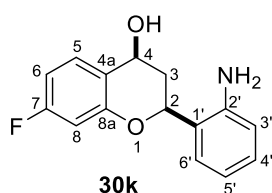
### 2-(2-aminophenyl)-3,4-dihydro-7-methyl-2H-1-benzopyran-4-ol (**30i**)



Prepared according to general procedure E. Flash column chromatography eluting with 10-50% [DCM:EtOH:NH<sub>4</sub>OH (50:8:1)] in DCM afforded the desired product **30i** (58.60mg, 0.23 mmol, 83%) as pale yellow solid (dr. 15:1). **<sup>1</sup>H-NMR** (600 MHz, CDCl<sub>3</sub>, OH and NH<sub>2</sub> not observed): δ 7.40 (1H, d, *J* 7.9, 1.0 Hz, 5-H), 7.22 (1H, dd, *J* 7.6, 1.5 Hz, 6'-H), 7.18 (1H, td, *J* 7.6, 1.6 Hz, 5'-H), 6.91-6.84 (2H, m, 3'-H and 4'-H), 6.80 (1H, d, *J* 7.9, 1.7 Hz, 6-H), 6.69 (1H, s, 8-H), 5.20 (1H, dd, *J* 12.0, 2.0 Hz, 2-H), 5.09 (1H, dd, *J* 10.5, 6.5 Hz, 4-H), 2.53-2.48 (1H, m, 3-H<sub>a</sub>), 2.44-2.39 (1H, m, 3-H<sub>b</sub>), 2.25 (3H, s, CH<sub>3</sub>). **<sup>13</sup>C NMR** (151 MHz, CDCl<sub>3</sub>): δ 154.1 (8a-C), 142.9 (2'-C), 139.4 (7-C), 129.6 (5'-C), 127.5 (6'-C), 127.1 (5-C), 125.6 (4a-C), 123.3 (1'-C), 120.3 (4'-C), 118.3 (3'-C), 117.1 (8-C), 75.8 (2-C), 65.9 (4-C), 36.6 (3-C), 21.2 (CH<sub>3</sub>). **FT-IR**: 3372, 2923, 1621, 1575, 1499, 1458, 1300, 1243. **HR-MS**: calc. for [M+H]<sup>+</sup> C<sub>15</sub>H<sub>11</sub>O<sub>4</sub>N: 256.1332, found: 256.1329.

**2-(2-aminophenyl)-3,4-dihydro-6-chloro-2H-1-benzopyran-4-ol (30j)**

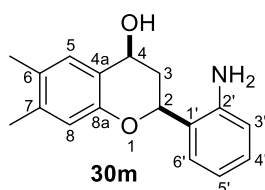
Prepared according to general procedure E. Flash column chromatography eluting with 10-50% [DCM:EtOH:NH<sub>4</sub>OH (50:8:1)] in DCM afforded the desired product **30j** (102.50 mg, 0.32 mmol, 49%) as pale yellow solid (dr. >10:1), NMR assignments belong to the major isomer. **<sup>1</sup>H-NMR** (400 MHz, CDCl<sub>3</sub>, OH and NH<sub>2</sub> not observed): δ 7.40 (1H, d, *J* 8.2 Hz), 7.23-7.16 (2H, m, 4'-H and 5'-H), 7.15-7.09 (1H, m, 6-H), 7.04 (1H, s, 8-H), 6.85 (1H, t, *J* 7.7 Hz, 5'-H), 6.80 (1H, d, *J* 7.9 Hz, 3'-H), 5.24 (1H, d, *J* 11.6 Hz, 2-H), 5.06 (1H, dd, *J* 10.4, 6.3 Hz, 4-H), 2.58-2.38 (2H, m, 3-H<sub>a</sub> and 3-H<sub>b</sub>). **<sup>13</sup>C NMR** (176 MHz, CDCl<sub>3</sub>): δ 154.8 (8a-C), 142.7 (2'-C, HMBC), 131.6 (7-C), 129.7 (4'-C), 129.4, 128.6 (5-C), 127.3 (6'-C), 125.1 (4a-C), 124.5 (6-C), 123.0 (1'-C), 119.7 (8-C), 118.1 (5'-C), 118.0 (3'-C), 76.0 (2-C), 65.6 (4-C), 36.0 (3-C).

**2-(2-aminophenyl)-3,4-dihydro-2H-1-benzopyran-4-ol (30k)**

Prepared according to general procedure E. Flash column chromatography eluting with 10-50% [DCM:EtOH:NH<sub>4</sub>OH (50:8:1)] in DCM afforded the desired product **30k** (171.70 mg, 0.66 mmol, 73%) as pale yellow solid (dr. 10:2), NMR assignments belong to the major isomer. **<sup>1</sup>H-NMR** (600 MHz, CDCl<sub>3</sub>, OH and NH<sub>2</sub> not observed): δ 7.53-7.48 (1H, m, 5-H), 7.22-7.15 (2H, m, 6'-H and 4'-H), 6.85-6.79 (1H, m, 5'-H), 6.78-6.70 (2H, m, 6-H and 3'-H), 6.57 (1H, dd, *J* 10.0, 2.5 Hz, 8-H), 5.24 (1H, dd, *J* 12.0, 1.9 Hz, 4-H), 5.09 (1H, dd, *J* 10.6, 6.4 Hz, 2-H), 2.60-2.53 (1H, m, 3-H<sub>a</sub>), 2.52-2.40 (1H, m, 3-H<sub>b</sub>). **<sup>13</sup>C NMR** (151 MHz, CDCl<sub>3</sub>): δ 163.2 (*J*<sub>CF</sub> 245.9 Hz, 7-C), 155.5 (*J*<sub>CF</sub> 12.0 Hz, 8a-C), 145.5 (2'-C), 129.9 (6'-C or 4'-H), 128.7 (*J*<sub>CF</sub> 9.9 Hz, 5-C), 127.4 (6'-C or 4'-H), 123.6 (1'-C), 122.2 (*J*<sub>CF</sub> 3.0 Hz, 4a-C), 119.0 (5'-C), 117.3 (3'-C), 108.8 (*J*<sub>CF</sub> 21.6 Hz, 6-C), 103.8 (*J*<sub>CF</sub> 24.5 Hz, 8-C), 76.4 (2-C), 65.9 (4-C), 36.0 (3-C). **<sup>19</sup>F NMR** (565 MHz, CDCl<sub>3</sub>) δ -110.90- -111.00 (m, minor isomer), -112.51- -112.61 (m, major isomer). **FT-IR**: 3376, 1737, 1597, 1496, 1458, 1434, 1301, 1259. **HR-MS**: calc. for [M+H]<sup>+</sup> C<sub>15</sub>H<sub>15</sub>O<sub>2</sub>NF: 260.1081, found: 260.1078.

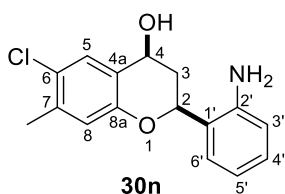
## Experimental

### 2-(2-aminophenyl)-3,4-dihydro-7-fluoro-2*H*-1-benzopyran-4-ol (**30m**)

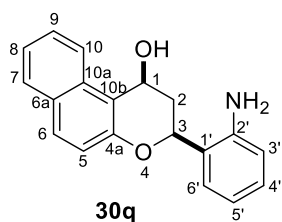


Prepared according to general procedure E. Flash column chromatography eluting with 10-50% [DCM:EtOH:NH<sub>4</sub>OH (50:8:1)] in DCM afforded the desired product **30m** (155.70 mg, 0.58 mmol, 30%) as pale yellow solid (dr. 15:1). **<sup>1</sup>H-NMR** (500 MHz, CDCl<sub>3</sub>, OH and NH<sub>2</sub> not observed): δ 7.29 (1H, s, 5-H), 7.20-7.14 (2H, m, 6'-H and 4'-H), 6.82-6.78 (1H, m, 5'-H), 6.76-6.73 (1H, m, 3'-H), 6.67 (1H, s, 8-H), 5.16 (1H, dd, *J* 11.8, 1.9 Hz, 2-H), 5.09 (1H, dd, *J* 10.5, 6.6 Hz, 4-H), 2.58-2.50 (1H, m, 3-H<sub>a</sub>), 2.49-2.41 (1H, m, 3-H<sub>b</sub>), 2.22 (3H, s, CH<sub>3</sub>), 2.20 (3H, s, CH<sub>3</sub>). **<sup>13</sup>C NMR** (151 MHz, CDCl<sub>3</sub>): δ 13C NMR (126 MHz, CDCl<sub>3</sub>) δ 152.2 (8a-C), 145.4 (2'-C), 138.0 (7-C), 129.9 (6-C), 129.5 (4'-C), 127.9 (5-C), 127.4 (6'-C), 124.1 (4a-C), 123.3 (1'-C), 118.8 (5'-C), 117.5 (8-C), 117.1 (3'-C), 75.9 (2-C), 66.1 (4-C), 36.3 (3-C), 19.8 (CH<sub>3</sub>), 19.1 (CH<sub>3</sub>). **FT-IR**: 3368, 1619, 1485, 1459, 1252, 1193, 1139. **HR-MS**: calc. for [M+H]<sup>+</sup> C<sub>17</sub>H<sub>20</sub>O<sub>2</sub>N: 270.1489 found: 270.1485.

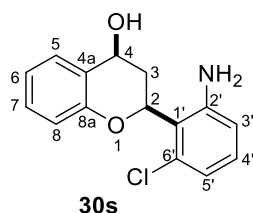
### 2-(2-aminophenyl)-3,4-dihydro-6-chloro-7-methyl-2*H*-1-benzopyran-4-ol (**30n**)



Prepared according to general procedure E. Flash column chromatography eluting with 10-50% [DCM:EtOH:NH<sub>4</sub>OH (50:8:1)] in DCM afforded the desired product **30n** (79.50 mg, 0.27 mmol, 74%) as pale yellow solid (dr. 10:3f), NMR assignments belong to the major isomer. **<sup>1</sup>H-NMR** (600 MHz, CDCl<sub>3</sub>, OH not observed): 7.51 (1H, s, 5-H), 7.19-7.15 (2H, m, 4'-H and 6'-H), 6.84-6.78 (1H, m, 5'-H), 6.76-6.72 (2H, m, 3'-H and 8-H), 5.18 (1H, dd, *J* 11.9, 1.9 Hz, 2-H), 5.07 (1H, s, 4-H), 4.04 (2H, s, NH<sub>2</sub>), 2.55-2.50 (1H, m, 3-H<sub>a</sub>), 2.49-2.43 (1H, m, 3-H<sub>b</sub>), 2.31 (3H, s, CH<sub>3</sub>). **<sup>13</sup>C NMR** (151 MHz, CDCl<sub>3</sub>): δ 152.6 (8a-C), 145.5 (2'-C), 137.2 (7-C), 129.7 (4-C), 127.4 (5-C), 127.3 (6'-C), 126.7 (6-C), 125.2 (4a-C), 123.6 (1'-C), 118.8 (5'-C), 118.8 (8-C), 117.1 (3'-C), 76.1 (2-C), 65.8 (4-C), 35.8 (3-C), 20.1 (CH<sub>3</sub>). **FT-IR**: 3377, 3181, 1609, 1567, 1482, 1449, 1394, 1376, 1304, 1289, 1252 **HR-MS**: calc. for [M+H]<sup>+</sup> C<sub>16</sub>H<sub>17</sub>O<sub>2</sub>NCl: 290.0942 found 290.0941; calc. for [M+H]<sup>+</sup> C<sub>16</sub>H<sub>17</sub>O<sub>2</sub>N<sup>37</sup>Cl: 292.0913 found 290.0911.

**3-(2-aminophenyl)-1H,2H,3H-naphtho[2,1-b]pyran-1-ol (30q)**

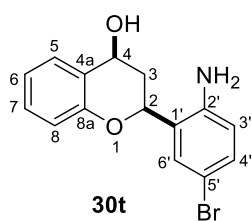
Prepared according to general procedure E. Flash column chromatography eluting with 10-50% [DCM:EtOH:NH<sub>4</sub>OH (50:8:1)] in DCM afforded the desired product **30q** (34.50 mg, 0.12 mmol, 26%) as pale yellow solid (dr. 10:2), NMR assignments belong to the major isomer. **<sup>1</sup>H-NMR** (700 MHz, CDCl<sub>3</sub>, OH and NH<sub>2</sub> not observed): δ 8.09 (1H, d, *J* 8.4 Hz, 10-H), 7.79 (1H, d, *J* 8.1 Hz, 7-H), 7.73 (1H, d, *J* 8.9 Hz, 6-H), 7.57-7.53 (1H, m, 9-H), 7.39 (1H, t, *J* 8.1 Hz, 8-H), 7.32-7.29 (1H, m, 6'-H), 7.18 (1H, td, *J* 7.7, 1.3 Hz, 4'-H), 7.12 (1H, d, *J* 8.9 Hz, 5-H), 6.85 (1H, t, *J* 7.1 Hz, 5'-H), 6.73 (1H, d, *J* 7.7 Hz, 3'-H), 5.43-5.37 (2H, m, 1-H and 3-H), 3.57 (NH<sub>2</sub>), 2.48-2.42 (1H, m, 2-H<sub>a</sub>), 2.41-2.36 (1H, m, 2-H<sub>b</sub>). **<sup>13</sup>C NMR** (176 MHz, CDCl<sub>3</sub>): δ 152.8 (10b-C), 145.0 (2'-C), 132.9 (10a-C), 130.7 (7-C), 129.5 (4a-C), 129.4 (4'-C), 128.8 (7-C), 127.5 (6'-C or 9-C), 127.4 (6'-C or 9-C), 124.3 (1'-C), 123.9 (8-C), 122.2 (10-C), 119.1 (5-C), 118.9 (5'-C), 117.0 (3'-C), 115.1 (6a-C), 71.6 (3-C), 60.9 (1-C), 34.5 (2-C). **FT-IR:** 3390 3211, 2067, 1821, 1622, 1599, 1500, 1459, 1436, 1402, 1335, 1267, 1234. **HR-MS:** calc. for [M+H]<sup>+</sup> C<sub>19</sub>H<sub>18</sub>O<sub>2</sub>N: 292.1332, found: 292.1331.

**2-(2-amino-6-chloro-phenyl)-3,4-dihydro-2H-1-benzopyran-4-ol (30s)**

Prepared according general procedure E. Flash column chromatography eluting with 10-50% [DCM:EtOH:NH<sub>4</sub>OH (50:8:1)] in DCM afforded the desired product **30s** (86.40 mg, 0.31 mmol, 41%) as pale yellow solid (dr. 10:2), NMR assignments belong to the major isomer. **<sup>1</sup>H-NMR** (700 MHz, CDCl<sub>3</sub>, OH and NH<sub>2</sub> not observed): δ 7.57 (1H, d, *J* 7.7 Hz, 5-H), 7.18 (1H, app. s, 7-H), 7.07-6.98 (2H, m, 6-H and 4'-H), 6.89 (1H, dd, *J* 8.2, 1.0 Hz, 8-H), 6.81 (1H, d, *J* 7.5 Hz, 5'-H), 6.65-6.57 (1H, m, 3'-H), 5.89 (1H, d, *J* 11.6 Hz, 2-H), 5.14 (1H, dd, *J* 10.5, 6.7 Hz, 4-H), 2.64-2.56 (1H, m, 3-H<sub>a</sub>), 2.36 (1H, ddd, *J* 13.3, 6.7, 2.0 Hz, 3-H<sub>b</sub>). **<sup>13</sup>C NMR** (176 MHz, CDCl<sub>3</sub>, 2'-C not observed): δ 153.8 (8a-C), 133.4 (6'-C), 129.6 (4'-C), 129.3 (7-C), 127.5 (5-C), 126.4 (4a-C), 121.9 (6-C), 120.9 (1'-C), 119.9 (5'-C), 116.8 (8-C), 116.4 (3'-C), 75.6 (2-C), 65.7 (4-C), 34.1 (3-C). **FT-IR:** 3381, 3174, 2349, 1871, 1600, 1573, 1482, 1446, 1321, 1289, 1272, 1256, 1233. **HR-MS:** calc. for [M+H]<sup>+</sup> C<sub>15</sub>H<sub>15</sub>O<sub>2</sub>NCl: 276.0786, found: 276.0784, calc. for [M+H]<sup>+</sup> C<sub>15</sub>H<sub>15</sub>O<sub>2</sub>N<sup>37</sup>Cl: 278.0756, found: 278.0753.

## Experimental

### 2-(2-amino-5-bromo-phenyl)-3,4-dihydro-2H-1-benzopyran-4-ol (**30t**)

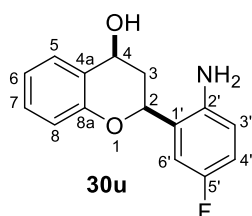


Prepared according to general procedure E. Flash column

chromatography eluting with 10-50% [DCM:EtOH:NH<sub>4</sub>OH (50:8:1)] in DCM afforded the desired product **30t** (237.40 mg, 0.74 mmol, 58%) as pale yellow solid (dr. 10:2), NMR assignments belong to the major isomer. <sup>1</sup>H-NMR (600 MHz, CDCl<sub>3</sub>, OH and NH<sub>2</sub> not observed): δ

7.55 (1H, d, *J* 7.6 Hz, 5-H), 7.32 (1H, d, *J* 2.3 Hz, 6'-H), 7.27-7.23 (1H, m, 4'-H), 7.23-7.19 (1H, m, 7-H), 7.02 (1H, td, *J* 7.6, 1.1 Hz, 6-H), 6.86 (1H, dd, *J* 8.2, 0.9 Hz, 8-H), 6.62 (1H, dd, *J* 8.5, 3.1 Hz, 3'-H), 5.17-5.10 (2H, m, 2-H and 4-H), 2.52 (1H, ddd, *J* 12.9, 6.4, 1.8 Hz, 3-H<sub>a</sub>), 2.45-2.39 (1H, m, 3-H<sub>b</sub>). <sup>13</sup>C NMR (151 MHz, CDCl<sub>3</sub>): δ 154.0 (8a-C), 144.5 (2'-C), 132.2 (4'-C), 130.1 (6'-C), 129.4 (7-C), 127.2 (5-C), 126.1 (4a-C), 125.8 (1'-C), 121.7 (6-C), 118.6 (3'-C), 116.7 (8-C), 110.4 (5'-C), 75.3 (2-C), 66.0 (4-C), 35.9 (3-C). **FT-IR:** 3319, 1883, 1633, 1580, 1480, 1453, 1414, 1393, 1291, 1272, 1220. **HR-MS:** calc. for [M+H]<sup>+</sup> C<sub>15</sub>H<sub>15</sub>O<sub>2</sub>NBr: 320.0281 found 320.0284, calc. for [M+H]<sup>+</sup> C<sub>15</sub>H<sub>15</sub>O<sub>2</sub>N<sup>81</sup>Br: 322.060 found 322.0261.

### 2-(2-amino-5-fluoro-phenyl)-3,4-dihydro-2H-1-benzopyran-4-ol (**30u**)

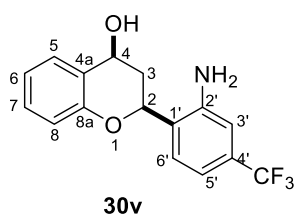


Prepared according to general procedure E. Flash column chromatography eluting with 10-50% [DCM:EtOH:NH<sub>4</sub>OH (50:8:1)] in DCM afforded the desired product **30u** (234.90 mg, 0.91 mmol, 56%) as pale yellow solid (dr. 10:2), NMR assignments belong to the major isomer. <sup>1</sup>H-NMR (600 MHz, CDCl<sub>3</sub>, OH and NH<sub>2</sub> not observed): δ 7.54

(1H, d, *J* 7.6 Hz, 5-H), 7.17 (1H, t, *J* 8.2 Hz, 7-H), 7.02-6.93 (2H, m, 6-H and 6'-H), 6.90 (1H, td, *J* 8.4, 2.8 Hz, 4'-H), 6.86 (1H, d, *J* 8.2 Hz, 2-H, 8-H), 6.75 (1H, dd, *J* 8.7, 4.8 Hz, 3'-H), 5.18 (1H, d, *J* 10.8 Hz, 2-H), 5.12 (1H, dd, 10.5, 6.5 Hz, 4-H), 2.56-2.50 (1H, m, 3-H<sub>a</sub>), 2.41-2.34 (1H, m, 3-H<sub>b</sub>). <sup>13</sup>C NMR (151 MHz, CDCl<sub>3</sub>): δ 156.9 (d, *J*<sub>CF</sub> 237.7 Hz, 5'-C), 154.0 (8a-C), 139.8 (2'-C), 129.3 (7-C), 127.3 (5-C), 126.4 (d, *J*<sub>CF</sub> 5.1 Hz, 1'-C), 126.1 (4a-C), 121.7 (6-C), 118.8 (d, *J*<sub>CF</sub> 7.4 Hz, 3'-C), 116.7 (8-C), 116.0 (d, *J*<sub>CF</sub> 22.3 Hz, 4-C), 114.0 (d, *J*<sub>CF</sub> 23.5 Hz, 6'-C), 74.9 (2-C), 65.9 (4-C), 36.2 (3-C). **FT-IR:** 3191, 1824, 1610, 1582, 1502, 1484, 1457, 1437, 1248. **HR-MS:** calc. for [M+H]<sup>+</sup> C<sub>15</sub>H<sub>15</sub>O<sub>2</sub>NF: 260.1081, found: 260.1079.

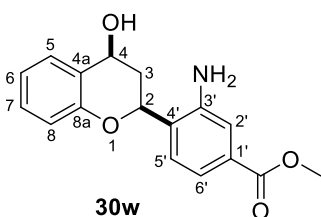


### 2-(2-amino-5-bromo-phenyl)-3,4-dihydro-2H-1-benzopyran-4-ol (**30v**)



Prepared according to general procedure E. Flash column chromatography eluting with 10-50% [DCM:EtOH:NH<sub>4</sub>OH (50:8:1)] in DCM afforded the desired product **30v** (154.70 mg, 0.50 mmol, 51%) as pale yellow solid (dr. 10:2), NMR assignments belong to the major isomer. <sup>1</sup>H-NMR (600 MHz, CDCl<sub>3</sub>, OH and NH<sub>2</sub> not observed): δ 7.56 (1H, d, *J* 7.6 Hz, 5-H), 7.30 (1H, d, *J* 8.0 Hz, 6'-H), 7.21 (1H, t, *J* 7.2 Hz, 7-H), 7.06-7.01 (2H, m, 5'-H and 6-H), 6.98 (1H, s, 3'-H), 6.87 (1H, d, *J* 8.1 Hz, 8-H), 5.23 (1H, dd, *J* 11.9, 1.8 Hz, 2-H), 5.15 (1H, dd, *J* 10.5, 6.6 Hz, 4-H), 2.58-2.51 (1H, m, 3-H<sub>a</sub>), 2.50-2.43 (1H, m, 3-H<sub>b</sub>). <sup>13</sup>C NMR (151 MHz, CDCl<sub>3</sub>): δ 153.9 (8a-C), 145.4 (2'-C), 131.7 (q, *J* 32.3 Hz, 4'-C), 129.4 (7-C), 127.9 (6'-C), 127.3 (5-C), 127.2 (1'-C), 126.1 (4a-C), 124.1 (q, *J*<sub>CF</sub> 272.2, CF<sub>3</sub>), 121.8 (6-C), 116.7 (8-C), 115.4 (5'-C), 113.7 (3'-C), 75.6 (2-C), 65.9 (4-C), 35.9 (3-C). <sup>19</sup>F NMR (565 MHz, CDCl<sub>3</sub>) δ -63.0. FT-IR: 3247, 1637, 1586, 1485, 1457, 1435, 1339, 1264, 1222. HR-MS: calc. for [M+H]<sup>+</sup> C<sub>15</sub>H<sub>15</sub>O<sub>2</sub>NF: 310.1049 found 310.1051.

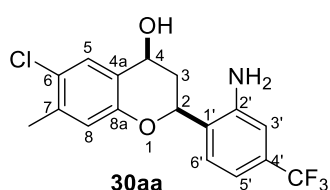
### Methyl-3-amino-4-(4-hydroxy-3,4-dihydro-2H-1-benzopyran-2-yl)benzoate (**30w**)



Prepared according to general procedure E. Flash column chromatography eluting with 10-50% [DCM:EtOH:NH<sub>4</sub>OH (50:8:1)] in DCM afforded the desired product **30w** (99.80 mg, 0.33 mmol, 30%) as pale yellow solid (dr. >10:1), NMR assignments belong to the major isomer. <sup>1</sup>H-NMR (600 MHz, CDCl<sub>3</sub>, OH and NH<sub>2</sub> not observed): δ 7.55 (1H, dt, *J* 7.6, 1.3 Hz, 5-H), 7.47 (1H, dd, *J* 8.0, 1.7 Hz, 6'-H), 7.43 (1H, d, *J* 1.7 Hz, 2'-H), 7.26 (1H, d, *J* 8.0 Hz, 5'-H), 7.19 (1H, td, *J* 7.9, 1.7 Hz, 7-H), 7.01 (1H, td, *J* 7.6, 1.2 Hz, 6-H), 6.87 (1H, d, *J* 8.2 Hz, 8-H), 5.24 (1H, dd, *J* 11.9, 2.0 Hz, 2-H), 5.14 (1H, dd, *J* 10.6, 6.5 Hz, 4-H), 3.90 (3H, s, CH<sub>3</sub>), 2.53 (1H, ddd, *J* 13.0, 6.5, 2.1 Hz, 3-H<sub>a</sub>), 2.46 (1H, ddd, *J* 13.0, 11.9, 10.6 Hz, 3-H<sub>b</sub>). <sup>13</sup>C NMR (151 MHz, CDCl<sub>3</sub>): δ 167.0 (COOCH<sub>3</sub>), 153.9 (8a-C), 144.9 (3'-C), 131.2 (1'-C), 129.4 (7-C), 128.7 (4'-C), 127.5 (5-C), 127.3 (5'-C), 126.1 (4a-C), 121.7 (6-C), 120.2 (6'-C), 118.2 (3'-C), 116.7 (8-C), 75.7 (2-C), 65.9 (4-C), 52.3 (CH<sub>3</sub>), 36.0 (3-C). FT-IR: 3448, 3360, 2951, 2157, 2028, 1703, 1626, 1582, 1487, 1461, 1437, 1298, 1244. HR-MS: calc. for [M+H]<sup>+</sup> C<sub>17</sub>H<sub>18</sub>O<sub>4</sub>N: 300.1230, found: 300.1232.

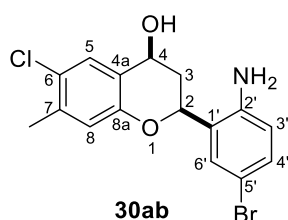
## Experimental

### 2-(2-amino-4-trifluoromethyl-phenyl)-6-chloro-7-methyl-3,4-dihydro-2H-1-benzopyran-4-ol (30aa)



Prepared according to general procedure E. Flash column chromatography eluting with 10-50% [DCM:EtOH:NH<sub>4</sub>OH (50:8:1)] in DCM afforded the desired product **30aa** (27.10 mg, 0,08 mmol, 28%) as pale yellow solid (dr. 10:5), NMR assignments belong to the major isomer. **<sup>1</sup>H-NMR** (500 MHz, CDCl<sub>3</sub>, OH not observed): δ 7.50 (1H, s, 5-H), 7.28-7.25 (1H, m, 6'-H), 7.03 (1H, d, *J* 8.1 Hz, 5'-H), 6.95 (1H, s, 3'-H), 6.74 (8-H), 5.18 (1H, dd, *J* 11.9, 2.1 Hz, 2-H), 5.07 (1H, dd, *J* 10.7, 6.5 Hz, 4-H), 4.22 (NH<sub>2</sub>), 2.49 (1H, ddd, *J* 13.1, 6.5, 2.1 Hz, 3-H<sub>a</sub>), 2.41 (1H, ddd, *J* 13.1, 11.9, 10.7 Hz, 3-H<sub>b</sub>), 2.31 (3H, s, CH<sub>3</sub>). **<sup>13</sup>C NMR** (126 MHz, CDCl<sub>3</sub>, CF<sub>3</sub> not observed): δ 152.2 (8a-C), 145.7 (2'-C), 137.3 (7-C), 131.7 (q, *J*<sub>CF</sub> 32.2 Hz, 4'-C), 127.9 (6'-C), 127.5 (4a-C), 127.4 (5-C), 126.6 (1'-C), 124.9 (6-C), 118.8 (8-C), 115.2 (q, *J*<sub>CF</sub> 3.8 Hz, 5'-C), 113.5 (q, *J*<sub>CF</sub> 3.8 Hz, 3'-C), 75.7 (2-C), 65.5 (4-C), 35.6 (3-C), 20.1 (CH<sub>3</sub>). **<sup>19</sup>F NMR** (565 MHz, CDCl<sub>3</sub>) δ -63.0. **FT-IR**: 3375, 2930, 2290, 2050, 1623, 1568, 1517, 1484, 1439, 1399, 1333, 1253. **HR-MS**: calc. for [M-OH]<sup>+</sup> C<sub>17</sub>H<sub>14</sub>O<sub>1</sub>N: 340.0711 found 340.0711.

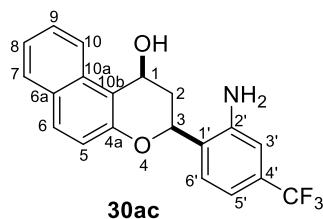
### 2-(2-amino-5-bromo-phenyl)-3,4-dihydro-2H-1-benzopyran-4-ol (30ab)



Prepared according to general procedure E. Flash column chromatography eluting with 10-50% [DCM:EtOH:NH<sub>4</sub>OH (50:8:1)] in DCM afforded the desired product **30ab** (145.70 mg, 0.40 mmol, 63%) as pale yellow solid (dr.>20:1), NMR assignments belong to the major isomer. **<sup>1</sup>H-NMR** (700 MHz, CDCl<sub>3</sub>, OH and NH<sub>2</sub> not observed): δ 7.50 (1H, s, 5-H), 7.31 (1H, d, *J* 2.4 Hz, 6'-H), 7.26 (1H, dd, *J* 2.4, 8.4 Hz, 4'-H), 6.74 (1H, s, 8-H), 6.64 (1H, d, *J* 8.4 Hz, 3'-H), 5.11 (1H, dd, *J* 12.0, 1.9 Hz, 2-H), 5.05 (1H, dd, *J* 10.7, 6.5 Hz, 4-H), 2.49 (1H, ddd, *J* 13.1, 6.5, 1.9 Hz, 3-H<sub>b</sub>), 2.39-2.31 (1H, m, 3-H<sub>b</sub>), 2.29 (3H, s, CH<sub>3</sub>). **<sup>13</sup>C NMR** (176 MHz, CDCl<sub>3</sub>): δ 152.3 (8a-C), 144.4 (2'-C), 137.3 (6-C or 7-C), 132.3 (4'-C), 130.1 (6'-C), 127.4 (5-C), 127.0 (6-C or 7-C), 125.6 (1'-C), 125.0 (4a-C), 118.8 (3'-C or 8-C), 118.7 (3'-C or 8-C), 110.5 (5'-C), 75.4 (2-C), 65.6 (4-C), 35.8 (3-C), 20.1 (CH<sub>3</sub>). **FT-IR**: 3378, 3215, 1621, 1564, 1480, 1448, 1415, 1391, 1376, 1337 1318, 1306, 1282, 1248 1239, 1203. **HR-MS**: calc. for [M-OH]<sup>+</sup> C<sub>16</sub>H<sub>14</sub>ONBrCl: 351.9922 found: 351.9919.

### 3-[2-amino-4-(trifluoromethyl)phenyl]-1*H*-2*H*-3*H*-naphtho[2,1-*b*]pyran-1-ol (30ac)

Prepared according to general procedure E. Flash column chromatography eluting with 10-

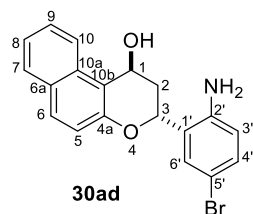


50% [DCM:EtOH:NH<sub>4</sub>OH (50:8:1)] in DCM afforded the desired product **30ac** (17.00 mg, 47.31 μmol, 21%) as pale yellow solid (dr.

10:5pp), NMR assignments belong to the major isomer. **<sup>1</sup>H-NMR** (500 MHz, CDCl<sub>3</sub>, OH not observed): δ 8.13 (1H, d, *J* 8.4 Hz, 10-H), 7.81 (1H, d, *J* 8.1 Hz, 7-H), 7.77 (1H, d, *J* 8.9 Hz, 6-H), 7.61-7.55 (1H, m, 9-H), 7.45-7.38 (2H, m, 6'-H and 8-H), 7.14 (1H, d, *J* 8.9 Hz, 5-H), 7.07 (1H, d, *J* 7.9 Hz, 5'-H), 6.97 (1H, s, 3'-H), 5.50 (1H, app. s, 3-H), 5.45 (1H, dd, *J* 11.6, 2.7 Hz, 2-H), 4.25 (2H, s, NH<sub>2</sub>), 2.54-2.37 (2H, m, 2-H<sub>a</sub> and 2-H<sub>b</sub>). **<sup>13</sup>C NMR** (126 MHz, CDCl<sub>3</sub>, CF<sub>3</sub> and 4'-C not observed): δ 152.5 (10a-C), 145.4 (2'-C), 132.7 (4a-C), 130.9 (6-C), 129.6 (6a-C), 128.9 (7-C), 127.9 (6'-C), 127.7 (9-C), 127.3 (1'-C), 124.2 (8-C), 122.0 (10-C), 118.9 (5-C), 115.2 (q, *J*<sub>CF</sub> 3.5 Hz, 5'-C), 115.1 (10b-C), 113.2 (q, *J*<sub>CF</sub> 3.5 Hz, 3'-C), 71.5 (3-H), 60.7 (1-H), 34.3 (2-H). **<sup>19</sup>F NMR** (565 MHz, CDCl<sub>3</sub>) δ -63.0. **FT-IR**: 3383, 2927, 2349, 2263, 1624, 1598, 1515, 1465, 1437, 1402, 1332, 1267, 1233, 1216. **HR-MS**: calc. for [M-OH]<sup>+</sup> C<sub>20</sub>H<sub>15</sub>ONF<sub>3</sub>: 342.1101 found 342.1103.

### 3-[2-amino-5-bromophenyl]-1*H*-2*H*-3*H*-naphtho[2,1-*b*]pyran-1-ol (30ad)

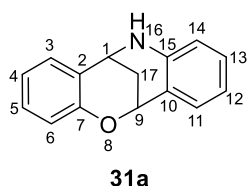
Prepared according to general procedure E. Flash column chromatography eluting with 10-



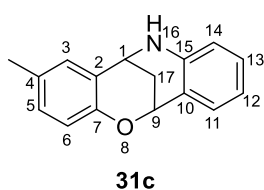
50% [DCM:EtOH:NH<sub>4</sub>OH (50:8:1)] in DCM afforded the desired product **30ad** (59.20 mg, 0.16 mmol, 24%) as pale yellow solid (dr. 2:1),

NMR assignments belong to the major isomer. Major differences in the spectra indicate the formation of the trans isomer as major isomer in this reaction. **<sup>1</sup>H-NMR** (700 MHz, CDCl<sub>3</sub>, NH<sub>2</sub> and OH not observed): δ 8.07 (1H, d, *J* 8.5 Hz, 10-H), 7.80-7.75 (1H, m, 7-H), 7.71 (1H, dd, *J* 11.4, 8.9 Hz, 6-H), 7.57-7.53 (1H, m, 9-H), 7.43 (1H, d, *J* 2.3 Hz, 6'-H), 7.41-7.37 (1H, m, 8-H), 7.23 (1H, d, *J* 8.5 Hz, 4'-H), 7.11 (1H, d, *J* 8.9 Hz, 5-H), 6.61-6.59 (1H, m, 3'-H), 5.39 (1H, t, *J* 2.8 Hz, 3-H), 5.35-5.29 (1H, m, 1-H), 2.42-2.26 (2H, m, 2-H<sub>a</sub> and 2-H<sub>b</sub>). **<sup>13</sup>C NMR** (176 MHz, CDCl<sub>3</sub>): δ 152.6 (10a-C), 144.06 (2'-C), 132.7 (4a-C), 131.9 (4'-C), 130.8 (6-C), 129.5 (6'-C), 128.8 (7-C), 127.6 (Ar-C<sub>q</sub>), 127.0 (9-C), 125.8 (Ar-C<sub>q</sub>), 124.1 (8-C), 122.1 (10-C), 119.0 (5-C), 118.6 (3'-C), 117.1 (Ar-C<sub>q</sub>), 110.7 (Ar-C<sub>q</sub>), 70.6 (3-C), 60.8 (1-C), 34.6 (2-C). **FT-IR**: 3379, 3056, 2922, 1623, 1598, 1513, 1489, 1465, 1437, 1400, 1263, 1230. **HR-MS**: calc. for [M-OH]<sup>+</sup> C<sub>19</sub>H<sub>15</sub>ONBr: 354.0312 found 354.0313.

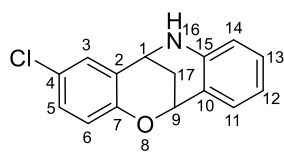
## Preparation of Chromalines

**8-oxa-16-azatetracyclo[7.7.1.0<sup>2,7</sup>.0<sup>10,15</sup>]heptadeca-2,4,6,10,12,14-hexaene (31a)**

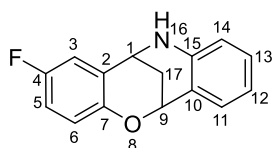
Prepared according to general procedure F. Flash column chromatography eluting with 2.5-10% EtOAc in *n*-pentane afforded the desired product **31a** (24.1 mg, 0.11 mmol, 52%) as white solid. <sup>1</sup>H-NMR (500 MHz, CDCl<sub>3</sub>, NH not observed): δ 7.32 (d, *J* = 7.6 Hz, 1H, 11-H), 7.18 (d, *J* = 7.5 Hz, 1H, 3-H), 7.14 – 7.07 (m, 2H, 5-H and 13-H), 6.85 (d, *J* = 7.5 Hz, 1H, 4-H), 6.81 (d, *J* = 8.1 Hz, 1H, 6-H), 6.75 (d, *J* = 7.6 Hz, 1H, 12-H), 6.59 (d, *J* = 7.9 Hz, 1H, 14-H), 5.34 (br s, 1H, 9-H), 4.42 (br s, 1H, 1-H), 2.37 (dt, *J* = 13.3, 3.3 Hz, 1H, 17-H<sub>a</sub>), 2.24 (dt, *J* = 13.3, 2.7 Hz, 1H, 17-H<sub>b</sub>). <sup>13</sup>C NMR (126 MHz, CDCl<sub>3</sub>): δ 153.02 (7-C), 143.01 (15-C), 131.24 (11-C), 129.92 (13-C), 129.25 (3-C or 5-C), 129.16 (3-C or 5-C), 125.17 (2-C), 122.08 (10-C), 120.43 (4-C), 118.73 (12-C), 117.35 (6-C), 116.11 (14-C), 69.46 (9-C), 46.03 (1-C), 26.55 (17-C). **FT-IR:** 3379, 2964, 2934, 1784, 1607, 1581, 1495, 1483, 1456, 1427, 1347, 1321, 1301, 1275, 1210. **HR-MS:** calc. for [M+H]<sup>+</sup> C<sub>15</sub>H<sub>14</sub>ON: 224.1069 found 224.1068.

**4-methyl-8-oxa-16-azatetracyclo[7.7.1.0<sup>2,7</sup>.0<sup>10,15</sup>]heptadeca-2,4,6,10,12,14-hexaene (31c)**

Prepared according to general procedure F. Flash column chromatography eluting with 2.5-10% EtOAc in *n*-pentane afforded the desired product **31c** (13.7 mg, 57.73 μmol, 49%) as white solid. <sup>1</sup>H-NMR (600 MHz, CDCl<sub>3</sub>, NH not observed): δ 7.31 (1H, dd, *J* 7.6, 1.6 Hz, 11-H), 7.10-7.06 (1H, m, 13-H), 6.96 (1H, d, *J* 2.2 Hz, 3-H), 6.94-6.90 (1H, m, 5-H), 6.76-6.70 (2H, m, 6-H and 12-H), 6.56 (1H, dd, *J* 8.1, 1.1 Hz, 14-H), 5.33-5.28 (1H, m, 9-H), 4.36-4.34 (1H, m, 1-H), 2.35 (1H, dt, *J* 13.1, 3.2 Hz, 17-H<sub>a</sub>), 2.25 (3H, s, CH<sub>3</sub>), 2.21 (1H, dt, *J* 13.1, 2.7 Hz, 17-H<sub>b</sub>). <sup>13</sup>C NMR (151 MHz, CDCl<sub>3</sub>): δ 150.7 (7-C), 143.4 (15-C), 131.2 (11-C), 129.9 (4-C), 129.8 (5-C), 129.6 (13-C), 129.4 (3-C), 125.1 (2-C), 122.0 (10-C), 118.4 (12-C), 117.0 (6-C), 115.9 (14-C), 69.4 (9-C), 46.1 (1-C), 26.7 (17-C), 20.6 (CH<sub>3</sub>). **FT-IR:** 3369, 2919, 2110, 1877, 1609, 1584, 1494, 1428, 1347, 1315, 1275, 1241, 1202. **HR-MS:** calc. for [M+H]<sup>+</sup> C<sub>16</sub>H<sub>16</sub>ON: 238.1226, found: 238.1225.

**4-chloro-8-oxa-16-azatetracyclo[7.7.1.0<sup>2,7</sup>.0<sup>10,15</sup>]heptadeca-2,4,6,10,12,14-hexaene (31d)****31d**

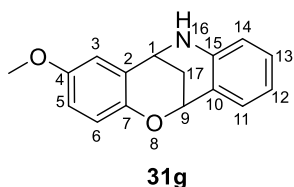
Prepared according to general procedure F. Flash column chromatography eluting with 2.5-10% EtOAc in *n*-pentane afforded the desired product **31d** (24.1 mg, 0.11 mmol, 52%) as white solid. **<sup>1</sup>H-NMR** (500 MHz, CDCl<sub>3</sub>, NH not observed): δ **<sup>1</sup>H NMR** (Chloroform-*d*, 600 MHz) δ 7.35 (1H, dd, *J* 7.5, 1.2 Hz, 11-H), 7.28 (1H, s, 3-H), 7.18-7.14 (1H, m, 13-H), 7.07 (1H, dt, *J* 8.7, 2.5 Hz, 5-H), 6.89 (1H, t, *J* 7.5 Hz, 12-H), 6.81 (1H, d, *J* 5.7 Hz, 14-H), 6.74 (1H, d, *J* 8.7 Hz, 6-H), 5.36-5.34 (1H, m, 9-H), 4.51 (1H, br s, 1-H), 2.38-2.34 (2H, m, 17-H<sub>a</sub> and 17-H<sub>b</sub>). **<sup>13</sup>C NMR** (151 MHz, CDCl<sub>3</sub>): δ 151.8 (7-C), 136.3 (15-C), 131.4 (11-C), 131.0 (Ar-C<sub>q</sub>), 130.3 (13-C), 129.7 (5-C), 129.4 (3-C), 129.2 (Ar-C<sub>q</sub>), 125.3 (Ar-C<sub>q</sub>), 119.1 (12-C), 118.9 (6-C), 117.5 (14-C), 69.2 (9-C), 46.1 (1-C), 26.1 (17-C). **FT-IR**: 3400, 2559, 1735, 1735, 1720, 1607, 1581, 1492, 1472, 1431, 1411, 1368, 1348, 1311, 1262. **HR-MS**: calc. for [M+H]<sup>+</sup> C<sub>15</sub>H<sub>13</sub>ONCl: 258.0680, found: 258.0680, calc. for [M+H]<sup>+</sup> C<sub>15</sub>H<sub>13</sub>ON<sup>37</sup>Cl: 260.0651, found: 260.0650.

**4-fluoro-8-oxa-16-azatetracyclo[7.7.1.0<sup>2,7</sup>.0<sup>10,15</sup>]heptadeca-2,4,6,10,12,14-hexaene (31e)****31e**

Prepared according to general procedure 70. Flash column chromatography eluting with 2.5-10% EtOAc in *n*-pentane afforded the desired product **31e** (3.9 mg, 16.27 μmol, 14%) as white solid. **<sup>1</sup>H-NMR** (700 MHz, CDCl<sub>3</sub>, NH not observed): δ 7.32 (1H, dd, *J* 7.6, 1.5 Hz, 11-H), 7.12 (1H, td, *J* 8.1, 1.6 Hz, 13-H), 6.90 (1H, dd, *J* 8.4, 3.0 Hz, 3-H), 6.84-6.79 (2H, m, 5-H and 12-H), 6.74 (1H, dd, *J* 8.9, 4.6 Hz, 6-H), 6.64 (1H, d, *J* 8.1 Hz, 14-H), 5.33-5.29 (1H, m, 9-H), 4.42-4.40 (1H, m, 1-H), 2.35 (1H, dt, *J* 13.3, 3.2 Hz, 17-H<sub>a</sub>), 2.26 (1H, dt, *J* 13.3, 2.6 Hz, 17-H<sub>b</sub>). **<sup>13</sup>C NMR** (176 MHz, CDCl<sub>3</sub>): δ 157.5 (d, *J*<sub>CF</sub> 239.0 Hz, 5-C), 149.0 (d, *J*<sub>CF</sub> 2.1 Hz, 7-C), 142.0 (15-C), 131.3 (11-C), 130.1 (13-C), 125.4 (2-C), 122.3 (10-C), 119.7 (12-C), 118.4 (d, *J*<sub>CF</sub> 7.8 Hz, 6-C), 116.5 (14-C), 116.3 (d, *J*<sub>CF</sub> 23.1 Hz, 3-C), 115.0 (d, *J*<sub>CF</sub> 22.6 Hz, 3-C), 69.3 (9-C), 46.1 (1-C), 26.3 (17-C). **<sup>19</sup>F NMR** (470 MHz, CDCl<sub>3</sub>) δ -75.7. **FT-IR**: 3384, 2967, 1740, 1666, 1610, 1582, 1491, 1424, 1348, 1312, 1262. **HR-MS**: calc. for [M+H]<sup>+</sup> C<sub>15</sub>H<sub>13</sub>ONF: 242.0976 found 242.0974.

## Experimental

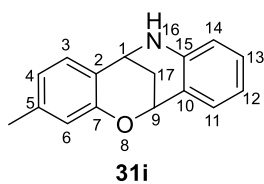
### 4-methoxy-8-oxa-16-azatetracyclo[7.7.1.0<sup>2,7</sup>.0<sup>10,15</sup>]heptadeca-2,4,6,10,12,14-hexaene (31g)



Prepared according to general procedure F. Flash column chromatography eluting with 2.5-10% EtOAc in *n*-pentane afforded the desired product **xx** (10.5 mg, 38.61  $\mu$ mol, 50%) as white solid.

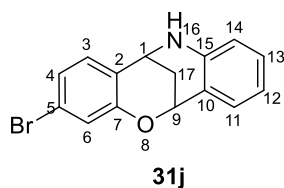
**<sup>1</sup>H-NMR** (500 MHz, CDCl<sub>3</sub>, NH not observed):  $\delta$  7.31 (1H, dd, *J* 7.6, 1.5 Hz, 11-H), 7.11-7.06 (1H, m, 13-H), 6.76-6.72 (2H, m, 5-H and 12-H), 6.71-6.68 (2H, m, 3-H and 6-H), 6.57 (1H, d, *J* 7.9 Hz, 14-H), 5.28 (1H, br. s, 9-H), 4.34 (1H, br. s, 1-H), 3.74 (3H, s, OCH<sub>3</sub>), 2.35 (1H, dt, *J* 13.2, 3.3 Hz, 17-H<sub>a</sub>), 2.21 (1H, dt, *J* 13.2, 2.7 Hz, 17-H<sub>b</sub>). **<sup>13</sup>C NMR** (126 MHz, CDCl<sub>3</sub>):  $\delta$  153.4 (4-C), 146.8 (7-C), 143.3 (15-C), 131.2 (11-C), 129.8 (13-C), 125.7 (2-C), 122.0 (10-C), 118.6 (5-C or 12-C), 117.9 (5-C or 12-C), 115.9 (14-C), 115.2 (6-C), 113.6 (3-C), 69.3 (9-C), 55.9 (OCH<sub>3</sub>), 46.3 (1-C), 26.7 (17-C). **FT-IR**: 3382, 2941, 2082, 1812, 1606, 1579, 1489, 1464, 1454, 1442, 1423, 1344, 1333, 1314, 1266, 1247, 1224.20. **HR-MS**: calc. for [M+H]<sup>+</sup> C<sub>16</sub>H<sub>16</sub>O<sub>2</sub>N: 254.1176 found 254.1167.

### 5-methyl-8-oxa-16-azatetracyclo[7.7.1.0<sup>2,7</sup>.0<sup>10,15</sup>]heptadeca-2,4,6,10,12,14-hexaene (31i)

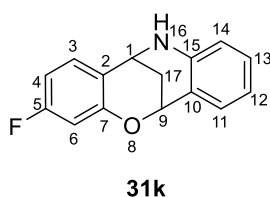


Prepared according general procedure XX. Flash column chromatography eluting with 2.5-10% EtOAc in *n*-pentane afforded the desired product **31i** (8.5 mg, 25.82  $\mu$ mol, 46%) as white solid. **<sup>1</sup>H-NMR** (700 MHz, CDCl<sub>3</sub>, NH not observed): 7.31 (1H, dd, *J* 7.6, 1.4 Hz, 11-H), 7.09-7.06 (1H, m, 13-H), 7.04 (1H, d, *J* 7.6 Hz, 3-H), 6.73 (1H, t, *J* 7.6 Hz, 12-H), 6.67 (1H, d, *J* 7.6 Hz, 4-H), 6.63 (1H, s, 6-H), 6.56 (1H, d, *J* 8.0 Hz, 14-H), 5.32-5.29 (1H, m, 9-H), 4.37 (1H, br. s, 1-H), 2.34 (1H, dt, *J* 13.1, 3.2 Hz, 17-H<sub>a</sub>), 2.24-2.19 (4H, m, 17-H<sub>b</sub> and CH<sub>3</sub>).

**<sup>13</sup>C NMR** (176 MHz, CDCl<sub>3</sub>):  $\delta$  152.8 (7-C), 143.3 (15-C), 139.3 (5-C), 131.2 (11-C), 129.9 (13-C), 128.9 (3-C), 122.5 (2-C), 122.1 (10-C), 121.4 (4-H), 118.5 (12-C), 117.7 (6-C), 116.0 (14-C), 69.5 (9-C), 45.8 (1-C), 26.8 (17-C), 21.3 (CH<sub>3</sub>). **FT-IR**: 3376, 2323, 1873, 1608, 1577, 1494, 1416, 1353, 1320, 1276, 1240. **HR-MS**: calc. for [M+H]<sup>+</sup> C<sub>16</sub>H<sub>16</sub>ON: 238.1226 found 238.1224.

**5-bromo-8-oxa-16-azatetracyclo[7.7.1.0<sup>2,7</sup>.0<sup>10,15</sup>]heptadeca-2,4,6,10,12,14-hexaene (31j)**

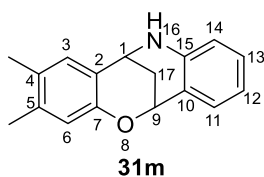
Prepared according to general procedure F. Flash column chromatography eluting with 2.5-10% EtOAc in *n*-pentane afforded the desired product **31j** (8.0 mg, 26.48  $\mu$ mol, 28%) as white solid. **<sup>1</sup>H-NMR** (500 MHz, CDCl<sub>3</sub>, NH not observed):  $\delta$  7.32 (1H, dd, *J* 7.6, 1.6 Hz, 11-H), 7.12 (1H, ddd, *J* 8.1, 7.3, 1.6 Hz, 13-H), 7.07 (1H, d, *J* 8.5 Hz, 3-H), 7.00-6.96 (2H, m, 4-H and 6-H), 6.80 (1H, td, *J* 7.6, 1.2 Hz, 12-H), 6.65 (1H, dd, *J* 8.1, 1.1 Hz, 14-H), 5.34 (1H, td, *J* 2.7, 1.4 Hz, 9-H), 4.43 (1H, td, *J* 3.2, 1.4 Hz, 1-H), 2.33 (1H, dt, *J* 13.4, 3.2 Hz, 17-H<sub>b</sub>), 2.28 (1H, dt, *J* 13.4, 2.7 Hz, 17-H<sub>a</sub>). **<sup>13</sup>C NMR** (126 MHz, CDCl<sub>3</sub>):  $\delta$  154.0 (7-C), 142.1 (15-C), 131.3 (11-C), 130.5 (3-C), 130.2 (13-C), 123.8 (2-C), 123.7 (4-C or 6-C), 122.2 (5-C), 122.0 (10-C), 120.5 (4-C or 6-C), 119.5 (12-C), 116.5 (14-C), 69.6 (9-C), 45.7 (1-C), 26.3 (17-C). **FT-IR**: 3231, 3028, 2926, 2850, 2055, 1978, 1891, 1723, 1592, 1571, 1483, 1443, 1407, 1371, 1345, 1327, 1313, 1253, 1223, 1212. **HR-MS**: calc. for [M+H]<sup>+</sup> C<sub>15</sub>H<sub>13</sub>ONBr: 302.0175 found: 302.0178, : calc. for [M+H]<sup>+</sup> C<sub>15</sub>H<sub>13</sub>ON<sup>81</sup>Br: 304.0155 found: 304.0157.

**5-fluoro-8-oxa-16-azatetracyclo[7.7.1.0<sup>2,7</sup>.0<sup>10,15</sup>]heptadeca-2,4,6,10,12,14-hexaene (31k)**

Prepared according to general procedure F. Flash column chromatography eluting with 2.5-10% EtOAc in *n*-pentane afforded the desired product **31k** (18.4 mg, 75.21  $\mu$ mol, 65%) as white solid. **<sup>1</sup>H-NMR** (600 MHz, CDCl<sub>3</sub>, NH not observed):  $\delta$  7.32 (1H, dd, *J* 7.6, 1.5 Hz, 11-H), 7.17-7.10 (2H, m, 3-H and 13-H), 6.79 (1H, td, *J* 7.6, 1.0 Hz, 12-H), 6.64 (1H, d, *J* 8.1 Hz, 14-H), 6.57 (1H, td, *J* 8.3, 2.5 Hz, 4-H), 6.52 (1H, dd, *J* 10.3, 2.5 Hz, 6-H), 5.34 (1H, br s, 9-H), 4.43 (1H, br s, 1-H), 2.33 (1H, dt, *J* 13.3, 3.2 Hz, 17-H<sub>a</sub>), 2.26 (1H, dt, *J* 13.3, 2.6 Hz, 17-H<sub>b</sub>). **<sup>13</sup>C NMR** (151 MHz, CDCl<sub>3</sub>):  $\delta$  163.1 (d, *J*<sub>CF</sub> 245.4 Hz, 5-C), 154.4 (d, *J*<sub>CF</sub> 12.3 Hz, 7-C), 142.4 (15-C), 131.4 (11-C), 130.3 (3-C or 12-C), 130.2 (3-C or 12-C), 122.0 (10-C), 121.0 (2-C), 119.3 (12-C), 116.5 (14-C), 107.9 (d, *J*<sub>CF</sub> 245.4 Hz, 4-C), 104.5 (d, *J*<sub>CF</sub> 24.2 Hz, 6-C), 69.6 (9-C), 45.7 (1-C), 26.6 (17-C). **<sup>19</sup>F NMR** (565 MHz, CDCl<sub>3</sub>)  $\delta$  -112.2. **FT-IR**: 3391, 2946, 1863, 1608, 1493, 1434, 1341, 1318, 1258, 1221. **HR-MS**: calc. for [M+H]<sup>+</sup> C<sub>15</sub>H<sub>13</sub>ONF: 242.0976, found: 242.0973.

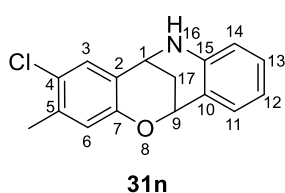
## Experimental

### 4,5-dimethyl-8-oxa-16-azatetracyclo[7.7.1.0<sup>2,7</sup>.0<sup>10,15</sup>]heptadeca-2,4,6,10,12,14-hexaene (31m)



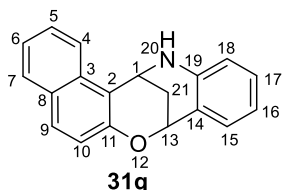
Prepared according to general procedure F. Flash column chromatography eluting with 2.5-10% EtOAc in *n*-pentane afforded the desired product **31m** (8.0 mg, 31.83  $\mu$ mol, 29%) as yellow solid. **<sup>1</sup>H-NMR** (500 MHz, CDCl<sub>3</sub>, NH not observed):  $\delta$  7.30 (1H, dd, *J* 7.5, 1.5 Hz, 11-H), 7.10-7.04 (1H, m, 13-H), 6.91 (1H, s, 3-H), 6.73 (1H, td, *J* 7.5, 1.1 Hz, 12-H), 6.61 (1H, s, 6-H), 6.56 (1H, d, *J* 7.9 Hz, 14-H), 5.31-5.24 (1H, m, 9-H), 4.33 (1H, br. s, 1-H), 2.33 (1H, dt, *J* 13.1, 3.3 Hz, 17-H<sub>a</sub>), 2.19 (1H, dt, *J* 13.1, 2.6 Hz, 17-H<sub>b</sub>), 2.15 (3H, s, CH<sub>3</sub>), 2.13 (3H, s, CH<sub>3</sub>). **<sup>13</sup>C NMR** (126 MHz, CDCl<sub>3</sub>):  $\delta$  150.7 (7-C), 143.3 (15-C), 137.8 (5-C), 131.2 (11-C), 129.8 (2-C, 13-C and 3-C), 128.5 (2-C), 122.5 (4-C), 122.2 (10-C), 118.5 (12-C), 118.0 (6-C), 116.1 (14-C), 69.3 (9-C), 45.7 (1-C), 26.9 (17-C), 19.8 (CH<sub>3</sub>), 18.9 (CH<sub>3</sub>). **FT-IR**: 3381, 2922, 1739, 1609, 1581, 1493, 1450, 1406, 1352, 1338, 1323, 1307, 1272, 1202. **HR-MS**: calc. for [M+H]<sup>+</sup> C<sub>17</sub>H<sub>18</sub>ON: 252.1383, found: 252.1381.

### 4-chloro-5-methyl-8-oxa-16-azatetracyclo[7.7.1.0<sup>2,7</sup>.0<sup>10,15</sup>]heptadeca-2,4,6,10,12,14-hexaene (31n)

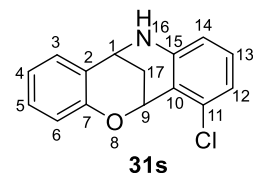


Prepared according to general procedure F. Flash column chromatography eluting with 2.5-10% EtOAc in *n*-pentane afforded the desired product **31n** (10.8 mg, 39.74  $\mu$ mol, 38%) as yellow solid. **<sup>1</sup>H-NMR** (500 MHz, CDCl<sub>3</sub>, NH not observed):  $\delta$  7.30 (1H, dd, *J* 7.6, 1.5 Hz, 11-H), 7.14 (1H, s, 3-H), 7.12-7.08 (1H, m, 13-H), 6.75 (1H, td, *J* 7.5, 1.1 Hz, 12-H), 6.68 (1H, s, 6-H), 6.59 (1H, d, *J* 8.1 Hz, 14-H), 5.32-5.28 (1H, m, 9-H), 4.36-4.33 (1H, m, 1-H), 2.31 (1H, dt, *J* 13.3, 3.2 Hz, 17-H<sub>a</sub>), 2.25-2.20 (4H, m, 17-H<sub>b</sub> and CH<sub>3</sub>). **<sup>13</sup>C NMR** (126 MHz, CDCl<sub>3</sub>):  $\delta$  151.4 (7-C), 142.9 (15-C), 136.9 (4-C), 131.2 (11-C), 130.1 (13-C), 128.9 (3-C), 125.4 (2-C), 124.3 (5-C), 121.8 (10-C), 119.5 (6-C), 118.9 (12-C), 116.1 (14-C), 69.5 (9-C), 45.5 (1-C), 26.6 (17-C), 20.1 (CH<sub>3</sub>). **FT-IR**: 3382, 2925, 1739, 1609, 1582, 1564, 1493, 1475, 1447, 1394, 1378, 1352, 1337, 1324, 1306, 1273, 1243, 1220. **HR-MS**: calc. for [M+H]<sup>+</sup> C<sub>16</sub>H<sub>15</sub>ONCl: 272.0837, found: 272.0837, calc. for [M+H]<sup>+</sup> C<sub>16</sub>H<sub>15</sub>ON<sup>37</sup>Cl: 274.0807, found: 274.0804.



**12-oxa-20-azapentacyclo[11.7.1.0<sup>2,11</sup>.0<sup>3,8</sup>.0<sup>14,19</sup>]henicososa-2(11),3,5,7,9,14,16,18-octaene****(31q)**

Prepared according to general procedure F. Flash column chromatography eluting with 2.5-10% EtOAc in *n*-pentane afforded the desired product **31q** (19.5 mg, 38.61  $\mu$ mol, 50%) as white solid. **<sup>1</sup>H-NMR** (700 MHz, CDCl<sub>3</sub>, NH not observed):  $\delta$  7.97 (1H, d, *J* 8.4 Hz, 4-H), 7.75 (1H, d, *J* 1.3 Hz, 7-H), 7.62 (1H, d, *J* 8.9 Hz, 9-H), 7.58-7.53 (1H, m, 5-H), 7.41-7.33 (2H, m, 6-H and 15-H), 7.08-7.03 (2H, m, 10-H and 17-H), 6.78-6.73 (1H, m, 16-H), 6.59 (1H, d, *J* 8.1 Hz, 18-H), 5.44-5.40 (1H, m, 13-H), 5.11 (1H, br s, 1-H), 2.47-2.34 (2H, m, 21-H<sub>a</sub> and 21-H<sub>b</sub>). **<sup>13</sup>C NMR** (176 MHz, CDCl<sub>3</sub>):  $\delta$  150.8 (11-C), 143.4 (Ar-C<sub>q</sub>), 132.2 (Ar-C<sub>q</sub>), 131.3 (15-C), 129.9 (17-C), 129.5 (9-C), 129.3 (Ar-C<sub>q</sub>), 129.1 (7-C), 127.2 (5-C), 123.4 (6-C), 122.1 (Ar-C<sub>q</sub>), 120.5 (4-C), 119.3 (10-C), 118.9 (16-C), 116.4 (18-C), 116.0 (Ar-C<sub>q</sub>), 69.5 (13-C), 41.7 (1-C), 26.6 (21-C). **FT-IR**: 3366, 2921, 2850, 2108, 1731, 1609, 1515, 1489, 1464, 1435, 1399, 1330, 1306, 1269, 1236. **HR-MS**: calc. for [M+H]<sup>+</sup> C<sub>15</sub>H<sub>11</sub>O<sub>4</sub>N: 274.1226 found 274.1226.

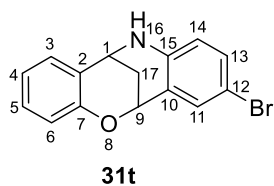
**8-oxa-11-chloro-16-azatetracyclo[7.7.1.0<sup>2,7</sup>.0<sup>10,15</sup>]heptadeca-2,4,6,10,12,14-hexaene (31s)**

Prepared according to general procedure F. Flash column chromatography eluting with 2.5-10% EtOAc in *n*-pentane afforded the desired product **31s** (13.9 mg, 53.94  $\mu$ mol, 50%) as white solid. **<sup>1</sup>H-NMR** (700 MHz, CDCl<sub>3</sub>, NH not observed):  $\delta$  7.19-7.12 (2H, m, 3-H and 5-H), 6.98 (1H, t, *J* 8.1 Hz, 13-H), 6.88-6.84 (2H, m, 4-H and 6-H), 6.77 (1H, d, *J* 8.1 Hz, 12-H), 6.46 (1H, d, *J* 8.1 Hz, 14-H), 5.83-5.76 (1H, m, 9-H), 4.43-4.30 (1H, m, 1-H), 2.40 (1H, dt, *J* 13.3, 3.3 Hz, 17-H<sub>a</sub>), 2.15 (1H, dt, *J* 13.3, 2.7 Hz, 17-H<sub>b</sub>). **<sup>13</sup>C NMR** (176 MHz, CDCl<sub>3</sub>):  $\delta$  153.4 (7-C), 144.9 (15-C), 136.0 (11-C), 130.1 (13-C), 129.3 (3-C or 5-C), 129.1 (3-C or 5-C), 124.8 (2-C), 120.5 (4-C), 119.3 (10-C), 119.0 (12-C), 117.6 (6-C), 114.4 (14-C), 65.7 (9-C), 45.7 (1-C), 26.6 (17-C). **FT-IR**: 3373, 2966, 2944, 1455, 1431, 1345, 1316, 1268. **HR-MS**: calc. for [M+H]<sup>+</sup> C<sub>15</sub>H<sub>13</sub>ONCl: 258.0680 found 258.0679, calc. for [M+H]<sup>+</sup> C<sub>15</sub>H<sub>13</sub>ON<sup>37</sup>Cl: 260.0651 found 258.0646.

## Experimental

### 8-oxa-12-bromo-16-azatetracyclo[7.7.1.0<sup>2,7</sup>.0<sup>10,15</sup>]heptadeca-2,4,6,10,12,14-hexaene (31t)

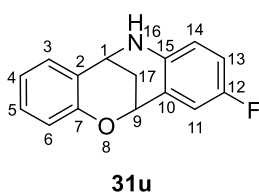
Prepared according to general procedure F. Flash column chromatography eluting with 2.5-



10% EtOAc in *n*-pentane afforded the desired product **31t** (4.1 mg, 14.48  $\mu\text{mol}$ , 14%) as white solid.  $^1\text{H-NMR}$  (700 MHz,  $\text{CDCl}_3$ , NH not observed):  $\delta$  7.46 (1H, d,  $J$  2.3 Hz, 11-H), 7.22-7.18 (2H, m, 3-H and 6-H), 7.16-7.13 (1H, m, 3-H), 6.88 (1H, td,  $J$  7.4, 1.1 Hz, 6-H), 6.82

(1H, d,  $J$  8.0 Hz, 13-H), 6.58 (1H, d,  $J$  8.0 Hz, 14-H), 5.28 (1H, s, 9-H), 4.48 (1H, br s, 1-H), 2.37 (1H, dt,  $J$  13.3, 3.2 Hz, 17-H<sub>a</sub>), 2.26 (1H, d,  $J$  13.3 Hz, 17-H<sub>b</sub>).  $^{13}\text{C NMR}$  (176 MHz,  $\text{CDCl}_3$ ):  $\delta$  152.8 (7-C), 140.8 (15-C), 133.8 (11-C), 132.8 (13-C), 129.7 (3-C or 5-C), 129.4 (3-C or 5-C), 124.6 (4-C), 123.9 (2-C), 120.8 (10-C), 118.4 (12-C), 117.4 (6-C), 112.3 (14-C), 68.7 (9-C), 46.1 (1-C), 26.2 (17-C). **FT-IR**: 3370, 2923, 1782, 1602, 1582, 1490, 1456, 1431, 1410, 1349, 1328, 1298, 1274, 1211. **HR-MS**: calc. for  $[\text{M}+\text{H}]^+$   $\text{C}_{15}\text{H}_{13}\text{ONBr}$ : 302.0175 found 301.0174, calc. for  $[\text{M}+\text{H}]^+$   $\text{C}_{15}\text{H}_{13}\text{ON}^{81}\text{Br}$ : 304.0155 found 304.0152.

### 8-oxa-12-fluoro-16-azatetracyclo[7.7.1.0<sup>2,7</sup>.0<sup>10,15</sup>]heptadeca-2,4,6,10,12,14-hexaene (31u)

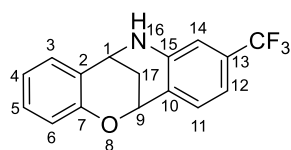


Prepared according to general procedure F. Flash column chromatography eluting with 2.5-10% EtOAc in *n*-pentane afforded the desired product **31u** (13.9 mg, 53.94  $\mu\text{mol}$ , 50%) as white solid.  $^1\text{H-NMR}$  600 MHz,  $\text{CDCl}_3$ , NH not observed):  $\delta$  7.21 (1H, dd,  $J$  7.6, 1.4 Hz, 3-H), 7.16-7.12 (1H, m, 5-H), 7.06 (1H, dd,  $J$  8.7, 2.9 Hz, 11-H),

6.88 (1H, td,  $J$  7.4, 1.0 Hz, 4-H), 6.84 (1H, td,  $J$  8.6, 2.9 Hz, 13-H), 6.81 (1H, d,  $J$  8.3 Hz, 6-H), 6.62 (1H, dd,  $J$  8.6, 4.5 Hz, 14-H), 5.28 (1H, br s, 9-H), 4.45 (1H, br s, 1-H), 2.38 (1H, dt,  $J$  13.3, 3.2 Hz, 17-H<sub>a</sub>), 2.26 (1H, dt,  $J$  13.3, 2.5 Hz, 17-H<sub>b</sub>).  $^{13}\text{C NMR}$  (151 MHz,  $\text{CDCl}_3$ ):  $\delta$  156.6 (d,  $J_{\text{CF}}$  238 Hz, 12-C), 152.9 (7-C), 138.3 (15-C), 130.9, 129.9, 129.6 (5-C), 129.4 (3-C), 124.3 (2-C), 123.5 (10-C), 120.8 (4-C), 117.8 (d,  $J_{\text{CF}}$  6.0 Hz, 14-C), 117.2 (d,  $J_{\text{CF}}$  18.2 Hz, 11-C), 117.1 (d,  $J_{\text{CF}}$  16.9 Hz, 13-C) 117.0 (6-C), 68.9 (9-C), 46.2 (1-C), 26.3 (17-C).  $^{19}\text{F NMR}$  (570 MHz,  $\text{CDCl}_3$ ) -125.7. **FT-IR**: 3386, 2924, 1607, 1583, 1501, 1457, 1433, 1350, 1328, 1311, 1278, 1253.02, 1213. **HR-MS**: calc. for  $[\text{M}+\text{H}]^+$   $\text{C}_{15}\text{H}_{13}\text{ONF}$ : 242.0976, found: 242.0973.

**8-oxa-13-trifluoromethyl-16-azatetracyclo[7.7.1.0<sup>2,7</sup>.0<sup>10,15</sup>]heptadeca-2,4,6,10,12,14-hexaene (31v)**

Prepared according to general procedure F. Flash column chromatography eluting with 2.5-

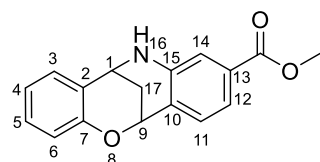


**31v**

10% EtOAc in *n*-pentane afforded the desired product **31v** (13.9 mg, 53.94  $\mu$ mol, 50%) as white solid. <sup>1</sup>H-NMR (500 MHz, CDCl<sub>3</sub>, NH not observed):  $\delta$  7.44 (1H, d, *J* 7.9 Hz, 11-H), 7.20 (1H, dd, *J* 7.5, 1.7 Hz, 3-H), 7.15 (1H, ddd, *J* 8.5, 7.2, 1.7 Hz, 5-H), 7.02 (1H, dd, *J* 7.9,

2.0 Hz, 12-H), 6.91-6.87 (2H, m, 4-H and 14-H), 6.82 (1H, dd, *J* 8.5, 1.1 Hz, 6-H), 5.39-5.35 (1H, m, 9-H), 4.54-4.49 (1H, m, 1-H), 2.42 (1H, d, *J* 13.4 Hz, 17-H<sub>a</sub>), 2.27 (1H, dd, *J* 13.4, 1.1 Hz, 17-H<sub>b</sub>). <sup>13</sup>C NMR (176 MHz, CDCl<sub>3</sub>):  $\delta$  158.58 (q, *J*<sub>CF</sub> 41.8 Hz, CF<sub>3</sub>), 152.8 (7-C), 142.9 (15-C), 132.07 (q, *J* 32.2 Hz, 13-C) 131.9 (11-C), 129.6 (5-C), 129.2 (3-C), 125.3 (10-C), 124.3 (2-C), 123.9 (q, *J*<sub>CF</sub> 272.5 Hz, 12-C), 120.9 (4-C), 117.4 (6-C), 115.3 (12-C), 114.8 (q, *J*<sub>CF</sub> 285.8 Hz, 14-C), 68.7 (9-C), 45.9 (1-C), 26.1 (17-C). <sup>19</sup>F NMR (470 MHz, CDCl<sub>3</sub>)  $\delta$  -63.0. **FT-IR:** 3375, 2107, 1782, 1620, 1585, 1485, 1433, 1352, 1318, 1277, 1245, 1214. **HR-MS:** calc. for [M+H]<sup>+</sup> C<sub>15</sub>H<sub>13</sub>ONF: 292.0944, found:292.0944.

**methyl-8-oxa-16-azatetracyclo[7.7.1.0<sup>2,7</sup>.0<sup>10,15</sup>]heptadeca-2(7),3,5,10,12,14-hexaene-13-carboxylate (31w)**



**31w**

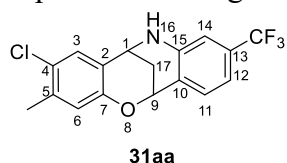
Prepared according to general procedure F. Flash column chromatography eluting with 2.5-10% EtOAc in *n*-pentane afforded the desired product **31w** (4.6 mg, 16.35  $\mu$ mol, 16%) as white solid. <sup>1</sup>H-NMR 500 MHz, CDCl<sub>3</sub>, NH not observed):  $\delta$  7.44-

7.37 (2H, m, 11-H and 12-H), 7.30 (1H, s, 14-H), 7.19 (1H, dd, *J* 7.5, 1.5 Hz, 3-H), 7.14-7.10 (1H, m, 5-H), 6.87 (1H, td, *J* 7.5, 1.1 Hz, 4-H), 6.80 (1H, d, *J* 9.2 Hz, 6-H), 5.37-5.34 (1H, m, 9-H), 4.47 (1H, s, 1-H), 3.84 (3H, s, CH<sub>3</sub>), 2.40 (1H, dt, *J* 13.3, 3.2 Hz, 17-H<sub>a</sub>), 2.25 (1H, dt, *J* 13.3, 2.6 Hz, 17-H<sub>b</sub>). <sup>13</sup>C NMR (126 MHz, CDCl<sub>3</sub>):  $\delta$  167.0 (C=O<sub>2</sub>CH<sub>3</sub>), 152.8 (7-C), 142.8 (13-C), 131.6 (15-C), 131.3 (12-C), 129.5 (5-C), 129.2 (3-C), 126.4 (10-C), 124.6 (2-C), 120.8 (4-C), 119.8 (11-C), 117.5 (14-C), 117.3 (6-C), 68.9 (9-C), 52.3 (CH<sub>3</sub>), 46.0 (1-C), 26.3 (17-C). **FT-IR:** 3366, 2952, 2115, 1698, 1604, 1578, 1514, 1486, 1454, 1436, 1410, 1346, 1319, 1288, 1239. **HR-MS:** calc. for [M+H]<sup>+</sup> C<sub>17</sub>H<sub>16</sub>O<sub>3</sub>N: 282.1125, found: 282.1127.

## Experimental

### 4-chloro-5-methyl-13-(trifluoromethyl)-8-oxa-16-azatetracyclo[7.7.1.0<sup>2,7</sup>.0<sup>10,15</sup>]heptadeca-2(7),3,5,10,12,14-hexaene (31aa)

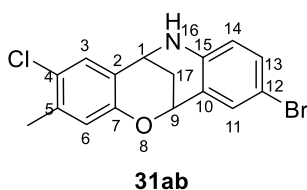
Prepared according to general procedure F. Flash column chromatography eluting with 2.5-



31aa

10% EtOAc in *n*-pentane afforded the desired product **31aa** (2.7 mg, 7.95  $\mu$ mol, 11%) as white solid. <sup>1</sup>H-NMR 700 MHz, CDCl<sub>3</sub>, NH not observed):  $\delta$  7.31 (1H, d, *J* 8.0 Hz, 11-H), 7.05 (1H, s, 3-H), 6.87 (1H, d, *J* 8.0 Hz, 12-H), 6.71 (1H, s, 6-H), 6.62 (1H, s, 14-H), 5.25 (1H, br s, 9-H), 4.30 (1H, br s, 1-H), 2.28 (1H, dt, *J* 13.3, 3.2 Hz, 17-H<sub>a</sub>), 2.17 (3H, s, CH<sub>3</sub>), 2.10 (1H, dt, *J* 13.3, 2.7 Hz, 17-H<sub>b</sub>). <sup>13</sup>C NMR (176 MHz, CDCl<sub>3</sub>, CF<sub>3</sub> not observed):  $\delta$  151.1 (7-C), 143.5 (Ar-C<sub>q</sub>), 137.1 (Ar-C<sub>q</sub>), 131.6 (11-C), 128.7 (3-C), 125.6 (Ar-C<sub>q</sub>), 124.3 (Ar-C<sub>q</sub>), 123.9 (Ar-C<sub>q</sub>), 119.4 (14-C), 114.5 (q, *J*<sub>CF</sub> 3.9, 12-C), 112.3 (q, *J*<sub>CF</sub> 4.0, 14-C), 68.7 (9-C), 45.2 (1-C), 26.1 (17-C), 19.9 (CH<sub>3</sub>). <sup>19</sup>F NMR (565 MHz, CDCl<sub>3</sub>)  $\delta$  -63.1. FT-IR: 3366, 2952, 2075.33, 1966.16, 1587, 1520, 1496, 1456, 1434, 1394, 1379, 1355, 1334, 1321, 1247, 1222.74. HR-MS: calc. for [M+H]<sup>+</sup> C<sub>17</sub>H<sub>16</sub>O<sub>3</sub>N: 340.0711, found: 340.0715.

### 4-chloro-5-methyl-(12-bromo)-8-oxa-16-azatetracyclo[7.7.1.0<sup>2,7</sup>.0<sup>10,15</sup>]heptadeca-2(7),3,5,10,12,14-hexaene (31ab)

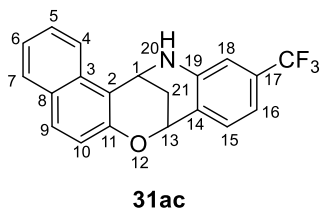


31ab

Prepared according to general procedure F. Flash column chromatography eluting with 2.5-10% EtOAc in *n*-pentane afforded the desired product **31ab** (4.6 mg, 16.35  $\mu$ mol, 16%) as white solid.

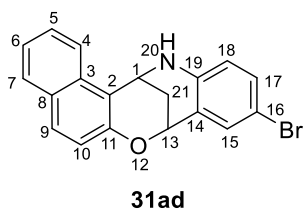
<sup>1</sup>H-NMR 600 MHz, CDCl<sub>3</sub>, NH not observed):  $\delta$  7.40 (1H, d, *J* 2.3 Hz, 11-H), 7.16 (1H, dd, *J* 8.6, 2.3 Hz, 13-H), 7.10 (1H, s, 3-H), 6.69 (1H, s, 6-H), 6.43 (1H, d, *J* 8.6 Hz, 14-H), 5.25-5.17 (1H, m, 9-H), 4.35-4.26 (1H, m, 1-H), 2.30 (1H, dt, *J* 13.3, 3.2 Hz, 17-H<sub>a</sub>), 2.24 (3H, s, CH<sub>3</sub>), 2.15 (1H, dt, *J* 13.3, 2.6 Hz, 17-H<sub>b</sub>). <sup>13</sup>C NMR (151 MHz, CDCl<sub>3</sub>):  $\delta$  151.1 (7-C), 142.3 (15-C), 137.0 (4-C or 5-C), 133.5 (11-C), 132.6 (13-C), 128.7 (3-C), 125.4 (4-C or 5-C), 124.0 (2-C), 123.2 (10-C), 119.4 (6-C), 117.3 (14-C), 109.7 (12-C), 68.8 (9-C), 45.2 (1-C), 26.2 (17-C), 19.9 (CH<sub>3</sub>). FT-IR: 3378, 2927, 2098, 2012, 1777, 1734, 1494, 1433, 11395, 1373, 1351, 1330, 1312, 1296, 1273, 1244. HR-MS: calc. for [M+H]<sup>+</sup> C<sub>16</sub>H<sub>14</sub>ONBrCl: 349.9942, found: 349.9945, calc. for [M+H]<sup>+</sup> C<sub>16</sub>H<sub>14</sub>ON<sup>81</sup>BrCl: 351.9921, found: 351.9921, calc. for [M+H]<sup>+</sup> C<sub>16</sub>H<sub>14</sub>ONBr<sup>37</sup>Cl: 353.9892, found: 345.39895.

**17-(trifluoromethyl)-12-oxa-20-azapentacyclo[11.7.1.0<sup>2,11</sup>.0<sup>3,8</sup>.0<sup>14,19</sup>]henicososa-2(11),3,5,7,9,14,16,18-octaene (31ac)**



Prepared according to general procedure F. Flash column chromatography eluting with 2.5-10% EtOAc in *n*-pentane afforded the desired product **31ac** (2.8 mg, 8.20  $\mu$ mol, 20%) as white solid. **<sup>1</sup>H-NMR** (600 MHz, CDCl<sub>3</sub>, NH not observed):  $\delta$  7.94 (1H, d, *J* 8.4 Hz, 4-H), 7.77 (1H, d, *J* 8.1 Hz, 7-H), 7.63 (1H, d, *J* 8.9 Hz, 9-H), 7.57 (1H, ddd, *J* 8.4, 7.0, 1.4 Hz, 5-H), 7.44 (1H, d, *J* 8.0 Hz, 15-H), 7.39-7.34 (1H, m, 6-H), 7.04 (1H, d, *J* 8.9 Hz, 10-H), 6.93 (1H, d, *J* 8.0 Hz, 16-H), 6.76 (1H, s, 18-H), 5.48-5.42 (1H, m, 9-H), 5.16-5.05 (1H, m, 1-H), 2.47 (1H, dt, *J* 13.2, 3.2 Hz, 21-H<sub>a</sub>), 2.34 (1H, dt, *J* 13.3, 2.6 Hz, 21-H<sub>b</sub>). **<sup>13</sup>C NMR** (151 MHz, CDCl<sub>3</sub>, CF<sub>3</sub> not observed):  $\delta$  150.6 (11-C), 144.3 (19-C), 132.0 (15-C), 131.80 (d, *J*<sub>CF</sub> 20.0 Hz, 17-C), 131.8 (Ar-C<sub>q</sub>), 129.7 (9-C), 129.4 (Ar-C<sub>q</sub>), 129.2 (7-C), 127.3 (5-C), 124.7 (8-C or 2-C), 123.6 (6-C), 120.3 (4-C), 119.2 (16-C), 116.0 (8-C or 2-C), 114.6 (q, *J*<sub>CF</sub> 3.7 Hz, 16-C), 112.6 (q, *J*<sub>CF</sub> 4.1 Hz, 18-C), 68.8 (13-C), 41.4 (1-C), 26.4 (21-C). **<sup>19</sup>F NMR** (565 MHz, CDCl<sub>3</sub>)  $\delta$  -63.1. **FT-IR**: 3375, 2921, 2109, 1625, 1597, 1516, 1487, 1434, 1398, 1355, 1336, 1322, 1308, 1244. **HR-MS**: calc. for [M+H]<sup>+</sup> C<sub>20</sub>H<sub>15</sub>ONF<sub>3</sub>: 342.1100 found 342.110.

**16-bromo-12-oxa-20-azapentacyclo[11.7.1.0<sup>2,11</sup>.0<sup>3,8</sup>.0<sup>14,19</sup>]henicososa-2(11),3,5,7,9,14,16,18-octaene (31ad)**



Prepared according to general procedure F. Flash column chromatography eluting with 2.5-10% EtOAc in *n*-pentane afforded the desired product **31ad** (21.2 mg, 60.19  $\mu$ mol, 74%) as white solid. **<sup>1</sup>H-NMR** (600 MHz, CDCl<sub>3</sub>, NH not observed):  $\delta$  7.92 (1H, d, *J* 8.4 Hz, 4-H), 7.77 (1H, d, *J* 8.1 Hz, 7-H), 7.63 (1H, d, *J* 8.9 Hz, 9-H), 7.58-7.54 (1H, m, 5-H), 7.50-7.44 (1H, m, 15-H), 7.42-7.32 (1H, m, 6-H), 7.12 (1H, dt, *J* 8.6, 1.7 Hz, 10-H), 7.05 (1H, dd, *J* 8.9, 1.1 Hz, 17-H), 6.40 (1H, dd, *J* 8.6, 1.1 Hz, 18-H), 5.40-5.34 (1H, m, 9-H), 5.07 (1H, t, *J* 3.0 Hz, 1-H), 2.45-2.36 (1H, m, 21-H<sub>a</sub>), 2.31 (1H, dt, *J* 13.2, 2.5 Hz, 21-H<sub>b</sub>). **<sup>13</sup>C NMR** (151 MHz, CDCl<sub>3</sub>):  $\delta$  150.5 (11-C), 143.0 (19-C), 133.5 (15-C), 132.4 (10-C), 131.9 (Ar-C<sub>q</sub>), 129.4 (9-C), 129.2 (Ar-C<sub>q</sub>), 129.1 (7-C), 127.1 (5-C), 123.4 (Ar-C<sub>q</sub>), 123.3 (6-C), 120.3 (4-C), 119.1 (17-C), 117.5 (18-C), 116.0 (Ar-C<sub>q</sub>), 109.6 (Ar-C<sub>q</sub>), 68.8 (9-C), 41.3 (1-C), 26.3 (21-C). **FT-IR**: 3390, 3056, 2952, 2025, 1623, 1601, 1514, 1486, 1435, 1398, 1355, 1315, 1296, 1268, 1234, 1215. **HR-MS**: calc. for

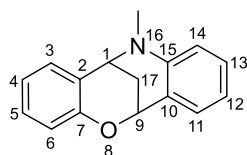
## Experimental

$[M+H]^+$  C<sub>20</sub>H<sub>15</sub>ONBr: 352.0332, found:352.0332, calc. for  $[M+H]^+$  C<sub>20</sub>H<sub>15</sub>ON<sup>81</sup>Br: 354.0311, found:354.0311.

### Functionalisation of the chromaline-amine (N-R)

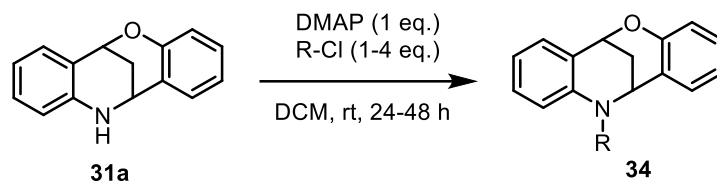
#### Preparation of compound 33

##### 16-methyl-8-oxa-16-azatetracyclo[7.7.1.0<sup>2,7</sup>.0<sup>10,15</sup>]heptadeca-2,4,6,10,12,14-hexaene (33)

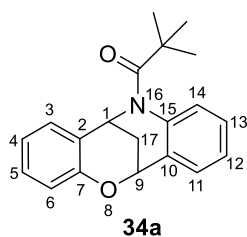


**33**

To a stirred solution of **31a** (20 mg, 1.0 eq.) in anhydrous DMF (0.5 mL) was added portionwise NaH (60% dispersion in mineral oil, 2.5 eq, 4.3 mg.) at rt. The reaction mixture was stirred for 1 h, then MeI (1.1 eq., 6.1  $\mu$ L) was added dropwise. The reaction mixture was stirred for 17 h, then quenched with sat. aq. brine solution (20 mL). The resulting solution was extracted with DCM (3  $\times$  1 mL), then the combined organics were dried over MgSO<sub>4</sub>, filtered, and concentrated in vacuo. Flash column chromatography eluting with 5-20% EtOAc in *n*-pentane gave the desired product **33** (9.0 mg, 37.93  $\mu$ mol, 42%) as white solid. **<sup>1</sup>H-NMR** (600 MHz, CDCl<sub>3</sub>):  $\delta$  7.32 (1H, dd, *J* 7.5, 1.7 Hz, 11-H), 7.22-7.15 (2H, m, 3-H and 13-H), 7.14-7.09 (1H, m, 5-H), 6.84-6.80 (2H, m, 4-H and 6-H), 6.71 (1H, td, *J* 7.4, 1.1 Hz, 12-H), 6.61 (1H, d, *J* 8.3 Hz, 14-H), 5.36-5.31 (1H, m, 9-H), 4.30-4.23 (1H, m, 1-H), 3.07 (3H, s, CH<sub>3</sub>), 2.36-2.31 (1H, m, (17-H<sub>a</sub>), 2.28 (1H, dt, *J* 13.1, 2.7 Hz, 17-H<sub>b</sub>). **<sup>13</sup>C NMR** (126 MHz, CDCl<sub>3</sub>):  $\delta$  13C NMR (151 MHz, CDCl<sub>3</sub>)  $\delta$  153.1 (7-C), 145.3 (15-C), 131.1 (11-C), 130.2 (13-C), 129.3 (3-C), 129.2 (5-C), 122.0 (2-C or 10-C), 122.0 (2-C or 10-C), 119.7 (4-C), 117.3 (4-C or 6-C), 117.2 (12-C), 112.4 (14-C), 70.2 (9-C), 54.3 (1-C), 38.2 (CH<sub>3</sub>), 26.9 (17-C). **FT-IR**: 2920, 2849, 1603, 1579, 1494, 1480, 1451, 1432, 1371, 1346, 1321, 1265, 1218, 1209. **HR-MS**: calc. for  $[M+H]^+$  C<sub>16</sub>H<sub>16</sub>ON: 238.1226 found 238.128.

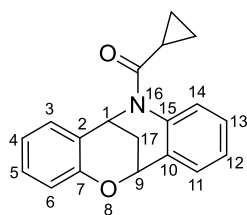
**General procedure G:** functionalisation of the chromaline amine

Chromaline **31a** (15-20 mg, 1 equiv) was dissolved in 500  $\mu\text{L}$  DCM in an argon flushed reaction vial. DMAP (1 eq.) was added to the mixture at 0  $^{\circ}\text{C}$  and the temperature maintained. Acid chloride (1-4 eq.) were added, and the reaction monitored via TLC. After 24-48 h, the reaction was quenched by addition of saturated ammonium chloride solution (aq., 1 mL). The aqueous phase was extracted with DCM (3x5 mL), the combined organics dried over  $\text{Mg}_2\text{SO}_4$  and the solvents removed under reduced pressure. Flash column chromatography eluting with 10-50% EtOAc in *n*-pentane gave compound **34**.

**2,2-dimethyl-1-{8-oxa-16-azatetracyclo[7.7.1.0<sup>2,7</sup>.0<sup>10,15</sup>]heptadeca-2(7),3,5,10(15),11,13-hexaen-16-yl}propan-1-one (34a)**

Prepared according to general procedure G. 18 mg 31a and 5 eq. acid chloride were used. Flash column chromatography eluting with 10-20% EtOAc in *n*-pentane afforded the desired product **34a** (5.8 mg, 18.87  $\mu\text{mol}$ , 23%) as white solid.  $^1\text{H-NMR}$  (700 MHz,  $\text{CDCl}_3$ ):  $\delta$  7.46 (1H, dd,  $J$  7.6, 1.7 Hz, 11-H), 7.42-7.36 (2H, m, 3-H and 6-H), 7.15 (1H, ddd,  $J$  8.3, 7.2, 1.6 Hz, 4-H or 5-H), 7.11 (1H, ddd,  $J$  8.3, 7.2, 1.6 Hz, 13-H), 7.07 (1H, td,  $J$  7.4, 1.2 Hz, 4-H or 5-H), 6.84 (1H, td,  $J$  7.6, 1.2 Hz, 12-H), 6.72 (1H, dd,  $J$  8.3, 1.2 Hz, 14-H), 5.66-5.61 (1H, m, 9-H), 5.37-5.32 (1H, m, 1-H), 2.43 (1H, ddd,  $J$  13.3, 3.6, 2.5 Hz, 17-H<sub>a</sub>), 2.30 (1H, ddd,  $J$  13.3, 3.0, 2.2 Hz, 17-H<sub>b</sub>), 1.55 (9H, s, *t*-Butyl).  $^{13}\text{C NMR}$  (176 MHz,  $\text{CDCl}_3$ ): 178.5 ( $\underline{\text{C}}\text{O}$ ), 153.1 (7-C), 139.1 (15-C), 130.3 (3-C or 6-C), 130.0 (13-C), 129.3 (11-C), 128.3 (4-C or 5-C), 126.2 (3-C or 6-C), 125.0 (4-C or 5-C), 121.8 (Ar-C<sub>q</sub>), 121.8 (Ar-C<sub>q</sub>), 120.7 (12-C), 117.6 (14-C), 69.5 (9-C), 48.4 (1-C<sub>9</sub>), 41.3 (17-C), 29.8 ( $\underline{\text{C}}(\text{CH}_3)_3$ ), 29.6 ( $\text{C}(\underline{\text{C}}\text{H}_3)_3$ ). **FT-IR**: 2958, 2929, 2040, 1648, 1609, 1584, 1485, 1457, 1430, 1401, 1371, 1347, 1292. **HR-MS**: calc. for  $[\text{M}+\text{H}]^+$   $\text{C}_{20}\text{H}_{22}\text{O}_2\text{N}$ : 308.1645, found: 308.1646.

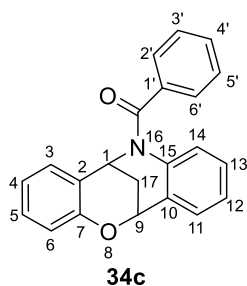
**16-cyclopropanecarbonyl-8-oxa-16-azatetracyclo[7.7.1.0<sup>2,7</sup>.0<sup>10,15</sup>]heptadeca-2(7),3,5,10(15),11,13-hexaene (34b)**



34b

Prepared according to general procedure G. 20 mg **31a** and 5 eq. acid chloride were used. Flash column chromatography eluting with 10-20% EtOAc in *n*-pentane afforded the desired product **34b** (21.0 mg, 72.08  $\mu$ mol, 80%) as white solid. **<sup>1</sup>H-NMR** (700 MHz, CDCl<sub>3</sub>):  $\delta$  7.51-7.43 (2H, m, 3-H and 11-H), 7.36 (1H, dd, *J* 7.7, 1.7 Hz, 6-H), 7.22-7.15 (1H, m, 12-H), 7.13-7.05 (2H, m, 4-H and 13-H), 6.84 (1H, td, *J* 7.5, 1.2 Hz, 5-H), 6.71 (1H, dd, *J* 8.3, 1.2 Hz, 14-H), 6.08 (1H, d, *J* 3.2 Hz, 9-H), 5.38 (1H, td, *J* 2.8, 1.2 Hz, 1-H), 2.43-2.39 (1H, m, 17-H<sub>a</sub>), 2.30 (1H, dt, *J* 13.5, 2.7 Hz, 17-H<sub>b</sub>), 2.22-2.08 (1H, m, CH), 1.51-1.41 (1H, m, CH<sub>2</sub>), 1.13-1.01 (2H, m, 2 CH<sub>2</sub>), 0.90-0.79 (1H, m, CH<sub>2</sub>). **<sup>13</sup>C NMR** (126 MHz, CDCl<sub>3</sub>):  $\delta$  173.3 (CO), 153.1 (7-C), 138.0 (15-C), 131.0 (3-C), 130.5 (6-C), 129.6 (4-C), 128.7 (12-C), 126.5 (2-C), 124.5 (13-C), 123.1 (11-C), 121.9 (10-C), 120.7 (12-C), 117.1 (14-C), 69.7 (9-C), 46.8 (-C), 28.7 (17-C), 15.0 (CH), 10.5 (CH<sub>2</sub>), 9.5 (CH<sub>2</sub>). **FT-IR**: 3038, 2663, 2383, 2349, 1651, 1607, 1582, 1484, 1456, 1398, 1342, 1314, 1296, 1281, 1266. **HR-MS**: calc. for [M+H]<sup>+</sup> C<sub>23</sub>H<sub>22</sub>O<sub>3</sub>N: 360.1594, found: 360.1594.

**16-benzoyl-8-oxa-16-azatetracyclo[7.7.1.0<sup>2,7</sup>.0<sup>10,15</sup>]heptadeca-2(7),3,5,10(15),11,13-hexaene (34c)**

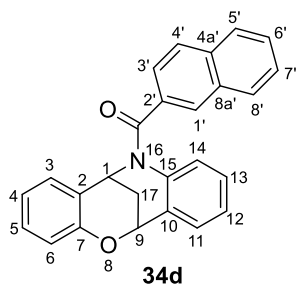


34c

Prepared according to general procedure G. 20 mg **31a** and 1.1 eq. acid chloride were used. Flash column chromatography eluting with 10-20% EtOAc in *n*-pentane afforded the desired product **34c** (16.0 mg, 48.87  $\mu$ mol, 55%) as white solid. **<sup>1</sup>H-NMR** (500 MHz, CDCl<sub>3</sub>):  $\delta$  7.54-7.48 (3H, m, 3-H, 2'-H and 6'-H), 7.48-7.41 (2H, m, 4'-H and 11-H), 7.41-7.35 (2H, m, 3'-H and 5'-H), 7.12 (1H, ddd, *J* 8., 7.2, 1.7 Hz, 6-H), 6.99 (1H, td, *J* 7.4, 1.2 Hz, 12-H), 6.92-6.84 (2H, m, 4-H and 13-H), 6.73 (1H, dd, *J* 8.3, 1.2 Hz, 5-H), 6.68 (1H, d, *J* 8.3 Hz, 14-H), 6.00-5.92 (1H, m, 9-H), 5.46-5.33 (1H, m, 1-H), 2.54-2.41 (2H, m, 17-H<sub>a</sub> and 17-H<sub>b</sub>). **<sup>13</sup>C NMR** (126 MHz, CDCl<sub>3</sub>):  $\delta$  170.0 (CO), 153.1 (7-C), 137.9 (15-C), 136.4 (1'-C), 130.9 (11-C), 130.9 (4'-C), 130.6 (3-C), 129.9 (6-C), 128.7 (3'-C and 5'-C), 128.6 (4-C), 128.4 (2'-C or 6'-C), 125.7 (2-C), 124.4 (12-C), 124.2 (14-C), 121.6 (10-C), 120.9 (13-C), 117.2 (5-C), 69.6 (9-C), 48.2 (1-C), 28.7 (17-C). **FT-IR**: 3023, 3007, 2948, 1640, 1604, 1576, 1484, 1456, 1448, 1375, 1352, 1344, 1330, 1318, 1291, 1269, 1239. **HR-MS**: calc. for [M+H]<sup>+</sup> C<sub>23</sub>H<sub>22</sub>O<sub>3</sub>N: 328.1332, found: 328.1336.



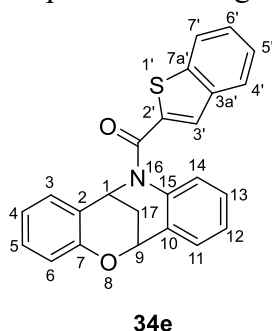
**16-(naphthalene-2-carbonyl)-8-oxa-16-azatetracyclo[7.7.1.0<sup>2,7</sup>.0<sup>10,15</sup>]heptadeca-2(7),3,5,10(15),11,13-hexaene (34d)**



Prepared according to general procedure G. 20 mg **31a** and 1 eq. acid chloride were used. Flash column chromatography eluting with 10-20% EtOAc in *n*-pentane afforded the desired product **34d** (21.9 mg, 58.02  $\mu$ mol, 65%) as white solid. <sup>1</sup>H-NMR (500 MHz, CDCl<sub>3</sub>):  $\delta$  8.12 (1H, s, 1'-H), 7.88-7.82 (2H, m, 4'-H, one out of 5' to 8'), 7.80 (1H, d, *J* 8.5 Hz, 3'-H), 7.61-7.42 (5H, m, 3-H, 11-H and 5'-H to 8'-

H (except one)), 7.12 (1H, ddd, *J* 8.3, 7.3, 1.7 Hz, 6-H), 6.97 (1H, td, *J* 7.5, 1.2 Hz, 12-H), 6.90 (1H, td, *J* 7.5, 1.2 Hz, 4-H), 6.78 (1H, ddd, *J* 8.8, 7.3, 1.6 Hz, 13-H), 6.75 (1H, dd, *J* 8.3, 1.2 Hz, 5-H), 6.67 (1H, d, *J* 8.4 Hz, 14-H), 6.05-5.94 (1H, m, 9-H), 5.47 (1H, td, *J* 2.8, 1.3 Hz, 1-H), 2.58-2.44 (2H, m, 17-H<sub>a</sub> and 17-H<sub>b</sub>). <sup>13</sup>C NMR (126 MHz, CDCl<sub>3</sub>):  $\delta$  169.9 (CO), 153.2 (7-C), 137.9 (15-C), 134.3 (Ar-C<sub>q</sub>), 133.7 (Ar-C<sub>q</sub>), 132.9 (Ar-C<sub>q</sub>), 130.9 (11-C), 130.6 (3-C), 129.9 (5'-, 6'-, 7'- or 8'-C), 129.4 (5'-, 6'-, 7'- or 8'-C), 128.9 (1'-C), 128.5 (4'-C), 128.3 (Ar-C<sub>q</sub>), 127.9 (5'-, 6'-, 7'- or 8'-C), 127.8 (13-C), 126.9 (3'-C), 125.7 (5'-, 6'-, 7'- or 8'-C), 125.2 (2-C), 124.4 (6-C), 124.1 (14-C), 121.7 (10-C), 120.9 (4-C), 117.2 (5-C), 69.7 (9-C), 48.2 (1-C), 28.7 (17-C). FT-IR: 2930, 2516, 2178, 2159, 2024, 1971, 1638, 1606, 1578, 1484, 1456, 1373. HR-MS: calc. for [M+H]<sup>+</sup> C<sub>26</sub>H<sub>20</sub>O<sub>2</sub>N: 378.1489, found: 378.1488.

**16-(1-benzothiophene-2-carbonyl)-8-oxa-16-azatetracyclo[7.7.1.0<sup>2,7</sup>.0<sup>10,15</sup>]heptadeca-2(7),3,5,10(15),11,13-hexaene (34e)**



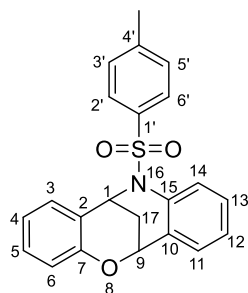
Prepared according to general procedure G. 20 mg **31a** and 5 eq. acid chloride were used. Flash column chromatography eluting with 10-20% EtOAc in *n*-pentane afforded the desired product **34e** (27.5 mg, 71.71  $\mu$ mol, 80%) as white solid. <sup>1</sup>H-NMR (500 MHz, CDCl<sub>3</sub>):  $\delta$  7.84 (1H, d, *J* 7.5 Hz, 7'-H), 7.75 (1H, d, *J* 7.5 Hz, 4'-H), 7.58 (1H, dd, *J* 7.7, 1.7 Hz, 3-H), 7.52 (1H, s, 3'-H), 7.50-7.46 (1H, m, 11-H), 7.45-7.33 (2H, m, 5'-H and 6'-H), 7.13 (1H, ddd, *J* 8.2, 7.3, 1.7 Hz, 13-H), 7.05 (1H, td, *J* 7.4, 1.2 Hz, 5-H),

7.01 (1H, dd, *J* 8.4, 1.3 Hz, 6-H), 6.95-6.87 (2H, m, 4-H and 12-H), 6.74 (1H, dd, *J* 8.2, 1.2 Hz, 14-H), 6.00-5.97 (1H, m, 9-H), 5.49-5.44 (1H, m, 1-H), 2.52-2.49 (2H, m, 17-H<sub>a</sub> and 17-H<sub>b</sub>). <sup>13</sup>C NMR (126 MHz, CDCl<sub>3</sub>): 163.7 (CO), 153.2 (7-C), 141.1 (Ar-C<sub>q</sub>), 138.6 (Ar-C<sub>q</sub>), 138.2 (Ar-C<sub>q</sub>), 137.7 (15-C), 130.9 (11-C), 130.7 (3-C), 130.0 (13-C), 128.6 (4-C or 12-C), 128.1 (3'-C), 126.5, 125.9 (2-C), 125.2 (4'-C), 125.0 (5-C), 125.0 (5'-C or 6'-C), 124.1 (6-C), 122.7 (7'-C), 121.3 (10-C), 121.0 (4-C or 12-C), 117.2 (14-C), 69.5 (9-C), 49.0 (1-C), 29.0

## Experimental

(17-C). **FT-IR:** 1630, 1607, 1578, 1517, 1483, 1456, 1432, 1375, 1337, 1314, 1292, 1270, 1213. **HR-MS:** calc. for  $[M+H]^+$   $C_{24}H_{18}O_2NS$ : 384.1053, found: 384.1057.

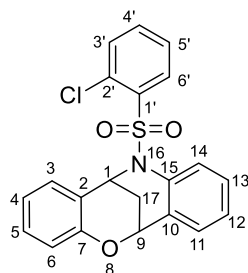
### 16-(4-methylbenzenesulfonyl)-8-oxa-16-azatetracyclo[7.7.1.0<sup>2,7</sup>.0<sup>10,15</sup>]heptadeca-2(7),3,5,10(15),11,13-hexaene (31a)



**34f**

Prepared according to general procedure G. 20 mg **31a** and 2 eq. acid chloride were used. Flash column chromatography eluting with 10-20% EtOAc in *n*-pentane afforded the desired product **34f** (16.1 mg, 42.64  $\mu$ mol, 47%) as white solid. **<sup>1</sup>H-NMR** (500 MHz,  $CDCl_3$ ):  $\delta$  7.86 (1H, dd, *J* 8.5, 1.1 Hz, 11-H), 7.67-7.57 (2H, m, 2'-H and 6'-H), 7.41-7.32 (2H, m, 3-H and 5-H), 7.28-7.20 (3H, m, 3'-H, 5'-H and 12-H), 7.16-7.06 (2H, m, 6-H and 13-H), 6.88 (1H, td, *J* 7.5, 1.2 Hz, 4-H), 6.70 (1H, dd, *J* 8.3, 1.1 Hz, 14-H), 5.68-5.58 (1H, m, 9-H), 5.17-5.09 (1H, m, 1-H), 2.39 (3H, s,  $CH_3$ ), 2.11 (1H, dt, *J* 13.8, 3.0 Hz, 17-H<sub>a</sub>), 1.69 (1H, dt, *J* 13.8, 2.7 Hz, 17-H<sub>b</sub>). **<sup>13</sup>C NMR** (126 MHz,  $CDCl_3$ ):  $\delta$  152.8 (7-C), 144.2 (4'-C), 137.3 (1'-C), 135.8 (15-C), 131.3 (3-C or 5-C), 130.7 (3-C or 5-C), 130.2 (3'-C and 5'-C), 130.0 (6-C or 13-C), 129.8 (12-C), 127.1 (2'-C and 6'-C), 126.2 (2-C), 124.8 (13-C or 6-C), 122.9 (11-C), 121.1 (10-C), 121.0 (4-H), 117.2 (14-C), 69.0 (9-C), 50.0 (1-C), 25.3 (17-C), 21.7 ( $CH_3$ ). **FT-IR:** 2922, 2851, 1605, 1582, 1483, 1454, 1359, 1342, 1307, 1289, 1273, 1213. **HR-MS:** calc. for  $[M+H]^+$   $C_{24}H_{18}O_2NS$ : 378.1158 found: 378.11589.

### 16-(2-chloro-benzenesulfonyl)-8-oxa-16-azatetracyclo[7.7.1.0<sup>2,7</sup>.0<sup>10,15</sup>]heptadeca-2(7),3,5,10(15),11,13-hexaene (34g)



**34g**

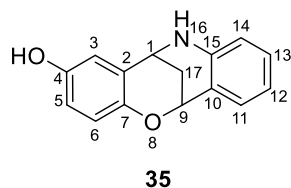
Prepared according to general procedure G. 20 mg **31a** and 5 eq. acid chloride were used. Flash column chromatography eluting with 10-20% EtOAc in *n*-pentane afforded the desired product **34g** (17.6 mg, 44.23  $\mu$ mol, 44%) as white solid. **<sup>1</sup>H-NMR** (500 MHz,  $CDCl_3$ ):  $\delta$  8.18-8.13 (1H, m, 6'-H), 7.58 (1H, dd, *J* 8.4, 1.1 Hz, 11-H), 7.54-7.49 (2H, m, 4'-H and 3'-H), 7.45-7.38 (3H, m, 3-H, 12-H and 5'-H), 7.21-7.11 (2H, m, 5-H and 13-H), 7.05 (1H, td, *J* 7.5, 1.1 Hz, 6-H), 6.88 (1H, td, *J* 7.5, 1.2 Hz, 4-H), 6.75 (1H, dd, *J* 8.2, 1.2 Hz, 14-H), 5.78-5.54 (1H, m, 9-H), 5.34-5.25 (1H, m, 1-H), 2.37-2.24 (2H, m, 17-H<sub>a</sub> and 17-H<sub>b</sub>). **<sup>13</sup>C NMR** (126 MHz,  $CDCl_3$ ):  $\delta$  152.8 (7-C), 137.6 (Ar-C<sub>q</sub>), 135.8 (Ar-C<sub>q</sub>), 134.3 (3'-C or 4'-C), 132.6 (Ar-C<sub>q</sub>), 132.5 (3'-C or 4'-C), 132.4 (6'-C), 131.6 (3-C, 12-C or 5'-C), 130.5 (5-C or 13-C), 130.3 (3-C, 12-C or 5'-C), 129.7 (5-C or 13-C), 127.3 (3-C, 12-C or 5'-C), 125.5 (2-C), 124.0 (6-C), 121.1 (10-C), 121.0 (4-C), 120.8 (11-C), 117.2 (14-C), 69.2 (9-C), 49.7 (1-C), 26.4 (17-C). **FT-IR:** 3076, 2955, 2360,

2222, 2211, 2162, 2150, 2036, 1994, 1963, 1606, 1583, 1486, 1455, 1430, 1344, 1293, 1279, 1255, 1217. **HR-MS**: calc. for  $[M+H]^+$   $C_{24}H_{18}O_2NS$ : 398.0611, found: 398.0612.

### Functionalisation of compound **31g** (C-R)

#### Preparation of compound **35**

#### 4-hydroxy-5-methyl-8-oxa-16-azatetracyclo[7.7.1.0<sup>2,7</sup>.0<sup>10,15</sup>]heptadeca-2,4,6,10,12,14-hexaene (**35**)



A vacuum dried schlenck vial was equipped with a stirring bar and 65 mg **31g**. The compound was dissolved in anhydrous dichloromethane (7.8 mL). Borontribromide (5 eq., 225  $\mu$ L) was added under a stream of argon at 0 °C. The reaction was allowed to warm to ambient temperature and stirred at this temperature for 1.5 hour. *Besides formation of the desired product, the formation of a ring-opened side product (internal ether cleavage and aromatisation to quinoline) was observed.* The reaction was quenched by addition 25% aqueous ammonia solution (5 mL), followed by addition of water (5 mL) at 0 °C and the mixture was stirred for 15 min, then extracted with DCM (3x15 mL). The organic phases were combined, washed with saturated brine, and dried over  $Mg_2SO_4$ . The crude material was concentrated under reduced pressure and purified by silica flash column chromatography eluting with 20-40% EtOAc in *n*-pentane to afford product **35** (62.3 mg, 0.26 mmol, 66%). **<sup>1</sup>H-NMR** (500 MHz,  $CDCl_3$ , NH, OH not observed):  $\delta$  7.31 (1H, dd, *J* 7.6, 1.5 Hz, 11-H), 7.08 (1H, ddd, *J* 8.0, 7.3, 1.5 Hz, 13-H), 6.77 (1H, td, *J* 7.3, 1.2 Hz, 12-H), 6.69 (1H, d, *J* 2.9 Hz, 3-H), 6.66 (1H, d, *J* 8.7 Hz, 5-H or 6-H), 6.63-6.57 (2H, m, 5-H or 6-H and 14-H), 5.37-5.05 (1H, m, 9-H), 4.40-4.29 (1H, m, 1-H), 2.33 (1H, dt, *J* 13.2, 3.2 Hz, 17-H<sub>a</sub>), 2.23-2.19 (1H, m, 17-H<sub>b</sub>). **<sup>13</sup>C NMR** (126 MHz,  $CDCl_3$ ):  $\delta$  149.0 (4-C), 146.7 (7-C), 142.3 (15-C), 131.1 (11-C), 129.8 (13-C), 125.2 (2-C), 122.3 (10-C), 119.1 (12-C), 117.9 (5-C or 6-C), 116.6 (5-C or 6-C and 14-C), 115.0 (3-C), 69.0 (9-C), 46.1 (1-C), 26.4 (17-C). **FT-IR**: 3494, 3366, 2961, 2114, 1605, 1494, 1483, 1440, 1346, 1335, 1325, 1278. **HR-MS**: calc. for  $[M+H]^+$   $C_{15}H_{14}O_2N$ : 240.1019 found 240.1022.

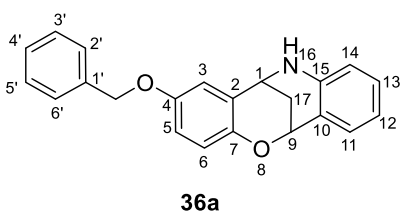
## Experimental

### General Procedure H: Preparation of chromaline ethers

**35** (15 mg, 1 eq.) and triphenylphosphine (1.3 eq.) were taken under argon in a vacuum-dried schlenk vial. 0.4 mL of dry THF were added and the solids dissolved, then isopropanol was added, and the solution was cooled to 0 °C. Diisopropylazodicarboxylate (DIAD) (1.3 equiv.) was added carefully, and the mixture was then stirred for 15 min at 0 °C, before it was allowed to warm to rt and stirred for 5 h. After complete conversion of starting material, the reaction was diluted with 3 mL *n*-pentane and passed through a syringe filter (3x). Then the solvents were removed under reduced pressure and the crude material purified by flash column chromatography using 10-50% EtOAc in *n*-pentane.

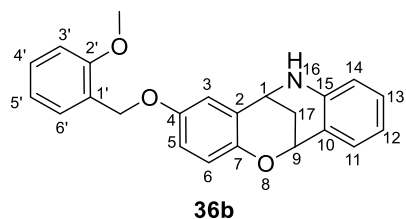
### Preparation of chromaline ethers (36)

#### 5-(benzyloxy)-8-oxa-16-azatetracyclo[7.7.1.0<sup>2,7</sup>.0<sup>10,15</sup>]heptadeca-2,4,6,10,12,14-hexaene (36a)



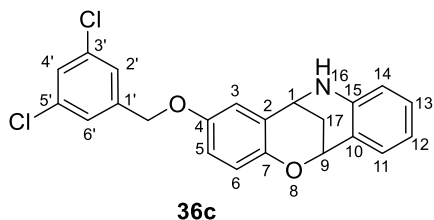
Prepared according to procedure H to afford product **36a** (16.5 mg, 50.09  $\mu$ mol, 80%). **<sup>1</sup>H-NMR** (500 MHz, CDCl<sub>3</sub>, OH not observed):  $\delta$  7.42-7.35 (4H, m, 2'-H, 3'-H, 5'-H and 6'-H), 7.34-7.30 (2H, m, 4'-H and 11-H), 7.09 (1H, ddd, *J* 8.3, 7.2, 1.5 Hz, 13-H), 6.81-6.71 (3H, m, 3-H, 5-H, 6-H, and 12-H), 6.59 (1H, d, *J* 8.3 Hz, 14-H), 5.30-5.26 (1H, m, 9-H), 4.98 (2H, s, CH<sub>2</sub>), 4.37-4.28 (1H, m, 1-H), 2.35 (1H, dt, *J* 13.2, 3.2 Hz, 17-H<sub>a</sub>), 2.21 (1H, dt, *J* 13.2, 2.6 Hz, 17-H<sub>b</sub>). **<sup>13</sup>C NMR** (126 MHz, CDCl<sub>3</sub>):  $\delta$  152.7 (4-C), 147.0 (7-C), 143.1 (15-C), 137.3 (1'-C), 131.2 (11-C), 129.9 (13-C), 128.7 (3'-C and 5'-C), 128.1 (4'-C), 127.6 (2'-C and 6'-C), 125.6 (2-C), 122.1 (10-C), 118.7 (12-H), 117.9 (5-C or 6-C), 116.2 (14-C), 116.0 (5-C or 6-C), 114.9 (3-C), 70.9 (CH<sub>2</sub>), 69.3 (9-C), 46.3 (1-C), 26.7 (17-C). **FT-IR**: 3420, 3351, 3033, 2928, 1608, 1492, 1466, 1454, 1430, 1422, 1384, 1353, 1341, 1313, 1266, 1243, 1213. **HR-MS**: calc. for [M+H]<sup>+</sup> C<sub>22</sub>H<sub>20</sub>O<sub>2</sub>N: 330.1489 found 330.1486.

**5-(2-methoxy-benzyloxy)-8-oxa-16-azatetracyclo[7.7.1.0<sup>2,7</sup>.0<sup>10,15</sup>]heptadeca-2,4,6,10,12,14-hexaene (36b)**



Prepared according to procedure H to afford product **36b** (8.8 mg, 24.48  $\mu\text{mol}$ , 29%). **<sup>1</sup>H-NMR** (500 MHz,  $\text{CDCl}_3$ , NH not observed):  $\delta$  7.43 (1H, d,  $J$  6.0 Hz, 6'-H), 7.32-7.27 (2H, m, 4'-H and 11-H), 7.11-7.06 (1H, m, 13-H), 6.98-6.94 (1H, m, 5'-H), 6.90 (1H, d,  $J$  8.2 Hz, 3'-H), 6.80-6.76 (2H, m, 3-H and 5-H), 6.76-6.70 (2H, m, 6-H and 12-H), 6.56 (1H, d,  $J$  8.1 Hz, 14-H), 5.28 (1H, br s, 9-H), 5.02 (2H, s,  $\text{CH}_2$ ), 4.33 (1H, br s, 1-H), 3.85 (3H, s,  $\text{OCH}_3$ ), 2.35 (1H, dt,  $J$  13.1, 3.2 Hz, 17-H<sub>a</sub>), 2.20 (1H, dt,  $J$  13.1, 2.6 Hz, 17-H<sub>b</sub>). **<sup>13</sup>C NMR** (126 MHz,  $\text{CDCl}_3$ ):  $\delta$  156.9 (2'-C), 152.9 (4-C), 146.9 (7-C), 142.1 (15-C), 131.2 (11-C), 129.8 (13-C), 129.0 (4'-C), 128.8 (6'-C), 125.7 (1'-C), 125.6 (2-C), 122.0 (10-C), 120.7 (5'-C), 118.5 (12-C), 117.9 (6-C), 116.2 (3-C or 5-C), 115.9 (14-C), 114.8 (3-C or 5-C), 110.3 (3'-C), 69.3 (9-C), 65.9 ( $\text{CH}_2$ ), 55.5 ( $\text{OCH}_3$ ), 46.3 (1-C), 26.7 (17-C). **FT-IR**: 3382, 2931, 2524, 2182, 2156, 2026, 1974, 1605, 1588, 1491, 1463, 1437, 1379, 1343, 1312, 1272, 1243. **HR-MS**: calc. for  $[\text{M}+\text{H}]^+$   $\text{C}_{23}\text{H}_{22}\text{O}_3\text{N}$ : 360.1594, found: 360.1593.

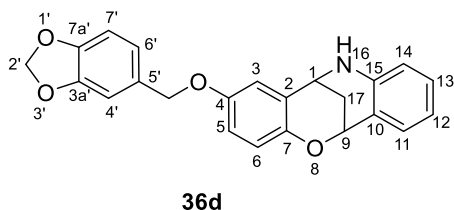
**5-(3,5-dichloro-benzyloxy)-8-oxa-16-azatetracyclo[7.7.1.0<sup>2,7</sup>.0<sup>10,15</sup>]heptadeca-2,4,6,10,12,14-hexaene (36c)**



Prepared according to procedure H to afford product **36c** (7.8 mg, 19.58  $\mu\text{mol}$ , 23%). **<sup>1</sup>H-NMR** (500 MHz,  $\text{CDCl}_3$ , NH not observed):  $\delta$  7.34-7.28 (4H, m, 2'-H, 4'-H, 6'-H and 11-H), 7.14-7.06 (1H, m, 13-H), 6.76-6.69 (4H, m, 3-H, 5-H, 6-H and 12-H), 6.56 (1H, d,  $J$  7.9 Hz, 14-H), 5.29 (1H, br s, 9-H), 4.97-4.87 (2H, m,  $\text{CH}_2$ ), 4.33 (1H, br s, 1-H), 2.35 (1H, dt,  $J$  13.3, 3.3 Hz, 17-H<sub>a</sub>), 2.20 (1H, dt,  $J$  13.3, 2.6 Hz, 17-H<sub>b</sub>). **<sup>13</sup>C NMR** (126 MHz,  $\text{CDCl}_3$ )  $\delta$  152.1 (4-C), 147.5 (7-C), 143.4 (15-C), 140.9 (1'-C), 135.3 (3'-C and 5'-C), 131.2 (11-C), 129.9 (13-C), 128.1 (4'-C), 126.1 (2-C), 125.6 (2'-C and 6'-C), 121.8 (10-C), 118.5 (3-C, 5-C or 6-C), 118.1 (12-C), 116.0 (3-C, 5-C or 6-C), 115.8 (14-C), 115.1 (3-C, 5-C or 6-C), 69.4 ( $\text{CH}_2$ ), 69.4 (9-C), 46.2 (1-C), 26.6 (17-C). **FT-IR**: 3381, 2929, 2851, 2083, 1608, 1571, 1491, 1431, 1370, 1344, 1312, 1273, 1258, 1243. **HR-MS**: calc. for  $[\text{M}+\text{H}]^+$   $\text{C}_{22}\text{H}_{18}\text{O}_2\text{NCl}_2$ : 398.0709, found: 398.0705, calc. for  $[\text{M}+\text{H}]^+$   $\text{C}_{22}\text{H}_{18}\text{O}_2\text{NCl}^{37}\text{Cl}$ : 400.0679, found: 400.074, calc. for  $[\text{M}+\text{H}]^+$   $\text{C}_{22}\text{H}_{18}\text{O}_2\text{N}^{37}\text{Cl}_2$ : 402.0650, found: 402.0646.

## Experimental

### 5-[(2H-1,3-benzodioxol-5-yl)methoxy]-8-oxa-16-azatetracyclo[7.7.1.0<sup>2,7</sup>.0<sup>10,15</sup>]heptadeca-2,4,6,10,12,14-hexaene (36d)

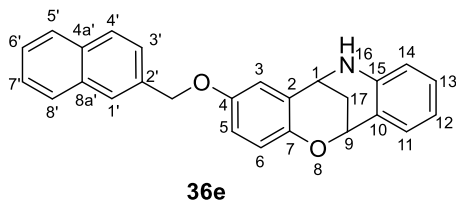


36d

Prepared according to procedure H to afford product **36d** (7.8 mg, 19.58  $\mu\text{mol}$ , 23%). <sup>1</sup>H-NMR (500 MHz, CDCl<sub>3</sub>, NH not observed):  $\delta$  7.32 (1H, dd, *J* 7.6, 1.5 Hz, 11-H), 7.11 (1H, ddd, *J* 8.1, 7.3, 1.5 Hz, 13-H), 6.90 (1H, d, *J* 1.7 Hz, 4'-H), 6.85 (1H, dd, *J* 7.9, 1.7 Hz, 6'-H),

6.82-6.70 (5H, m, 3-H, 5-H, 6-H, 12-H and 7'-H), 6.64 (1H, d, *J* 8.1 Hz, 14-H), 5.96 (2H, s, 2'-CH<sub>2</sub>), 5.30-5.26 (1H, m, 9-H), 4.88-4.86 (2H, m, CH<sub>2</sub>), 4.40-4.36 (1H, m, 1-H), 2.36 (1H, dt, *J* 13.3, 3.2 Hz, 17-H<sub>a</sub>), 2.25 (1H, dt, *J* 13.3, 2.6 Hz, 17-H<sub>b</sub>). <sup>13</sup>C NMR (126 MHz, CDCl<sub>3</sub>)  $\delta$  152.6 (4-C), 148.0 (3a'-C or 7a'-C), 147.5 (3a'-C or 7a'-C), 147.0 (7-C), 142.3 (15-C), 131.3 (11-C), 131.1 (5'-C), 129.9 (13-C), 125.1 (2-C), 122.5 (10-C), 121.4 (6'-C), 119.3 (12-C), 118.3, 118.0 (3-C, 5-C or 6-C), 116.5 (14-C), 116.4 (3-C, 5-C or 6-C), 114.9 (7'-C), 108.6 (3-C, 5-C or 6-C), 108.5 (4'-C), 101.2 (2'-CH<sub>2</sub>), 70.8 (CH<sub>2</sub>), 69.2 (9-C), 46.4 (1-C), 26.6 (17-C). **FT-IR:** 3375, 2924, 2349, 2322, 2097, 1608, 1582, 1496, 1455, 1443, 1423, 1351, 1313, 1270, 1250, 1234. **HR-MS:** calc. for [M+H]<sup>+</sup> C<sub>23</sub>H<sub>20</sub>O<sub>4</sub>N: 374.1387, found: 374.1384.

### 5-[(naphthalen-2-yl)methoxy]-8-oxa-16-azatetracyclo[7.7.1.0<sup>2,7</sup>.0<sup>10,15</sup>]heptadeca-2,4,6,10,12,14-hexaene (36e)



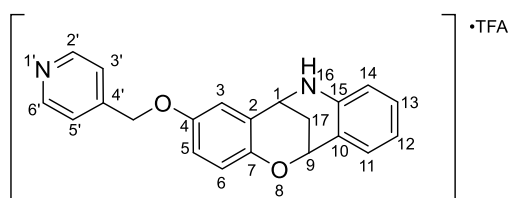
36e

Prepared according to procedure H to afford product **36e** (7.8 mg, 19.58  $\mu\text{mol}$ , 23%). <sup>1</sup>H-NMR (600 MHz, CDCl<sub>3</sub>, NH not observed):  $\delta$  8.04 (1H, d, *J* 8.1 Hz, 3'-H or 4'-H), 7.90 (1H, d, *J* 7.4 Hz, 5'-H or 8'-H), 7.85 (1H, d, *J* 8.0 Hz, 5'-H or 8'-H), 7.59-7.50 (3H, m, 1'-H, 3'-H

or 4'-H and 7'-H or 6'-H), 7.46 (1H, t, *J* 7.4 Hz, 7'-H or 6'-H), 7.32 (1H, d, *J* 7.6 Hz, 11-H), 7.10 (1H, t, *J* 7.9 Hz, 13-H), 6.87-6.82 (2H, m, 3-H and 5-H), 6.80-6.71 (2H, m, and 12-H and 6-H), 6.57 (1H, d, *J* 7.9 Hz, 14-H), 5.44-5.38 (2H, m, CH<sub>2</sub>), 5.31-5.27 (1H, m, 9-H), 4.33 (1H, s, 1-H), 2.39-2.30 (1H, m, 17-H<sub>a</sub>), 2.23-2.17 (1H, m, 17-H<sub>b</sub>). <sup>13</sup>C NMR (126 MHz, CDCl<sub>3</sub>)  $\delta$  152.8 (4-C), 147.2 (7-C), 143.5 (15-C), 133.9 (naphthalene-Ar-C<sub>q</sub>), 132.7 (naphthalene-Ar-C<sub>q</sub>), 131.7 (naphthalene-Ar-C<sub>q</sub>), 131.2 (11-C), 129.9 (13-C), 129.1 (naphthalene-C), 128.8 (naphthalene-C), 126.7 (naphthalene-C), 126.6 (naphthalene-C), 126.0 (naphthalene-C), 126.0 (2-C), 125.5 (naphthalene-C), 123.9 (naphthalene-C), 121.9 (10-C), 118.4 (12-C), 118.0 (6-C), 116.2 (5-C), 115.8 (14-C), 115.0 (3-C), 69.5 (CH<sub>2</sub>), 69.4 (9-C), 46.3 (1-C), 26.7 (17-C). **FT-**

**IR:** 2926, 2365, 2175, 2158, 2026, 2008, 1976, 1607, 1490, 1437, 1380, 1345, 1312, 1267, 1235. **HR-MS:** calc. for  $[M+H]^+$   $C_{26}H_{22}O_2N$ : 380.1645, found: 380.1645.

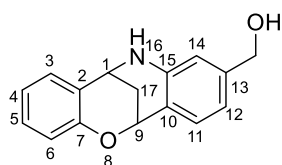
**5-[(pyridin-4-yl)methoxy]-8-oxa-16-azatetracyclo[7.7.1.0<sup>2,7</sup>.0<sup>10,15</sup>]heptadeca-2,4,6,10,12,14-hexaene (36f)**



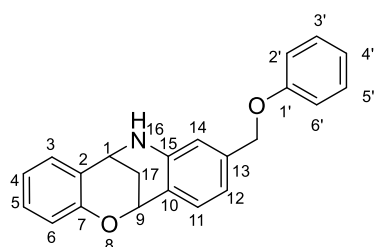
**36f**

Prepared according to procedure H to afford product **36f** (3.3 mg, 7.43  $\mu$ mol, 23%). The product was additionally purified by preparative HPLC (to remove TPPO), after acidic HPLC the TFA salt of **36f** was obtained. **<sup>1</sup>H-NMR** (600 MHz,  $CDCl_3$ , NH

not observed):  $\delta$  8.78 (2H, app. d,  $J$  6.2 Hz, 2'-H and 6'-H), 7.76 (2H, app. d,  $J$  5.6 Hz, 3'-H and 5'-H), 7.30 (1H, dd,  $J$  7.6, 1.6 Hz, 11-H), 7.11-7.06 (1H, m, 13-H), 6.80-6.71 (4H, m, 3-H, 5-H, 6-H and 12-H), 6.55 (1H, d,  $J$  8.1 Hz, 14-H), 5.32-5.27 (1H, m, 9-H), 5.17 (2H, s,  $CH_2$ ), 4.36-4.31 (1H, m), 2.34 (1H, dt,  $J$  13.2, 3.2 Hz, 17-H<sub>a</sub>), 2.21 (1H, dt,  $J$  13.2, 2.6 Hz, 17-H<sub>b</sub>). **<sup>13</sup>C NMR** (126 MHz,  $CDCl_3$ )  $\delta$  154.5 (4'-C), 151.3 (4-C), 148.1 (7-C), 144.2 (2'-C and 6'-C), 143.3 (15-C), 131.3 (11-C), 130.0 (13-C), 126.5 (2-C), 123.3 (3'-C and 5'-C), 121.7 (10-C), 118.5 (3-C, 5-C or 6-C), 118.4 (12-C), 115.9 (3-C, 5-C or 6-C), 115.7 (14-C), 115.2 (3-C, 5-C or 6-C), 69.5 (9-C), 68.5 ( $CH_2$ ), 46.1 (1-C), 26.6 (17-C). **FT-IR:** 3354, 2924, 1675, 1608, 1494, 1426, 1312. **HR-MS:** calc. for  $[M+H]^+$   $C_{21}H_{19}O_2N_2$ : 331.1441, found: 331.1439.

**Functionalisation of compound 31t (Q-R)****Preparation of compound 37****{8-oxa-16-azatetracyclo[7.7.1.0<sup>2,7</sup>.0<sup>10,15</sup>]heptadeca-2(7),3,5,10(15),11,13-hexaen-13-yl}methanol (37)****37**

**31t** (30 mg, 1 eq.) was dissolved in anhydrous THF (0.5 mL) and LiAlH<sub>4</sub> (2eq) was added at 0°C. The mixture then was allowed to warm to rt stirred for 1 h, until full reduction of the ester (uHPLC-MS). The reaction was quenched by careful addition of MeOH (0.1 mL) then add water (1 mL). Then, the aqueous phase was extracted (3x DCM), the organics combined and dried over Mg<sub>2</sub>SO<sub>4</sub> and the solvents removed under reduced pressure. Flash column chromatography eluting with 10 to 50% EtOAc in *n*-pentane gave the title compound **37** (3.3 mg, 7.43 μmol, 23%). **<sup>1</sup>H-NMR** (500 MHz, CDCl<sub>3</sub>, NH not observed): δ 7.29 (1H, d, *J* 7.8 Hz, 11-H), 7.15 (1H, dd, *J* 7.4, 1.7 Hz, 3-H), 7.10 (1H, ddd, *J* 8.5, 7.4, 1.7 Hz, 5-H), 6.85 (1H, td, *J* 7.4, 1.1 Hz, 4-H), 6.80 (1H, dd, *J* 8.5, 1.1 Hz, 6-H), 6.69 (1H, dd, *J* 7.8, 1.6 Hz, 12-H), 6.57 (1H, d, *J* 1.6 Hz, 14-H), 5.33-5.25 (1H, m, 9-H), 4.53 (2H, s, CH<sub>2</sub>), 4.41-4.33 (1H, m, 1-H), 2.36 (1H, dt, *J* 13.2, 3.3 Hz, 17-H<sub>a</sub>), 2.20 (1H, dt, *J* 13.2, 2.7 Hz, 17-H<sub>b</sub>). **<sup>13</sup>C NMR** (126 MHz, CDCl<sub>3</sub>) δ 152.8 (7-C), 143.6 (15-C), 142.7 (13-C), 131.4 (11-C), 129.1 (5-C), 128.9 (3-C), 125.3 (2-C), 121.1 (10-C), 120.3 (4-C), 117.2 (6-C), 116.8 (12-C), 113.9 (14-C), 69.2 (9-C), 65.2 (CH<sub>2</sub>), 45.8 (1-C), 26.5 (17-C). **FT-IR**: 3192, 2937, 2833, 1625, 1580, 1524, 1483, 1455, 1420, 1346, 1319, 1280, 1248, 1213. **HR-MS**: calc. for [M+H]<sup>+</sup> C<sub>16</sub>H<sub>16</sub>O<sub>2</sub>N: 254.1176, found: 254.1175.

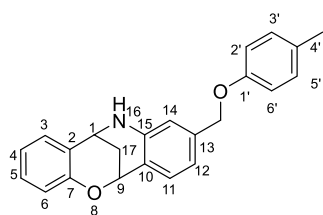
**Preparation of chromaline ethers (38)****13-(phoxymethyl)-8-oxa-16-azatetracyclo[7.7.1.0<sup>2,7</sup>.0<sup>10,15</sup>]heptadeca-2(7),3,5,10(15),11,13-hexaene (38a)****38a**

Prepared according to procedure H to afford product **38a** (9.5 mg, 28.84 μmol, 73%). **<sup>1</sup>H-NMR** (700 MHz, CDCl<sub>3</sub>, NH not observed): δ 7.32 (1H, d, *J* 7.8 Hz, 11-H), 7.29-7.25 (2H, m, 2'-H and 6'-H), 7.15 (1H, dd, *J* 7.6, 1.7 Hz, 3-H), 7.11 (1H, ddd, *J* 8.2, 7.6, 1.7 Hz, 5-H), 6.96-6.91 (3H, m, 3'-H, 4'-H and 5'-H), 6.85 (1H, td, *J* 7.6, 1.2 Hz, 4-H), 6.81 (1H, dd, *J* 8.2, 1.2 Hz, 6-H), 6.77 (1H, dd, *J* 7.8, 1.6 Hz, 12-H), 6.65 (1H, d, *J* 1.6 Hz, 14-H), 5.38-5.30 (1H, m, 9-H), 4.91 (2H, s, CH<sub>2</sub>), 4.42-4.34 (1H, m, 1-H), 2.36 (1H, dt, *J* 13.1, 3.2 Hz, 17-H<sub>a</sub>), 2.21 (1H,



dt,  $J$  13.1, 2.6 Hz, 17-H<sub>b</sub>).  $^{13}\text{C}$  NMR (176 MHz, CDCl<sub>3</sub>) 158.9 (1'-C), 153.0 (7-C), 143.7 (15-C), 138.9 (13-C), 131.5 (11-C), 129.6 (2'-C and 6'-C), 129.2 (3-C or 5-C), 129.1 (3-C or 5-C), 125.4 (2-C), 121.5 (10-C), 121.0 (4'-C), 120.5 (4-C), 117.4 (6-C or 12-C), 117.3 (6-C or 12-C), 114.9 (3'-C and 5'-C), 114.5 (14-C), 69.8 (CH<sub>2</sub>), 69.3 (9-C), 46.0 (1-C), 26.6 (17-C). **FT-IR:** 3382, 2929, 2852, 2160, 2035, 2013, 1971, 1963, 1731, 1621, 1598, 1583, 1484, 1456, 1434, 1376, 1347, 1321, 1301, 1277. **HR-MS:** calc. for [M+H]<sup>+</sup> C<sub>22</sub>H<sub>20</sub>O<sub>2</sub>N: 330.1488, found: 330.1487.

**13-[(4-methylphenoxy)methyl]-8-oxa-16-azatetracyclo[7.7.1.0<sup>2,7</sup>.0<sup>10,15</sup>]heptadeca-2(7),3,5,10(15),11,13-hexaene (SZ591)**



Prepared according to procedure H to afford product **38b** (3.6 mg, 10.48  $\mu\text{mol}$ , 27%).  $^1\text{H-NMR}$  (700 MHz, CDCl<sub>3</sub>, NH not observed):  $\delta$  7.31 (1H, d,  $J$  7.8 Hz, 11-H), 7.15 (1H, dd,  $J$  7.4, 1.7 Hz, 3-H), 7.11 (1H, ddd,  $J$  8.2, 7.4, 1.7 Hz, 5-H), 7.07-7.03 (2H, m, 2'-H and 6'-H), 6.85 (1H, td,  $J$  7.4, 1.2 Hz, 4-H), 6.83-6.79 (3H, m, 6-H and 3'-H and 5'-H), 6.76 (1H, dd,  $J$  7.8, 1.6 Hz, 12-H), 6.65 (1H, s, 14-H), 5.33 (1H, td,  $J$  2.7, 1.4 Hz, 9-H), 4.88 (2H, s, CH<sub>2</sub>), 4.41-4.37 (1H, m, 1-H), 2.36 (1H, dt,  $J$  13.1, 3.2 Hz, 17-H<sub>a</sub>), 2.27 (3H, s, CH<sub>3</sub>), 2.21 (1H, dt,  $J$  13.1, 2.7 Hz, 17-H<sub>b</sub>).  $^{13}\text{C}$  NMR (176 MHz, CDCl<sub>3</sub>):  $\delta$  156.8 (1'-C), 153.0 (7-C), 139.1 (15-C), 131.5 (11-C), 130.3 (4'-C), 130.0 (2'-C and 6'-C), 129.2 (3-C), 129.1 (5-C), 125.4 (2-C), 121.5 (10-C), 120.5 (4-C), 117.4 (12-C or 6-C), 117.4 (12-C or 6-C), 114.7 (3'-C and 5'-C), 114.6 (14-C), 70.0 (CH<sub>2</sub>), 69.3 (9-C), 46.0 (1-C), 26.6 (17-C), 20.6 (17-C). **FT-IR:** 3379, 2925, 2858, 1723, 1620, 1582, 1510, 1483, 1457, 1431, 1375, 1348, 1322, 1292, 1240, 1212. **HR-MS:** calc. for [M+H]<sup>+</sup> C<sub>23</sub>H<sub>22</sub>O<sub>2</sub>N: 344.1645, found: 344.1641.

### 6.3. Materials, Instruments and Methods for Biological Experiments

<b>Name</b>	<b>Supplier</b>
<b>6-well plate</b>	6-well plate, clear, flat bottom Sarstedt AG & Co
<b>96-well plate, clear, conical bottom</b>	Sarstedt AG & Co
<b>96-well plate, clear, flat bottom</b>	Greiner falcon
<b>Acrylamide / Bisacrylamide solution</b>	AppliChem
<b>Ammonium persulfate (APS)</b>	Serva
<b>Bovine serum albumin (BSA)</b>	Serva
<b>Bromophenol blue</b>	Carl Roth
<b>Cell culture flask T175</b>	Sarstedt AG & Co
<b>Cell culture flask T25</b>	Sarstedt AG & Co
<b>Cell culture flask T75</b>	Sarstedt AG & Co
<b>CellCarrier-384 Ultra</b>	PerkinElmer
<b>Dimethyl sulfoxide (DMSO)</b>	Sigma-Aldrich
<b>Ethylene diamine tetraacetic acid (EDTA)</b>	Gerbu
<b>Fetal bovine serum (FBS)</b>	Gibco
<b>Hoechst-33342</b>	Invitrogen
<b>Hydrochloric acid (HCl)</b>	AppliChem
<b>MEM non-essential amino acids</b>	PAN Biotech
<b>Methylene blue</b>	Fisher Scientific GmbH
<b>Micro reaction tube 0.5 mL</b>	Sarstedt AG & Co
<b>Micro reaction tube, 1.5 mL</b>	Sarstedt AG & Co
<b>Micro reaction tube, 1.5 mL, protein low-binding</b>	Eppendorf AG
<b>Micro reaction tube, 2.0 mL</b>	Sarstedt AG & Co
<b>Milk powder, non-fat dy</b>	AppliChem
<b>NP-40 alternative</b>	Calbiochem
<b>PBS tablets</b>	Jena Bioscience
<b>PBS-based Odyssey® Blocking buffer</b>	Li-COR Biosciences
<b>Pipette tips, 10 µL Sarstedt AG &amp; Co</b>	Sarstedt AG & Co
<b>Pipette tips, 1000 µL</b>	Diagonal GmbH & Co. KG
<b>Pipette tips, 200 µL</b>	Diagonal GmbH & Co. KG

Name	Supplier
<b>Polycarbonate ultracentrifugation tubes, 0.5 mL</b>	Beckman Coulter Inc
<b>Polysorbate 20 (Tween® 20)</b>	Sigma-Aldrich
<b>Polyvinylidene difluoride (PVDF) membrane</b>	Merck KGaA
<b>Sample tube, 15 mL</b>	Sarstedt AG & Co
<b>Sample tube, 50 mL</b>	Sarstedt AG & Co
<b>Serological pipette, 1 mL</b>	Sarstedt AG & Co
<b>Serological pipette, 10 mL</b>	Sarstedt AG & Co
<b>Serological pipette, 25 mL</b>	Sarstedt AG & Co
<b>Serological pipette, 5 mL</b>	Sarstedt AG & Co
<b>Serological pipette, 50 mL</b>	Sarstedt AG & Co
<b>Trypsin/EDTA solution</b>	Pan Biotech

### Buffer

Name	Composition
<b>NP-40 lysis buffer</b>	50 mM Tris-HCl, pH 8.0 150 mM NaCl 1 % NP-40 alternative
<b>Phosphate-buffered saline (PBS)</b>	2.7 mM KCl 1.5 mM KH <sub>2</sub> PO <sub>4</sub> 136.9 mM NaCl 8.1 mM Na <sub>2</sub> HPO <sub>4</sub> pH 7.4
<b>PBS-T</b>	0.1 % (v/v) Tween® 20
<b>SDS running buffer (10x) 250 mM Tris</b>	2.5 M glycine 35 mM SDS SDS sample buffer (5x) 0.5 M Tris-HCl, pH 6.8 40 % (v/v) glycerol 277 mM SDS

## Experimental

<b>Name</b>	<b>Composition</b>
	400 mM DTE 0.3 mM bromophenol blue
<b>SDS separating gel buffer</b>	1.5 M Tris pH 8.8
<b>SDS stacking gel buffer</b>	1.0 M Tris pH 6.8
<b>Transfer buffer</b>	25 mM Tris 188 mM glycine 10 % (v/v) methanol
<b>Tris-buffered saline (TBS)</b>	50 mM Tris-HCl 150 mM NaCl pH 7.5
<b>TBS-T</b>	TBS 0.1 % (v/v) Tween® 20

## Cell culture media

<b>Name</b>	<b>Supplements</b>	<b>Product number</b>	<b>Supplier</b>
<b>DMEM-based growth medium</b>	10 % (v/v) FBS 1 mM sodium pyruvate 1x MEM non-essential aminoacids	P04-03550	PAN Biotech GmbH, Germany
<b>DMEM-based growth Medium (w/o glucose)</b>	10 % (v/v) FBS 1 mM sodium pyruvate 1x MEM non-essential aminoacids	P04-01548S1	PAN Biotech GmbH, Germany
<b>MEM-based growth medium</b>	10 % (v/v) FBS 1 mM sodium pyruvate 1x MEM non-essential aminoacids	P04-08500	PAN Biotech GmbH, Germany

**Antibodies**

<b>Antigen</b>	<b>Origin</b>	<b>Supplier</b>	<b>Blocking buffer</b>	<b>Dilution</b>	<b>Product number</b>
<b>Vinculin</b>	mouse	ThermoFisher	5% milk (TBS)	1:10000	V9131
<b>PI3 Kinase Class III (D4E2)</b>	Rabbit	Cell Signalling	Odyssey blocking buffer containing 0.2% Tween-20	1:5000	mAb #3358
<b>IRDye® 800CW (anti-Rabbit IgG)</b>	Donkey	LiCOR	Odyssey blocking buffer containing 0.2% Tween-20 and 0.1 % SD	1:10000	P/N 925-32213

**Instruments**

<b>Description</b>	<b>Name</b>	<b>Supplier</b>
<b>Automated Fluorescence Microscope</b>	IncuCyte S3	Sartorius AG
<b>Centrifuge</b>	5810R	Eppendorf AG
	5417R	Eppendorf AG
	5424R	Eppendorf AG
	5430	Eppendorf AG
<b>Clean bench (Cell culture)</b>	NU-437-400E	ibs tecnomara GmbH
<b>Gel and blot documentation system.</b>	ChemiDoc™ MP	Bio-Rad Laboratories, Inc
<b>Gradient thermal cycler</b>	Mastercycler ep gradient	Eppendorf AG
<b>Plate reader</b>	Sparcs	Tecan Group AG

**Software**

<b>Description</b>	<b>Name</b>	<b>Supplier</b>
<b>Data analysis software</b>	Prism	GraphPad Software
	Excel	Microsoft Corporation
<b>Gel / Immunoblot analysis software</b>	ImageLab	Bio-Rad Laboratories, Inc
<b>Microscopy &amp; image analysis software</b>	IncuCyte® S3 2019B Rev2	Sartorius AG
	MetaMorph Molecular	Devices, LLC

## 6.4 Biological Methods

### 6.4.1 Cell Culture

MCF7 cells stably transfected with eGFP-LC3 (MCF7-GFP-LC3) were cultured at 37 °C with 5% CO<sub>2</sub> using Eagle's MEM (Gibco cat# 21090-022) containing 10% FBS (Invitrogen cat# 10500-084), 1% L-Glutamine (Invitrogen cat# 25030-081), 1% sodium pyruvate (PAN Biotech cat# P04-43100), 1% NEAA (PAN Biotech cat# P08-32100), 0.01 mg/mL bovine insulin (Sigma Aldrich cat# I9278) and 200 µg/ml G418 as the medium.

MCF7 wt (#2011) cells were cultured in standard DMEM (PAN Biotech, cat# P04-03500) supplemented with 10% FBS (Invitrogen cat# 10500-084), 1% sodium pyruvate (PAN Biotech, cat# P04-43100), 1% NEAA (PAN Biotech, cat# P08-32100) and 0.01 mg/mL bovine insulin (Sigma Aldrich cat# I9278) at 37 °C with 5% CO<sub>2</sub>.

Hek293A EGFP-WIPI2b cells were cultured in standard DMEM (PAN Biotech, cat# P04-03500) supplemented with 10% FBS (Invitrogen cat# 10500-084), 1% sodium pyruvate (PAN Biotech, cat# P04-43100) and 1% NEAA (PAN Biotech, cat# P08-32100) at 37 °C with 5% CO<sub>2</sub>.

**Passaging of Mammalian Cells:** After cells were grown to 70-80% confluency in cell culture flasks, cells were sub-cultured and added with fresh media. All used solutions and media were warmed to 37 °C in a water bath before usage. In a first step the old medium was removed and cells washed with sterile PBS. To detach cells from the tissue flask surface, a trypsin/EDTA solution was added, and the cells incubated for 2-5- min (37 °C, 5% CO<sub>2</sub>) until complete detachment of the cells. Then fresh medium was added, and the desired cell suspension volume transferred to a fresh culture flask.

**Long-Term Storage of Cells:** For cryo-conservation, cells were grown to confluence, detached from the culturing flask (Trypsin/EDTA) counted by automatic cell counting and subsequently centrifuged (350 g, 5 min). The cell-pellet was then resuspended in the respective medium containing 5% (v/v) DMSO to obtain an approximate density of  $1 \times 10^6$  cells/mL. The cell suspension was subsequently transferred to cryovials and placed into a freezing container (Mr. Frosty™) to allow a slow and even reduction of the temperature. After a 24 h storage at -80 °C, cell vials were transferred to a liquid nitrogen tank for long-term storage.

**Automated Cell Counting and Cell Seeding:** Cells were counted using the automated cell counter Countess™ II Automated Cell Counter according to the manufacturers' instructions

and the Countess® Cell Counting Chamber Slide (Thermo Fisher Scientific, Cat. No. C10228) For the identification of dead cells, Trypan blue (1:1 ratio with cell suspension) was used. Based on the cell number, the cell suspension was further diluted with medium to give the desired cell number to reach the cell density required for the applied assay.

#### **6.4.2 Phenotypic Assays**

##### **6.4.2.1 High Content Screening for Autophagy Inhibitors**

For the phenotypic autophagy assay, 4000 MCF7-GFP-LC3 cells per well were seeded in 25  $\mu$ l medium in a 384 well Greiner  $\mu$ clear plate (cat# 781080, lid cat# 656191) and incubated (37 °C, 5% CO<sub>2</sub>) overnight. Cells were then washed by a plate washer (Biotek, ELx405) three times with 1X PBS followed by a final aspiration of the washing buffer. The addition of 25 nl of compound solution (10 mM stock solution in DMSO) was then carried out with an echo dispenser (Labcyte, Echo 520 dispenser). Addition of medium to induce autophagy was carried out with a Multidrop Combi (Thermo Scientific). 25  $\mu$ L Earle's Balanced Salt Solution (EBSS, Sigma Aldrich, cat# E3024-500ml) containing 50  $\mu$ M Chloroquine (Sigma Aldrich, cat# C6628-25g) was used for starvation-induced autophagy and 25  $\mu$ L medium containing 50  $\mu$ l Chloroquine and 100 nM Rapamycin (Biomol, cat# Cay13346)-1 was used for rapamycin-induced autophagy screening. After incubation (37 °C, 5% CO<sub>2</sub>) for three hours cells were fixed by addition of 25  $\mu$ L 1:4 formaldehyde in 1X PBS + 1:500 Hoechst (stock: 1 mg/mL, Sigma Aldrich cat# B2261-25 mg) and incubation for 20 min at room temperature. Cells were then washed three times with 1X PBS. Four images per well were taken with ImageXpress Micro XL (Molecular Devices) at 20x. Automated image analysis was performed using the granularity setting of MetaXpress Software (Molecular Devices).

##### **6.4.2.2 Cell Painting Assay**

The cell painting assay was performed by the COMAS center and closely followed the method described by Bray *et al.*<sup>[115]</sup>

5  $\mu$ L U2OS medium were added to each well of a 384-well plate (PerkinElmer CellCarrier-384 Ultra), followed by subsequent addition of 1600 U2OS cells in 20  $\mu$ L medium. Incubation at ambient temperature for 5 min was followed by incubation at 37°C (5% CO<sub>2</sub>) for 4 h. Then the cells were treated with compounds by employing the Echo 520 acoustic dispenser (Labcyte) to reach the final concentrations of 3, 10, 30 and 50  $\mu$ M and incubated for 20 h (37 °C, 5%

## Experimental

CO<sub>2</sub>). To reduce plate effects, replicates were performed on different plates and in different plate positions.

After incubation, the mitochondria were stained with Mito Tracker Deep Red (Thermo Fisher Scientific, Cat. No. M22426). After dilution of a concentrated stock solution (1 mM) with prewarmed medium to a concentration of 100 nM, 15 µL medium from the cell plate were removed and replaced with 25 µL of the Mito Tracker solution. After 30 min incubation in darkness (37 °C, 5% CO<sub>2</sub>) the cells were fixed by addition of formaldehyde (3.7%) in PBS. An additional incubation in the dark for 20 min (37 °C, 5% CO<sub>2</sub>) was followed by a PBS washing step applying the Biotek Washer Elx405 (3x70 µL). The final 70 µL PBS were left in each well. Subsequently, a staining solution containing 1% BSA, 50 µL phalloidin (Thermo Fisher Scientific, A12381), 25 µg/ml concanavalin A (Thermo Fisher Scientific, Cat. No. C11252), 50 µL/ml Hoechst 33342 (Sigma, Cat. No. B2261-25mg), 15 µl/ml WGA-Alexa594 conjugate (Thermo Fisher Scientific, Cat. No. W11262) and 0.3 µL/ml SYTO 14 solution (Thermo Fisher Scientific, Cat. No. S7576) was added to each well. After a last incubation in darkness (30 min, 37 °C, 5% CO<sub>2</sub>) cells were washed again with PBS (3x 70 µL) leaving 70 µL in each well after the last washing step. Then the plate was sealed and centrifuged (1 min at 500 rpm).

The fluorescence readout was performed by a Micro XL High-Content Screening System (Molecular Devices, 5 channels, 9 sites per well, 20x magnification, binning 2). The obtained microscope figures were analysed with a computing cluster of the Max Planck Society by employing the CellProfiler package (<https://cellprofiler.org/>) to extract 1716 features. A subset of 579 characteristic parameters that show high reproducibility were identified in previous studies using the method published by Woehrmann *et al.*<sup>[116]</sup>

For the creation of phenotypic profiles for each tested compound, the Z-scores for each feature was calculated. The Z-scores can be derived from the deviation of the measured feature value of the test compound (measured) to the median of controls divided by the Median Absolute Deviation (MAD) of the controls. The list of obtained Z-scores represents the morphological profile (fingerprint) of a compound.

$$z - score = \frac{value_{measured} - median_{controls}}{MAD_{controls}}$$

The induction-value was calculated as a percentage of the number of significantly changed parameters compared to the DMSO control fingerprint.



$$\text{Induction [\%]} = \frac{\text{number of parameters with abs. values} > 3}{\text{total number of parameters}}$$

Biosimilarities between morphological profiles were calculated from the correlation distances between two profiles and additionally, a dimension reduction analysis (Principal Component Analysis, short PCA) was employed to evaluate the compound sets. In the PCA the whole profiles. Thereby, all morphological information (features) from the profiles are reduced to three components. For the PCA, a 'row' normalization in which each profile was normalised according to the parameter with the highest z-score was employed.

### 6.4.3 Biochemical and Cell-based Assays

#### 6.4.3.1 Kinase Panel

**Detection of the biochemical inhibition of 485 kinases was carried out by Life Technologies Ltd (United Kingdom).** The screen was performed in three different assays formats: Adapta (activity-based), Z-Lyte (activity-based) and Lantha (binding-based) at a concentration of 10  $\mu$ M of azaquindole-1 (6s). VPS34 IC<sub>50</sub> values for 5 selected compounds were measured in the Adapta assay.

Information on how each assay was completed can be found using the following link: <https://www.thermofisher.com/nz/en/home/products-and-services/services/custom-services/screening-and-profiling-services/selectscreen-profiling-service/selectscreen-kinase-profiling-service.html> (last accessed 25.05.2022).

#### 6.4.3.2 Immunoblotting (LC3 and ULK1/pULK1)

**This experiment was performed by Dale Corkery.** Cells were lysed in ice cold lysis buffer (20 mM Tris-HCl pH 8, 300 mM KCl, 10% Glycerol, 0.25% Nonidet P-40, 0.5 mM EDTA, 0.5 mM EGTA, 1 mM PMSF, 1x complete protease inhibitor) and passed 5X through a 21G needle. After clearance by centrifugation protein concentrations were determined via Bradford assay (Bio-Rad Protein Reagent, cat# 5000006) and lysates normalised. Lysates were mixed with 4X sample buffer, boiled for 10 min, proteins separated by SDS-PAGE, then transferred to nitrocellulose membrane (Bio-Rad, cat# 1704159) using a Trans-Blot Turbo transfer system (Bio-Rad). Membranes were blocked with 5% skim milk (in TBS-T) and incubated with primary antibody overnight at 4°C. Membranes were washed with TBST and incubated with an HRP-conjugated secondary antibody diluted in 5% skim milk for 1 h at room temperature. After washing, protein detection was carried out using chemiluminescence and imaged using a ChemiDoc imaging system (Bio-Rad).

#### 6.4.3.3 Selective Viability Assay

To test the selective viability of cells under autophagy activation or standard conditions, 5000 MFC7 cells per well (100  $\mu$ L medium) were seeded into a clear, flat-bottom 96 well plate and incubated overnight (37 °C, 5% CO<sub>2</sub>). Following, the medium was removed and replaced with 80  $\mu$ L either glucose rich or glucose deprived medium, both added with propidium iodide (1:60). On a separate dilution plate, compound solutions in the same media were prepared and 20  $\mu$ L added to the cells to reach the nine final concentrations in the cell plate wells DMSO (0.1%) and nocodazole (10  $\mu$ M) were used as controls. The cell growth was monitored for 72 h using the IncuCyte® ZOOM for 72 h. Two images per well

were taken at 10-fold magnification every 2 h in the fluorescent red and in the phase channel. The resulting images were analysed with the IncuCyte® ZOOM software.

#### 6.4.3.4 Live-Cell Microscopy

**This experiment was performed by Dale Corkery.** For live-cell imaging of Hek293A EGFP-WIP12b cells, cells were seeded on poly-l-lysine coated 8-well cover glass bottom chamber slides (Sarstedt, cat# 94.6190.802) and incubated for 24 h. Imaging was performed on a Zeiss Cell Observer spinning disk confocal (ANDOR iXon Ultra ) (Carl Zeiss) equipped with a 63x immersion oil objective lens (Plan-Apochromat 1.40 Oil DIC M27) and a temperature-controlled hood maintained at 37°C and 5% CO<sub>2</sub>. Quantification of puncta was performed using the spot tracking function of the open-source bioimage processing software, Icy.

#### 6.4.3.5 Cellular Thermal Shift Assay (CETSA)

##### CETSA in Lysates

Two T75 cell culture Flasks were seeded with each  $6 \times 10^5$  MCF7#2011 cells in 12 mL DMEM and incubated at 37°C and 5% CO<sub>2</sub> for three days. Cells were detached, transferred to two separate tubes, and washed three times with PBS. Then 0.6 mL PBS containing 0.04% NP-40 Alternative were added to each tube and cells were lysed by means of freeze and thaw. Either 50 µM of Azaquindole-1 or DMSO were added to the lysates, samples were mixed and incubated for 10 min. Treated and non-treated lysates were divided into ten aliquots, each 50 µL in PCR tubes. The aliquots were individually heated at different temperatures (*Eppendorf Mastercycler ep Gradient S*). After the heat treatment the cell lysates were completely transferred to polycarbonate tubes and centrifuged (*Beckman Optima MAX-TL*) at 100,000 g, 4°C for 25 min. 16 µL of each supernatant was added with 4 µL of 5x loading buffer and incubated for 5 min at 95°C, before samples were analysed by Immunoblotting. Proteins were separated by SDS-PAGE and transferred to PDVF membrane using wet transfer. The membranes were blocked with Odyssey Blocking Buffer (TBS; *Li-Cor*) for 1 h and incubated with the primary antibody (PI3 Kinase Class III (D4E2) Rabbit mAb #3358 Cell Signalling in Odyssey blocking buffer containing 0.2% Tween-20) at 4°C, overnight. After washing with TBS-T (TBS containing 0.1 % Tween) the membrane was incubated with the secondary antibody coupled to IRDye® 800CW (Donkey anti-Rabbit IgG, *Li-COR*) for 1 h, in Odyssey blocking buffer containing 0.2% Tween-20 and 0.1 % SDS at room temperature. Membranes were washed with TBS-T, then TBS before images were taken (*Bio-Rad ChemiDoc™ MP Imaging System*).

## Experimental

### In-Cell CETSA

Two T75 cell culture Flasks were seeded with each  $6 \times 10^5$  MCF7#2011 cells in 12 mL DMEM and incubated at 37°C and 5% CO<sub>2</sub> for three days. The media was subsequently removed and replaced with 3 mL medium containing either 50 μM of Azaquindole-1 or DMSO. After incubation for 1 h at 37°C and 5% CO<sub>2</sub> the medium was removed, and cells were detached using 1.5 mL trypsin and collected in 0.6 mL PBS each. Treated and non-treated cell suspensions were divided into ten aliquots, each 50 μL in PCR tubes. The aliquots were individually heated at different temperatures (*Eppendorf Mastercycler ep Gradient S*). After the heat treatment, 5 μL PBS containing 4.4% NP-40 Alternative were added to each sample and cells lysed by freeze and thaw. The cell lysates were completely transferred to polycarbonate tubes and centrifuged (*Beckman Optima MAX-TL*) at 100,000 g, 4°C for 25 min. 16 μL of each supernatant were added with 4 μL of 5x loading buffer and incubated for 5 min at 95°C, before samples were analysed by Immunoblotting. Proteins were separated by SDS-PAGE and transferred to PDVF membrane using wet transfer. The membranes were blocked with Odyssey Blocking Buffer (TBS; *Li-Cor*) for 1 h and incubated with the primary antibody (PI3 Kinase Class III (D4E2) Rabbit mAb #3358 Cell Signalling in Odyssey blocking buffer containing 0.2% Tween-20) at 4°C, overnight. After washing with TBS-T (TBS containing 0.1 % Tween) the membrane was incubated with the secondary antibody coupled to IRDye® 800CW (Donkey anti-Rabbit IgG, *Li-COR*) for 1 h, in Odyssey blocking buffer containing 0.2% Tween-20 and 0.1 % SDS at room temperature. Membranes were washed with TBS-T, then TBS before images were taken (*Bio-Rad ChemiDoc™ MP Imaging System*).

**Analysis:** Images were analysed with ImageJ (FUJI). Normalisation and all calculations were done with PRISM. (Curves: IC<sub>50</sub> variable slope → turning points correspond to melting temperature in obtained curves).

#### 6.4.3.6 Kinase Kinetic Experiments (VPS34)

**The experiments were performed by SignalChem.** Three independent profiling runs of azaquindole-1 (**6s**) against VPS34 at 5 compound concentrations and 6 ATP concentration were performed using the ADP Glo™ assay to determine K<sub>i</sub>. VPS34 was cloned, expressed, and purified in-house at SignalChem and the ADP-Glo™ assay kit purchased from Promega. Data were analysed by nonlinear regression (curve fit) – mixed model inhibition analysis in GraphPad Prism using the obtained velocity data.

## 6.4. Cheminformatic Analysis

All cheminformatic analyses were performed by Axel Pahl. (Similar as in: Grigalunas *et al. Nat Commun* **2021** *12* 1-11.)<sup>[15]</sup> using Python 3.8, the cheminformatics toolkit RDKit [RDKit: Open-Source Cheminformatics Software, (v 2020.03.6, <http://www.rdkit.org/>), and KNIME (v 4.2.3, <https://www.knime.com>). The Python part of the analysis was performed in JupyterLab Notebooks in a conda environment.

### 6.4.1 Reference Data Sets

**ChEMBL NP 30:** Entries which had the "J. Nat. Prod" OR "J Nat Prod" as journal source were extracted from the ChEMBL database (v30). Molecular standardisation and diverse filtering steps gave the final dataset (45679 entries).

**DrugBank:** The approved and experimental data sets from DrugBank (v 5.1.8) were downloaded and standardised to obtain 8204 entries.

**Enamine:** The full Advanced Screening Collection was downloaded (>50000 compounds). A random set of 50000 compounds was filtered and standardised to give a reference dataset consisting of 49968 unique structures.

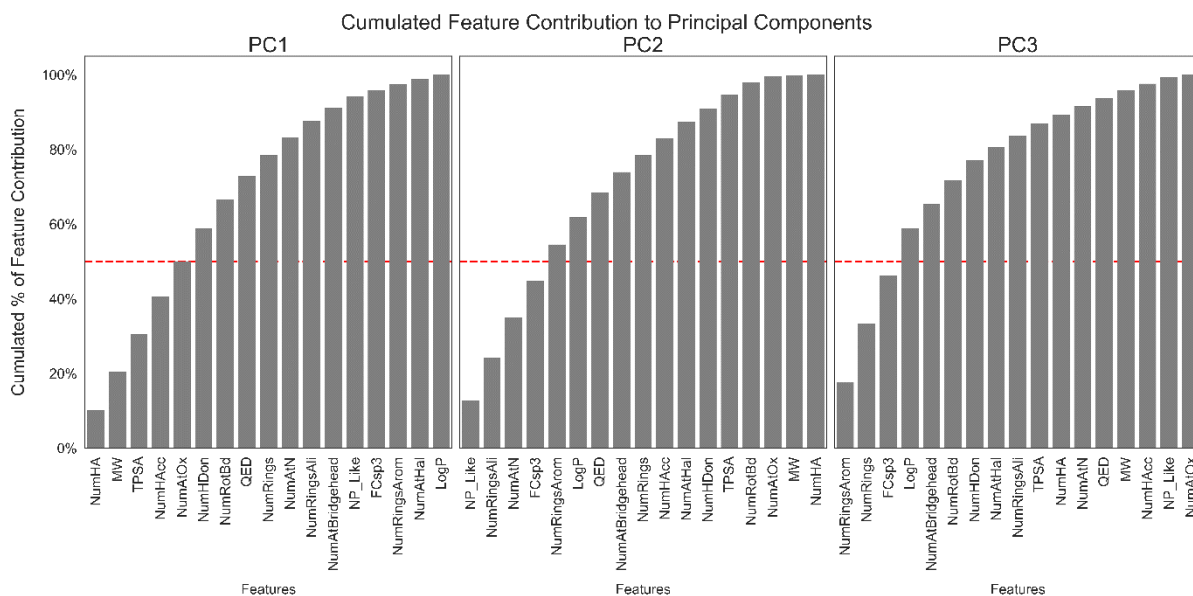
### 6.4.2 Molecular and Physiochemical Investigations

**Principal Moment of Inertia (PMI):** The principal moments of inertia were calculated using RDKit and plots were produced using matplotlib.

**NP Likeness and QED Scores:** NP Likeness Scores and QED scores were calculated with the implementations in the RDKit.

**Principal Component Analysis of Molecular Descriptors:** The PCA of 17 molecular descriptors was performed to investigate the chemical space occupied by the chromaline PNP class compared to the reference data sets. The analysis was performed using the scikit-learn Python package and the contribution of molecular features for each principal component were calculated as shown in the plots below.

## Experimental



**Chemical Similarity:** The chemical similarities of chromalines, chromopyrones and pyroquinolines were calculated using a fingerprint implemented in the RDKit: ECFP6 (a bit fingerprint of length 1024 with radius 3).

**Biological Similarities:** Class based similarities of morphological profiles were calculated from comparison of 579 features by Distance Correlation (scipy 'spatial distance'). The similarity is: 1- Distance Correlation. Negative values were set zero and the similarity is given in percent.



**7.Abbreviations**

$\mu$ w microwave

**A**

ACN Acetonitrile

AMP adenosine monophosphate

AMPK 5'-AMP-activated kinase

AMRA1 activating molecule in Beclin-1 regulated autophagy

APS ammonium persulfate

ATG Autophagy-related gene

ATP adenosine triphosphate

AZA azaquindole-1

**B**

BIOS biology oriented synthesis

BS biosimilarity

BSA bovine serum albumin

**C**

C chromanone

CETSA cellular thermal shift assay

ChEMBL Chemical database of bioactive molecules of the European Molecular Biology Laboratory

COMAS Compound Management and Screening Center

Comp principal component

CPA cell painting assay

CQ chlorouine

CS chemical similarity

CtD complexity to diversity

**D**

DABCO 1,4-diazabicyclo[2.2.2]octane

DAPI 4', 6-diamidino-2-phenylindole, dihydrochloride

DCM dichloromethane

DIAD diisopropyl azodicarboxylate



DMAP	4-(Dimethylamino)pyridine
DMAP	dimethylamino-pyridine
DMEM	Dulbecco's Modified Eagle Medium
DMF	N,N-Dimethylformamid
DMSO	dimethyl sulfoxide
DMSO	dimethyl sulfoxide
<b>E</b>	
EBSS	Earle's Balanced Salt Solution
EDTA	ethylenediaminetetraacetic acid
eGFP	enhanced green fluorescent protein
eGFP	enhanced green fluorescent protein
EGTA	ethylene glycol-bis( $\beta$ -aminoethyl ether)- <i>N,N,N',N'</i> -tetraacetic acid
eq.	equivalent
ER	endoplasmic reticulum
ESI	electrospray ionization
et a.	<i>lat. et alia, and others</i>
Et <sub>3</sub> N	triethylamine
EtOAc	ethylacetate
Expl. Var-	explained variance
<b>F</b>	
FBDD	fragment based drug discovery
FBS	fetal bovine serum
FCsp <sup>3</sup>	fraction of sp <sup>3</sup> carbons
FDA	U.S. Food and Drug Administration
FT-IR	fourier-transform infrared spectroscopy
<b>G</b>	
GF	griseofulvin
GFP	green fluorescent protein
<b>H</b>	
h	hours

## Abbreviations

HBD	hydrogen bond donator
HPLC	High-performance liquid chromatography
HPLC-MS	High-performance liquid chromatography with mass spectrometry
HR-MS	high resolution-mass spectrometry
HTS	high throughput screening

### I

I	indole
IC	isocoumarin
IC <sub>50</sub>	half maximal inhibitory concentration
IND	induction

### K

<i>K<sub>i</sub></i>	inhibitor constant
<i>K<sub>M</sub></i>	Michaelis-Menten constant

### L

LC3	microtubule-associated protein 1A/1B-light chain 3
LiAlH <sub>4</sub>	lithium aluminium hydride

### M

MAD	mean absolute deviation
MBS	median biosimilarity
MBS	median biosimilarity
MEM	Modified Eagle Medium
MeOH	methanol
min	minutes
MOA	mode of action
MOI	mode of inhibition
MS	mass spectrometry
mTOR	mammalian target of rapamycin
MVK	methylvinylketone

### N

nd	not detected
NEAA	non-essential amino acids
NMR	nuclear magnetic resonance
NP	natural product
NP-40	4-nonylphenyl-polyethylene glycol
<b>P</b>	
PAS	phagophore assembly site
PBS	phosphate buffered saline
PCA	principal component analysis
PCR	polymerase chain reaction
PE	phosphatidyl ethanolamine
PI	phosphatidylinositol
PMI	principal moments of inertia
PNP	Ppseudo-natural product
PVDF	polyvinylidene-difluoride
<b>Q</b>	
QCI	quincorine
QD	quinidine
QED	quantitative estimation of drug-likeness
QN	quinine
<b>R</b>	
<i>rt</i>	room temperature
<b>S</b>	
SAR	structure activity relationship
SAR	structure activity relationship
SCONP	structural classification of natural products
SDS	sodium dodecyl sulfate
SDS-PAGE	sodium dodecylsulfate polyacrylamide gel electrophoresis
SM	sinomenine

## Abbreviations

SNARE	soluble NSF attachment receptor
SPR	structure phenotype relationship
<b>T</b>	
<i>T</i>	temperature
<i>t</i>	time
TBAF	tetra-n-butylammonium fluoride
TBDMS	<i>tert</i> -butyldimethylsilyl
TBS	tris buffered saline
TFA	trifluoroacetic acid
THF	tetrahydrofuran
THF	tetrahydrofuran
THPI	tetrahydropyran-indole
THQ	tetrahydroquinoline
TLC	thin layer chromatography
<b>U</b>	
U-2OS	human bone osteosarcoma epithelial cells
uHPLC	Ultra-high-performance liquid chromatography
ULK1	Unc-51-like-kinase 1
<b>V</b>	
<i>v</i>	velocity (of an enzymatically catalysed reaction)
$v_{\max}$	maximum velocity (of an enzymatically catalysed reaction)
VPS34	vacuolar protein sorting 34
<b>W</b>	
WIPI	WD repeat domain phosphoinositide-interacting protein



## 8. References

- [1] B. R. Stockwell, *Nature* **2004**, *432*, 846–854.
- [2] H. J. Jung, H. J. Kwon, *Arch Pharmacol Res* **2015**, *38*, 1627–1641.
- [3] J.-L. Reymond, M. Awale, *ACS Chem Neurosci* **2012**, *9*, 649–657.
- [4] M. Grigalunas, S. Brakmann, H. Waldmann, *J Am Chem Soc* **2022**, *144*, 3314–3329.
- [5] K. Kumar, H. Waldmann, *Isr J Chem* **2019**, *59*, 41–51.
- [6] D. J. Newman, G. M. Cragg, *J Nat Prod* **2020**, *83*, 770–803.
- [7] J. Clardy, C. Walsh, *Nature* **2004**, *6*, 829–837.
- [8] S. Wetzel, R. S. Bon, K. Kumar, H. Waldmann, *Angew Chem Int Ed* **2011**, *50*, 10800–10826.
- [9] H. van Hattum, H. Waldmann, *J Am Chem Soc* **2014**, *136*, 11853–11859.
- [10] G. Karageorgis, H. Waldmann, *Synthesis* **2019**, *51*, 55–66.
- [11] W. Wilk, T. J. Zimmermann, M. Kaiser, H. Waldmann, *Biol Chem* **2010**, *391*, 491–497.
- [12] R. I. Sadreyev, N. v. Grishin, *BMC Struct. Biol.* **2006**, *6*, 1–14.
- [13] M. A. Koch, A. Schuffenhauer, M. Scheck, et al., *Proc Natl Acad Sci U S A* **2005**, *102*, 17272–17277.
- [14] J. Liu, G. S. Cremonesi, F. Otte, et al., *Angew Chem Int Ed* **2021**, *60*, 4648–4656.
- [15] M. Grigalunas, A. Burhop, S. Zinken, et al., *Nat Commun* **2021**, *12*, 1–11.
- [16] G. Karageorgis, D. J. Foley, L. Laraia, H. Waldmann, *Nat Chem* **2020**, *12*, 227–235.
- [17] S. E. Motika, P. J. Hergenrother, *Nat Prod Rep* **2020**, *37*, 1395–1403.
- [18] W. H. I. Robert, K. C. Morrison, R. W. Hicklin, T. A. Flood, P. J. Richter, Michelle F., Hergenrother, *Nat. Chem.* **2013**, *5*, 195–202.
- [19] K. C. Morrison, P. J. Hergenrother, *Nat Prod Rep* **2014**, *31*, 6–14.
- [20] D. A. Erlanson, R. S. McDowell, T. O'Brien, *J Med Chem* **2004**, *47*, 3463–3482.
- [21] S. Knight, D. Gianni, A. Hendricks, *SLAS Discov* **2022**, *27*, 3–7.

- [22] E. A. Crane, K. Gademann, *Angew Chem Int Ed* **2016**, *55*, 3882–3902.
- [23] A. Pahl, H. Waldmann, K. Kumar, *CHIMIA* **2017**, *71*, 653.
- [24] G. Karageorgis, E. S. Reckzeh, J. Ceballos, et al., *Nat Chem* **2018**, *10*, 1103–1111.
- [25] M. Akbarzadeh, J. Flegel, S. Patil, et al., *Angew Chem* **2022**, e202115193.
- [26] A. Burhop, S. Bag, M. Grigalunas, et al., *Adv Sci* **2021**, *8*, 2102042.
- [27] H. Waldmann, J.-M. Gally, A. Pahl, P. Czodrowski, *Arkivoc* **2021**, *4*, 89–104.
- [28] C. J. O’connor, L. Laraia, D. R. Spring, *Chem Soc Rev* **2011**, *40*, 4332–4345.
- [29] B. R. Stockwell, *Trends Biotechnol* **2000**, *18*, 449–455.
- [30] M. Schenone, V. Dančík, B. K. Wagner, P. A. Clemons, *Nat Chem Biol* **2013**, *9*, 232–240.
- [31] R. P. Hertzberg, A. J. Pope, *Curr Opin Chem Biol* **2000**, *4*, 445–451.
- [32] A. T. Plowright, L. Drowley, *Annu Rep Med Chem* **2017**, *50*, 263–299.
- [33] M. Prior, C. Chiruta, A. Currais, et al., *ACS Chem Neurosci* **2014**, *5*, 503–513.
- [34] W. Zheng, N. Thorne, J. C. McKew, *Drug Discov Today* **2013**, *18*, 1067–1073.
- [35] J. Inglese, R. L. Johnson, A. Simeonov, et al., *Nat Chem Biol* **2007**, *3*, 466–479.
- [36] D. C. Rubinsztein, P. Codogno, B. Levine, *Nat Rev Drug Discov* **2012**, *11*, 709–730.
- [37] I. Dikic, Z. Elazar, *Nat Rev Mol Cell Biol* **2018**, *19*, 349–364.
- [38] D. J. Klionsky, K. Abdelmohsen, A. Abe, et al., *Autophagy* **2016**, *12*, 1–222.
- [39] I. Orhon, F. Reggiori, *Cells* **2017**, *6*, 1–13.
- [40] N. Mizushima, A. Yamamoto, M. Matsui, T. Yoshimori, Y. Ohsumi, *Mol Biol Cell* **2004**, *15*, 1101–1111.
- [41] A. D. Balgi, B. D. Fonseca, E. Donohue, et al., *PLOS ONE* **2009**, *4*, e7124.
- [42] M. A. Bray, S. Singh, H. Han, et al., *Nat Protoc* **2016**, *11*, 1757–1774.
- [43] A. Pahl, S. Sievers, *Methods Mol Biol* **2019**, *1888*, 115–126.

## References

- [44] S. Ziegler, S. Sievers, H. Waldmann, *Cell Chem Biol* **2021**, *28*, 300–319.
- [45] D. Ausgabe, A. Christoforow, J. Wilke, et al., *Angew Chem* **2019**, *131*, 14857–14865.
- [46] L. Laraia, G. Garivet, D. J. Foley, et al., *Angew Chem Int Ed* **2020**, *59*, 5721–5729.
- [47] D. C. Rubinsztein, P. Codogno, B. Levine, *Nat Rev Drug Discov* **2012**, *11*, 709–730.
- [48] N. Mizushima, T. Noda, T. Yoshimori, et al., *Nature* **1998**, *395*, 395–398.
- [49] Y. Ohsumi, *Cell Res* **2013**, *24*, 9–23.
- [50] J. A. Nguyen, R. M. Yates, *Front Immunol* **2021**, *12*, 209.
- [51] G. Manic, F. Obrist, G. Kroemer, I. Vitale, L. Galluzzi, *Mol Cell Oncol* **2014**, *1*, e29911.1-e29911.11.
- [52] F. Tang, P. Hu, Z. Yang, et al., *Oncol Rep* **2017**, *37*, 3449–3458.
- [53] D. Schlütermann, M. A. Skowron, N. Berleth, et al., *Urol Oncol: Semin Orig* **2018**, *36*, 160.e1-160.e13.
- [54] M. Dyczynski, Y. Yu, M. Otrocka, et al., *Cancer Lett* **2018**, *435*, 32–43.
- [55] L. Galluzzi, J. M. B. S. Pedro, S. Demaria, S. C. Formenti, G. Kroemer, *Nat Rev Clin Oncol* **2017**, *14*, 247–258.
- [56] K. M. Kacprzak, in *Natural Products*, Springer, Berlin, Heidelberg, **2013**, pp. 605–641.
- [57] J. Pelletier, J. B. Caventon, *J B Ann Chim Phys* **1820**, *14*, 69-.
- [58] T. S. Kaufman, E. A. Rfflveda, T. S. Kaufman, E. A. Rfflveda, *Angew Chem Int Ed* **2005**, *44*, 854–885.
- [59] K. Kacprzak, *Synthesis* **2001**, *7*, 961–998.
- [60] C. von Riesen, H. M. R. Hoffmann, *Chem. Eur. J.* **1996**, *2*, 680–684.
- [61] L. Laraia, K. Ohsawa, G. Konstantinidis, et al., *Angew Chem Int Ed* **2017**, *56*, 2145–2150.
- [62] F. de Sa Alves, E. Barreiro, C. Manssour Fraga, *Mini Rev Med Chem* **2009**, *9*, 782–793.
- [63] E. Martino, G. Casamassima, S. Castiglione, et al., *Bioorg Med Chem Lett* **2018**, *28*, 2816–2826.



- [64] S. Siddiqui, S. S. Ahmad, S. I. Haider, B. S. Siddiqui, *Phytochem* **1987**, *26*, 875–877.
- [65] C. Chen, D. R. Lieberman, R. D. Larsen, T. R. Verhoeven, P. J. Reider, *J Org Chem* **1997**, *9*, 2676–2677.
- [66] J. Frackenpohl, H. M. R. Hoffmann, *J Org Chem* **2000**, *65*, 3982–3996.
- [67] A. J. Mancuso, D. Swern, *Synthesis* **1981**, *3*, 165–185.
- [68] B. Singh, S. Bhaskar, *Methods Mol Biol* **2019**, *2045*, 245–258.
- [69] A. Kuma, M. Matsui, N. Mizushima, *Autophagy* **2007**, *3*, 323–328.
- [70] C. G. Towers, D. Wodetzki, A. Thorburn, *J Cell Biol* **2020**, *219*, 1–15.
- [71] L. C. Crowley, A. P. Scott, B. J. Marfell, et al., *Cold Spring Harb Protoc* **2016**, *2016*, 647–651.
- [72] R. J. Vasquez, B. Howell, A. M. C. Yvon, P. Wadsworth, L. Cassimeris, *Mol Biol Cell* **2017**, *8*, 973–985.
- [73] A. Christoforow, J. Wilke, A. Binici, et al., *Angew Chem Int Ed* **2019**, *58*, 14715–14723.
- [74] “Adapta® Universal Kinase Assay and Substrates | Thermo Fisher Scientific - DE,” can be found under <https://www.thermofisher.com/de/de/home/industrial/pharmabiopharma/drug-discovery-development/target-and-lead-identification-and-validation/kinasebiology/kinase-activity-assays/adapta-universal-kinase-assay.html>, **05.2022**.
- [75] “SelectScreen Kinase Profiling Services | Thermo Fisher Scientific - DE,” can be found under <https://www.thermofisher.com/de/de/home/products-and-services/services/custom-services/screening-and-profiling-services/selectscreen-profiling-service/selectscreen-kinase-profiling-service.html>, **05.2022**.
- [76] L. Robke, Y. Futamura, G. Konstantinidis, et al., *Chem Sci* **2018**, *9*, 3014–3022.
- [77] A. S. Rosenthal, C. Tanega, M. Shen, et al., *Bioorg Med Chem Lett* **2011**, *21*, 3152–3158.
- [78] M. Muraki, B. Ohkawara, T. Hosoya, et al., *J Biol Chem* **2004**, *279*, 24246–24254.
- [79] J. Kim, M. Kundu, B. Viollet, K. L. Guan, *Nat Cell Biol* **2011**, *13*, 132–141.

## References

- [80] R. C. Russell, Y. Tian, H. Yuan, et al., *Nat Cell Biol* **2013**, *15*, 741.
- [81] H. E. J. Polson, J. de Lartigue, D. J. Rigden, et al., *Autophagy* **2010**, *6*, 506–522.
- [82] D. M. Molina, R. Jafari, M. Ignatushchenko, et al., *Science* **2013**, *341*, 84–87.
- [83] B. Seashore-Ludlow, H. Axelsson, T. Lundbäck, *SLAS Discov* **2020**, *25*, 118–126.
- [84] M. S. Celej, G. G. Montich, G. D. Fidelio, *Protein Sci* **2003**, *12*, 1496–1506.
- [85] J. Strelow, W. Dewe, P. W. Iversen, et al., in *Assay Guidance Manual*, Eli Lilly & Company and the National Center for Advancing Translational Sciences, Bethesda, **2012**, pp. 60–86.
- [86] V. L. Michaelis, M. L. Maud Menten, *Biochem* **1913**, *49*, 333–369.
- [87] I. T. Jolliffe, J. Cadima, *Philos Trans Royal Soc A* **2016**, *374*, 20150202.1–16.
- [88] A. Saeed, *European J Med Chem* **2016**, *116*, 290–317.
- [89] H. Kumagai, K. Wakazono, N. Agata, et al., *J Antibiot* **2005**, *58*, 202–205.
- [90] K. Nozawa, M. Yamada, Y. Tsuda, K. ichi Kawai, S. Nakajima, *Chem Pharm Bull* **1981**, *29*, 2689–2691.
- [91] A. Casnati, R. Maggi, G. Maestri, N. della Ca, E. Motti, *J Org Chem* **2017**, *82*, 8296–8303.
- [92] A. Saeed, M. Haroon, F. Muhammad, et al., *J Organomet Chem* **2017**, *834*, 88–103.
- [93] V. Kavala, C. C. Wang, D. K. Barange, et al., *J Org Chem* **2012**, *77*, 5022–5029.
- [94] “Dictionary of Natural Products 30.2 Chemical Search,” can be found under <https://dnp.chemnetbase.com/faces/chemical/ChemicalSearch.xhtml>, **05.2022**.
- [95] K. I. Nakashima, M. Oyama, T. Ito, et al., *Tetrahedron* **2012**, *68*, 2421–2428.
- [96] G. D. A. Martin, L. T. Tan, P. R. Jensen, et al., *J Nat Prod* **2007**, *70*, 1406–1409.
- [97] H. Eshghi, M. Rahimizadeh, S. M. Mousavi, *Nat Prod Res* **2014**, *28*, 438–443.
- [98] V. Kavala, C. Lin, C. W. Kuo, H. Fang, C. F. Yao, *Tetrahedron* **2012**, *68*, 1321–1329.
- [99] M. S. Yusubov, V. v. Zhdankin, *Resource-Efficient Techn* **2015**, *1*, 49–67.
- [100] Y. al Jasem, R. El-Esawi, T. Thiemann, *J Chem Res* **2014**, *38*, 453–463.

- [101] R. E. Gawley, *Synthesis* **1976**, 1976, 777–794.
- [102] S. Llona-Minguez, S. P. Mackay, *Beilstein J Org Chem* **10:135** **2014**, 10, 1333–1338.
- [103] “Home - Enamine,” can be found under <https://enamine.net/>, **05.2022**.
- [104] “DrugBank Online | Database for Drug and Drug Target Info,” can be found under <https://go.drugbank.com/>, **05.2022**.
- [105] “ChEMBL Database,” can be found under <https://www.ebi.ac.uk/chembl/>, **05.2022**.
- [106] J. Meyers, M. Carter, N. Y. Mok, N. Brown, *Future Med Chem* **2016**, 8, 1753–1767.
- [107] M. Aldeghi, S. Malhotra, D. L. Selwood, A. W. E. Chan, *Chem Biol Drug Des* **2014**, 83, 450–461.
- [108] F. Lovering, J. Bikker, C. Humblet, *J Med Chem* **2009**, 52, 6752–6756.
- [109] W. Wei, S. Cherukupalli, L. Jing, X. Liu, P. Zhan, *Drug Discov* **2020**, 25, 1839–1845.
- [110] K. V. Jayaseelan, P. Moreno, A. Truszkowski, P. Ertl, C. Steinbeck, *BMC Bioinform* **2012**, 13, 1–6.
- [111] P. Ertl, S. Roggo, A. Schuffenhauer, *J Chem Inf Model* **2008**, 48, 68–74.
- [112] C. A. Lipinski, F. Lombardo, B. W. Dominy, P. J. Feeney, *Adv Drug Deliv Rev* **2012**, 64, 4–17.
- [113] G. R. Bickerton, G. v. Paolini, J. Besnard, S. Muresan, A. L. Hopkins, *Nat Chem* **2012**, 4, 90–98.
- [114] T. J. Ritchie, S. J. F. Macdonald, *Drug Discov* **2014**, 19, 489–495.
- [115] M. A. Bray, S. Singh, H. Han, et al., *Nat Protoc* **2016** 11:9 **2016**, 11, 1757–1774.
- [116] M. H. Woehrmann, W. M. Bray, J. K. Durbin, et al., *Mol Biosyst* **2013**, 9, 2604–2617.

